# Effects of Tree Canopy on Pavement Condition, Safety and Maintenance - Phase 2


*Prepared by:*

Bhaven Naik, PhD, PE, PTOE, RSP
Glenn Matlack, PhD
Issam Khoury, PhD, PE
Gaurav Sinha, PhD
Deborah S. McAvoy, PhD, PE, PTOE
Andrea Horn, MS
O. Ryan Gassaway


*Prepared for:*

The Ohio Department of Transportation
Office of Statewide Planning and Research


State Job No. 135566

PID: 105899

September 2020

Final Report



OHIO UNIVERSITY

**Ohio Research Institute for Transportation and the Environment**


RESEARCH

U.S. Department of Transportation
Federal Highway Administration

## Technical Report Documentation Page

| 1. Report No. | 2. Government Accession No. | 3. Recipient's Catalog No. |
|---|---|---|
| **FHWA/OH-2020-17** | | |

| 4. Title and Subtitle | 5. Report Date |
|---|---|
| **Effects of Tree Canopy on Pavement Condition, Safety and Maintenance - Phase 2** | **September 2020**<br>6. Performing Organization Code |

| 7. Author(s) | 8. Performing Organization Report No. |
|---|---|
| **Bhaven Naik (ORCID 0000-0003-0436-885X), Glenn Matlack (ORCID 0000-0002-9628-0937), Issam Khoury (ORCID 0000-0003-4856-7535), Gaurav Sinha (ORCID 0000-0002-1280-6269), Deborah S. McAvoy (ORCID 0000-0002-0411-0034), Andrea Horn, and O. Ryan** | |

| 9. Performing Organization Name and Address | 10. Work Unit No. (TRAIS) |
|---|---|
| **Ohio University**<br>**Department of Civil Engineering**<br>**231 Stocker Center**<br>**Athens OH 45701-2979** | 11. Contract or Grant No.<br>**PID: 105899**<br>**SJN: 135566** |

| 12. Sponsoring Agency Name and Address | 13. Type of Report and Period Covered |
|---|---|
| **Ohio Department of Transportation**<br>**1980 West Broad Street**<br>**Columbus, Ohio 43223** | **Final Report**<br>14. Sponsoring Agency Code |

15. Supplementary Notes

**Prepared in cooperation with the Ohio Department of Transportation (ODOT) and the U.S. Department of Transportation, Federal Highway Administration.**

16. Abstract

**Tree canopies are common alongside and above rural highways in Ohio. Consequently, ODOT wants to know how a tree canopy affects pavement condition and road safety. A review of published research conducted for Phase I of this study suggested that tree canopies extend the life of asphalt pavement and improve road safety. Road managers and highway officials said roadside trees were believed to negatively impact the pavement surface directly below the canopy, according to the report's survey and anecdotal accounts. These impacts included increases in moisture and temperature variation, reductions of pavement longevity, and undermined road safety. These observations have not been rigorously verified, and there is a lack of prior research on the topic. This study seeks to determine if tree canopies affect asphalt pavement in Ohio, quantify any effects, and recommend best management practices. The research was approached with controlled experiments on small plots concerning microclimate and pavement condition and observations and measurements on in-service pavements covering microclimate, pavement condition, and safety.**

**The net results show tree canopies substantially reduce thermal loading, snow accumulation, and moisture in light to moderate rainstorms. Canopies also increase the persistence of moisture on stretches of shaded pavement. Snow and ice persistence were controlled by drainage and compaction by traffic, rather than the presence of tree canopies. In addition, a negative relationship exists between pavement surface texture and tree cover, landscape position, and traffic loading, but the effects on surface texture were apparent only under unusual conditions. No significant effects on pavement cracking were found. Crash data showed improvements in safety that can be attributed to roadside maintenance activities (trimming and pruning), but not specifically to the removal of tree canopy. There were no conclusive effects to driving behavior that can be related to tree canopy cover. Consequently, this report concludes that neither pavement condition nor driving behavior should be considered sufficient justification for removal or pruning of tree canopies as a form of routine maintenance on Ohio's rural roadways.**

| 17. Key Words | 18. Distribution Statement |
|---|---|
| Pavement condition; Tree canopy; Tree removal; Microclimate; Asphalt degradation; Pavement environment | **No Restrictions. This document is available to the public through the National Technical Information Service, Springfield, Virginia 22161** |

| 19. Security Classification (of this report) | 20. Security Classification (of this page) | 21. No. of Pages | 22. Price |
|---|---|---|---|
| **Unclassified** | **Unclassified** | **211** | |

# SI* (MODERN METRIC) CONVERSION FACTORS

## APPROXIMATE CONVERSIONS TO SI UNITS

| Symbol | When You Know | Multiply By | To Find | Symbol |
|---|---|---|---|---|
| **LENGTH** | | | | |
| in | inches | 25.4 | millimeters | mm |
| ft | feet | 0.305 | meters | m |
| yd | yards | 0.914 | meters | m |
| mi | miles | 1.61 | kilometers | km |
| **AREA** | | | | |
| $in^2$ | square inches | 645.2 | square millimeters | $mm^2$ |
| $ft^2$ | square feet | 0.093 | square meters | $m^2$ |
| $yd^2$ | square yards | 0.836 | square meters | $m^2$ |
| ac | acres | 0.405 | hectares | ha |
| $mi^2$ | square miles | 2.59 | square kilometers | $km^2$ |
| **VOLUME** | | | | |
| fl oz | fluid ounces | 29.57 | milliliters | mL |
| gal | gallons | 3.785 | liters | L |
| $ft^3$ | cubic feet | 0.028 | cubic meters | $m^3$ |
| $yd^3$ | cubic yards | 0.765 | cubic meters | $m^3$ |
| NOTE: Volumes greater than 1000 L shall be shown in $m^3$. | | | | |
| **MASS** | | | | |
| oz | ounces | 28.35 | grams | g |
| lb | pounds | 0.454 | kilograms | kg |
| T | short tons (2000 lb) | 0.907 | megagrams (or "metric ton") | Mg (or "t") |
| **TEMPERATURE (exact)** | | | | |
| °F | Fahrenheit temperature | 5(°F-32)/9 or (°F-32)/1.8 | Celsius temperature | °C |
| **ILLUMINATION** | | | | |
| fc | foot-candles | 10.76 | lux | lx |
| fl | foot-Lamberts | 3.426 | candela/$m^2$ | $cd/m^2$ |
| **FORCE and PRESSURE or STRESS** | | | | |
| lbf | poundforce | 4.45 | newtons | N |
| $lbf/in^2$ or psi | poundforce per square inch | 6.89 | kilopascals | kPa |

## APPROXIMATE CONVERSIONS FROM SI UNITS

| Symbol | When You Know | Multiply By | To Find | Symbol |
|---|---|---|---|---|
| **LENGTH** | | | | |
| mm | millimeters | 0.039 | inches | in |
| m | meters | 3.28 | feet | ft |
| m | meters | 1.09 | yards | yd |
| km | kilometers | 0.621 | miles | mi |
| **AREA** | | | | |
| $mm^2$ | square millimeters | 0.0016 | square inches | $in^2$ |
| $m^2$ | square meters | 10.764 | square feet | $ft^2$ |
| $m^2$ | square meters | 1.195 | square yards | $yd^2$ |
| ha | hectares | 2.47 | acres | ac |
| $km^2$ | square kilometers | 0.386 | square miles | $mi^2$ |
| **VOLUME** | | | | |
| mL | milliliters | 0.034 | fluid ounces | fl oz |
| L | liters | 0.264 | gallons | gal |
| $m^3$ | cubic meters | 35.71 | cubic feet | $ft^3$ |
| $m^3$ | cubic meters | 1.307 | cubic yards | $yd^3$ |
| **MASS** | | | | |
| g | grams | 0.035 | ounces | oz |
| kg | kilograms | 2.202 | pounds | lb |
| Mg (or "t") | megagrams (or "metric ton") | 1.103 | short tons (2000 lb) | T |
| **TEMPERATURE (exact)** | | | | |
| °C | Celsius temperature | 1.8°C + 32 | Fahrenheit temperature | °F |
| **ILLUMINATION** | | | | |
| lx | lux | 0.0929 | foot-candles | fc |
| $cd/m^2$ | candela/$m^2$ | 0.2919 | foot-Lamberts | fl |
| **FORCE and PRESSURE or STRESS** | | | | |
| N | newtons | 0.225 | poundforce | lbf |
| kPa | kilopascals | 0.145 | poundforce per square inch | $lbf/in^2$ or psi |

* SI is the symbol for the International Symbol of Units. Appropriate rounding should be made to comply with Section 4 of ASTM E380.

(Revised September 1993)

# Effects of Tree Canopy on Pavement Condition, Safety and Maintenance - Phase 2

Prepared by:

Bhaven Naik, PhD, PE, PTOE, RSP[1]

Issam Khoury, PhD, PE

Deborah S. McAvoy, PhD, PE, PTOE

Andrea Horn, MS

Department of Civil Engineering
Ohio University

Glenn Matlack, PhD

Department of Environmental and Plant Biology
Ohio University

Gaurav Sinha, PhD

Department of Geography
Ohio University

O. Ryan Gassaway, ISA-Certified Arborist

Woodsong Tree Care, LLC

September 2020

Prepared in cooperation with the Ohio Department of Transportation
and the U.S. Department of Transportation, Federal Highway Administration.

## ACKNOWLEDGEMENTS

The Ohio University research team would like to gratefully acknowledge the Ohio Department of Transportation technical panel members for their valuable contributions and assistance throughout this project. The technical panel members include:

- Mr. Scott E. Lucas, MBA, CPM – ODOT Office of Maintenance Operations (Tech Lead),
- Mr. Adam Au, P.E. – ODOT Office of Pavement Engineering,
- Mr. Matt Perlik, MS. – ODOT Office of Environmental Services;
- Mr. Eric Biehl, P.E. – ODOT Office of Materials Management, and
- Mr. Aric A. Morse, P.E. – ODOT Office of Pavement Engineering.

The research team would also like to gratefully acknowledge the time, assistance, and management from Ms. Kelly Nye in the Office of Statewide Planning and Research. Additionally, we would also like to thank the numerous individuals that contributed and were involved with this project in one way or the other.

Finally, the authors wish to thank Ohio University Civil Engineering undergraduate (Isaac Koroma, Braydon Putnam, and Autumn Watkins) and graduate (Jacob Campbell, Johnnatan Garcia, and Derar Tarawneh) students for their assistance with this project. Also, of assistance were research engineers Mary Robbins, Roger Green, and Andrew Russ.

**TABLE OF CONTENTS**

## LIST OF FIGURES

## LIST OF TABLES

## 1.0 EXECUTIVE SUMMARY

An integral part of Ohio's roadscape is the tree canopy cover alongside and above the pavement – abundant along a significant mileage of low-to-medium-volume roads in both urban and rural areas. Research in forest microclimates, environmental effects on pavement, and urban microclimates suggests that tree canopies affect the process of pavement degradation and the drivability of the pavement surface by altering the pavement microclimate. This study seeks to determine if/how tree canopies affect asphalt pavement in Ohio's climate, to quantify such effects, and to recommend best management practices.

The research was approached in four stages beginning with controlled experiments and progressively scaling up to real management units: First, microclimate effects were documented in small plots with basic physical properties measured under controlled conditions. Second, environmental effects on pavement condition were measured in small plots under actual road conditions to determine the contribution of tree canopies relative to other environmental factors. Third, road conditions as a function of tree coverage were compared at the scale of actual management units in the field. Fourth, safety was assessed in terms of crash data from real road sections. Data were recorded over a period of 24-months in approximately 270 permanent small plots on rural roads in Athens County, OH; and at 39 selected road sections spread across Ohio DOT's eastern districts.

The small-plot data show tree canopies substantially reduce thermal loading, reduce snow accumulation, and reduce moisture in light-moderate rainstorms, potentially extending pavement life. Canopies also increase the persistence of moisture on stretches of shaded pavement, potentially decreasing service life. Snow and ice persistence were controlled by drainage and compaction by traffic and appeared to be unrelated to presence of tree canopies. The findings from road sections at the scale of management units were akin to those observed from the small plot analysis.

Observations of small plots under natural road conditions showed a significant negative relationship between pavement surface texture and tree cover, landscape position, and traffic loading. However, the influence of tree cover on surface texture was only apparent under unusual conditions: 95% canopy cover (>90% is rare on rural roads; 0-60% cover is more usual), or in pavement surfaces >10 years old and at end of service life. Road plots under moderate canopy (40-60% cover; the majority of forest roads) showed no degradation that could be linked to presence of roadside trees. In contrast to the case of surface texture, pavement cracking was not significantly related to tree proximity or canopy cover under any circumstances.

Road sections described at the scale of management units showed no significant differences in pavement condition between shaded and unshaded sections. Pavement core samples showed greater interstitial voids under tree canopies, suggesting a canopy effect, but the small sample size prevents drawing firm conclusions at this point. Crash data showed improvements in safety that can be attributed to roadside maintenance activities (e.g. trimming and pruning), but not specifically to the removal of tree canopy. Surrogate measures of safety showed no conclusive effects to driving behavior/performance that can be related to tree canopy cover.

Recommendations: Based on these observations, it is recommended in this report that removal or pruning of tree canopies should not be practiced as routine maintenance for Ohio

highways as a means of extending the life of pavement. Canopy pruning or removal should only be applied to individual trees in specific cases justified by actual tree cover and pavement data. There may also be other reasons for tree maintenance which were outside the scope of this study, including health of the tree or line of sight problems. Potential reasons for removal include >95% measured canopy cover paired with degraded pavement or presence of a demonstrably dead tree likely to fall on the road. Results from this analysis support the view that, in general, tree canopies overtop rural highways should not be removed as a means of extending the life of pavement. This is consistent with the well-known economic and suggested safety benefits accruing from roadside trees, and (hence) the enormous public support that exists for protecting trees.

## 2.0 PROJECT BACKGROUND

An integral part of Ohio's roadscape is the trees that are abundant along a significant mileage of roads in both urban and rural settings. These trees create canopies and they are widely valued by the public, and support is often expressed in public forums [Lohr et al., 2004; Wolf, 2005]. However, within the Ohio Department of Transportation (Ohio DOT), it has been long thought that the shading from tree canopies influences the condition, safety, and maintenance of the pavement in various ways such as accelerated pavement deterioration and limited solar heating reducing the effectiveness of deicers; tree canopies are also thought to present a safety issue from falling limbs (ODOT, 2017). The Ohio DOT's current practice is to remove the tree canopy from the roadway where practical. This practice has been widely criticized by the general public, but possible effects of the tree canopy on pavement condition and safety have not been demonstrated in a rigorous scientific/engineering study.

The research team, with funding from the Ohio DOT, completed a literature review and synthesis as Phase 1 of this project (SJN No. 135320) to gain an understanding of the potential influence of tree canopy on pavement integrity, drivable surface condition, safety, and any maintenance practices [Naik et al., 2017]. This review of published research suggested that trees extend the life of asphalt pavement by reducing radiation loading, thermal cycling, and surface moisture, and improve road safety by affecting driving behavior. However, a survey of practice by Ohio DOT road managers and anecdotal reports suggested that roadside trees were believed to negatively impact the pavement surface directly below the canopy [Naik et al., 2017]. Specifically, a tree canopy is believed to cause increases in moisture and temperature variation, subsequently impairing the pavement's structural performance. The perceived impacts included accelerated moisture damage, poor density attainment, differential rutting, and raveling; all of which are believed by road managers to reduce the pavement longevity with an undesirable increase in the maintenance and rehabilitation costs. Tree canopy alongside the roadway is also believed to undermine road safety because of reduced skid resistance due to fallen leaves, limited direct sunlight promoting formation of black ice and fog; and entire trees, and branches and/or fruits falling on passing vehicles or blocking traffic lanes.

The consensus among Ohio DOT respondents is that a minimum clearance of 30 ft (0.9 m) from the centerline on both sides – available Right-of-Way (ROW) must be maintained. Some respondents mentioned removing all trees within the ROW, while others mentioned the removal of all trees except those trees having a trunk diameter of less than 12 in (300 mm). In conditions where the ROW is limited such as embankments, hills, curves and dips, and residential areas, the edge of the roadway (white line) was used to determine the clearance area. No specifics were provided on the vertical extent of the clearance, which was dependent on the reach of available trimming equipment such as a bucket truck or "sky trimmer".

Observations on tree canopy and pavement condition have been largely indirect, so there is not enough information directly addressing the tree canopy/pavement interaction. Therefore, the question of how a tree canopy alongside and overtop the roadway affects pavement condition and road safety is ripe for scientific exploration.

## 3.0 RESEARCH CONTEXT

The objective of this research project was to determine the effects of tree canopy on pavement in terms of pavement condition, maintenance, and safety. More specifically, this research work attempts to fill the gap in the body of knowledge pertaining to tree canopies overtop rural roadways and their effects on the pavement surface in Ohio, which has a cool-temperate climate. The research team formulated the problem in terms of four specific questions:

1. Does pavement quality differ between canopied, partially canopied, and open-sky plots?
2. How does the effect of shading due to tree canopy compare with effects of other factors which commonly contribute to pavement deterioration?
3. Do observations of microclimate and pavement condition made at the scale of individual trees also apply at the larger scale of highways and/or byways?
4. Does a tree canopy cause changes to the pavement condition that can subsequently create hazards for drivers? If 'yes', then what factors specifically contribute to the hazards?

To answer the four specific questions above, the research team set out to verify the following testable predictions (or hypotheses):

I. Tree canopy alongside and overtop the roadway influences the pavement structure. It is predicted that there will be differences in surface condition and differential setting between sections with and without tree canopies. These differences are likely to affect the life expectancy of pavement overlays, patching, and resurfacing.

II. Tree canopies act on pavement by moderating thermal cycling. In this case, there would be less block and transverse cracking under trees.

III. Tree canopies affect pavement by catching moisture on their foliage, thereby reducing the amount of moisture reaching the pavement. The research team predicts pavement under trees will have less alligator cracking in wheel tracks than exposed pavement, less debonding, and less fine-scale cracking throughout.

IV. Where the moisture from rainfall does reach the pavement, tree canopy can reduce evaporation, thereby accelerating moisture damage and water infiltration in the pavement sub-structure. This would be supported by observation of more serious edge cracking and debonding of pavement under trees than under an open sky. There will be moisture-related differences in pavement deterioration between shaded pavements and open-sky pavements.

V. Tree canopies act on pavement by absorbing soil moisture, thereby reducing the amount of moisture reaching the pavement from below. There should be less subsidence and expansion cracking of pavement under trees than under an open sky.

VI. If tree canopies cause pavement deterioration and in turn affect road safety, then all measures of deterioration and safety are expected to be proportional to the size, age, and canopy density of overhanging trees.

VII. If tree canopies influence pavement condition, this will subsequently affect the comfort and safety of the roadway. Differences between wet/dry/slick pavement surfaces will likely affect crashes or driving behavior.

The answers to the research questions and evaluations of the testable predictions then informed the development of recommendations contained in this report on tree canopy maintenance practices to maximize pavement longevity and performance while ensuring the safety of motorists.

## 4.0 RESEARCH APPROACH

This research was conducted as two parallel sub-projects examining canopy effects at different scales. First a detailed comparison of small patches of pavement (the "small plot study") focused on the effects on microclimate due to canopy presence and on the contribution to pavement condition by other aspects of the road environment. The second part was a comparison of larger pavement segments in a "road section study" which included microclimate impacts, pavement condition, and safety effects at the scale of real management units. Both parts involved the selection of study sites, data collection, data analysis, and interpretation of results.

This section of the report summarizes 1. Small plot evaluation of microclimate, 2. Small plot evaluation of pavement condition, 3. Road segment evaluation of microclimate, 4. Road segment evaluation of pavement condition, and 5. Road segment evaluation of safety. In each section, the method is described, and concise results are presented. More detailed and complete descriptions of methods and results are provided in the appendices.

### 4.1 Small Plot Study on Effects of Tree Canopy on Pavement Microclimate.

This section presents an abridged version of the research work performed at the *small plot level* to determine how tree canopy affects the pavement microclimate. A detailed presentation of the analysis can be found in Appendix A.

#### 4.1.1 Methods

*Study Sites*

Microclimate was described in experimental pavement plots established on residential streets in the City of Athens, Ohio. The plots consisted of 20 in × 20 in (50 cm × 50 cm) squares that were permanently located 20 to 40 in (50 to 100 cm) from the pavement edge. The pavement was asphalt concrete placed 2 to 8 years before, with modest slope and a surface course showing only minimal wear. Plots were established in triplets – "Under" (>95% canopy cover); "Partial" (45% to 55% canopy cover); and "Open" (no canopy cover). Plots were established under 23 trees (N = 69 plots).

Experimental trees ranged from 12 to 35 in (30 to 90 cm) in diameter; and were greater than 50 years in age. All trees had a uniformly dense, apparently healthy canopy with no obvious dead tissue. Species were typical of roadside trees in the Ohio Valley region: predominantly red maple (*Acer rubrum*), sugar maple (*Acer saccharum*), willow oak (*Quercus phellos*), and red oak (*Quercus rubrum*), with occasional sycamore (*Platanus occidentalis*), sweetgum (*Liquidambar styraciflua*), and locust (*Robinia pseudoacacia*). Most pavement variables were measured between June and September 2018 when all trees were fully leafed, presenting the maximum canopy density. Snow and ice were surveyed in January 2018 when all trees had shed their leaves and only bare branches remained. No evergreen tree species were used.

*Data*

- Pavement temperature; measured sequentially in experimental plots on June 6, 2018 from before sunrise (6:05AM) to after sunset (8:52PM) with an approximately 50-minute rotation. All three plots at each tree were measured within 60 seconds.
- Pavement wetness; measured as electrical conductivity at 3 to 5-minute intervals before and during natural rain showers in mid-late summer 2018. Measurement began on dry pavement, proceeded as rain began to fall, and ended when "Under" canopy plots showed wetness values comparable to "Open" plots.
- Moisture persistence; measured by experimentally wetting and then monitoring the drying of pavement plots. One liter (34 fl oz) of water was poured onto plots equivalent to a 0.39 in (1 cm) rain event. All plots were wetted before sunrise to ensure equal temperatures under all canopy conditions. Moisture was monitored in all plots at 40 to 50-minute intervals until metered moisture levels dropped to levels observed before wetting.
- Snow/Ice accumulation; measured immediately after a storm on January 13, 2018, and at daily intervals until no snow or ice remained. Snow depth was measured visually using a plastic scale inserted into undisturbed snow. Ice was assessed on the pavement as the proportion of the study plot covered.

### 4.1.2 Results

*Pavement Temperature.*

Figure 1 shows two representative examples of pavement temperature measured over the course of a day. The pavement was coolest before dawn and heated up as it absorbed solar radiation. The "open" plot pavement temperatures peaked at 113 to 122°F (45 to 50°C) during 1:00 to 3:00PM. By contrast, plots under the canopy heated substantially more slowly, with pavement temperatures peaking at only 82 to 90°F (28 to 32°C). Air temperatures ranged from 64.8°F (18.2°C) at sunrise to 78.6°F (25.9°C) at 6:00PM, normal values for a sunny day at this time of year. Peak temperatures under the canopy tended to occur early (8:00 to 10:00AM) or late (4:00 to 6:00PM) in the day as lateral radiation extended diagonally under the edge of the canopy.

Canopy classes differed significantly in maximum temperature (Kruskal-Wallis $\chi^2 = 31.577$, $p = 0.000$) and individual classes were easily distinguishable (Wilcoxon probabilities 0.0000-0.0002) increasing in proportion to canopy openness (Figure 2, left). In minimum temperature, canopy classes differed with lowest temperatures in "open" plots as depicted in Figure 2, center ($\chi^2 = 12.796$, $p = 0.002$). The greatest contrast in pavement temperature occurred between "open" and "under" plots (mean $\Delta$=24.8±1.9°C (44.6±3.4°F)) while smaller contrasts were observed between "open" and "partial" plots (18.5 ± 4.1°C (33.3±7.4°F)), as seen in Figure 2, right.

Maples (*Acer spp.*) allowed both warmer maximum and minimum pavement temperatures than oaks (*Quercus spp.*). Site aspect and tree diameter showed no relationship with either maximum or minimum pavement temperatures.

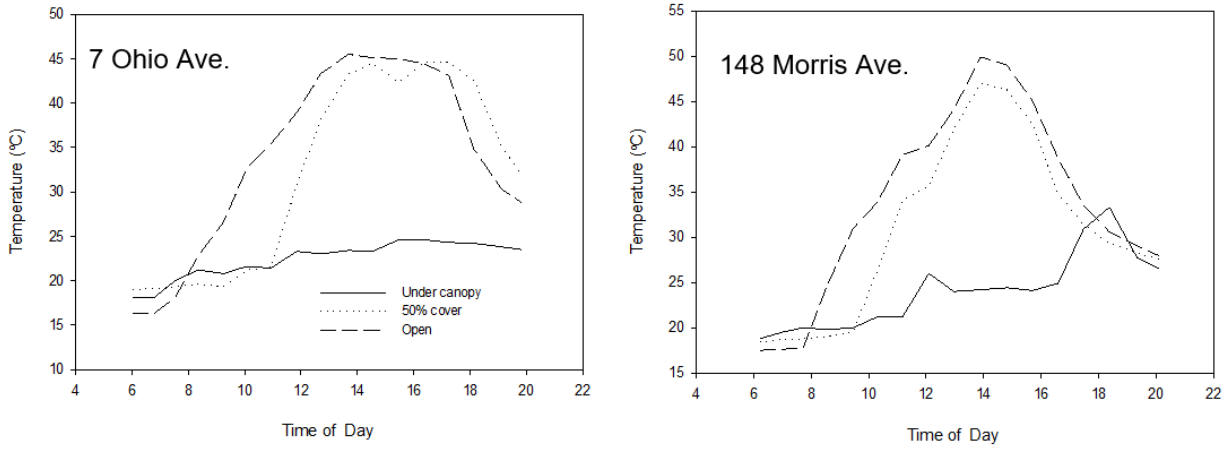


***Figure 1. Pavement Surface Temperature Through the Day on June 6, 2018 in Selected Pavement Plots Under and Adjacent to two Tree Canopies.***

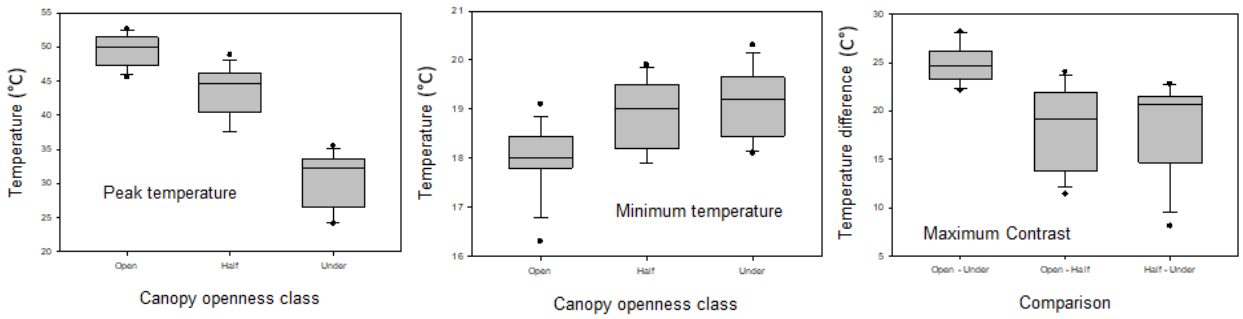


***Figure 2. Temperature Extremes in Pavement Plots Under and Adjacent to Tree Canopies. Left: peak temperature between sunrise and sunset (scale range 68-131°F). Center: minimum temperature (scale range 61-70°F). Right: maximum temperature contrast (1°C = 1.8°F).***

*Pavement Wetting.*

Wetting was measured during natural rainfall under six trees. Rain typically began with gentle sprinkling and intensity increased over a span of 30 to 40 minutes, as in the examples in Figure 3. Wetness for "under" plots was lower than for "open" plots for approximately 30 minutes (median) although there was substantial variation between trials related to the intensity and speed of development of individual rainstorms (range: 3 to 77 minutes). In "partial" plots, wetness was detected as soon as in "open" plots (median delay = 0 minutes) though, the degree of wetness in "partial" plots reached that of "open" plots after a median delay of 22 minutes (range: 0 to 74 minutes).

Very little rain was necessary to cause a wetness response in "partial" and "under" plots (unmeasurable – 0.45 mm). "Partial" plots reached levels of wetness equivalent to "open" plots after 0.029 in (0.74 mm) of rain. "Under" plots reached wetness levels equal to "open" plots after 0.050 in (1.27 mm) median.

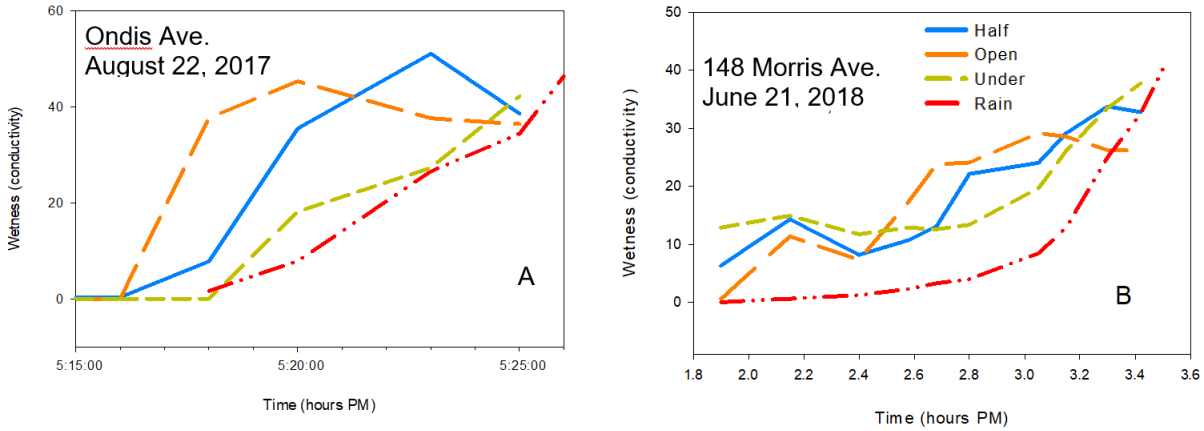


***Figure 3. Accumulation of Moisture Through the Course of Rain Showers on Test Plots at trees in Athens, Ohio. Two trees are shown as examples.***

*Pavement Drying.*

Figure 4 shows drying timelines for examples of experimentally wetted pavement plots. As expected, "open" plots dried faster than "under" plots. "Open" plots dried to 50% of the initial wetness value in 82 minutes (median), whereas "under" plots required 199 minutes. "Partial" plots required 124 minutes. Considerable variation was present within each canopy class (Figure 5). Significant contrasts were observed between canopy openness classes in 50% remaining ($\chi^2$ = 11.88, p = 0.003) and 10% remaining ($\chi^2$ = 8.23, p = 0.016). "Open" plots were distinguishable from "under" at both 50 and 10% dryness (p = 0.004 and 0.031, respectively). "Partial" plots were distinguishable from "open" in each measure (p = 0.072, 0.077), but only distinguishable from "under" at 50% dryness (p < 0.076).

Although pavement drainage was not quantified in this study, drainage was clearly important to drying rate. Plots with a pronounced camber (local slope within the plot) and a smooth surface drained rapidly; plots with a rough pavement surface, obvious cracks, or little slope gradient retained water longer even in full sun.

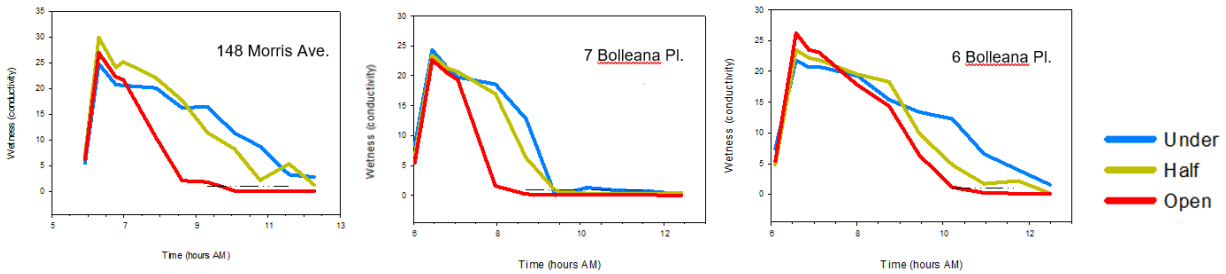


***Figure 4. Drying of Experimentally Wetted Pavement Plots Under and Adjacent to Trees in Athens, Ohio. Three trees are shown as examples.***

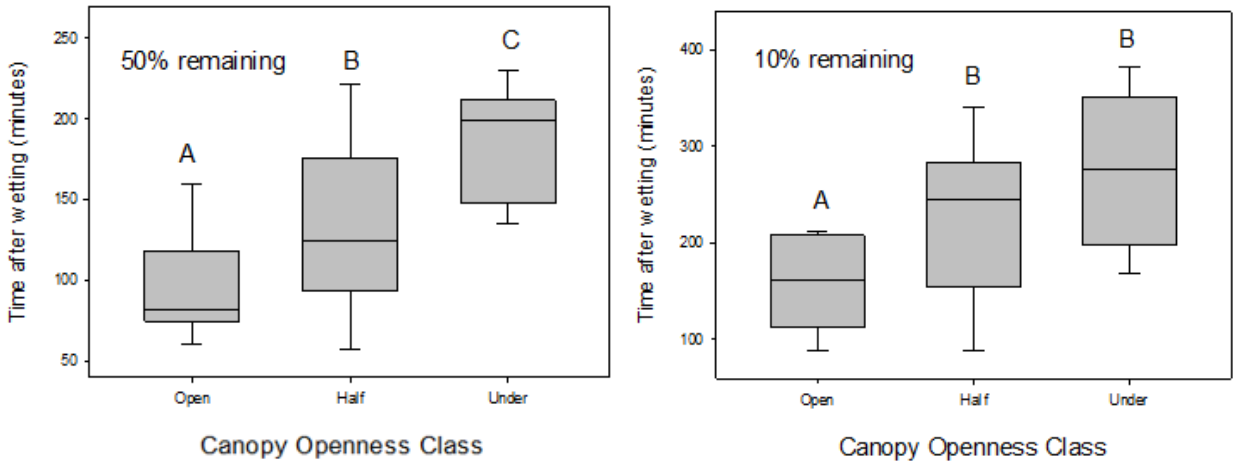


***Figure 5. Drying Rates of Experimentally Wetted Pavement Under and Adjacent to Tree Canopies. Left: time to 50% of initial wetness value; Right: time to 10% of initial wetness value. Letters indicate groups distinguishable by Wilcoxon Comparisons (p < 0.05)***

*Snow and Ice.*

Approximately 4 in (100 mm) of snow accumulated on January 13, 2018, supplemented by an additional 0.4 to 0.8 in (10 to 20 mm) on January 16. Maximum daily temperature remained below 32°F (0°C) though January 18 ensuring persistence of snow until January 19 (Figure 6). After the initial storm, snow depth under tree canopy was significantly less than in open plots ($\chi^2$ = 6.010, p = 0.050; Wilcoxon under/open p = 0.050) with a difference of about 21%.

No tree-canopy difference was detectable in ice cover (p > 0.40). After mean daily temperatures rose above freezing, snow and ice rapidly melted (Figure 6). Snow melted significantly faster under a tree canopy than under open sky ($\chi^2$ = 6.122, p = 0.047; Wilcoxon p = 0.066).

Although the research team did not systematically measure drainage or traffic volume, it became obvious that ice formation depended on two processes: packing of snow by passing vehicles and re-freezing of melt water when drainage was impeded by piles of plowed snow.

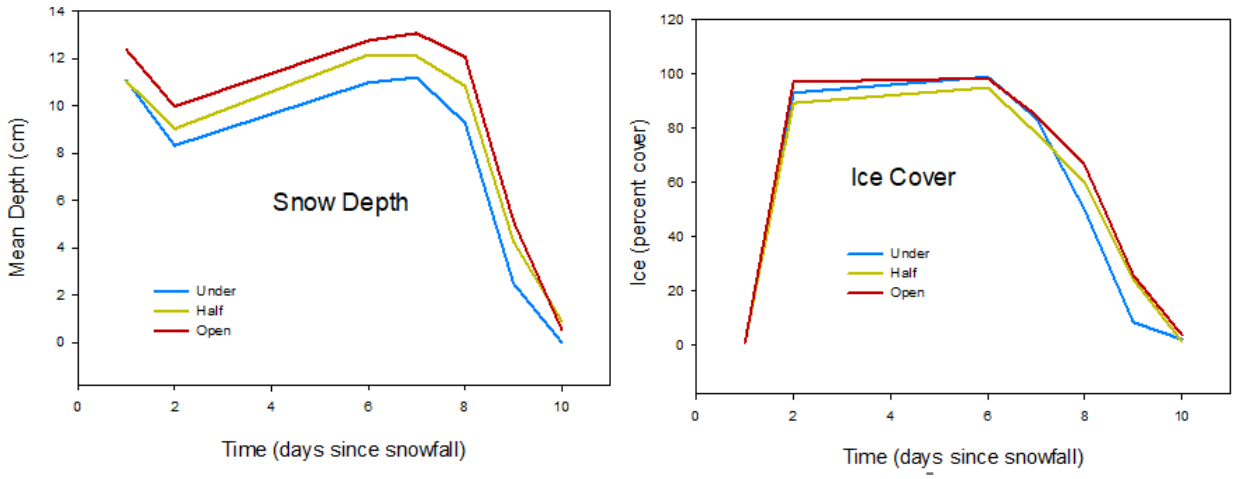


***Figure 6. Snow Depth and Ice Cover on Pavement Under and Adjacent to Tree Canopies. Left: Snow depth; Right: Ice cover. (1 cm = 0.39 in).***

### 4.2 Small Plot Study on Effects of Tree Canopy on Pavement Condition.

This section presents an abridged version of the research work performed at the *small plot level* to determine how the total road environment, including tree canopy, affects the condition of the pavement beneath. A detailed presentation of the analysis can be found in Appendix B.

#### 4.2.1 Methods

*Study Sites*

Pavement condition was assessed at 75 sites in rural Athens County, Ohio. Sites were standardized to a pavement age of 10 to 12 years to ensure comparability between sites and to allow maximum opportunity for pavement degradation. All sites were surfaced with the original asphalt concrete; sites showing evidence of surface amendments such as chip-seal or patching were avoided. At each site, three 6.6 ft × 6.6 ft (2m × 2m) permanent experimental plots were established to allow comparison between canopy conditions – "under" plots (>95% canopy); "partial" plots (45% to 55% canopy), and "open" plots (no canopy). All three plots were situated on the same section of pavement.

*Data*

At each small plot, 14 variables related to roadway, canopy, and pavement condition were collected including:

- Roadway parameters
  - width,
  - proximity of plot to pavement edge, elevation of the pavement surface above soil at the edge (Dropoff),
  - cross-slope (Camber); and location of plot within any curvature,
  - location in the larger landscape (Landscape); assigned to one of five categories: "upland", "high slope", "mid slope", "low slope", and "flood plain" and
  - soil compaction; measured just outside the pavement edge.

- Canopy related parameters
    - tree size (Diameter),
    - number of trunks (Number) > 4 in (100 mm) diameter within 33 ft (10 m) of the plot,
    - position of tree (Nearest); in terms of distance from the plot to the nearest trunk > 4 in (100 mm) diameter, and
    - species identity of the nearest tree.
- Pavement condition parameters
    - texture (SUBJ); quantified as a visual estimate based on Ohio DOT PCR,
    - mean texture depth (MTD); volumetric method of measuring pavement texture (ASTM E965-96),
    - crack presence (Presence), and
    - total length (Length) of crack in each plot.

### 4.2.2 Results

The Width, Camber (local cross-slope), and edge Dropoff of rural roads was significantly related to their landscape position. Roads tended to be wider at mid-slope than at low-slope or floodplain positions (Kruskal-Wallis, $\chi^2 = 11.791$, $p = 0.018$); slope sites had a slightly greater drop-off at the pavement edge than uplands or flood plains ($\chi^2 = 13.015$, $p = 0.011$), and floodplain roads showed substantially less camber than any other landscape position ($\chi^2 = 45.971$, $p = 0.000$). Soil was significantly softer at mid slope than in other landscape positions ($\chi^2=12.238$, $p=0.016$). Landscape position did not affect the proximity of roadside trees, nor their size, stem density, or openness of the tree canopy (probabilities > 0.10).

Twenty-two tree species were encountered as "nearest trees", with strong representation of sugar maple (*Acer saccharum)* (27 plots), black walnut (*Juglans nigra*) (21 plots), and hickory (*Carya* spp.) (18 plots). Species identity did not correspond with variation in any other environmental variable (Kruskal-Wallis probabilities > 0.10).

Pavement was significantly more degraded in road plots than bike path plots, which carried no car or truck traffic, in every measure of pavement condition except Crack length (Table 1).

***Table 1. Comparison of pavement conditions at road and bike path (no-traffic) sites in Athens County, Ohio. Numbers indicate mean, standard deviation, and median. Comparison by Kruskal-Wallis test except in the case of Crack presence/absence, which is compared to pavement type by a $\chi^2$ test.***

| Pavement measure | | Road sites | Bike path sites | $\chi^2$ | p |
|---|---|---|---|---|---|
| **Subjective** | mean | 3.114 | 2.164 | 72.33 | 0 |
| | std.dev. | 0.461 | 0.347 | | |
| | median | 3 | 2 | | |
| **Mean Texture Depth (mm)** | mean | 4.37 | 2.78 | 53.592 | 0 |
| | std.dev. | 1.35 | 0.34 | | |
| | median | 4.04 | 2.74 | | |
| **Mean Texture Depth (in)** | mean | 0.172 | 0.109 | 53.592 | 0 |
| | std.dev. | 0.053 | 0.013 | | |
| | median | 0.159 | 0.108 | | |
| **Crack presence (%)** | | 58.3 | 24.2 | 10.553 | 0.0012 |
| **Crack length (m)** | mean | 2502.02 | 33.29 | 0.559 | 0.3856 |
| | std.dev. | 23528.83 | 24.15 | | |
| | median | 38.32 | 34.07 | | |
| **Crack length (ft)** | mean | 8208.73 | 109.22 | 0.559 | 0.3856 |
| | std.dev. | 77194.32 | 79.23 | | |
| | median | 125.72 | 111.78 | | |

Pavement condition differed significantly according to nearest tree species. The subjective PCR-derived index was highest near white oak (*Quercus alba*) and lowest near box elder (*Acer negundo*) (Kruskal-Wallis $\chi^2 = 14.289$, $p = 0.075$) although the median difference was only 0.6 on a scale of 1.0 to 5.0. MTD returned the highest values (greatest degradation) near hickory (*Carya* spp.) and lowest near box elder (*Acer negundo*) ($\chi^2 = 19.786$, $p = 0.011$). Road curvature, did not significantly affect any measure of pavement condition (probabilities > 0.05).

Within each road site, pavement condition differed between canopy openness classes (Table 2). Canopy openness class significantly separated plots on the basis of the subjective (PCR derived) index (Subj; Kruskal-Wallis $\chi^2 = 24.017$, $p = 0.000$) with significantly higher values (more degraded pavement) in Under plots than either Open or Partial plots. However, the difference was minor (a median difference of 0.2 on a scale of 1.0 to 5.0). MTD showed greater depth under a tree canopy implying greater degradation, although the separation of median values between treatments was only 8.5% ($\chi^2 = 7.652$, $p = 0.022$). Cracks were marginally more common in Under plots (68%) than in Partial (48%) or Open (59%). However, total crack length was not significantly distinguishable between the canopy treatments.

***Table 2. Pavement condition under tree canopies at 162 rural road plots in Athens County, Ohio. Plots are >95% covered by leafy foliage (Under), 45-55% covered (Partial), and 0-5% covered (Open). Numbers show (top to bottom) mean value, standard deviation, and median, except in the case of Crack Presence/Absence. Highest values in each category are highlighted.***

| Pavement | Under | Partial | Open |
|---|---|---|---|
| **Subjective** | | | |
| Mean | 3.260 | 3.166 | 2.921 |
| Std dev | 0.457 | 0.457 | 0.408 |
| Median | 3.2 | 3.0 | 3.0 |
| CV | 0.140 | 0.144 | 0.140 |
| **Crack length (m)** | | | |
| Mean | 48.88 | 57.06 | 89.67 |
| Std dev | 57.97 | 48.58 | 83.27 |
| Median | 28.66 | 47.96 | 60.53 |
| CV | 1.186 | 0.851 | 0.929 |
| **Crack length (ft)** | | | |
| Mean | 160.37 | 187.20 | 294.19 |
| Std dev | 190.19 | 159.38 | 273.20 |
| Median | 94.03 | 157.35 | 198.59 |
| CV | 1.186 | 0.851 | 0.929 |
| **Crack presence (percent)** | | | |
| Present | 66.7 | 47.3 | 55.8 |
| **Mean Texture Depth (mm)** | | | |
| Mean | 4.726 | 4.212 | 4.158 |
| Std dev | 1.494 | 1.249 | 1.137 |
| Median | 4.366 | 4.033 | 4.023 |
| CV | 0.3161 | 0.2965 | 0.2734 |
| **Mean Texture Depth (in)** | | | |
| Mean | 0.1861 | 0.1658 | 0.1637 |
| Std dev | 0.0588 | 0.0492 | 0.0448 |
| Median | 0.1719 | 0.1588 | 0.1584 |
| CV | 0.3161 | 0.2965 | 0.2734 |

Best models for each pavement-condition metric are listed in Table 3. The subjective index was strongly dependent on canopy openness, with higher values in more open plots suggesting less degraded pavement under a closed tree canopy. Curvature and Opposite slopes also contributed although weakly. However, median values in Under plots are only 6.7% greater than Open plots demonstrating only a minor difference in pavement condition.

Crack presence was positively affected by soil compaction, suggesting that a harder substrate is more likely to cause cracking; crack length appeared to respond to edge drop-off (more cracking at plots with a greater drop). Crack length was strongly dependent on

environmental variation within sites (only 8.8% attributed to variation between sites). In contrast, Crack presence was strongly influenced by variation between sites (52.5% between).

Mean Texture Depth (MTD) responded only to canopy openness (Table 3), showing shallower crevices under an open sky consistent with Table 2. It is notable that substantially greater variation was accounted for by site than canopy condition implying a relatively weak canopy contribution (Table 3); the difference between median values in Under and Open plots was only 8.5%.

It is important to note that these results are strongly influenced by the inclusion of plots having >95% canopy cover; little difference was observed between plots with partial cover (40-60% cover) and plots open to the sky (<10% cover). Although the natural frequency of canopy cover was not quantified, two important observations emerge: First, >90% canopy cover is rare on rural roads, even in road sections running through forests (40-60% cover is much more common in forests). Thus, the actual effect of tree canopy on rural pavement condition is negligible.

***Table 3. Best-fit regression models for four metrics of pavement condition at rural road sites in Athens County, Ohio. Mixed models with "site" as a random effect. Predictor variables are centered and scaled, allowing comparison of coefficients. Only predictor variables with coefficients > the respective standard errors are shown. Significance of predictor variables is tested by likelihood comparisons.***

| Pavement | Predictor | Coefficient | Test statistic | Probability |
|---|---|---|---|---|
| **MTD** | **Intercept** | 0.437 | | |
| Site 56.9% of variance | **Open** | -0.0232 | $\chi^2 = 6.858$ | 0.0088 |
| **Crack length (log)** | **Intercept** | 8.069 | | |
| Site 8.8% | Edge | -0.23 | $\chi^2 = 2.469$ | 0.1161 |
| | **Dropoff** | -0.25 | 3.098 | 0.0784 |
| | Penmin | 0.177 | 1.938 | 0.1639 |
| | Opposite | 1.097 | 1.097 | 0.295 |
| | Diameter | -1.889 | 1.688 | 0.1878 |
| **Crack presence** | Intercept | 0.393 | t = 1.617 | 0.1059 |
| Site 52.5% | Open | -0.357 | 1.61 | 0.1073 |
| Binomial | Edge | 0.164 | 0.725 | 0.4683 |
| | **Penmin** | 0.473 | 1.985 | 0.0471 |
| | Dropoff | -0.273 | 1.207 | 0.2275 |
| | Diameter | -0.195 | 0.902 | 0.3669 |
| **Subjective (PCR derived)** | **Intercept** | 3.133 | | |
| Site 46.4% | **Open** | -0.104 | $\chi^2 = 11.596$ | 0.0007 |
| | Curvature | 0.045 | 2.085 | 0.1488 |
| | Opposite | 0.048 | 1.617 | 0.2035 |
| | Adjacent | 0.038 | 1.225 | 0.2684 |
| | Edge | -0.054 | 2.577 | 0.1084 |

Second, canopy density changes on a scale of a few yards or meters. Thus, canopy density measurements at a single point on a rural road cannot be generalized over tens or hundreds of yards of road; an accurate description of the tree canopy must include individual canopy measurements every 5-10 yards (5-10 m).

### 4.3 Road Section Study on Effects of Tree Canopy on Pavement Microclimate.

This section presents an abridged version of the research work performed on *road sections* to determine how small plot results scale up to actual management units. A detailed presentation of this research work can be found in Appendix C.

#### 4.3.1 Methods

*Study Sites*

Test road sections were confined to the eastern part of the state of Ohio and specifically to Ohio DOT Districts 5, 9, 10, 11, and 12. These Ohio DOT districts were selected due to (i) the climatic variations and precipitation levels, (ii) their proximity to the Ohio University Athens campus, and (iii) the perceived abundance of tree canopied roads. A total of 39 roadway segments were selected as test sites. These sites were selected first using GIS records of roadways and tree canopies, discussions of candidate sites with local Ohio DOT personnel with knowledge of the sites, and examination of sites via PathWeb (Ohio DOT's digital photolog). Canopied sections were verified by field inspection before final selection.

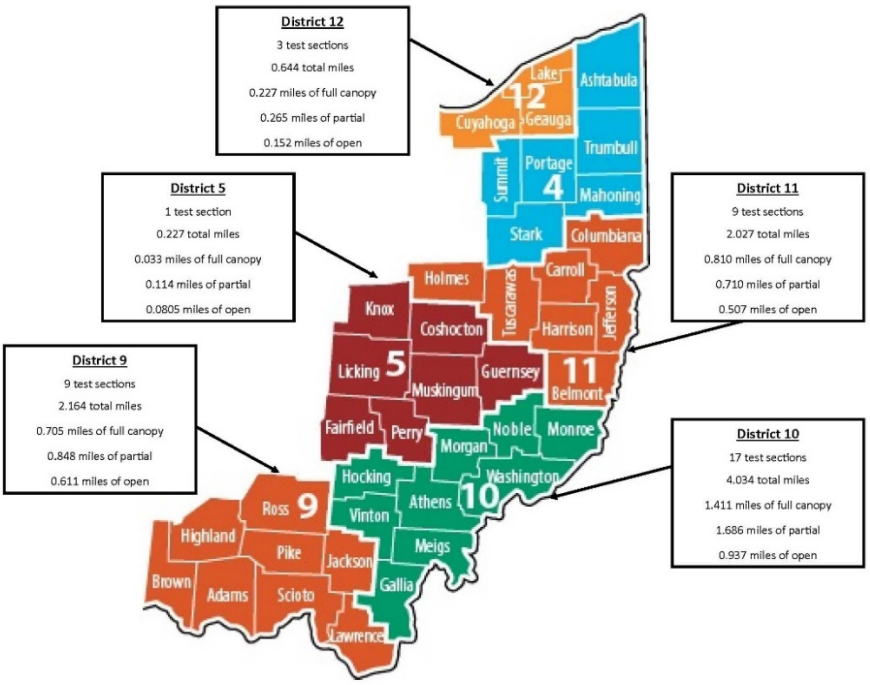


***Figure 7. Summary of Selected Test Locations in Ohio DOT Districts 5, 9, 10, 11, and 12.***

Each test site comprised a roadway segment with portions that had no canopy, had partial canopy, and had full canopy. Note that test segments were of different lengths and depended on the amount of tree canopy present. Figure 7 depicts the Ohio DOT Districts considered in this research study and information on the selected test segments including number of sites, total mileage, "under" (full) canopy mileage, "partial" canopy mileage and "open" (no canopy) mileage.

*Data*

- Pavement moisture: measured using an instrumented vehicle with GPS driven along each test segment at approximately 15 mph (24 km/h) or below and collected data every second in both directions of travel. The data were collected within 24 hours after a rain event and also includes date and time information; location information (latitude/longitude); condition of roadway (i.e., dry, wet, icy); pavement surface temperature (in °C at an accuracy of ±0.8°C (±1.4°F) at 0°C (32°F)); presence of moisture (film height) to an accuracy of 10%; and coefficient of friction of the pavement surface.
- Pavement temperature: measured along test segments with the MARWIS and a FLIR E6 infrared camera. With the FLIR E6 camera, measurements were at 25 ft (7.6 m) intervals along the center of each lane for each segment.

### 4.3.2 Results

*Pavement Moisture.*

In general, the results from Kruskal-Wallis H tests indicated that for over half of the test sites, there were statistically significant differences in moisture film height between open, partial, and full canopy sections. Additionally, some specific general conclusions based on results from Mann-Whitney U tests with Bonferroni correction include the following:

(a) difference in moisture levels between partial canopy and open (no canopy) sections was on average +3.88 µm (0.15 mil);
(b) difference in moisture levels between full canopy and open (no canopy) sections was on average +4.42 µm (0.17 mil); and
(c) difference in moisture levels between full canopy and partial canopy sections was on average +1.50 µm (.06 mil).

Note that the statistical testing was performed on the moisture data as individual sites, aggregated by Ohio DOT Districts, and for ALL sites; the results provided above were consistent. Additionally, observations of time lapse videos from sites on US-56 and US-374 showed that pavement under full canopy stayed wet for a longer time (approximately 6 to 7 hours) after a rain event relative to areas without a tree canopy.

*Temperature.*

In general, pavement surface temperatures were higher in open canopy compared to under both partial and full canopy. More specific conclusions based on the results include:

(a) difference in temperature levels between open (no canopy) and partial canopy sections was on average +3.29°F (+1.83°C),

(b) difference in temperature levels between open (no canopy) and full canopy sections was on average +5.09°F (+2.83°C), and
(c) difference in temperature levels between partial canopy and full canopy sections was on average +1.97°F (+1.09°C).

Note that the statistical testing was performed on the moisture data as individual sites, aggregated by Ohio DOT Districts, and for ALL sites; the results provided above were consistent.

### 4.4 Road Section Study on Effects of Tree Canopy on Pavement Condition.

This section presents an abridged version of the research work performed on *road sections* to determine how small plot results scale up actual management units. A detailed presentation of the research work can be found in Appendix C and Appendix D.

#### 4.4.1 Methods

*Study Sites*

The set of study sites included in this analysis was that used in the microclimate analysis as noted in Section 4.3.1 above.

*Data*

- Pavement condition rating (PCR): measured in accordance with the Ohio DOT PCR manual [Ohio DOT, 2006]. For each test segment, the pavement was rated by direction and by canopy coverage level (i.e., PCR (by direction) for the "under", "partial", and "open" canopy portions,
- Density (air voids): extracted from pavement cores in accordance with AASHTO T269 and ODOT 1036 specifications,
- Tensile strength ratio (TSR): extracted from pavement cores in accordance with AASHTO T283 and Ohio DOT S1051 specifications, and
- Mass Loss (ML): extracted from pavement cores using Cantabro test in accordance with AASHTO TP108 specifications.

#### 4.4.2 Results

*Pavement Condition Rating.*

The overall results, based on the directional average PCR values from all 38 sites, indicated there were no discernable differences in PCR between canopy levels as depicted in Table 4. By ODOT standards, these average PCR values all translate to a "GOOD" rating (i.e., 75 ≤ PCR < 90 = GOOD).

***Table 4. Descriptive statistics on PCR data.***

| Canopy Level | N | Mean | Median | Std. Deviation |
|---|---|---|---|---|
| Open | 76 | 86.13 | 85.59 | 8.49 |
| Partial | 76 | 84.23 | 84.86 | 9.12 |
| Full | 76 | 83.41 | 83.63 | 9.35 |

These ratings were analyzed further (refer to Horn [2019]), and the following conclusions were drawn:

(a) there was no statistically significant difference in PCR values between the different canopy levels (Kruskal-Wallis $\chi^2$ (2) = 3.298, $p$= 0.193) with a mean rank PCR value of 125.23 for open, 111.91 for partial; and 106.36 for full.
(b) based on PCR values alone, the open (no canopy) sections of roadway ranked higher than partial canopy sections; and both ranked higher than full canopy sections of roadway.

*Density (Air Voids).*

The average densities and air voids for both canopy and no-canopy sections are shown in Table 5. The average density under canopy was found to be higher (and more consistent), 92.5%, than for no canopy, 94.1%.

***Table 5. Density (air voids) test results.***

| Type | Number of Samples | Average Density (%) | Average Air Voids (%) | Std Dev (%) | Std Error | CoV (%) |
|---|---|---|---|---|---|---|
| Canopy | 9 | 92.5 | 7.5 | 1.4 | 0.5 | 19.2 |
| No Canopy | 11 | 94.1 | 5.9 | 2.6 | 0.8 | 43.1 |

*Tensile Strength Ratio.*

The tensile strength, average conditioned (dry) and unconditioned (wet) tensile strength and TSR values for the canopy and no-canopy sections are summarized in Table 6. Cores from pavement under canopy exhibited higher susceptibility to moisture damage (TSR = 0.71) than the cores from pavement under no-canopy conditions (TSR = 0.85). Figure 8 depicts the

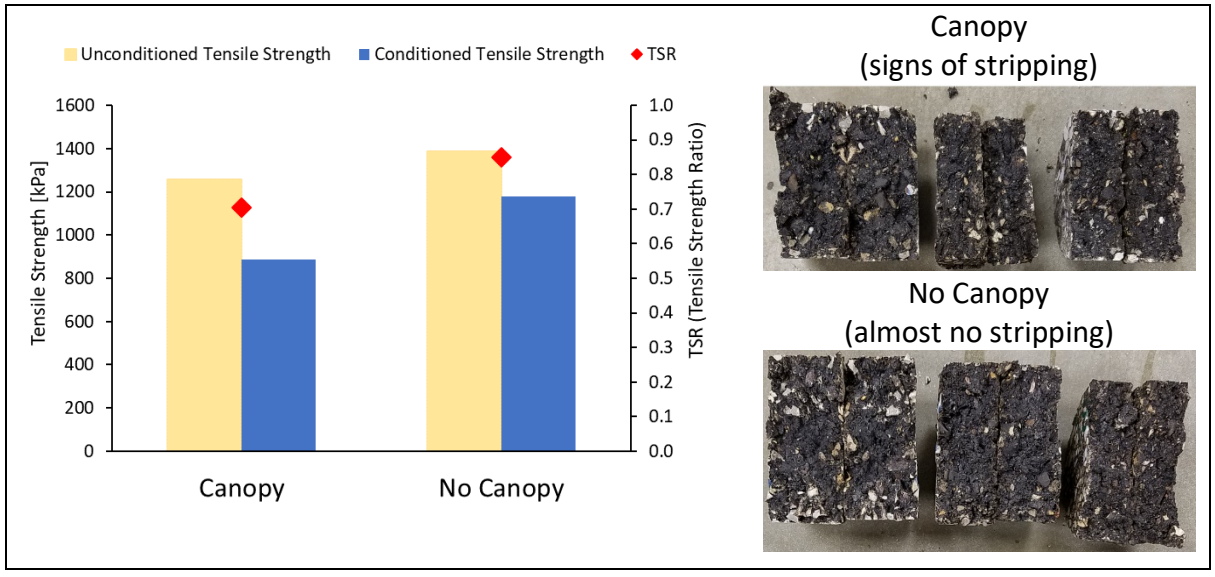


***Figure 8. Tensile Strength and TSR Values for Canopy and No-canopy Conditions.***

unconditioned indirect tensile strength, which was found, as expected, to be on average higher where exposure to moisture was minimized (i.e. no-canopy sections). Additionally, visual inspection of the specimens revealed the presence of stripping (physical separation of the asphalt cement and aggregate surface) where tree canopy is present.

***Table 6. Moisture susceptibility TSR test results. SI units at top and English units below.***

| Moisture condition | Sample ID | Density (%) | Average density (%) | Air voids (%) | Average air voids (%) | Thickness (mm) | Diameter (mm) | Maximum Load (N) | Tensile strength (kPa) | Average tensile strength (kPa) | TSR |
|---|---|---|---|---|---|---|---|---|---|---|---|
| Dry | 7 | 92.8 | 93.3 | 7.2 | 6.7 | 33.1 | 100.4 | 7784.7 | 1490.6 | 1255.7 | 0.71 |
| | 11 | 94.6 | | 5.4 | | 39.2 | 100.4 | 6142.3 | 992.9 | | |
| | 16 | 92.5 | | 7.5 | | 33.1 | 100.3 | 6691.1 | 1283.5 | | |
| Wet | 4 | 94.5 | 93.6 | 5.5 | 6.4 | 43.4 | 100.4 | 7126.5 | 1042.7 | 885.9 | |
| | 10 | 91.2 | | 8.8 | | 29.3 | 100.4 | 2970.1 | 642.2 | | |
| | 12 | 95.1 | | 4.9 | | 32.4 | 100.2 | 4965.7 | 972.9 | | |
| Dry | 1 | 97.2 | 95.0 | 2.8 | 5.0 | 33.5 | 100.4 | 9242.8 | 1751.9 | 1386.7 | 0.85 |
| | 8 | 90.8 | | 9.2 | | 30.8 | 100.1 | 6255.7 | 1293.1 | | |
| | 14 | 97.1 | | 2.9 | | 34.9 | 100.5 | 6146.4 | 1115.2 | | |
| Wet | 2 | 98.6 | 94.5 | 1.4 | 5.5 | 42.6 | 100.2 | 11560.1 | 1722 | 1177.6 | |
| | 17 | 91.5 | | 8.5 | | 36.3 | 100.8 | 6375.2 | 1109.3 | | |
| | 18 | 93.5 | | 6.5 | | 28.9 | 100.3 | 3192.5 | 701.5 | | |

| Moisture condition | Sample ID | Density (%) | Average density (%) | Air voids (%) | Average air voids (%) | Thickness (in) | Diameter (in) | Maximum Load (lb) | Tensile strength (kPa) | Average tensile strength (kPa) | TSR |
|---|---|---|---|---|---|---|---|---|---|---|---|
| Dry | 7 | 92.8 | 93.3 | 7.2 | 6.7 | 1.30 | 3.95 | 1750 | 216.2 | 182.1 | 0.71 |
| | 11 | 94.6 | | 5.4 | | 1.54 | 3.95 | 1381 | 144.0 | | |
| | 16 | 92.5 | | 7.5 | | 1.30 | 3.95 | 1504 | 186.2 | | |
| Wet | 4 | 94.5 | 93.6 | 5.5 | 6.4 | 1.71 | 3.95 | 1602 | 151.2 | 128.5 | |
| | 10 | 91.2 | | 8.8 | | 1.15 | 3.95 | 668 | 93.1 | | |
| | 12 | 95.1 | | 4.9 | | 1.28 | 3.94 | 1116 | 141.1 | | |
| Dry | 1 | 97.2 | 95.0 | 2.8 | 5.0 | 1.32 | 3.95 | 2078 | 254.1 | 201.1 | 0.85 |
| | 8 | 90.8 | | 9.2 | | 1.21 | 3.94 | 1406 | 187.5 | | |
| | 14 | 97.1 | | 2.9 | | 1.37 | 3.96 | 1382 | 161.7 | | |
| Wet | 2 | 98.6 | 94.5 | 1.4 | 5.5 | 1.68 | 3.94 | 2599 | 249.8 | 170.8 | |
| | 17 | 91.5 | | 8.5 | | 1.43 | 3.97 | 1433 | 160.9 | | |
| | 18 | 93.5 | | 6.5 | | 1.14 | 3.95 | 718 | 101.7 | | |

*Cantabro Mass Loss.*

The individual and average mass loss percentage (M.L.%) are presented in Table 7. In addition, Figure 9 depicts a comparison of the M.L.% against test duration for both canopy conditions. After 100 revolutions, the samples from canopy sections began to disintegrate much faster than samples from the no-canopy (open) sections. After 300 revolutions, the average mass loss was larger (69.8%) for the mixture under tree canopy than for the mixture in the no-canopy (open) section (33%). Figure 9 also shows the core remnant from the canopy section (residual) is much less than that from the no-canopy (open) section.

***Table 7. Cantabro mass loss test results.***

| Type | Sample ID | Density (%) | Average Density (%) | Air Voids (%) | Average Air Voids (%) | Thickness (mm) | Number of Revolutions | | | Average Mass Loss (%) |
|---|---|---|---|---|---|---|---|---|---|---|
| | | | | | | | 100 | 200 | 300 | |
| | | | | | | | Mass Loss (%) | | | |
| Canopy | 15 | 92.2 | 92.2 | 7.8 | 7.8 | 55.4 | 9.1 | 27.1 | 65.5 | 69.8 |
| | 9 | 92.2 | | 7.8 | | 46.9 | 33.0 | 64.7 | 74.1 | |
| No Canopy | 5 | 94.3 | 95.8 | 5.7 | 6.2 | 55 | 8.4 | 19.4 | 29.3 | 33.0 |
| | 19 | 93.2 | | 6.8 | | 41.4 | 24.7 | 32.9 | 36.6 | |

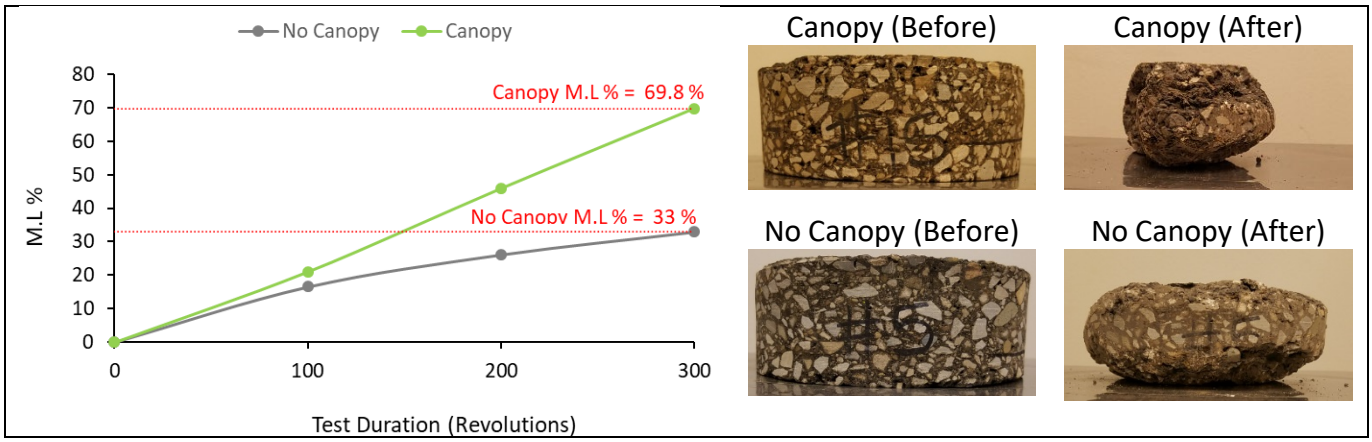


***Figure 9. Cantabro Mass Loss (M.L.%) for Canopy and No-canopy Conditions.***

### 4.5 Road Section Study on Effects of Tree Canopy on Safety.

Safety impacts from tree canopies were evaluated by comparing safety data before and after tree maintenance operations and by assessing surrogate safety measures. Full details of the safety assessment are in Appendix C.

#### 4.5.1 Methods

*Study Sites*

The before-after safety analysis performed for this project included 46 low-volume road segments in Ohio DOT Districts 4, 5, 9, 11, and 12 in Eastern Ohio at which tree related

maintenance operations had been performed, based on available records from Ohio DOT. The surrogate measures were obtained at study sites on SR 356 (Vinton County), SR 56 (Hocking County), and SR 374 (Hocking County), all in District 10.

*Data*

- Traffic crash data from 2009-2018 were obtained from Ohio DOTs GCAT system.
- Traffic volume data (per year) for the entire before-after study period were obtained from the Traffic Monitoring Management System.
- Roadway design elements, such as lane widths, shoulder widths, horizontal/vertical alignment parameters etc. were obtained using Google Earth and AutoCAD Civil 3D.
- Driver behavior, such as travel speeds and braking operations were measured as vehicles were observed travelling through study segments.

### 4.5.2 Results

*Before-After Crash Analysis.*

The results from a naïve analysis (i.e., basic comparison of observed crashes in before and after periods), showed an overall decrease in average crashes – approximately 23% for all crash types – attributed to tree maintenance (trimming/pruning). An Empirical Bayes analysis produced mixed findings, with 39 locations exhibiting safety improvements and 7 locations indicating no improvement in safety. Detailed results from the analysis are provided in Appendix C. The composite (project level) analysis found an overall 11% deterioration in safety at locations where tree maintenance operations (trimming/pruning) were performed, but this was not statistically significant at a 95% confidence level (Z-score = -1.43).

*Surrogate Measures of Safety - Speed Data.*

Overall, no discernable differences were observed in the average and 85$^{th}$ percentile speeds between canopy levels and/or day/night conditions. Additionally, a comparison of observed vehicle speeds between full and open canopy sections (see Table 8) indicated mixed findings with the 4 datasets from Hocking County exhibiting significant differences in speeds between canopy levels which the 2 datasets from Vinton County did not have. The datasets with a significant difference in speeds between canopy levels had higher average speeds within the full canopy sections.

Kruskal-Wallis H tests on the speed data under day or night conditions found some statistically significant differences under specific canopy levels for day and night conditions. Despite the statistically significant differences, interpretations cannot be made due to the mixed results. Average speeds were higher at night in some sections, but lower in others, and this is the case both for full canopy and open canopy sites.

***Table 8. Kruskal-Wallis H test results (speed by canopy level).***

| County | Route | Direction | Canopy | N | Mean Rank | Kruskal-Wallis H | Asymp. Sig. (p-value) |
|---|---|---|---|---|---|---|---|
| Vinton | SR 356 | NB | Open | 66 | 187.29 | 1.59 | 0.207 |
| | | | Full | 341 | 207.23 | | |
| | | SB | Open | 71 | 236.64 | 0.41 | 0.522 |
| | | | Full | 383 | 225.81 | | |
| Hocking | SR 56 | EB | Open | 1374 | 1062.66 | 422.81 | 0.000* |
| | | | Full | 1371 | 1684.02 | | |
| | | WB | Open | 1530 | 1302.16 | 200.69 | 0.000* |
| | | | Full | 1524 | 1753.73 | | |
| | SR 374 (3) | NB | Open | 3822 | 4094.88 | 106.18 | 0.000* |
| | | | Full | 3845 | 3574.68 | | |
| | | SB | Open | 3908 | 3835.69 | 26.44 | 0.000* |
| | | | Full | 3520 | 3579.95 | | |

Note: Routes with numbers in parenthesis correspond to multiple locations on the same route
*statistically significant (α=0.05)

*Surrogate Measures of Safety - Braking Data.*

Braking data were collected in both directions of travel from three test locations as drivers traveled through a section of tree-lined roadway during the fall (no leaves on trees) and during the spring (leaves on trees). At each test location, video cameras (placed at 200 ft (60 m) and 400 ft (120 m)) were used to observe the tail-lights for vehicles and subsequently assess if a driver was braking (or not) as he/she traversed the sections of roadway where canopy was present. Table 9 presents results from logistic regression analysis on the observed data. The results indicated mixed findings: Half (four) of the data sets indicated drivers are *more likely* to not brake when there is no canopy (no leaves on trees) and four other datasets indicating drivers are *less likely* to not brake when there is no canopy (no leaves on trees).

***Table 9. Results from braking analysis.***

| Leaves Present? | Number of Days monitored | Braking | No Braking | Odds Ratio | Percentage Braking | Percentage Not Braking |
|---|---|---|---|---|---|---|
| 400 ft (120 m) South of Full Canopy on SR 356 in Vinton County | | | | | | |
| Yes (spring) | 6 | 23 | 358 | 1.63 | 6% | 94% |
| No (autumn) | 5 | 23 | 219 | | 10% | 90% |
| 200 ft (60 m) South of Full Canopy on SR 356 in Vinton County | | | | | | |
| Yes (spring) | 5 | 8 | 307 | 2.59 | 3% | 97% |
| No (autumn) | 7 | 18 | 267 | | 6% | 94% |
| 200 ft (60 m) North of Full Canopy on SR 356 in Vinton County | | | | | | |
| Yes (spring) | 4 | 3 | 163 | 0.86 | 2% | 98% |
| No (autumn) | 6 | 4 | 253 | | 2% | 98% |
| 400 ft (120 m) North of Full Canopy on SR 356 in Vinton County | | | | | | |
| Yes (spring) | 4 | 3 | 408 | 7.68 | 1% | 99% |
| No (autumn) | 6 | 14 | 248 | | 5% | 95% |
| 200 ft (60 m) East of Full Canopy on SR 56 in Hocking County | | | | | | |
| Yes (spring) | 5 | 33 | 1229 | 0.3 | 3% | 97% |
| No (autumn) | 4 | 4 | 489 | | 1% | 99% |
| 400 ft (120 m) West of Full Canopy on SR 56 in Hocking County | | | | | | |
| Yes (spring) | 5 | 199 | 867 | 0.19 | 19% | 81% |
| No (autumn) | 4 | 26 | 589 | | 4% | 96% |
| 475 ft (145 m) South of Full Canopy on SR 374(3) in Hocking County | | | | | | |
| Yes (spring) | 2 | 43 | 387 | 0.17 | 10% | 90% |
| No (autumn) | 4 | 20 | 1037 | | 2% | 98% |
| 400 ft (120 m) North of Full Canopy on SR 374(3) in Hocking County | | | | | | |
| Yes (spring) | 2 | 40 | 586 | 1.43 | 6% | 94% |
| No (autumn) | 3 | 34 | 349 | | 9% | 91% |

## 5.0 RESEARCH FINDINGS

- Tree canopies do affect the microclimate beneath them, and shading does cause temperature differentials between the pavement surface beneath the canopy and the pavement surface exposed to the open sky. Ordinary heating was substantial, leading to a 52 to 61°F (29 to 34°C) diurnal variation of exposed pavement; in contrast, pavement under-canopy only experienced a 11 to 25°F (6 to 14°C) thermal cycling. The temperature differentials due to varying canopy levels have the potential to cause pavement cracking.
- Tree canopies delay the onset of wetting in convective summer rain showers and reduce total wetness for up to 30 minutes accounting for most summer rain events in southeastern Ohio. The amount of rain retained in the foliage depends on the species of the tree, its size, and branching structure. Also, it may take up to 7 hours longer for pavement to dry under overhanging tree canopies. On average, the water-film height on pavement under canopy was +4.42 µm (0.17 mil) more than that for open sky pavement with no canopy overtop. Open sky pavement generally showed concave drying curves suggesting immediate and rapid drying on exposure to direct sunlight, while canopy covered pavement dried slowly at first (convex curves). While there are differences in moisture amounts between canopy coverage levels, in practice these differences are negligible. With moisture levels well below 0.1 in (2.5 mm), there is a very small likelihood of drivers hydroplaning and subsequently impacting safety.
- The branches of deciduous trees blocked snowfall in our trial even though no leaves were present (median 12.9% lower under trees). Ice cover and persistence on pavement appeared to be unrelated to adjacent trees. Instead, most ice was generated by compaction of snow under car tires or by nocturnal freezing of meltwater in puddles.
- Incidental observations on the small plots during drying rate experiments indicated that pavement drainage (slope and surface texture) has much more of an effect on drying rate than absence of canopy.
- Pavement damage under the three canopy coverage levels showed statistically significant differences in terms of pavement condition rating (PCR) and mean texture depth (MTD). However, differences between canopy conditions were modest (<10%) and only evident under 95% canopy cover, a rare condition on rural roads. Canopy-covered pavement had lower values of MTD indicating less damage to the surface under trees. Crack length showed no relationship to tree cover. At the scale of road sections, no significant difference in PCR was detected with canopy cover.
- An analysis of pavement cores collected from road sections under canopy have lower density (more air voids) and are more susceptible to moisture damage (showing lower TSR values and more signs of stripping in the mixture) and degradation (showing larger percentage of Cantabro mass loss) than cores from road sections in open sky (no canopy). As such the average density, TSR, and average mass loss for canopy sections were 92.5%, 0.71, and 69.8%, respectively. By contrast, for open sky (no canopy) sections the average density, TSR, and average mass loss were 94.1%, 0.85, and 33%, respectively. However, these data were collected from a very limited number of sites.
- There was no correlation of tree location or proximity with pavement damage, providing no support for the idea that root penetration causes pavement degradation. Given the very

small differences in amount of pavement distress between sections with different levels of canopy cover, it is evident that the pavement distress is generally due to non-canopy related causes. Pavement distress may be due to a variety of other factors such as poor road design, poor construction, traffic loading, etc. which are beyond the scope of this study.

- Using available crash data, the safety analysis indicated that a composite (project) level view of roadside maintenance activities (i.e., trimming/pruning of trees) does not provide safety benefits. However, individual sites showed mixed results with 39 locations exhibiting safety improvements while seven locations had no improvement in safety.
- The analysis of surrogate measures of safety (vehicle speed and braking operations) did not provide any conclusive findings.

## 6.0 RECOMMENDATIONS FOR IMPLEMENTATION OF RESEARCH FINDINGS

Based on the findings of this research project, including the arborist's perspective in Appendix F, the following recommendations are suggested:

1. Tree canopies should not be removed along Ohio's rural routes as a routine management practice as means of preventing damage to pavement. Cutting should **only** be done on **individual** trees and in the following circumstances:

   a. There is >90% **measured** canopy cover and **measurable** pavement degradation.

   b. Dead or decayed individual trees threaten to fall in the road.

   c. Cutting should not be applied over sections longer than 10 to 20 yards (10 to 20 m). Because canopy density varies greatly on a fine scale, Canopy density should be re-measured every 10 yards (10 m).

   d. Maintenance crews should carry simple instruments (e.g. canopy densiometers) allowing them to make on-the-spot measurements of canopy density to guide cutting decisions.

   A hemispherical densiometer is an appropriate canopy measurement instrument.

2. The incidental relationship observed between drainage, ice, and traffic suggests drainage maintenance and snow removal are more important to minimizing moisture damage on a pavement surface than is tree maintenance. Scheduled routine or seasonal inspection and cleaning of culverts and drainage features should continue per usual practice. While it is beyond the scope of this project, the value of drainage maintenance and plowing should be assessed in future research.
3. It is necessary to consider using asphalt mixes which are not susceptible to stripping when paving on tree canopied roads.
4. Trees should be maintained to ensure safety in specific locations, i.e. in spots where trimming provides unobstructed sight distance, sign visibility, and enhanced margin of safety for errant vehicles. In locations where the right-of-way or lines of sight are limited (e.g. embankments, hills, curves and dips, and residential areas), branches should be

trimmed to provide vertical top-bottom clearance at a minimum 14.5 ft (4.4 m) and a desirable clearance of 16.5 ft (5.0 m) and at least 4.5-ft (1.4 m) horizontal clearance from the edge of the roadway (white line). It should be noted that any trimming/pruning work should be limited to the specific areas where a safety problem can be demonstrated.

**REFERENCES**


Horn, A.L. (2019) *Assessment of Tree Canopy Effects Overtop Low Volume Roadways*, Master of Science Thesis (Unpublished), Department of Civil Engineering, Ohio University, Athen, OH, August 2019.

Lohr, V.I., et al. (2004) How Urban Residents Rate and Rank the Benefits and Problems Associated with Trees in Cities. *Journal of Arboriculture* 30: 28-35.

Naik, B., et al. (2017) *Effects of Tree Canopy on Pavement Condition, Safety, and Maintenance: Phase 1*, Final Report No. FHWA/OH-2017/18 for Ohio Department of Transportation, February 2017. Available online at https://cdm16007.contentdm.oclc.org/digital/collection/p267401ccp2/id/14886

Ohio Department of Transportation (Ohio DOT). (2006) *Pavement Condition Rating Manual*. Ohio Department of Transportation, Office of Pavement Engineering, Columbus, Ohio.

Ohio Department of Transportation (Ohio DOT). (2017) *Effects of Tree Canopy on Pavement Condition, Safety, and Maintenance*. RFP Solicitation, Ohio Department of Transportation, Office of Statewide Planning and Research, Columbus, Ohio.

Wolf, K.L. (2005) Business District Streetscapes, Trees, and Consumer Response. *Journal of Forestry* 103: pp.396-400.

**APPENDIX A: EFFECT OF TREE CANOPY ON PAVEMENT MICROCLIMATE.**


## Abstract

Trees control the ground-level climate under their canopies, and climate is one of the important factors causing decay of asphalt pavement. However, it is not clear how roadside trees influence pavement microclimate or whether trees have the potential to cause or prevent pavement degradation. Most of the few studies on this topic have been done in hot and arid climates; we are aware of very few in wet-temperate climates. Our goal was to precisely document four forms of pavement microclimate and relate them to the size, species, aspect, and canopy coverage of adjacent trees. Twenty-three street-side trees were selected in a residential neighborhood in Athens, Ohio. Trees represented a variety of deciduous species, primarily from the genera *Acer* (maples) and *Quercus* (oaks). Study plots were established in triplets under full canopy coverage, under 45-55% coverage, and under open to the sky as a control condition. Pavement temperature, rainwater accumulation, drying, and accumulation and persistence of snow were documented near individual trees. Pavement temperature cycled diurnally in open-sky plots over a range of 29-34$^{o}$C, but only a range of 6-14$^{o}$C in plots under a canopy. Wetting of pavement under a canopy lagged 25 to 35 minutes behind wetting under an open sky, a delay equivalent to ca. 26% of rain events in the study region. Pavement drying was slower under a tree canopy corresponding to ca. 70% relative to open plots. In each of these metrics, partial-covered plots showed intermediate behavior consistent with the porous nature of the leafy canopy. Ten to twelve percent less snow was observed under the leafless canopy than under open sky areas without trees, and snow melted faster under a tree canopy. Ice was unrelated to canopy openness, but strongly influenced by traffic and drainage. Pavement microclimate did not differ significantly with tree size, aspect, species, or canopy porosity measured in hemispherical photos. We conclude that roadside trees influence pavement microclimate within ranges that potentially impact pavement service life. Some results (temperature, wetting, snow, and ice) suggest tree shading extends pavement service life; other results (drying) imply a reduction in service life. These findings require confirmation by comparison to pavement condition.

## Introduction

Weather is the most important factor controlling degradation of asphalt pavement. The average service life of asphalt pavements before a full-depth reconstruction is required ranges from approximately nine years in regions with wet climates and freezing winter temperatures to 20–40 years in dry regions, a generalization which holds across Asphalt Institute traffic classes I – IV [Boyer et al., 1999]. An extensive body of research in pavement engineering interprets regional differences in terms of the negative effects of ultraviolet radiation, temperature fluctuation, water penetration, and freeze-thaw cycling. A parallel body of research in forest ecology shows that overhanging trees strongly influence the microclimate near the ground, potentially controlling incident solar radiation, wetting in rainstorms, rate of water evaporation, and the deposition and melting of snow. Because trees are common along rural roads and some urban streets it is possible that roadside trees affect the rate of pavement degradation through their control of road surface microclimate. A small number of cross-disciplinary studies appear to support this thesis [McPherson and Muchnick, 2005; Mascaro, 2012] although they predominantly come from warm and dry regions and may not generalize to seasonally wet and cold regions such as Ohio. Our purpose here is to describe the capacity of roadside trees to modify pavement microclimate in a moist-temperate climate showing seasonal variation, and to compare observed values with the ranges shown to cause damage to asphalt pavement in laboratory trials.

*Asphalt pavement*

Climate acts on pavement through mechanical and chemical processes which are potentially influenced by overhanging trees. First, pavement is exposed to solar radiation, sensible as warm pavement on a summer day. Under an open sky, asphalt pavement may absorb 80-95% of incident radiation and reach temperatures as high as 67°C [150°F; Scott et al. 1999; US EPA 2008]. Daytime pavement temperatures above 50°C (122°F) are not unusual, reported from southern Brazil, central Arizona, northern England, southern India, central California, the Netherlands, and southern Australia [respectively, Mascaro, 2012; Golden et al., 2007; Armson et al., 2013; Vailshery et al., 2013; Scott et al., 1999; Klemm et al., 2015; Coutts et al., 2016]. Pavement shows higher surface temperatures than unpaved ground in many studies [e.g. Bowler et al., 2010; Stempihar et al., 2012]. The degree of solar heating is based on properties of the pavement material and its immediate environment including the specific heat capacity of the paving material, the thermal conductivity of the material (the ability to conduct heat away from the heated zone), the surface albedo (the reflectivity of the paving material), ambient humidity and the duration and intensity of solar input, and heat generated by traffic using the pavement [Bowler et al., 2010]. Absorption of solar energy declines with pavement age and traffic abrasion, which tend to increase albedo; after seven years, absorption may be reduced to 80% making the pavement proportionally cooler [Tran et al., 2009].

High temperatures soften the mastic binder potentially leading to rutting, shoving, and bleeding (exudation of binder) with traffic loading [Willway et al., 2008]. Conversely, cool pavement resists softening and deformation under traffic loading, and, so, lasts longer [Cominsky et al., 1994]. Modeling heating effects in the Los Angeles basin, Akbari et al. [2001] predicted that a 10°C (18°F) decrease in pavement temperature could lead to a 25-fold increase in longevity.

Daily solar heating drives a cycle of expansion and contraction which can lead to "fatigue" cracking analogous to fatigue failure in metals [Timm and Voller, 2003; Alavi et al., 2015]. Relative to other paving materials, asphalt shows stronger vertical gradients of temperature and more extreme diurnal fluctuation at the surface [Asaeda and Ca, 1993], which makes it particularly vulnerable to fatigue cracking. Thermal cycling aggravated by traffic loading causes many of the familiar patterns of cracking observed in asphalt pavement (e.g. alligator, longitudinal, transverse, block, reflective, and edge cracking) [Asphalt Institute, 2009]. Using data from Minnesota, Washington, and Virginia, Quiao et al. [2013] applied sensitivity analysis to judge the relative importance of temperature, precipitation, wind speed, percent sunshine, groundwater level, and temperature variation on four forms of pavement deterioration. In each case, temperature and temperature variation were most influential factors, potentially increasing longitudinal cracking, transverse fatigue cracking, and AC rutting.

Secondly, pavement is wetted by rainfall. Moisture influences the structure and properties of asphalt-based concrete in several ways which potentially accelerate pavement degradation. Water may penetrate natural pores in the pavement matrix (asphalt concrete is about 8% porous) or find its way into micro-cracks formed by thermal cycling [Si et al., 2014]. Water may also be suspended within the binder material [spontaneous emulsification; Little and Jones 2003]. The severity of most forms of pavement damage is greater with water present [Stidger, 2002]. Pavement stiffness, for example, can be dramatically reduced by water saturation [Schmidt and Graf, 1972] potentially losing as much as 50% of its tensile strength. Humidity at realistic levels (e.g. 80%) reduces pavement performance, and aged pavement appears to be more vulnerable than freshly laid [Yu et al., 2013]. Forms of deterioration unrelated to fatigue (shoving, pothole formation, raveling, bleeding) are also aggravated by water [Adlinge and Gupta, 2010].

Some mechanisms of water deterioration are based on chemical change, whilst others are primarily physical processes. Damage may occur within the asphalt binder or between the binder and the aggregate; water reduces both adhesive and cohesive strength [Little and Jones, 2003; Kim and Lutif, 2006]. Binder is then separated from the aggregate by the physical action of water in the micro-cracks [Willway et al., 2008]. Water exerts pore pressure on the surrounding asphalt matrix due to mechanical compression by heavy traffic ["pumping"; Little and Jones, 2003]. At freezing temperatures, ice forming in pores or cracks exerts pressure on the surrounding pavement matrix expanding existing cracks and initiating new ones. Ice formation can cause stripping and raveling effects similar to thermal or traffic-induced stripping at higher temperatures [Dawson, 2014].

*Microclimate under trees*

Trees control the physical environment under their leafy canopies in several ways which are potentially relevant to pavement condition. Most importantly, trees block sunlight and create shade at ground level controlling the absorption and dissipation of solar energy [Geiger, Aron, and Todhunter, 2009]. Incoming solar radiation is received at the earth's surface in the form of visible and ultraviolet light (0.2-5 μm wavelength) whereas outgoing radiation is in the form of heat (5-40 μm). During the day, surface temperature is dominated by incoming radiation as energy input exceeds energy loss by re-radiation. The surplus energy is either absorbed into

the ground, re-radiated to the air, evaporates moisture, or melts ice. At night, in the absence of solar input, the net radiation balance is dominated by outgoing radiation to the sky.

If plants are present, the uppermost layer of leaves becomes the thermodynamically active surface reflecting, absorbing, and transmitting portions of the incoming radiation. The forest canopy typically absorbs or reflects 75-90% of incoming radiation [McCaughy, 1987; Shuttleworth, 1989]. In deciduous species with spreading canopies (including most roadside tree species in Ohio), most light is absorbed or reflected by the top-most 1-2 layers of leaves. Only 1-3% of above-canopy radiation penetrates to half the height of a young beech or pine tree [Geiger et al., 2009]. In the Central Hardwood Forest of the eastern U.S. light at the forest floor may be as little as 1-5% of radiation falling on the crown canopy [Hutchinson and Mott, 1977; Matlack, 1993], and may have a much different spectral signature [Larcher, 2003].

Transmission through the canopy is controlled by canopy density (leaf layers per unit area, expressed as 'Leaf Area Index'), leaf spectral properties, solar elevation, tree height, and the size, shape, and orientation of individual leaves [Oke, 1987; Breman and Kessler, 1995; Lieffers et al., 1999; Parisi et al., 2001]. Because leaf morphology and branching architecture differ between species and between trees of different ages [Asner et al., 2003], tree age and species affect transmission of light to the ground [e.g. Heisler, 1986; Mitschrlich, 1940].

Light transmitted through the canopy warms the ground surface under a tree. During the day, low light levels under a tree canopy lead to low ground temperatures relative to open areas [Oliver et al., 1987; Geiger et al., 2009]. At night, downward reflectance by canopy foliage reduces energy loss by re-radiation from the ground leading to higher temperatures under the canopy. Thus, the ground under trees experiences less extreme thermal cycling than open ground in summer and less frequent freezing in winter [Nunez and Bowman, 1986].

Tree canopies also intercept incoming moisture, potentially holding moisture on leaf surfaces equivalent to 1-3 mm of rainfall [Shuttleworth, 1989; Xiao et al., 2000; Geiger, Amon, Todhunter, 2009]. Storage in the canopy translates into a drier ground layer under trees relative to adjacent open areas. Tree canopies may reduce wetting under them by as much as 50% in mild-moderate rainstorms [Linskens, 1952; Belsky et al., 1989]. A 20-40% reduction is typical of deciduous tree species such as we have in Ohio, with greater absorbing capacity in larger trees and those with denser foliage [Llorens and Domingo, 2007; Zimmerman et al., 2007]. Canopy storage can vary enormously depending on the species, size, and foliage density of a particular tree [e.g. Haworth and MacPherson, 1995]. Such studies suggest that in a season of light dew or brief showers, a substantial amount of moisture could be prevented from reaching the pavement surface.

In moderate-heavy showers, water falls through the leafy canopy and the ground is wetted. Xiao et al. [2000] estimated that a *Quercus suber* (cork oak) began stem flow and through-fall after 60 minutes of precipitation. Once the ground is wetted by rainfall or dew, trees potentially delay drying by blocking solar radiation which promotes cooler air temperatures and higher vapor pressure and reduces air movement which would otherwise cause evaporation. Species differ in their capacity for holding water, reflecting branching angles, bark texture, and leaf density [Xiao et al., 2000; Ovington, 1954].

In the temperate-zone winter, deciduous trees lose leaves so the moderating influence of the leafy canopy is theoretically lost. However, there is some evidence that even leafless tree canopies can influence snow accumulation and melting in forest situations [Geiger, Aron, and

Todhunter, 2009] leading to a moister ground surface [Boffa, 1999]. Because snow is an insulator the ground below is protected from extremely low temperatures [Jean and Payette, 2014; Sturm, 1992]. Trees may also collect snow, creating a local zone of shallow snow depth beneath the canopy. To the extent that trees block snow, they may increase the duration and thickness of frozen soil [Viereck, 1965].

*Trees and pavement*

Numerous studies have compared solar heating between tree-shaded and unshaded sites in urban settings. In most cases, pavement temperature was substantially lower in the shade than in adjacent open areas. Tree shade can reduce pavement temperature by as much as 11-25°C (20-45°F) relative to temperatures in nearby unshaded areas [Akbari et al., 1997], with maximum differences observed in early afternoon [e.g. Vailshery et al., 2013; Coutts et al., 2016]. At night, pavement temperature drops, equilibrating with air temperature [Stempihar et al., 2012].

Not all shade is equal. The radiation-blocking capacity of a tree canopy appears to vary considerably in pavement studies, with the degree of temperature buffering determined by foliage density and canopy structure [Mascaro, 2012; Golden et al., 2007; Napoli et al., 2016; Souch and Souch, 1993; Georgi and Zafiriadis, 2006; Shashua Bar et al., 2010; Zhang et al., 2013]. Contrasts in foliage density can be traced to differences between species; some species block significantly more light than others leading to lower pavement temperatures. Pavement and air temperature can also be linked to the height and crown size of individual trees [Gillner et al., 2015; Souch and Souch, 1993].

Only rarely has shading actually been linked to pavement condition. An innovative paper considered the shading of suburban streets in central California [McPherson and Muchnick, 2005]. McPherson and Muchnick [2005] compared the rate and extent of pavement degradation under tree canopies with pavement condition under the open sky. They reported that a dense street-tree canopy significantly reduced thermal cracking in the pavement below the canopy, potentially leading to an estimated 58% reduction in maintenance costs over 30 years.

Moisture effects under trees are less-well documented. Because tree canopies provide temporary storage of rainwater [Xiao et al., 2000], they potentially maintain a drier pavement underneath. Mathematical modelling of moisture interception by street trees [Xiao and McPherson, 2002] is consistent with casual observation of patterns of pavement wetting in light rainstorms [GRM personal observation]. Alternatively, a tree canopy may increase moisture exposure to the extent that it prevents evaporation from pavement below the canopy.

These interpretations are consistent with observations of tree microclimate in forest communities, but the effects on pavement remain speculative: Although thermal differences have often been reported, in road environments, they have not been related to laboratory studies of pavement performance. Many microclimate effects (e.g. accumulation and retention of moisture, snow, and ice) have rarely been measured on real roadways and accumulation and dissipation have not been documented on realistic time scales. Unfortunately, the small number of studies of pavement microclimate have largely occurred in dry, subtropical climates [e.g. McPherson and Muchnik, 2005; Mascaro, 2012]; it is unclear whether results from central California [McPherson and Muchnick, 2005] apply to pavement condition in Northeastern states such as Ohio where the climate is characterized by strong seasonality with extended periods of

freezing temperatures, pronounced wet and dry periods, and periods of freeze/thaw alternation [Coutts et al. 2016]. Because water plays an important role in pavement deterioration, failure to consider moist regions is a serious omission. The question of pavement microclimate also has ramifications for road safety. If trees shelter pavement from rain or snow, surface friction will be maintained in poor weather. Alternatively, if trees prevent thawing and drying of pavement, surface friction may be compromised.

A substantial portion of secondary rural and urban roadways are shaded by trees. A range of 1.8 - 27.6% shading was reported in a survey of Western cities [McPherson et al., 2005], and the proportion is probably higher in many older neighborhoods and rural areas, [GRM, personal observation]. If the benefit observed in McPherson and Muchnick [2005] can be generalized, these observations suggest enormous potential savings in maintenance costs nationwide. In this study we examine real road sections in a seasonally cold and wet temperate region. We document hourly, daily, and weekly variation in four important aspects of pavement microclimate and relate variation to critical ranges identified in lab trials to assess the potential for pavement damage under roadside trees.

## Site Selection, Description, and Locations

Microclimate was described in small pavement plots established on residential streets of the Near Eastside Neighborhood of Athens, Ohio (39°, 20’ N latitude; 82°, 6’ W longitude). Athens falls in the Köppen “humid subtropical” climate class with warm, humid summers and mild winters. Daily average January temperatures range from 18-39°F (-8-4°C) and July temperatures range from 61-86°F (16-30°C) [US Climate Data.com]. The region receives 39 in (100 cm) of precipitation annually, well distributed through the year. Freezing temperatures may occur anytime between November – March but temperature rarely remains below 32°F (0°C) for more than 7 or 8 days.

Study plots were 20 in × 20 in (50 cm × 50 cm) squares permanently located 20 – 40 in (50 – 100 cm) from the pavement edge. All pavement was asphalt concrete laid 2 – 8 years previously on level ground, and the plots had a minimal slope determined by road camber. Traffic was relatively light, consisting mainly of passenger cars. The surface course in all plots showed only modest wear with little loss of aggregate. Plots were established in triplets under, partially under, and away from canopies of individual trees. Under-canopy plots (“Under”) had >95% leafy canopy in a 90° region of interest directly above, measured using an optical densiometer [Lemmon, 1956]. Partial-canopy plots (“Partial”) showed 45% – 55% canopy cover corresponding to a position under the edge of the canopy. As a control for canopy effects, each triplet also included an open-sky plot (“Open”) having 100% canopy openness. Plots in each triplet were separated by < 66 ft (20 m) and situated on the same stretch of pavement, minimizing variation in pavement age, wear, and composition. Triplets were established under 23 trees (N = 69 plots); subsets of this group were used as appropriate to each measure of microclimate.

Experimental trees grew in the median strip between sidewalk and street pavement and ranged from 12-35 in (30-90 cm) in diameter. All trees had a uniformly dense, apparently healthy canopy with no obvious dead tissue. Presence in historical aerial photos indicated that all were > 50 years in age. Species were typical of roadside trees in the Ohio Valley region: predominantly *Acer rubrum* (red maple), *A. saccharum* (sugar maple), *Quercus phellos* (willow oak), and *Q. rubrum* (red oak), with occasional *Platanus occidentalis* (sycamore), *Liquidambar styraciflua*

(sweetgum), and *Robinea pseudoaccacia* (locust). Because of the small sample size, species were combined into *Quercus* spp (oaks), *Acer* spp (maples), and "other" in all analyses. Most pavement variables were measured between June and September 2018 when all trees were fully leafed, presenting the maximum canopy density. Snow and ice were surveyed in January 2018 when all trees had shed their leaves and only bare branches remained. No evergreen tree species were used.

## Data Collection Methods

**Pavement Temperature.**

Pavement temperature was measured in experimental plots under and beside trees through the course of a single day (June 6, 2018). Temperature was recorded to the nearest 0.18°F (0.10°C) using a handheld infrared thermometer (62 Max, Fluke Instruments, Everett, Washington). Plots were visited in sequence from before sunrise (6:05 AM on this date) to after sunset (8:52 PM) with an approximately 50-minute rotation. Thus, each plot was measured seventeen times through the course of the day.

Data recording began before sunrise, approximating the lowest nighttime temperature, and continued through the day until just after sunset. All three plots at each tree were measured within 60 seconds. In addition to temperature, incidence of direct sun was noted for each plot. Small fair-weather cumulus clouds drifted over the study site; they were noted as they occasionally shaded plots.

**Pavement Wetting.**

Wetness of the pavement was recorded at three to five minute intervals before and during natural rain showers in mid-late summer 2018. Wetness was measured as electrical conductivity between two probes of a handheld electronic moisture meter (Extech 230, Extech Instruments, Nashua, New Hampshire) applied to the surface of the pavement. Calibration trials showed values of 0.0-0.3 for dry surfaces, whereas immersion of probes in water produced a reading of 40.0. Conductivity was measured in each quadrant of the pavement plot and averaged for use in the analysis.

Measurement of wetting required discrete daytime rain events with a clearly defined starting point depositing rain on dry pavement. Rainfall was anticipated using real-time Doppler radar tracking [Weather Underground, 2018] and included frontal passage as well as local convective storm cells. Measurement began on dry pavement and proceeded as rain began to fall. Trials were ended when canopy plots showed values comparable to open-sky plots for at least four intervals.

Conductivity measurements were compared with actual rainfall collected with an array of rain gauges under an open sky. The large openings of the gauges 325 $in^2$ (2100 $cm^2$) ensured that stochastic effects of individual raindrops were averaged out, allowing estimation of rainfall to a precision of < 0.004 in (0.1 mm). Because of the difficulty in anticipating rain events and the discontinuous nature of small storms, only eight datasets were collected.

**Moisture Persistence.**

To explore the role of trees in controlling evaporation, pavement plots were experimentally wetted and monitored as they dried. One liter (34 fl oz) of water was poured into

a centered plastic frame enclosing 155 $in^2$ (1000 $cm^2$) equivalent to a 0.039 in (1 cm) rain event. The frame maintained water coverage over all parts of the pavement surface for four to five seconds, improving evenness of wetting. Then the frame was removed. Water was applied in all plots before sunrise to ensure equal temperatures under all canopy conditions and remove any effects of prior heating. Moisture was monitored in all wetted plots at 40 to 50 minute intervals until all visible moisture disappeared and metered moisture levels dropped to levels observed before wetting. Temperature was recorded in all plots at the beginning and end of the experiment.

The experiment was conducted in three groups of 4-5 plots for logistical reasons. All three trials were conducted on warm, predominantly sunny days corresponding to high barometric pressure. Moistness of the pavement was measured as electrical conductance using a handheld meter described above.

**Snow Accumulation and Persistence.**

Snow depth was measured immediately after a storm on January 13, 2018, and at one or two day intervals until no snow or ice remained. The storm deposited 3.5-4.7 in (9-12 cm) of snow. A minor storm three days later added an additional 0.8 in (2 cm). Temperatures remained below 32°F (0°C) until January 19 when air temperature abruptly rose to 39.2°F (4.0°C). Snow depth was measured visually using a plastic scale inserted into undisturbed snow. Because snow was plowed on most of the streets, snow was measured in undisturbed locations in the adjacent median strip rather than on the pavement itself. Median-strip locations were situated under full canopy, partial canopy, and open sky as near as possible to the corresponding pavement plots. Ice was assessed on the pavement as the proportion of the study plot covered.

**Environmental Parameters.**

Canopy cover was quantified using vertically oriented hemispherical digital photos following the method of Chianucci and Cutini [2013]. Tree canopies were photographed above pavement plots on overcast days to ensure uniform lighting. Images were then converted to an 8-bit greyscale, thresholded to maximized sky/canopy contrast, and quantified as the proportion of canopy within the region of interest using the ImageJ image analysis software [Schneider et al., 2012]. In each photo, density was assessed in a circular region-of-interest corresponding to 45° elevation from the horizon in all directions. This area included the portion of the tree canopy influencing rainfall and most solar heating; low elevation objects and those at a distance (i.e. neighboring trees and buildings) were excluded.

"Aspect" describes the location of the under-canopy plots relative to the trunk of the shading tree. As a result of a haphazard planting history, south-facing sites were over-represented (10/22 sites, 45%) and north-facing were under-represented (2/22 sites, 9%). Five sites faced east and four faced west.

## Data Analysis

Pairing of plots at individual trees allowed each under-canopy plot to be compared with a similar control (open sky) plot, thereby removing variation in pavement texture and chemistry, slope, exposure, and time of day. Pavement temperature was compared between open, partially open, and control plots by constructing a generalized linear model in which canopy openness was specified as a factor and individual tree was included as a random variable. Temperature values

were compared before sunrise, at the time of peak open-sky temperature, immediately after sunset, midway between sunrise and the maximum open-sky temperature, and midway between maximum and sunset.

Accumulation of moisture in rainfall was quantified as 1) the time elapsed between first wetting in the open plots and the first moisture recorded in the under-canopy plots, and 2) the time between first wetting in open plots and the point when wetness in under-canopy plots becomes equivalent to open plots. Wetting times were translated into amount of rainfall by comparison with progressive accumulation of water in the rainfall traps. Rainfall was then compared with the frequency distribution of rainfall in individual storms in the region between 2009-2018 [AWOS III, Albany, Ohio]. Wetting time and amount are presented graphically and tested for correlations with canopy openness.

Drying was quantified as the time elapsed between experimental wetting and 50% and 10% of the initial wetness value. To control for variation between individual sites, time elapsed in under-canopy and partial plots was expressed as a proportion of the wetness value in the respective open-sky plot. Times to 50% and 10% wetness were compared between canopy classes by Kruskal-Wallis tests, followed by pairwise Wilcoxon tests using the BH correction for multiple comparisons if appropriate. Environmental variables (hemispherical canopy openness, dbh, aspect, and species) were compared with rates of drying by visual inspection and calculation of correlation coefficients.

Snow accumulation was compared between canopy-openness classes immediately after the initial storm (January 13) and at the peak of snow depth (January 19) using Kruskal-Wallis tests. To separate rate of snow loss from snow accumulation, snow depth was standardized as a proportion of depth at the date of greatest snow depth in each plot, respectively, and the half-lives in each canopy class were compared by Kruskal-Wallis tests. Because the snow was preceded by freezing rain on the evening of January 12, all pavement was covered with a layer of 0.1-0.4 in (0.3-1.0 cm) of ice beneath the snow. Ice cover was compared between canopy classes on each of three dates during the period above 32°F (0°C) (January 19-21). Snow depth and half-life and ice cover were compared between tree aspect classes and species groups using Kruskal-Wallis tests. To compare snow and ice with tree size, correlation coefficients were calculated between each measure of snow and ice and tree diameter.

## Results

**Pavement Temperature.**

The pavement was coolest before dawn and heated during the day as it absorbed solar radiation (Figure A1). Open-sky plots peaked at 113-122°F (45-50°C) during 1:00-3:00PM. Plots under the canopy heated substantially more slowly, peaking at only 82-90°F (28-32°C). Peak temperatures under the canopy tended to occur early (8:00-10:00AM) or late (4:00-6:00PM) in the day as lateral radiation extended diagonally under the edge of the canopy, with the timing dependent on aspect and the distribution of surrounding trees. For example, the Bolleana 1 site (i.e., 7 Bolleana Pl.) faced eastward and under-canopy temperature peaked at approximately 10:30AM warmed by the rising sun (Figure A1). The Bolleana 2 site (i.e., 10 Bolleana Pl.) located approximately 160 ft (50 m) away on the other side of the same street, showed a peak under-canopy temperature at approximately 5:30PM as it received direct-beam radiation late in the

day. Partial canopy plots were intermediate, after tracking the temperature of open-sky plots for part of the day (for example 77 S. May Ave.), according to their position relative to the surrounding canopy.

Canopy classes differed significantly in maximum temperature (Kruskal-Wallis $\chi^2 = 31.577$, $p = 0.000$) and individual classes were easily distinguishable (Wilcoxon probabilities 0.0000-0.0002) increasing in proportion to canopy openness (Figure A2, top). In minimum temperature canopy classes differed in the opposite order, with lowest temperatures under an open sky (Figure A2, center). Canopy classes were significantly different ($\chi^2 = 12.796$, $p = 0.0017$) and open-sky plots were distinguishable from under and partial plots (probabilities = 0.0021 and 0.0189).

Individual trees differed in canopy density judged by hemispherical canopy photos of under-canopy trees. The Acer saccharum at 97 May Ave., for example, allowed 8.0% light transmission, whereas the A. saccharum at 152 Morris Ave. allowed only 2.1%. However, canopy transparency did not differ significantly with species or aspect (Kruskal-Wallis Probabilities >0.35). Correlations of under-canopy density with tree diameter, maximum temperature, and minimum temperature were weak (r values < 0. 30). Maximum and minimum temperatures in "under" plots were distinguishable by species ($\chi^2_{maximum} = 9.185$, $p = 0.0101$; $\chi^2_{minimum} = 6.0227$, $p = 0.0101$). *Acer spp* (maples) allowed both warmer maximum and minimum pavement temperatures than *Quercus spp* (oaks) as seen from Table A1. "Partial" plots showed a 1.8°F (1.0°C) median cooler minimum temperature under *Quercus spp* (oaks) than under *Acer spp* (maples) ($\chi^2 = 6.817$, $p = 0.0331$) but the effect was weak (Wilcoxon $p = 0.0830$).

Site aspect and tree diameter showed no relationship with either maximum or minimum pavement temperatures in either "under" or "partial" plots (probabilities > 0.30; $r < 0.20$). The greatest contrast in pavement temperature occurred between open-sky and completely shaded plots (mean $\Delta$=24.8 ± 1.9 SD); smaller contrasts were observed between Open and Partial plots (18.5 ± 4.1; Figure A2, bottom).

**Pavement Wetting.**

Wetting was measured during natural rainfall under six trees, two of which were measured twice. Rain typically began with gentle sprinkling and intensity increased over a span of 30-40 minutes (Figure A3). The sequence of rainfall was idiosyncratic, with intermittent breaks on some dates (e.g. Figure A3 a, b) and violent deluges on others (e.g. Figure A3 c, d). The first wetting under the canopy lagged slightly behind the onset of measurable moisture in the open (median 0.5 minutes), although it was as much as 18 minutes behind in one trial (Figure A3 e). Wetness (conductivity) under the canopy was lower than the respective open plots for approximately 30 minutes (median) although there was substantial variation between trials related to the intensity and speed of development of individual rainstorms (range: 3-77 minutes).

In Partial plots, wetness was detected as soon as in Open plots in most cases (Figure A4 top; median delay = 0 minutes). The degree of wetness in Partial plots reached Open levels after a median delay of 22 minutes (range: 0-74 minutes). Time and conductivity data were expressed as a proportion of the time to complete wetting (i.e. Under = Open) to correct for variation in individual rainstorms. The onset of wetting under and partial were simultaneous with first-wetting in Open plots in most cases (median proportion = 0.037). Partial plots reached the wetness of Open plots in 0.797 (median proportion) of the time in the respective Under plots (Table A1).

Time elapsed until wetting translated into amounts of rain fallen (Figure A4 center). Very little rain was necessary to cause a wetness response in Partial and Under plots (unmeasurable – 0.45 mm). Partial plots reached levels of wetness equivalent to Open plots after 0.029 in (0.74 mm) of rain (median; range: 0.021-0.083 in (0.54-2.1 mm)). Under plots reached Open plots after 0.05 in (1.27 mm) median with range 0.0307-0.161 in (0.780-4.090 mm). Graphing showed no obvious relation between canopy density and wetting onset or extent; correlations were generally weak ($r < 0.20$ for 14 of 16 tests, 87.5%) and differed strongly between individual trials.

**Pavement Drying.**

Pavement dries with the passage of time, reaching measurable dryness after 2-6 hours (Figure A5). In most cases Open plots dried most quickly (8/9 trials, 89%) and Under plots dried most slowly (8/9 cases, 89%). Open plots showed a somewhat concave decay curve (severe initial decline followed by slower rates of drying) whereas Under plots were usually somewhat convex. Partial plots were intermediate (7/9 trials, 78%). Open plots reached 50% of the initial wetness value in in 82 minutes (median; range 60-160), whereas Under plots required 199 minutes (median; range 135-230). This equates to a proportional median increase of 204% under a tree canopy. Partial plots required 124 minutes (median; range = 57-221), equivalent to a median proportional delay of 120% relative to Open plots. Considerable variation was present in each canopy class (Figure A5). Significant contrasts were observed between canopy openness classes in 50% remaining ($\chi^2 = 11.88$, $p = 0.0026$) and 10% remaining ($\chi^2 = 8.23$, $p = 0.0163$). Open plots were distinguishable from Under at both 50 and 10% dryness ($p = 0.0044$ and 0.0310, respectively). Partial plots were distinguishable from Open in each measure ($p = 0.072$, 0.077), but only distinguishable from Under at 50% dryness ($p < 0.076$).

It was not possible to link drying rate to pavement environment in statistical terms, in part because of the small sample size. Aspect was divided into "south-facing" (N = 4 trees) and north/northwest/west (N = 5 trees); no significant difference was detected in any measure of drying (probabilities > 0.10). Tree species was reduced to *Acer spp* (maples) (N = 5 trees) and "other" (N = 4 trees) but, again, no significant differences were detected. Hemispherical canopy openness and trunk diameter showed no correlations stronger than $r = 0.676$ and 0.473, respectively, and visual inspection suggests these were strongly influenced by isolated data points.

A lack of strong environment relationships should not be taken as an absence of environmental influence, however. The research team's emphasis on intensive sampling of individual trees necessitated a small sample size. More insight can be gained by examining the trajectories of individual plots. For example, Under and Partial plots at 7 Bolleana Pl. entered a period of rapid drying when those plots came into direct sunlight at 8:42AM. Similarly, Under plots at Ondis Ave. entered a rapid drying phase when direct-beam radiation fell on them at 8:43AM continuing to 10:44AM. Similar effects were observed in Under plots at 16 Morris Ave. between 8:40-9:28AM, and in Open plots at 7 Ohio Ave. beginning at 8:04AM. In contrast to these directly lit examples, plots at 6 Bolleana Pl., 148 Morris Ave., and 152 Morris Ave. were never observed to be in direct sunlight and have much more gradual drying trajectories.

Although drainage was not quantified in this study, drainage was clearly important to drying rate. Plots with a pronounced camber and a smooth surface drained rapidly; plots with a rough pavement surface, obvious cracks, or little slope gradient retained water even in full sun.

For example, the Under plot at 2 Wallace Dr. (Wallace 1) showed mean wetness values of zero over most of its surface, but 23.4 in cracks. At 148 Morris Ave., standing water was still present in flat areas in the sunny Open plot at 11:31AM despite near-complete dryness in the rest of the plot after 10:00AM. Similar examples are seen in the Partial plot at 152 Morris Ave. This residual puddling effect is why 10% wetness was chosen as a measure of wetness rather than complete dryness.

**Snow and Ice.**

Approximately 4 in (10 cm) of snow accumulated in the pre-dawn hours of January 13, 2019, supplemented by an additional 0.4-0.8 in (1-2 cm) on January 16. Maximum daily temperature remained below 32°F (0°C) though January 18 ensuring persistence of snow until January 19 (Figure A6). Immediately after the initial storm, snow depth under trees was significantly less than depth in Open plots ($\chi^2 = 6.010$, $p = 0.0495$; $\text{Wilcoxon}_{\text{under/open}}$ $p = 0.05$) with $\text{median}_{\text{under}} = 3.74$ in (9.5 cm) and $\text{median}_{\text{open}} = 4.72$ in (12.0 cm).

On January 19 (day of greatest snow depth), depth was marginally less in Under than Open plots ($\chi^2 = 4.99$, $p = 0.0825$; Wilcoxon = 0.09; $\text{median}_{\text{under}} = 4.33$ in (11.0 cm), $\text{median}_{\text{open}} =$ (4.72 in (12.0 cm)). No difference was detectable in ice cover ($p > 0.40$). After mean daily temperatures rose above freezing, snow and ice rapidly melted (Figure A6). The half-life of snow under a tree canopy was significantly less than under open sky ($\chi^2 = 6.122$, $p = 0.0468$; Wilcoxon $p = 0.066$). Ice cover declined rapidly when mean daily temperatures exceeded 32°F (0°C) but cover did not differ significantly between canopy classes on any of those days (probabilities > 0.12).

Tree species were assigned to three groups (*Acer spp* (maples) ~ 6 trees, *Quercus spp* (oaks) ~ 7 trees, other species ~ 5 trees). The greatest snow depth after the initial storm (13 in (33 cm)) was measured under a west-facing *Robinia pseudoacacia* (locust) 20 in (50 cm) in diameter, whereas the least depth (3.1 in (8 cm)) was measured under a 11.4 in (29 cm) south-facing *Acer rubrum* (red maple). Fastest snow loss (50% decline in 1.8 days) occurred under a 24 in (62 cm) *Acer saccharum* (sugar maple) facing east, whereas the slowest loss (> 4 days) was observed under a 22 in (55 cm) *Quercus phellos* (willow oak) facing south. The earliest ice loss was observed in four trees on January 14, and the last residual ice was observed beneath a west-facing *Quercus phellos* (willow oak) of 33 in (83 cm). No significant differences emerged between species groups or aspect classes in any of the measures of snow or ice accumulation or persistence (probabilities > 0.05). No correlations were observed between tree size (dbh) and any measure of snow or ice (r values < 0.36).

Although the research team did not quantify drainage or traffic, it became obvious that ice formation depended on two processes: packing of snow by passing vehicles and re-freezing of melt water when drainage was impeded by piles of plowed snow. Packing of snow into ice was noted at the 2 Wallace Dr., 152 Morris Ave., and Red Lot plots on January 13. Ice forming behind snow dams was noted at NE Wallace Dr. and 7 Ohio Ave. on January 20, after median daily temperatures had risen above 32°F (0°C), in addition to areas outside of trial plots.

## Discussion

In the select small study plots, tree canopy clearly affected the temperature, moisture, and snow accumulation over pavement below. These effects are easily understood in terms of blocking

solar radiation and falling rain in ways consistent with an understanding of microclimate in forests. However, these results provide new insights into the timing and degree of climate alteration, and such insight appears to be relevant to pavement condition.

*Pavement Temperature.*

Pavement heating can be interpreted in terms of exposure to direct-beam radiation on a minute-by-minute basis. Not surprisingly open-sky plots heated more and faster than Under plots, showing an Open/Under contrast of 72-82°F (22-28°C) in respective maximum temperatures. Under a tree canopy, direct heating included the minor peaks corresponding to lateral sun coming diagonally under the canopy at low solar angle early and late in the day. Similarly, Partial plots did not simply average the temperature of Open and Under plots; instead they tracked open-sky temperatures for the period in which they received direct radiation and dropped sharply when shaded. Thus, much of the variation in shaded pavement temperature was attributable to the distribution of neighboring trees and buildings which block lateral radiation; in retrospect a better design would have included the shade cast by an extended cluster of trees rather than a single individual.

Open-sky plots also showed significantly cooler minimum temperatures, in all cases just before sunrise, which can be linked to nighttime IR radiation. In the absence of a tree canopy to capture heat, open-canopy plots are losing more heat than those protected by a canopy [Geiger et al., 2009]. Thus, both daytime and nighttime radiation contribute to diurnal cycling in pavement temperature.

Heating under the canopy may be due to incidental exposure to flecks of light penetrating the canopy. The degree of heating differed significantly between tree genera (*Acer spp* (maples) allow marginally greater heating than *Quercus spp* (oaks)) but the mechanism is unclear as species were not distinguishable in canopy density. Through-canopy heating appears to be minor relative to direct beam heating; the rise in temperature of under-tree plots was minor in plots that did not receive lateral heating early in the day (see the 7 Ohio Ave. site in Figure A1). The size of the shading individual was not important; as long as the canopy filled the required arc of sky, a tree of small diameter buffered temperature as efficiently as a large tree.

Heating of pavement must be judged in the context of thermal expansion and contraction which can generate tensional stresses of 15-87 psi (0.1-0.6 MPa) at temperatures comparable to diurnal cycling in many temperate-zone climates [Tabatabaee et al., 2012]. As asphalt pavement cools, the asphalt matrix contracts more than the gravel aggregate, creating tensile stress between matrix and aggregate [Hussein and Halim, 1993] potentially inducing cracking. Ordinary heating was substantial, leading to a 52-61°F (29-34°C) diurnal variation in Open plots; in contrast, under-canopy plots only experienced a 11-25°F (6-14°C) thermal cycling.

Thermal stress (σ) generated by the daily temperature variation observed here can be calculated by equation 1 [Hills and Brien, 1966]:

$$\sigma = E \times CTC \times \Delta T \qquad (1)$$

Where: $E$ = modulus of elasticity of the pavement, $CTC$ = coefficient of thermal contraction, and $\Delta T$ = observed variation in temperature. Assuming a modulus of elasticity of 360,000-1,200,000 psi (2500-8300 MPa) at 77°F (25°C), appropriate to freshly laid asphalt pavement in SE Ohio [Masada et al., 2004], and using CTC values of 3.11 × 10-5 based on measurement of freshly laid SP III Superpave mix [Islam and Tarefder, 2015] the thermal stress experienced at Open plots can

be computed as 257-770 psi (1.77-5.31 MPa), whereas Partial plots experienced 200-599 psi (1.38-4.13 MPa), and Under plots experienced 94-284 psi (0.65-1.96 MPa). Based on the sampling in this study, it is evident that shading substantially reduces thermal stress, and a partial canopy also has an effect.

These estimates fall within the ranges demonstrated to cause fatigue cracking [Shahin and McCullough, 1972]. It must be noted that these estimates are based on freshly laid asphalt; tensile stress will increase as pavement ages [Alavi et al., 2015], making expansion and contraction destructive at progressively higher temperatures. In a Virginia trial, as little as 5% increase in temperature decreased the service life of asphalt pavement by more than 20% [Quiao et al., 2013]. We conclude that diurnal cycling in midsummer has the potential to cause pavement cracking in the seasonal climate of southeastern Ohio, and that even partial shading by a tree canopy has the potential to reduce that damage.

*Pavement Wetting.*

The results of this study show that an overhanging tree canopy delays the onset of wetting in convective summer rain showers and reduces total wetness for up to 30 minutes. This observation is consistent with canopy storage reported for other ecosystems [Calder et al., 1986; Vis, 1986], with the amount retained in the foliage depending on the species of the tree, reflected in its size and branching structure. Generally, soil is moister under tree canopies than in open areas notwithstanding the absorption by tree roots and decreased evaporation [Boffa, 1999]. A 20-40% reduction of rainfall is typical of deciduous tree species such as those found in Ohio, with greater absorbing capacity in larger trees and those with denser foliage [Llorens and Domingo, 2007; Zimmerman et al., 2007]. In this research study, water-holding capacity of the canopy is expressed as a delay in surface wetting relative to Open plots. In all rain events measured here, time elapsed between the onset of rain and Under pavement reaching the wetness of Open plots is a measure of canopy saturation.

At the beginning of each shower the profile of the tree was clearly visible as a dry circle under the canopy. However, moisture usually became detectable under the tree within 3-4 minutes indicating a degree of throughfall. More important is the delay of Under plots in reaching the degree of wetness of open-sky plots, which typically lasted 25-35 minutes. Compared with climate data for the region (Figure A7), this canopy-caused delay implies that under-canopy pavement never reaches complete wetting in 28 ± 11% of rainstorms. These are storms of short duration which are most common in this region; more extended storms result in equal wetting under and adjacent to the canopy. Inspection of cumulative rainfall (Figure A3) suggests a threshold behavior in which the Under plots were substantially less wet (0-40% of open-sky values) for most of the delay period. This delay appears to be a consequence of the pattern of accelerating rainfall in summer convective storms rather than a property of the tree canopies. Partial canopies offer some degree of pavement protection, delaying complete wetness in 13 ± 11% of storms.

The damaging effects of water penetration on pavement are widely recognized [e.g. Schmidt and Graf, 1972; Adlinge and Gupta, 2010; Yu et al., 2013], and exclusion of moisture is a major research and management objective. Because a tree canopy reduces water deposition, as these results demonstrate, roadside trees can potentially extend the service life of asphalt pavement. However, this conclusion needs to be qualified. The structural effects of moisture

duration and amount (the properties measured here) are not well understood. Future research needs to establish how rapidly water penetrates the pavement matrix, and how much hydrostatic pressure is exerted by the thin films of moisture observed here. Finally, it is worth noting that measurement was terminated in many of the study plots by flooding caused by particularly heavy rainfall (10/24 plots, 42%). Thus, pavement wetness is also dependent on drainage patterns and pavement engineering, factors unrelated to canopy coverage.

*Drying.*

Overhanging tree canopies caused a delay in drying pavement of 1-3 hours, consistent with blocking solar radiation. Open plots generally showed concave drying curves suggesting immediate and rapid drying on exposure to direct sunlight. In contrast to Open plots, Under plots dried slowly at first (convex curves) perhaps because drying was the cumulative effect of energy input from the air or from many small, transient rays ("sunflecks") penetrating the canopy. The effect of sunflecks is confirmed by direct observation of individual plots: rapid drying began when direct-beam radiation first reached them. Patchy light transmission is one of the essential properties of tree canopies differentiating them from the homogeneous filtering by engineered surfaces (e.g. a highway overpass).

Climate data [AWOS III, Albany, Ohio] show an average of 224.2 rainstorms per year over the ten-year period 2009-2018 (Figure A7). If the canopy of deciduous trees only affects pavement drying when they have leaves in the late spring, summer, and early fall (est. 58.3% of the year), it can be estimated that pavement in the small plot study area will influence pavement wetness in 131 rainstorms per year, each followed by a maximum of 161 minutes of wetness (based on a 10% measure of wetness in Open plots); equating to 21,091 minutes of wetness per year. Under tree canopies the period of wetness will be extended by an additional 14,785 minutes, and under partial canopies by 7,382 minutes.

To the extent that duration of wetness controls pavement degradation, tree shading appears to have the potential to reduce service life. However, this conclusion must be qualified. Drying trials were intentionally conducted on cloudless days in midsummer when differences in tree canopy were most likely to show differences in drying rate. Rain normally falls on days that are at least partially cloudy so road sections will show less contrast in solar energy than these data suggest. It is also worth noting that the delay in drying observed here can only happen during the daytime and during the seven months of the year (April – October) when deciduous trees have leaves. Because rain also falls at night, and during the winter when there is less solar energy to dry the pavement, the contrast between open-sky and canopy-covered road sections is probably substantially less distinct than reported here.

Although drainage was not explicitly quantified, the observations of puddling in some plots emphasize that water retention is not solely an issue of solar drying. Rural roads show a much greater range of roughness and camber than the city streets measured here, so one can expect a correspondingly lower contribution of solar drying to moisture retention in actual road sections.

*Snow and Ice.*

Air temperature was clearly the most important factor controlling persistence of ice and snow. However, tree canopies contributed to variation at fine scales 3.3-33.0 ft (1-10 m). It appears that the branches of deciduous trees block snowfall even when no leaves are present.

Tree canopy can account for a substantial reduction in snow accumulation (median 12.9% lower in Under plots; range 0-31%). Conifers have been reported to reduce snowfall under their canopies [Sturm, 1992] but this is the first report of deciduous tree limbs causing snow reduction. Less deposition potentially reduces the insulating quality of snow [Viereck, 1965]. Tensile cracking occurs at very low temperatures, approximately -22°F (-30°C) [Alavi et al., 2015] so it is possible that thinner snow layers would promote cracking in regions experiencing heavy snows and extreme cold.

As snow melted, plots under trees melted slightly faster even when corrected for the initially lower snow cover, a counterintuitive result because melting is driven by solar radiation. It is possible that Under plots melted disproportionately fast because the adjacent trunk absorbed and re-radiated solar energy, but the mechanism remains unclear. Although tree size, aspect, species all affect the amount of incident radiation [e.g. Heisler, 1986; Asner et al., 2003] their effects were insignificant in this trial. Leafless trees can block a significant portion of solar radiation [Heisler, 1986; van den Beldt and Williams, 1992; and see examples in Boffa, 1999] but accelerated snow loss observed here suggests the opposite effect.

Ice cover and persistence on pavement appeared to be unrelated to adjacent trees. Instead, most ice was generated by compaction of snow under car tires or by nocturnal freezing of meltwater in puddles. Although the research team did not measure these processes, their influence was obvious in the small plot sites. This observation suggests that ice can be managed by a) plowing promptly after a snowstorm, and b) by engineering roads with adequate camber and large gutters.

*Partial Coverage.*

In Bloomington, Indiana, zones at the edges of tree canopies were intermediate in air temperature between fully shaded and open locations suggesting a gradient of solar heating with canopy position [Souch and Souch, 1993]. In the present study, Partial plots showed intermediate values in all forms of microclimate, but intermediacy was not linearly related to canopy cover. In pavement heating, partially open plots were heated when exposed to direct beam radiation but quickly cooled when the sunfleck moved on. In drying, partially open plots were more similar to Under plots than to Open plots potentially because drying was based on cumulative heating of pavement. In both cases, the strength of the partial effect was linked to the rate of pavement heating and cooling, so it is important to know whether asphalt pavement has sufficient thermal inertia to integrate energy storage over the course of a day [Shahin and McCullough, 1972]. The results of this present study suggest absorption and re-radiation on a scale of 40-50 minutes rather than dawn-to-dusk, but laboratory trials are required to confirm this rate. In contrast to effects related to solar heating, effects based on precipitation show much less effect of partial canopy. In wetting Partial plots vary idiosyncratically, closely tracking Open or Under values in individual trees. Snow accumulation was intermediate between Open and Under, but Partial plots lost snow as rapidly as Open plots.

## Conclusion

The results confirm observations of forest microclimate: Trees control the energy budget of the ground beneath them and substantially affect the accumulation and persistence of moisture, factors known to be relevant to pavement condition. The range of temperature and moisture

described here is easily noticeable to humans, and potentially sufficient to affect the properties of asphalt pavement. This appears to be purely a shading effect. Although individual trees differ in species, size, and canopy architecture, such differences were rarely sufficient to affect pavement microclimate.

The results reported here both support the idea that a tree canopy extends pavement. service life (by buffering heating, wetting, and snow accumulation) and contradict it (by extending water retention). Thus, tree canopy appears to have some potential to cause degradation of rural roads. These results extend the conclusions of the study in the Central Valley of California which inspired this work [McPherson and Muchnick, 2005] by providing insight into moisture and snow deposition and retention. However, it is difficult to know whether the incremental effects measured here would be sufficient to cause pavement damage. Laboratory trials are required to calibrate the effects measured here to the material properties of asphalt concrete.

It is important to note that factors unrelated to tree canopy such as surface texture, traffic, and drainage affect pavement microclimate, particularly the retention of moisture. Thus, management of rural roads needs to balance canopy effects against the full spectrum of contributory factors, including pavement design and engineering. At this point, the pavement-protection hypothesis needs to be tested by comparing pavement microclimate with actual measures of pavement condition in rural roads.

## Bibliography.


Adlinge, S.S., A.K. Gupta. 2010. Pavement Deterioration and its Causes. *IOSR Journal of Mechanics and Civil Engineering* 2: pp.6-15.

Akbari, H., A.H. Rosenfeld, H.G. Taha. 1990. Summer Urban Heat Islands, Urban Trees and White Surfaces. ASHRAE Transactions, Atlanta Georgia.

Akbari, H., S. Davis, S. Dorsano, J. Huang, S. Winnett. 1992. Cooling our Communities: A Guidebook to Tree Planting and Light Colored Surfacing. US EPA Office of Policy Analysis, Climate Change Division, pp.217.

Alavi, M., N.E. Morian, E.Y. Hajj, P.E. Sebaaly. 2015. Influence of Asphalt Binder Oxidative Aging on Critical Thermal Cracking Characteristics of Asphalt Mixtures. *Journal of the Association of Asphalt Paving Technologists*, 84: pp.115-142.

Armson, D., M.A. Rahman, A.R. Ennos. 2013. A Comparison of the Shading Effectiveness of Fire Different Street Tree Species in Manchester, UK. *Arboriculture and Urban Forestry*. 39: pp.157-164.

Asaeda, T., V.T. Ca. 1993. The Subsurface Transport of Heat and Moisture and its Effect on the Environment: A Numerical Model. *Boundary Layer Meteorology* 65: pp.159-179.

Asner G.P., J.M. Scurlock, J.A. Hicke. 2003. Global Synthesis of Leaf Area Index Observations: Implications for Ecological and Remote Sensing Studies. *Global Ecology and Biogeography* 12: pp.191-205.

Asphalt Institute 2009. MS-16 Asphalt in Paving, Preservation & Maintenance 4th Edition. Lexington, Ky.

Belsky, A.J., R.G. Admundson, J.M. Duxbury, S.J. Riha, A.R. Ali, S.M. Mwonga. 1989. The Effects of Trees on their Physical, Chemical, and Biological Environments in a Semi-Arid Savanna in Kenya. *Journal of Applied Ecology* 26: pp.1005-1024.

Boffa, J.M. 1999. Biophysical Factors on Parkland Management - Influence of Trees on Microclimate. Chapter 3 in Agroforestry Parklands in Sub-Saharan Africa. United Nations Food and Agriculture Organization. Conservation Guide 34.

Bowler, D.E., L. Buyung-Ali, T.M. Knight, A.S. Pullin. 2010. Urban Greening to Cool Towns and Cities: A Systematic Review of the Empirical Evidence. *Landscape and Urban Planning* 97: pp.147-155.

Boyer, B., 1999. Life Cycle Performance. The Asphalt Institute. Available on line at http://www.asphaltmagazine.
com/archives/1999/Summer/Life_Cycle_Performance.pdf.

Bremen, H., J. J. Kessler. 1995. *Woody Plants in Agro-Ecosystems of Semi-Arid Regions*. Springer-Verlag.

Calder, I.R., I.R. Wright, D. Murdiyarso. 1986. A Study of Evaporation from Tropical Rainforest, West Java. *Journal of Hydrology* 89: pp.13-31.

Chianucci, F., A. Cutini. 2013. Estimation of Canopy Properties in Deciduous Forests with Digital Hemispherical and Cover Photography. *Agricultural and Forest Meteorology* 168: pp.130-139.

Cominsky, R.J., G.A. Huber, T.W. Kennedy, M. Anderson. 1994. The Superpave Mix Design Manual for New Construction and Overlays. SHRP-A-407. National Research Council, Washington.

Cool California. 2016. How cool pavements work. http://www.coolcalifornia.org/cool-pave-how

Coutts, A.M., E.C. White, N.J. Tapper, J. Beringer, S.J. Livesley. 2016. Temperature and Human Thermal Comfort Effects of Street Trees Across Three Contrasting Street Canyon Environments 124: pp.55-68.

Dawson, A. 2014. Anticipating and Responding to Pavement Performance as Climate Changes. Pages 127-157 in Climate Change, Energy, Sustainability and Pavements. (eds. K. Gopalakrishnan, W.J. Steyn, J. Harvey) Springer Verlag, Berlin.

Geiger, R., R.H. Aron, P. Todhunter. 2009. The Climate Near Ground. (7th Ed.) Rowman and Littlefield, Lanham, Maryland.

Georgi, N.J., K. Zafiriadis. 2006. The Impact of Park Trees on Microclimate in Urban Areas. *Urban Ecosystems* 9: pp.195-209.

Gillner, S., J. Vogt, A. Tharang, S. Dettmann, A. Roloff. 2015. Role of Street Trees in Mitigating Effects of Heat and Drought at Highly Sealed Urban Sites. *Landscape and Urban Planning* 143: pp.33-42.

Golden, J.S., J. Carlson, K.E. Kaloush, P. Phelan. 2007. A Comparative Study of the Thermal and Raitive Impacts of Photovoltaic Canopies on Pavement Surface Temperatures. *Solar Energy* 81: pp.872-883.

Haworth, K., E.G. McPherson. 1995. Effects of *Quercus Emory* Trees on Precipitation Distribution and Microclimate in a Semi-Arid Savanna. *Journal of Arid Environments* 31: pp.153-170.

Heisler, G.M. 1986. Energy Savings with Trees. *Journal of Arboriculture* 12: pp.113-125.

Hussein, H. E.L. Mohamed, A.O. Abd El Halim. 1993. Differential Thermal Expansion and Contraction: A Mechanistic Approach to Adhesion in Asphalt Concrete. *Canadian Journal of Civil Engineering* 20(3): pp.366-373.

Hutchinson, B. A., D.R. Mott. 1977. The Distribution of Solar Radiation Within a Deciduous Forest. *Ecological Monographs* 47, pp.185-207.

Islam, M.R., R.A. Tarefder. 2015. Coefficients of Thermal Contraction and Expansion of Asphalt Concrete in the Laboratory. *Journal of Materials in Civil Engineering* Vol 27 Issue 11.

Kim, Y.R., J.S. Lutif, J.S. 2006. Material Selection and Design Considerations for Moisture Damage of Asphalt Pavement. NDOR Research Project Number P564. Nebraska Department of Roads.

Klemm, W., B.G. Heusinkveld, S. Lenzholzer, B. van Hove. 2015. Street Greenery and its Physical and Psychological Impact on Thermal Comfort. *Landscape and Urban Planning* 138: pp.87-98.

Larcher, W., 2003. Physiological Ecology of Plants. (4th Ed.) Springer Verlag, Berlin.

Lemmon, P.E. 1956. A Spherical Densiometer for Estimating Forest Overstory Density. *Forest Science* 2(4), pp.314-320.

Llorens, P., F. Domingo. 2007. Rainfall Partitioning by Vegetation Under Mediterranean Condition. A Review of Studies in Europe. *Journal of Hydrology* 335, pp.37-54.

Lieffers, V. J., C. Messier, K.J. Stadt, F. Gendron, P.G. Comeau. 1999. Predicting and Managing Light in the Understory of Boreal Forests. *Canadian Journal of Forest Research* 29, pp.796-811.

Little, D.N., D.R. Jones. 2003. Chemical and Mechanical Processes of Moisture Damage in Hot-Mix Asphalt Pavements. National Seminar on Moisture Sensitivity in Asphalt Pavements. 37-70.

Mascaro, J. 2012. Shaded Pavements in the Urban Environment – A Case Study. *Road Materials and Pavement Design* 13 (3), pp.556-565.

Matlack, G.R. 1993. Microclimate Variation Within and Among Forest Edge Sites in the Eastern United States. *Biological Conservation* 66, pp.185-194.

McCaughey, J.H. 1987. The Albedo of a Mature Mixed Forest and a Clear-Cut Site at Petawawa, Ontario. *Agricultural and Forest Meteorology* 40: pp.251-263.

McPherson, E.G., J. Muchnik. 2005. Effects of Street Tree Shade on Asphalt Concrete Pavement Performance. *Journal of Arboriculture* 31, pp.303-310.

Mitscherlich, G. 1940. The Forest Office of Dietzhausen, *Journal of Forestry and Hunting*, 72: pp.149-188. (in German).

Napoli, M., L. Massetti, G. Brandani, M. Petralli, S. Orlandini. 2016. Modeling Tree Shade Effect on Urban Ground Surface Temperature. *Journal of Environmental Quality* 45: pp.146-156.

Nunez, M., D. Bowman. 1986. Nocturnal Cooling in a High Altitude Stand of Eucalyptus Delegatensis as Related to Stand Density. *Australian Journal of Forest Research* 16, pp.185-198.

Oke, T.R. 1987. Boundary Layer Climates, 2nd Edition. Methuen, London.

Oliver, S.A., H.R. Oliver, J.S. Wallace, A.M. Roberts. 1987. Soil Heat Flux and Temperature Variation with Vegetation, Soil Type and Climate. *Agriculture for Meteorology* 39: pp.257–269.

Ovington, J.D. 1954. A Comparison of Rainfall in Different Woodlands. *Forestry London* 27: pp.41-53.

Parisi, A.V., M.G. Kimlin, D. Turnbull. 2001. Spectral Shade Ratios on Horizontal and Normal Surfaces for Single Trees and Relatively Cloud Free Sky. *Journal of Photochemistry and Photobiology* B Biology 65, pp.151-156.

Qiao, Y., G.W. Flintsch, A.R. Dawson, T. Parry. 2013. Examining Effects of Climatic Factors on Flexible Pavement Performance and Service Life. *TRR* 2349: pp.100-107.

Schmidt, R.J, P.E. Graf. 1972. Effect of Water on Resilient Modulus of Asphalt-Treated Mixes. Proceedings of the Association of Asphalt Paving Technologists 41: pp.118-162.

*Schneider, C.A., W.S. Rasband, K.W. Eliceiri. 2012.* NIH Image to ImageJ: 25 years of image analysis*, Nature methods 9(7): pp.671-675.*

Scott, K.I., J.R. Simpson, E.G. McPherson. 1999. Effects of Tree Cover on Parking Lot Microclimate and Vehicle Emissions. *Journal of Arboriculture* 25: pp.129-142.

Shahin, M.Y, B.F. McCullough. 1972. Prediction of Low Temperature and Thermal-Fatigue Cracking in Flexible Pavements. Texas Highway Department, Research Report Number 123-14.

Shahrestani, M., R. Yao, Z. Luo, E. Turkbeyler, H. Davies. 2015. A Field Study of Urban Microclimates in London. *Renewable Energy* 73: pp.3-9.

Shashua-Bar, L., O. Potchter, A. Bitan, D. Boltansky, Y. Yaakov. 2010. Microclimate Modelling of Street Tree Species Effects Within the Varied Urban Morphology in the Mediterranean City of Tel Aviv, Israel. *International Journal of Climatology* 30: pp.44-57.

Shi, X., Y. Rew, C.S. Shon, P. Park. 2015. Controlling Thermal Properties of Asphalt Concrete and their Effects on Pavement Surface Temperature. Transportation Research Board Annual Meeting, Washington, D.C., Paper 15-3651.

Shuttleworth, W.J. 1989. Micrometeorology of Temperate and Tropical Forest. *Philosophical Transactions of the Royal Society of London*, B, 324: pp.299-334.

Si, W., B. Ma, N. Li, J.P. Ren, H.N. Wang. 2014. Reliability-Based Assessment of Deteriorating Performance to Asphalt Pavement Under Freeze-Thaw Cycles in Cold Regions. *Construction and Building Materials* 68: pp.572-579.

Souch, C.A., C. Souch. 1993. The Effect of Trees on Summertime Below Canopy Urban Climates: A Case Study Bloomington, Indiana. *Journal of Arboriculture* 19: pp.303-312.

Stempihar, J.J., T, Pourshams-Manzouri, K.K. Kaloush, M.C. Rodezono. 2012. Porous Asphalt Pavement Temperature Effects on Overall Urban Heat Island. Annual Meeting of the Transportation Research Board, Washington, D.C.

Stidger, R.W. 2002. Diagnosing Problem Pavements. *Better Roads*, June 2002.

Sturm, M. 1992. Snow Distribution and Heat Flow in the Tiaga. *Artic and Alpine Research* 24: pp.145-152.

Sydnor, T.D., D. Gamstetter, J. Nichols, B. Bishop, J. Favorite, C. Blazer, L. Turpin. 2000. Trees Are Not The Root of Sidewalk Problems. *Journal of Arboriculture* 26, pp.20-29.

Tabatabaee, H.A., R. Velasquez, H.U. Bahia. 2012. Predicting Low Temperature Physical Hardening in Asphalt Binders. *Journal of Construction and Building Materials* 34: pp.162-169.

Timm, D.H., V.R. Voller. 2003. Field Validation and Parametric Study of a Thermal Crack Spacing Model. Association of Asphalt Paving Technologists – *Proceedings of the Technical Sessions* 72, pp.356-387.

Tran, N., B. Powell, H. Marks, R. West, A. Kvasnak. 2009. Strategies for Design and Construction of High-Reflectance Asphalt Pavements. *TRR* 2098.

US Environmental Protection Agency. 2008. Cool Pavements. Reducing Urban Heat Islands: Compendium of Strategies.

US Climate Data. 2109. Athens, Ohio. https://www.usclimatedata.com/climate/athens/ohio/united-states/usoh0037

Vailshery, L.S., M. Jaganmohan, H. Nagendra. 2013. Effect of Street Trees on Microclimate and Air Pollution in a Tropical City. *Urban Forestry and Urban Greening* 12: pp.408-415.

van den Beldt, R.J., J.H. Williams. 1992. The Effect of Soil Surface Temperature on the Growth of Millet in Relation to the Effect of *Faidherbia albida* Trees. *Agricultural and Forest Meteorology* 60: pp.93–100.

Viereck, L.A. 1965. Relationship of White Spruce to Lenses of Perennially Frozen Ground, Mount McKinley National Park, Alaska. *Artic* 18: pp.262-267.

Vis, M. 1986. Ingterception, Drop Size Distribution and Rainfall Kinetic Energy in Four Colombian Forest Ecosystems. *Earth Surface Proceedings Landscape* 11: pp.591-603.

Weather Underground. 2018 Athens, Ohio. https://www.wunderground.com/wundermap?radar=1

Willway, T., S. Reeves, L. Baldachin. 2008. Maintaining Pavements in a Changing Climate, The Stationary Office, London.

Xiao, Q., E.G. McPherson, S.L. Ustin, M.E. Grismer, J.R. Simpson. 2000. Winter Rainfall Intercption by Two Mature Open-Grown Trees in Davis, California. *Hydrological Processes* 14: pp.763-784.

Xiao, Q., E.G. McPherson. 2002. Rainfall Interception by Santa Monica's Municipal Urban Forest. *Urban Ecosystems* 6: pp.291-2002.

Yu, X., J. Wei, Y. Lin, Y. Luo, Y. Wang, L. Yin. 2013. Effects of Moisture on Rheological Properties of PAV Aged Asphalt Binders. *China Petroleum and Petrochemical Technology*, 15: pp.38-44.

Zhang, Z., Y. Lu, H. Pan. 2013. Cooling and Humidifying Effect of Plant Communities in Subtropical Urban Parks. *Urban Forestry and Urban Cooling* 12: pp.323-329.

Zimmerman, A., W. Wilcke, H. Elsenbeer. 2007. Spatial and Temporal Patterns of Throughfall Quantity and Quality in a Tropical Montane Forest in Ecuador. *Journal of Hydrology* 343, pp.80-96.

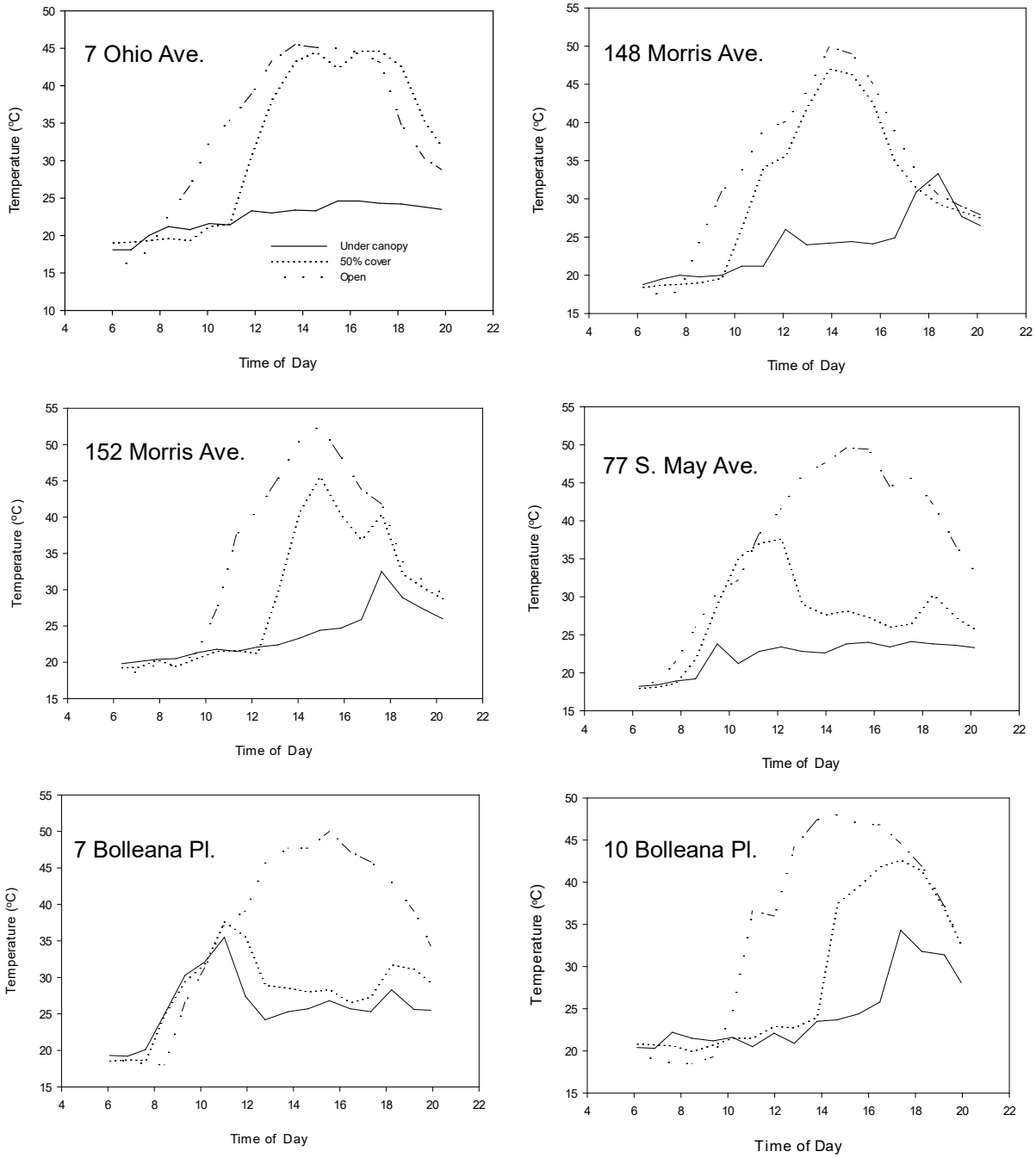


***Figure A1. Temperature through the Day in Selected Pavement Plots Under and Adjacent to Tree Canopies.***

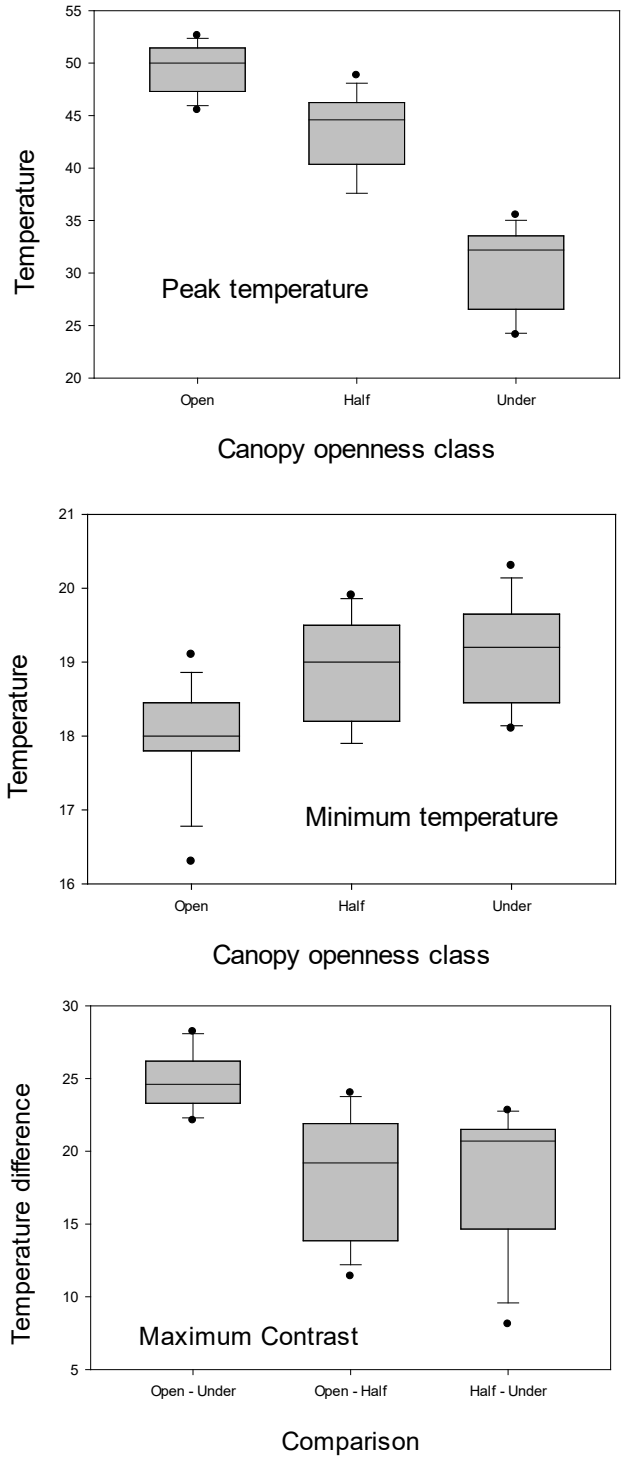


***Figure A2. Temperature Extremes in Pavement Plots Under and Adjacent to Tree Canopies. Top: peak temperature between sunrise and sunset (scale range 68-131°F). Center: minimum temperature (scale range 61-70°F). Bottom: maximum temperature contrast (1°C = 1.8°F).***

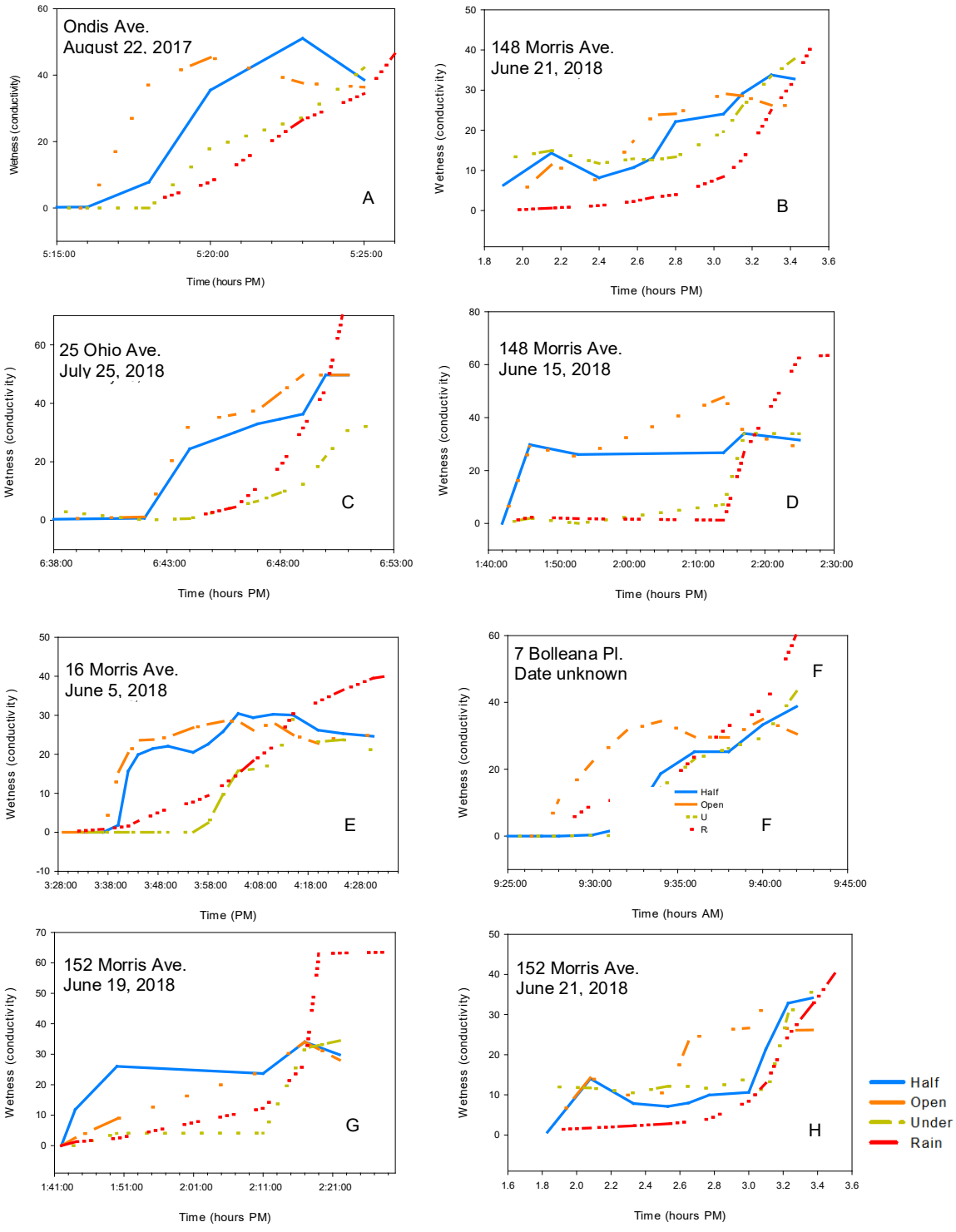


***Figure A3. Accumulation of Moisture through the Course of Rain Showers on Test Plots, mostly June and July 2018.***

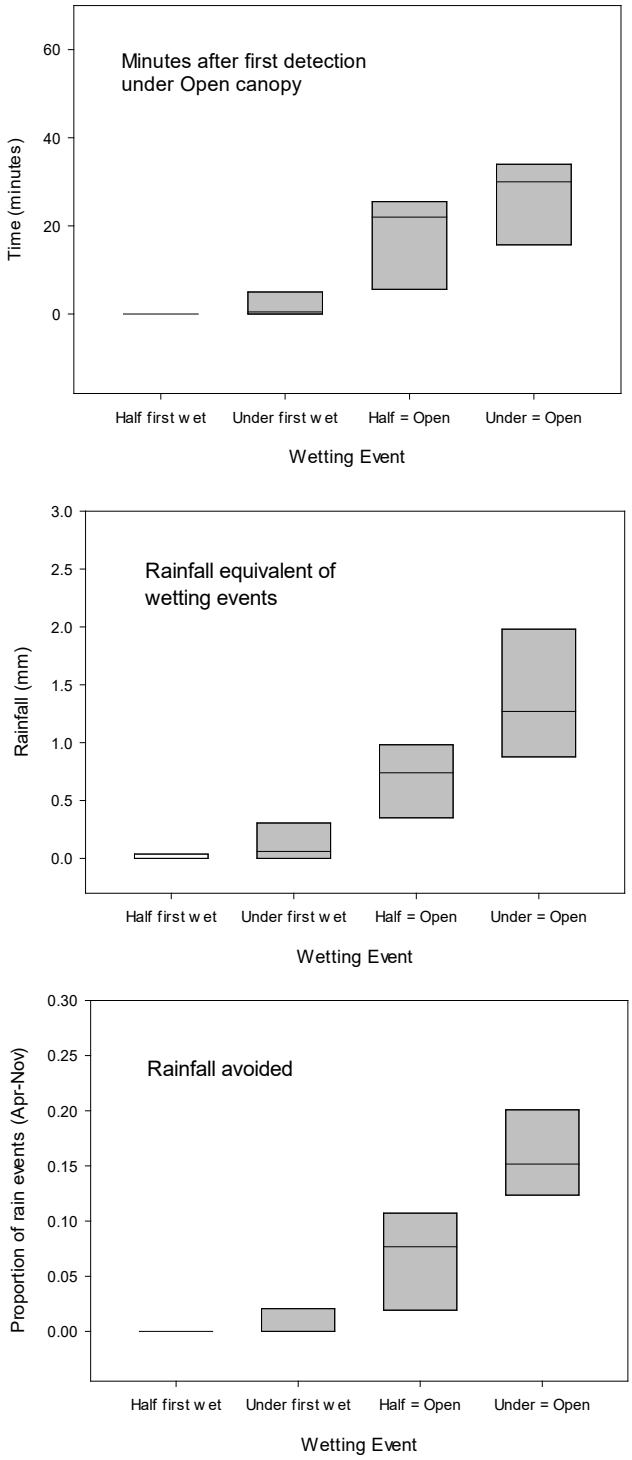


***Figure A4. Rainfall in Pavement Plots Under and Adjacent to Trees in Athens, Ohio. Top: Time elapsed after moisture first detected in open-sky plots; Center: Rainfall equivalents judged from on-site rain gauges (1 mm = 0.04 in); Bottom: Rain events entirely or partially avoided under a tree canopy.***

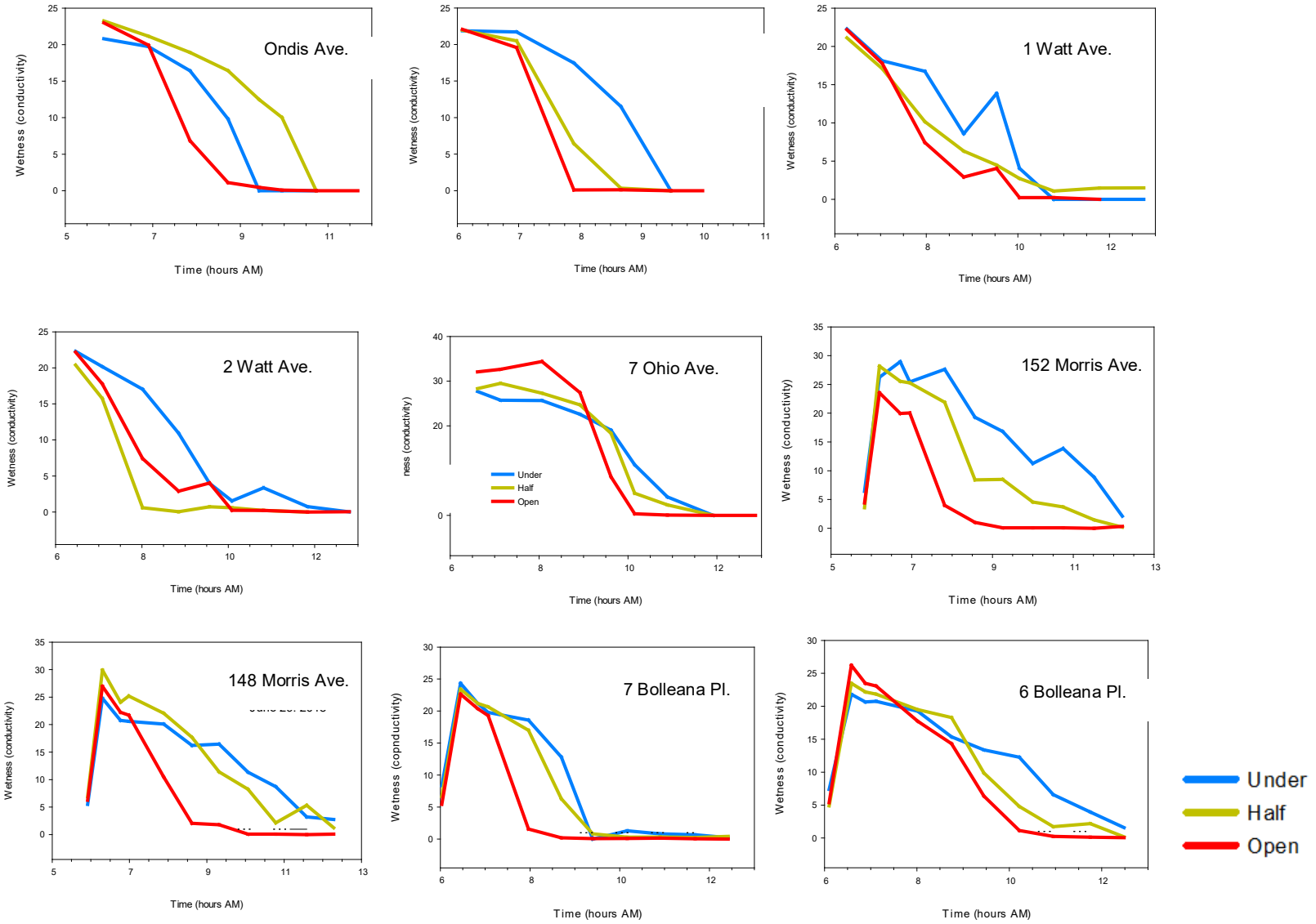


***Figure A5. Drying of Experimentally Wetted Pavement Plots Under and Adjacent to Trees in Athens, Ohio.***

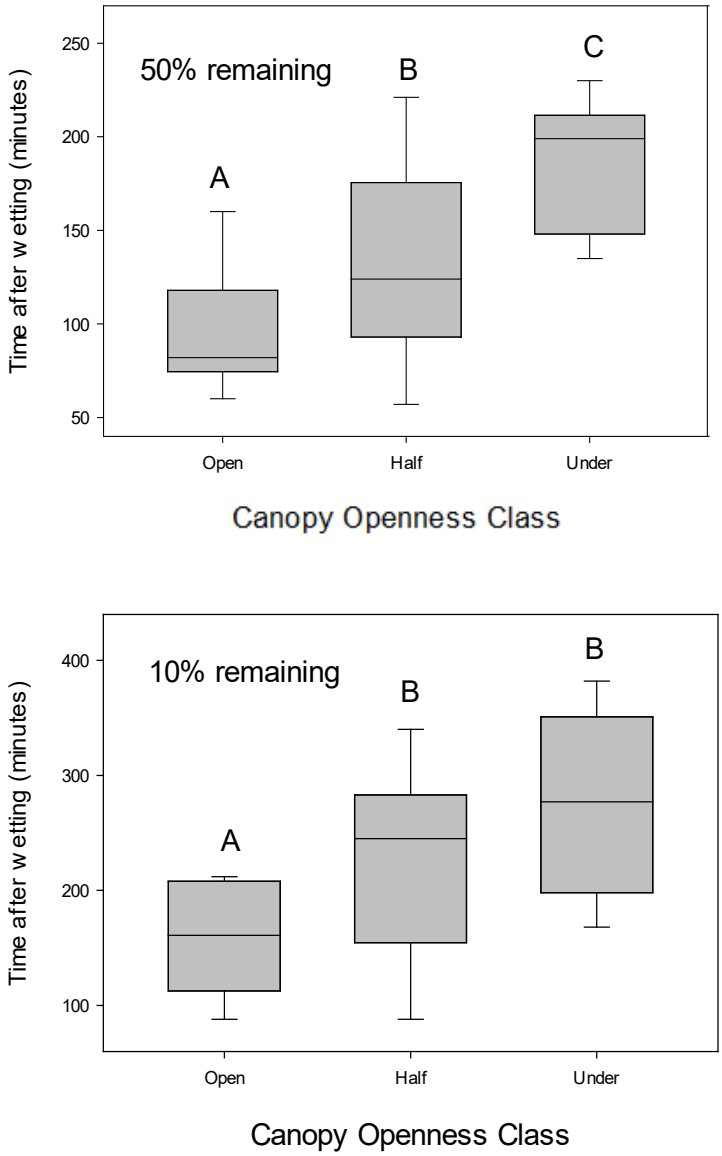


***Figure A6. Drying Rates of Experimentally Wetted Pavement Under and Adjacent to Tree Canopies. Top: time to 50% of initial wetness value; Bottom: time to 10% of initial wetness value. Letters indicate groups distinguishable by Wilcoxon Comparisons ($p < 0.05$).***

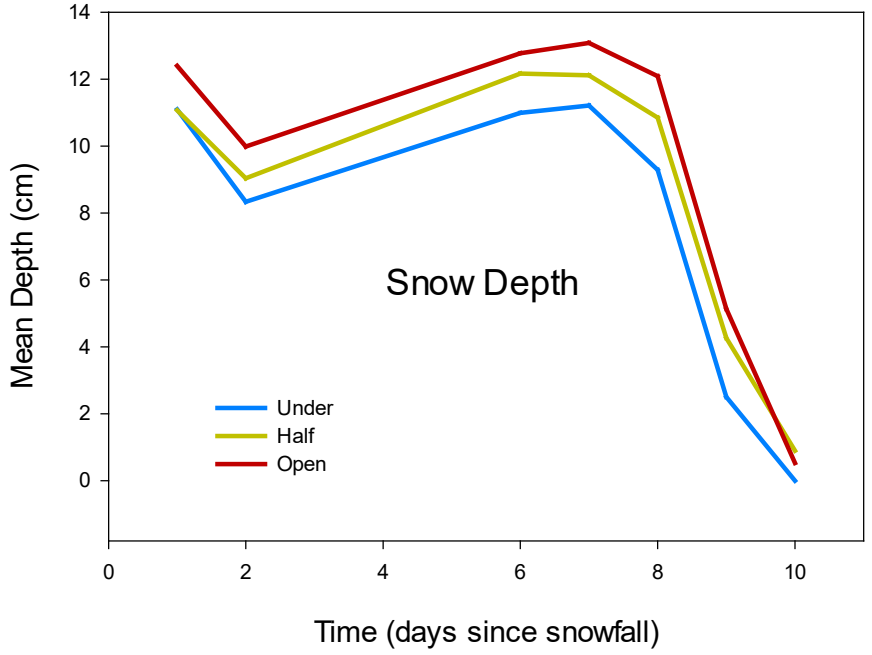


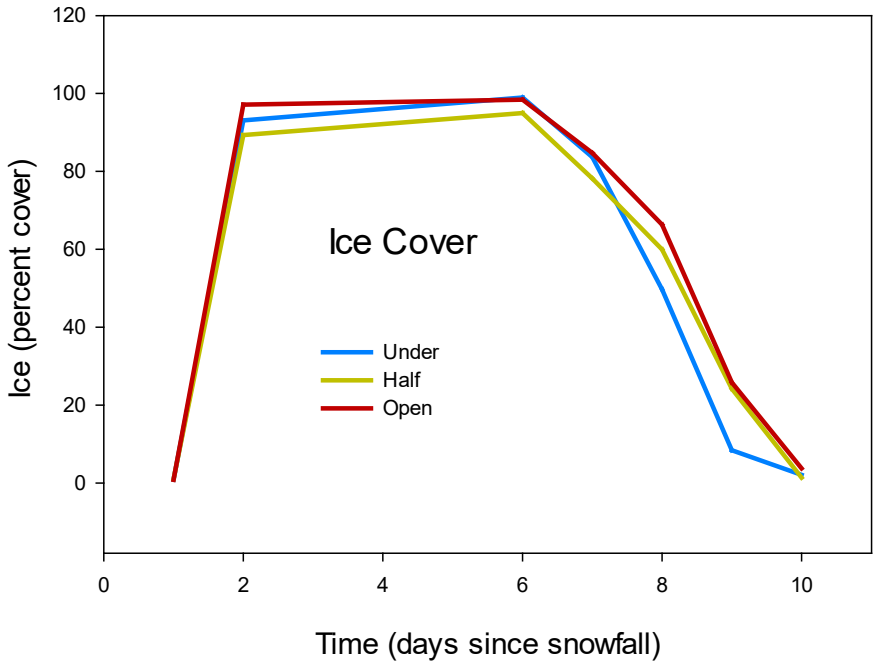


***Figure A7. Snow Depth and Ice Cover on Pavement Under and Adjacent to Tree Canopies. Top: Snow depth; Bottom: Ice cover. (1 cm = 0.39 in).***

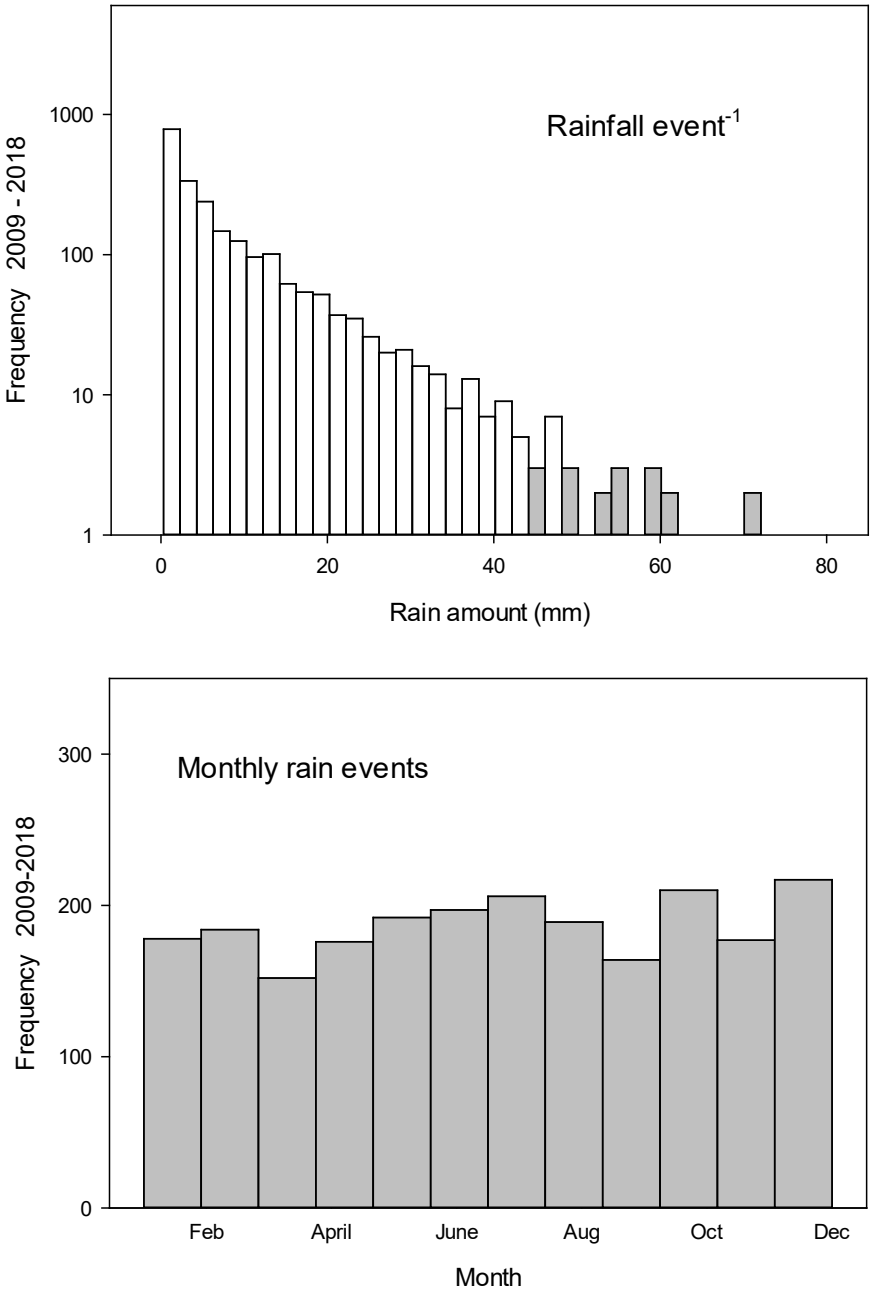


***Figure A8. Frequency of Rainfall Events at the Ohio University Airport, Albany, Ohio, 2009-2018. Top: Ranked by event size; Bottom: Frequency by month. (25 mm = 1 in).***

***Table A1. Rain wetting in twenty-four pavement plots under and adjacent to tree canopies. Wetting is described in Under and Partial plots as time and amount relative to Open plots. Deposition at first wetting and equivalence to Open is estimated by reference to rain gauges. Rainfall avoided is estimated as the proportion of storms depositing the observed amount of rainfall or less at a nearby airport over a ten-year period. Mean, standard deviation, and median values.***

| | | **First wetting occurs** | | **Wetness equivalent to Open** | |
|---|---|---|---|---|---|
| **Plot classification** | | Under | Partial | Under | Partial |
| **Time after Open (minutes)** | mean | 3.38 | 0.13 | 30.83 | 23.06 |
| | standard deviation | 6.26 | 0.35 | 21.2 | 22.79 |
| | median | 0.5 | 0 | 30 | 22 |
| **Deposition after Open (mm)** | mean | 0.14 | 0.02 | 1.62 | 0.8 |
| | standard deviation | 0.18 | 0.04 | 1.09 | 0.61 |
| | median | 0.06 | 0 | 1.27 | 0.74 |
| **Deposition after Open (in)** | mean | 0.0055 | 0.0008 | 0.0638 | 0.0315 |
| | standard deviation | 0.0071 | 0.0016 | 0.0429 | 0.0240 |
| | median | 0.0024 | 0.0000 | 0.0500 | 0.0291 |
| **Rainfall avoided (percent of storms)** | mean | 1.2 | 0 | 27.6 | 13.3 |
| | standard deviation | 2.1 | 0 | 10.7 | 11.1 |
| | median | 0 | 0 | 25.5 | 12.9 |

**APPENDIX B: EFFECTS OF TREE CANOPY ON PAVEMENT CONDITION.**


## Abstract

Tree canopies control the physical microenvironment below them suggesting that tree shading is relevant to asphalt pavement condition and service life. This study documents pavement condition under and adjacent to tree canopies in small plots along rural roads in southeastern Ohio. Six measures of pavement condition are compared with measures of canopy openness, tree size, proximity, and species identity to test the hypothesis that canopy cover affects pavement condition. Environmental gradients unrelated to trees are included in the analysis to judge the relative contribution of trees in the context of a realistic road environment. Four measures of surface texture were negatively related to canopy openness suggesting that tree canopies promote pavement degradation. However, the incremental effects of shading were small in absolute terms, and regression models indicate contributions from landform and pavement construction. Pavement of similar age on a nearby bike path showed no tree-canopy effect, suggesting an interaction of tree canopy with pavement loading. Presence and length of cracks showed minimal or no canopy openness effects in regression models, responding instead to measures of landform, soil density, and road engineering. Pavement condition in partial-covered plots (45-55% canopy cover) were indistinguishable from open-sky plots (100% open) but significantly different from completely covered plots (>95% covered). We conclude that tree canopy contributes to pavement surface condition in interaction with traffic loading but has no measurable effect on pavement cracking. Because partial coverage is typical of rural roads and complete coverage is rare, we conclude that tree canopies only rarely affect asphalt pavement condition. Considering the substantial aesthetic, climatic, and the suggested safety benefits of roadside trees, pruning to extend pavement surface life should be minimized, targeted to specific sites only as condition issues arise.

## Introduction

Trees are an integral part of the Ohio roadscape, abundant along a significant mileage of low- to medium-volume roads in both urban and rural areas. Because trees modify the microclimate beneath them, and because climate is an important contributor to pavement degradation, it has been suggested that trees determine the service life of asphalt pavement in rural roads [McPherson and Muchnick, 2005; Matlack et al., unpublished a]. Asphalt is the most common road surface used in the United States, comprising 95% of total lane length [Federal Highway Administration, 2015] and covering 99.8% of lane length in rural roads in Ohio. Several million dollars are spent annually on maintenance of rural roads in Ohio. Thus, if roadside trees can be shown to affect pavement condition there is considerable potential for financial benefit for the state of Ohio. However, the physical mechanism connecting trees and pavement condition is unclear. Trees potentially extends service life by protecting pavement from solar radiation and rainfall. Alternatively, trees may contribute to pavement degradation by delaying evaporative drying [Naik et al., 2017; Matlack et al., unpub a]. Although trees have been demonstrated to affect pavement microclimate in controlled trials, the effect of tree proximity has rarely been tested in realistically complex road environments. In this study, we examine pavement condition in actual traffic-bearing road sections in southeastern Ohio. This study compares pavement condition with tree size, coverage, proximity, and species and with a range of environmental gradients unrelated to trees, to partition the relative contribution of roadside trees to pavement condition.

*Pavement and climate*

Climate is one of the most important factors controlling the service life of asphalt pavement [Akbari et al., 2001; Zongzhi et al., 2002]. For example, solar heating softens the mastic binder potentially leading to rutting, shoving, and bleeding (exudation of binder) with traffic loading on a scale of months or years [Willway et al., 2008]. Solar heating causes loss of flexibility by oxidation and volatilization potentially resulting in failure of the binder under tire abrasion causing "raveling" of the pavement surface [ODOT, 2004]. Conversely, cool pavement resists softening and deformation under traffic loading, and, so, lasts longer [Cominsky et al., 1994]. At very low temperatures tensile cracking occurs in fresh asphalt, but cracking appears at progressively warmer temperatures as asphalt ages [Alavi et al., 2015].

On a daily time scale, solar heating drives a diurnal cycle of expansion and contraction which can lead to "fatigue" cracking analogous to fatigue failure in metals [Timm and Voller, 2003; Alavi et al., 2015]. Cracking, especially transverse cracking, appears to be caused by an interaction of thermal cycling with flexibility due to age, thermal cycling, and a large number of load cycles [Tabatabaee et al., 2012; Quiao et al., 2013]. Thermal cycling aggravated by traffic loading causes many of the familiar patterns of cracking observed in asphalt pavement (e.g. alligator, longitudinal, transverse, block, reflective, and edge cracking) [Asphalt Institute, 2009]. Modeling heating effects in the Los Angeles basin Akbari et al. [2001] predicted that a 10°C (18°F) decrease in pavement temperature could lead to a 25-fold increase in longevity.

Using data from Minnesota, Washington, and Virginia, Quiao et al. [2013] applied sensitivity analysis to judge the relative importance of temperature, precipitation, wind speed, percent sunshine, groundwater level, and temperature variation on four forms of pavement deterioration. In each case, temperature and temperature variation were most influential,

potentially increasing longitudinal cracking, transverse fatigue cracking, and AC rutting. In the Virginia trial, as little as 5% increase in temperature decreased the service life of asphalt pavement by more than 20%.

Climate also affects pavement in terms of moisture including condensation, evaporation, and rain wetting. Water may penetrate natural pores in the pavement matrix (asphalt concrete is naturally approx. 8% porous), or it may find its way into microcracks formed by thermal cycling or traffic loading [Si et al., 2014]. Water may also be suspended within the binder material [spontaneous emulsification; Little and Jones, 2003].

The severity of most forms of pavement damage is greater with water present [Stidger, 2002]. Pavement stiffness, for example, can be dramatically reduced by water saturation. Schmidt and Graf [1972]. Humidity at realistic levels (e.g. 80%) reduces pavement performance, and aged pavement appears to be more vulnerable than freshly laid. In lab simulations of pavement aging at varying levels of humidity [Yu et al., 2013], creep stiffness increased at high humidity and failure temperature decreased. Forms of deterioration unrelated to fatigue (shoving, pothole formation, raveling, bleeding) are also aggravated by water [Adlinge and Gupta 2010].

Damage may occur within the asphalt binder or between the binder and the aggregate; water reduces both adhesive and cohesive strength [Little and Jones, 2003]. Molecular detachment allows a thin film of water between aggregate and binder. Binder is then separated from the aggregate by the physical action of water in the micro-cracks [Willway et al., 2008]. Water exerts pore pressure on the surrounding asphalt matrix due to mechanical compression by heavy traffic ("pumping"); the rate of crack formation is proportional to the number of load cycles [Little and Jones, 2003]. Mechanical pumping can lead to raveling and visible crack formation [Wolters, 2003; Dawson, 2014].

The average service life of asphalt pavements before a full-depth reconstruction is required ranges from approximately nine years in regions with wet climates and freezing winter temperatures to 20–40 years in dry regions, a generalization which holds across Asphalt Institute traffic classes I – IV [Boyer et al., 1999] implying a pavement response to moisture. After approximately 40 years expensive replacement is necessary [Willway et al., 2008].

*Trees and pavement*

Numerous studies have compared solar heating between tree-shaded and unshaded pavement in urban settings [reviewed in Naik et al., 2017]. Several effects are immediately apparent. First, solar-heated pavement can become quite warm, sometimes exceeding 60°C [e.g. Scott et al., 1999; Golden et al., 2016; Klemm et al., 2017]. In Ezurum, eastern Turkey, asphalt concrete in early afternoon in summertime was 6.5°C (11.7°F) warmer than dry soil and 11.8°C (21.2°F) warmer than grass-covered soil, leading to a 5.2-7.5°C elevation in air temperature over pavement [Yilmaz et al., 2008]. In Phoenix, Arizona, pavement (67°C) was considerably warmer than air (38°C) at mid-afternoon in late summer, although pavement and air were almost equal at dawn [Stempihar et al., 2012].

Second, pavement temperature is consistently lower under a tree canopy than in adjacent open areas in all studies. Shade can reduce pavement temperature by as much as 11-25°C (20-45°F) relative to nearby unshaded areas [Akbari et al., 1997], with maximum differences observed in early afternoon [e.g. Vailshery et al., 2013; Coutts et al., 2016; Matlack et al., unpublished a].

As a result, thermal cycling is less pronounced in the shade of buildings or trees [Golden et al., 2007]. Similarly, shade reduces air temperature above pavement relative to nearby unshaded sites. Simpson [1998] estimated that midday air temperatures in urban areas can be reduced 0.04-0.2°C (0.7-0.4°F) for each 1% of additional canopy cover.

Relatively few studies have considered rain interception by trees, so generalization about tree effects on pavement moisture is difficult. The urban forest has been reported to intercept 15-27% of rainfall, preventing a proportion of rain from reaching the ground and potentially reducing standing water on pavement [Crockford and Richardson, 1990; Xiao et al., 2000; Xiao and McPherson, 2002; Matlack et al., unpublished a]. In light rainfall, a tree canopy may completely protect the pavement beneath although surrounding pavement is thoroughly wetted [GRM personal observation]. Deciduous trees monitored in Oakland, California, intercepted 14-27% of rainfall over a 7-month period [Xiao and McPherson, 2011], with degree of water capture and diversion differing between species. The water holding capacity of the crown was exceeded in large storms, so pavement protection is only available in small-moderate rainfall events. However, a leafy canopy can substantially reduce the amount of rain reaching the pavement when rainfall is distributed among many small events [Matlack et al., unpublished a].

Relative humidity is commonly higher under the urban tree canopy, confirming observations of trees in forests. Humidity can be as much as 27-33% higher under street trees than in nearby urban areas without a canopy [Souch and Souch, 1993; Georgi and Zafirdis, 2006] suggesting that trees delay evaporation of pavement moisture. On an individual tree basis, relative humidity in streets of Thessaloniki, Greece, correlated with the amount of light penetrating the canopy, which was related to species identity [Georgi and Zafirdis, 2006]. Trees may substantially extend the period of pavement wetness after a storm [Matlack et al., unpublished a] because they block solar radiation that would otherwise cause evaporation. There is also some evidence that trees extend pavement life by reducing deposition of snow [Matlack et al., unpublished a].

Pavement degradation by thermal cycling, aging, and moisture penetration all depend on exposure to the open sky so it is reasonable to assume that tree canopies, which block the sky, would mitigate such damage [Adlinge and Gupta, 2010]. An innovative study on suburban streets of Sacramento, California reported longer service life in pavement sections under tree canopies, an effect the authors attributed to reduced thermal cycling [McPherson and Muchnick, 2005].

It is also possible that trees aggravate moisture-driven forms of degradation by delaying evaporation in the shade of the canopy. Undoubtedly all of these processes work simultaneously, but the relative importance of each in a real pavement situation remains to be determined. It should be noted that the pavement microclimate in rural roads is also influenced by a variety of factors unrelated to tree shading including landscape position, drainage, traffic patterns, and slope. Landforms and buildings, for example, can block solar radiation. In some cases, urban geometry appears to be more important to pavement heating than the presence of trees [e.g. Johansson and Emmanuel, 2006; Coutts et al., 2016; Sanusi et al., 2016] – in some cases presence of trees was only secondarily important [Shahrestani et al., 2015].

Unfortunately, the small number of studies on shading and pavement condition have been limited to dry, subtropical climates with little seasonal variation [e.g. McPherson and Muchnik, 2005; Shashua-Bar et al., 2010; Mascaro, 2012]; less is known about urban microclimate in seasonally wet and cold regions such as Ohio [Coutts et al., 2016]. Because water

and temperature variation play important roles in pavement deterioration, failure to consider moist, seasonally cold regions is a serious omission. Anecdotal reports from road managers in Ohio suggest that roadside trees increase the amount and duration of pavement wetness and thereby reduce structural performance [Naik et al., 2017] but this remains to be tested.

The results described above demonstrate that the microclimatic effects observed in natural forests also apply in human-created landscapes. The ranges of temperature and humidity measured in urban studies are similar to ranges determined to be critical in laboratory studies of pavement performance suggesting that tree shading is relevant to pavement condition and service life [Matlack et al., unpublished a]. In this study we document pavement condition under tree canopies along rural roads in southeastern Ohio. Pavement condition is compared with measures of canopy density, tree size, proximity, and species identity to test the hypothesis that canopy cover affects pavement condition. Environmental gradients unrelated to trees are included in the analysis to judge the relative contribution of trees in the context of the real road environment. Three types of road are considered to shed light on the physical mechanisms of environmental effects.

## Site Selection, Description, and Location

Pavement condition was assessed at 75 pavement sites in rural Athens County, Ohio (39° 12' – 39° 26'N, 81° 56' – 82° 15' W). The dominant landform is a highly eroded peneplain dissected by many small, steep-sided stream valleys. Secondary and tertiary roads predominantly follow ridges or valley bottoms and show considerable variation in slope and landscape position. Soils are highly leached silt and sandy loams derived from Pennsylvanian parent material [Lucht et al., 1985]. Local concentrations of clay are susceptible to slumping and contraction, frequently distorting pavement on rural roads. Athens falls in the Köppen-Geiger "humid subtropical" climate zone with warm, humid summers and mild winters [Kotteck et al., 2003]. Daily average January temperatures range from 18°F (-8°C) – 39°F (4°C) and July temperatures range from 61°F (16°C) – 86°F (30°C) [PRISM Climate Group, 2015]. The region receives approximately 40 in (102 cm) of precipitation annually, well distributed through the year. Freezing temperatures may occur anytime between November and March, but temperature rarely remains below 32°F (0°C) for more than 7 or 8 days.

Roadside trees are generally deciduous species (species that lose their leaves in the winter) native to the Central Hardwoods forest type, or transplants from the moist-temperate zones of western Europe or eastern Asia [Zanon, 2014]. Common roadside species include *Carya spp* (Hickory species), *Quercus alba* (white oak), *Quercus rubrum* (red oak), *Acer rubrum* (red maple), *Acer saccharum* (sugar maple), *Juglans nigra* (black walnut), and *Prunus serotine* (black cherry); lowland sites frequently have *Platanus occidentalis* (sycamore) and *Acer negundo* (box elder). Forest covers approximately 68% of the study area as a result of widespread abandonment from agriculture in the early-mid twentieth century [Monsted, 2017], resulting in frequent shading of rural roads.

Road sites were standardized to a pavement age of 10-12 years to ensure comparability between sites and to allow maximum opportunity for pavement degradation. All sites were surfaced with the original asphalt concrete; sites showing evidence of surface amendments such as chip-and-seal or patching were avoided. At each site, three 6.6 ft × 6.6 ft (2m × 2m) permanent plots were established to allow comparison between canopy conditions. Plots were positioned

to avoid cracking obviously related to seams between pavement courses and to avoid slumping at the pavement edge, which is common in the study area. Potholes and other major forms of pavement failure were avoided. One of the three plots was positioned under the tree canopy ("Under"), one plot was partial under ("Partial"), and the third plot was exposed to open sky ("Open") to provide a control for local site conditions. Plots were selected with a spherical densiometer [Lemmon, 1956] based on canopy coverage in a 90$^{o}$ arc of sky immediately above the plot: Under plots were >95% covered; Partial plots were selected for 45% – 55% coverage, and Open plots had no canopy coverage (100% open sky). All three plots were situated on the same section of pavement ensuring consistent pavement age, structure, and composition at each site. All three plots at each site were within 330 ft (100 m); most were separated by < 130 ft (40m).

## Data Collection Methods

### Road Environment

Each plot was described in terms of fourteen environmental variables which have been shown elsewhere to affect pavement condition. Canopy openness was measured precisely by photographing the canopy with a hemispherical lens (F 11.5 ft (3.5 m), 167$^{o}$) on a horizontally mounted camera at 4.6 ft (1.4 m) above the road surface following the method of Chianucci and Cutini [2013]. Images were imported into the ImageJ image processing environment, and thresholded to maximize contrast between sky and foliage. Total foliage cover was measured in a circular RoI using the *histogram* function [Schneider et al., 2012].

At each plot, pavement width, proximity to the pavement edge, and elevation of the pavement surface above soil at the edge ("Dropoff") were measured. Camber (cross-slope) of the pavement ("Camber") was measured as the maximum vertical variation relative to a 6.6 ft (2 m) leveling rod within the plot. Position in the larger landscape ("Landscape") was assigned to one of five categories: "upland", "high slope", "mid slope", "low slope", and "flood plain". The immediate slope position of the plot was described in terms of vertical variation from the road surface to a point 32.8 ft (10 m) beyond the nearest pavement edge ("Adjacent") and at a similar point on the opposite side of the road ("Opposite").

Because force applied to the pavement is related to angular momentum of traffic, curvature of the road was measured. The position of each plot was documented using a hand-held geographic positioning unit (Etrex 25, Garmin Ltd, Olathe, Kansas) and compared with two points 66 ft (20 m) up and down the road axis, respectively. Curvature at each plot was estimated as the oblique angle of a triangle constructed using the three points. Location of the plot on the inside or outside of the curve was noted.

The size and position of roadside trees was described in terms of distance from the plot to the nearest trunk > 4 in (100 mm) diameter ("Nearest"), the diameter of the nearest trunk at 4.6 ft (1.4 m) above the ground ("Diameter"), and the number of trunks > 4 in (100 mm) diameter within 33 ft (10 m) of the plot ("Number"). Species identity of the nearest tree was recorded. Compaction of the soil was estimated at four points approximately 20 in (500 mm) from the pavement edge ("Penmin", "Penmax") using a pocket penetrometer (AMS Inc., American Falls, Idaho).

**Pavement Condition**

Pavement condition was assessed in each plot in terms of four measures of surface texture and two measures of cracking. First, texture was quantified as a subjective visual estimate (SUBJ) based on the pavement condition rating system used by ODOT [2006]. Plots were assigned to one of five categories: "1" freshly laid asphalt concrete with binder covering all surfaces, "2" aggregate exposed but firmly held within the binder matrix, "3" some aggregate removed from the surface layer, "4" much aggregate removed from the surface layer and some lower layers but the original pavement surface is still evident, and "5" substantial loss of aggregate through several layers such that the original road surface cannot be recognized. Intermediate conditions were assigned fractional values.

Second, texture was quantified as fractal dimension was calculated from photographs taken by a vertically mounted camera 5.6 ft (1.7 m) above the pavement surface. Fractal dimension ("D") is a measure of spatial complexity of a surface, which has been shown to correlate well with pavement condition in controlled trials [Matlack et al. unpublished b]. High values of D are observed in freshly laid pavement; values decline as pavement surface becomes rougher. Calculations used the *Fraclac* package in the ImageJ image analysis software package [Schneider et al. 2013].

Third, lacuniarity was calculated from pavement photographs using the ImageJ software package. Lacuniarity ("lambda") describes the relative size of gaps in a spatial pattern. Values of lambda have been shown to increase as the visual assessment of damage increases above Degradation Class 2 [Matlack et al. unpublished b].

Fourth, mean texture depth ("MTD") is a commonly used volumetric method of describing pavement texture based on penetration of a calibrated microsolid with fluid properties [Yaacob et al., 2014; Pratico and Vaian, 2015]. Following ASTM E965-96, a 6.8 fl oz (200 ml) volume of glass microspheres was spread in the center of each plot and the dimensions of the elliptical smear were recorded. MTD was calculated in millimeters by dividing the volume of sand by the area of the ellipse. Matlack et al. [unpublished b] found that MTD most clearly separated subjective texture classes among four methods compared.

Cracking was assessed as crack presence ("Presence") and total length ("Length") in each plot. Cracks, when present, were traced visually using the *line* tool in the ImageJ package [Schneider et al., 2012] and summed to give total crack length.

## Data Analysis

Data were analyzed in three groups to address specific questions. First, pavement plots under bridge overpasses (7 sites) allowed to test the potential of a simple opaque canopy to influence pavement condition – a control for the porous nature of a tree canopy. Second, plots on a community bike path (12 sites) allowed the effect of tree canopy to be tested in the absence of potentially confounding variation in pavement age, mix composition, slope, foundation material, landscape position, and traffic loading. Finally, plots on rural roads (56 sites) were used to test the effect of tree canopies in the context of the complex environmental gradients found in real road situations.

In the overpass and bike path groups, pavement condition was initially compared by canopy openness (Under, Partial, and Open) using pavement values normalized to the respective Open plot, thereby removing "site" as an independent variable. Due to the small sample sizes,

contrasts between canopy classes were examined by Kruskal Wallis tests, followed by pairwise Wilcoxon tests with significance levels adjusted by the BH method as appropriate for multiple comparisons [Benjamini and Hochberg, 1995].

In bike path and road sites, linear mixed models were constructed to judge the relative importance of environmental variables in determining pavement condition. Generalized or linear mixed models (*GLMR* and *LMER* packages, respectively) were used as appropriate in each case. "Site" was included as a random variable to control for spatial autocorrelation inherent in the use of pavement triplets. Spearman nonparametric correlations were calculated between all variables, and those that correlated above r = 0.40 were removed to reduce collinearity and prevent overfitting [Dormann et al., 2013]. Environmental variables were scaled and centered beforehand, and "site" was included as a random effect. In each group (overpass, bike path, or road) models were fit systematically following the protocol recommended by Zuur et al. [2009]. Nonsignificant environmental variables were progressively removed until a) all remaining variables made a significant contribution to pavement condition ($p < 0.05$) and b) further removal decreased the AIC by < 2%. The effect of canopy openness was tested by the likelihood ratio method comparing models with and without the openness variable. All statistical analyses were conducted in R [version 3.5.3; R Core Team, 2019].

Contrasts between plots and sites were examined by Nonmetric Multidimensional Scaling (package *metaNMS*; library *lme4*) using the reduced set of environmental variables. All variables were centered and scaled beforehand. The ordination was based on Euclidean distance due to negative values in some variables, and default values specific to vegetation analysis were turned off. The relative importance of individual variables in separating sites was assessed in terms of correlations with axis scores using the *envfit* function. Canopy classes were then compared by Permutational Analysis of Variance (PERMANOVA) using the *Adonis* function.

## Results

**Overpass Plots.**

Overpass plots showed little variation in landscape position (18/21 were on the floodplain of the Hocking River), and "nearest" trees were often so distant as to be irrelevant, so variables Position, Nearest, and Diameter were omitted from this section of the analysis. Collinearity was observed between pavement width, edge distance, slope at 32.8 ft (10 m) on either side, curvature, and edge dropoff, so the predictor group at overpass sites was reduced to six variables with $r < 0.40$ in correlations: curvature, edge-dropoff, 33 ft (10 m) slope on the opposite side, pavement slope, canopy openness, and minimum penetrometer depth. Hemispherical canopy photos showed that overpass plots were very close to the desired canopy openness (Figure B1a), with no overlap between the three openness classes (Kruskal-Wallis $\chi^2 = 18.065$, $p = 0.0001$). The other five environmental variables, normalized to the respective open-sky values, showed little variation between openness classes (Kruskal-Wallis; probabilities > 0.10). NMS converged after twenty interactions with a stress of 0.0138. In the ordination (not shown) openness classes overlapped extensively and were not distinguishable by PERMANOVA ($F_{canopy} = 0.8764$, $p = 0.442$). Thus, the overpass plots were all very similar in environmental terms.

Pavement condition ranged from moderate – good (e.g. Subj classes 2.0-3.0; MTD: 0.06 in (1.5 mm) – 0.15 in (4.0 mm). However, variation was minor when normalized to the respective

Open plots (Figure B1e, Figure B1c). Two measures of pavement condition differed between openness classes in overpass sites. Lacuniarity was significantly greater in Under and Partial plots than in the respective Open plots (Figure B1b; Kruskal-Wallis $\chi^2 = 7.632$, $p = 0.0220$). MTD was less in Under plots than in Partial or Open plots (Figure B1c; Kruskal-Wallis $\chi^2 = 10.682$, $p = 0.0048$). Crack length (Figure B1d) was strongly influenced by the large number of zero values (15/21 plots), so statistical testing was not used. However, it is notable that cracking was never observed in any Under plot. Subjective texture (Figure B1e) did not show a significant difference between openness classes ($p > 0.05$), but it should be noted that all Under values were ≥ the respective Open values. Fractal D (Figure B1f) showed no difference between pavement classes ($p > 0.05$).

**Bikepath Plots.**

The bikepath pavement was approximately 12 ft (3.6 m) wide at plot locations (Table B1), with plot centers approximately 5 ft (1.5 m) from the pavement edge. Plots were generally elevated above the adjacent landscape with little curvature, as expected on a re-purposed railroad grade (Adjacent, Opposite), although several plots were flanked by high banks where the rail grade cut into a hillside. Pavement sloped very little within plots (median camber 1% (1 in per 100 in or 2 cm per 2 m) and dropped off approximately 2¾ in (70 mm) at the pavement edge. Adjacent trees were 5.5 in (140 mm) to 15.7 in (400 mm) in diameter and fairly close to the pavement plot (median nearest 23.6 ft (7.2 m)), but not abundant (0-4 stems within 33 ft (10 m)). Adjacent soil was relatively soft (0.4 in (10 mm) to 1.2 in (30 mm) penetration).

Canopy openness was easily distinguishable between openness classes (Figure B2a). Distance to the nearest tree, trees within 33 ft (10 m), and canopy openness differed significantly between openness classes (Kruskal-Wallis probabilities < 0.0000), as would be expected in variables describing tree proximity, but other environmental variables showed no correlations with canopy openness. *Acer negundo* (box elder) was significantly more common than "other species" in sites with a steep negative slope (Opposite), indicating a flood plain (Kruskal-Wallis $\chi^2 = 4.000$, $p_{opposite} = 0.0455$), and tended to be smaller in diameter than "other species" ($\chi^2 = 4.167$, $p_{diameter} = 0.0412$).

Most environmental variables in bike path sites were only weakly correlated ($r < 0.40$). Tree variables were the exception, forming a clearly defined collinear group (Nearest, Canopy, and Number) with $|r|$ values ranging from 0.53-0.74. Pavement width was positively correlated with Curvature ($r = 0.65$). To reduce collinearity in predictor data sets, two of the variables related to tree position (Nearest, Number), and path curvature (Curvature) were removed from further analysis.

Nonmetric multidimensional scaling (NMDS) of plots on the basis of environmental variables converged in twenty interactions with a stress value of 0.0233. Nearest-species groups ("*Acer negundo*" (box elder) and "other") overlapped almost entirely in the ordination of NMDS scores (not shown), and PERMANOVA did not distinguish between them ($p = 0.113$). Similarly, openness classes overlapped in ordinations and were not distinguishable ($p = 0.377$). Thus, most environmental variables did not differ with openness classes either individually or considered collectively by NMDS.

Bikepath pavement was in good condition (Table B2), with mean and median values of SUBJ, crack length, D, lambda, and MTD corresponding to the "freshly laid" and "lightly abraded"

categories described by Matlack et al. [unpublished, b]. However, Fractal D differed between normalized openness classes (Figure B2b; Kruskal-Wallis $\chi^2 = 5.116$, $p = 0.0774$) with lower values in Partial plots than in Open plots (Wilcoxon pairwise test; $p = 0.0270$). Similarly, lacuniarity differed between canopy classes (Figure B2c; $\chi^2 = 13.793$, $p = 0.0010$) reflecting the distinctiveness of the Under plots ($p_{open\text{-}under} = 0.0007$; $p_{partial\text{-}under} = 0.0051$). Subjective pavement condition, crack length, and MTD showed no differences between canopy classes (probabilities = 0.4718 - 0.7141).

The best regression model for SUBJ related pavement condition to edge dropoff indicating greater degradation with greater edge thickness (Table B3). A large number of zero values appeared in Length (no cracks were observed in 27/36 plots (75%)), so presence/absence of cracks was considered separately from length of cracks, where present. The best model of binomial presence/absence included only Dropoff (Table B3) indicating greater likelihood of cracks with a greater pavement thickness. Cracked and non-cracked plots were then compared in multivariate environment space using the NMDS calculated above. Cracked and non-cracked plots overlapped substantially in the ordination (not shown) and PERMANOVA was not able to distinguish the two classes ($p=0.306$). Crack presence/absence was also unrelated to the species identity of adjacent trees in a $\chi^2$ comparison ($p > 0.10$). Non-zero values were observed in only nine plots, so correlations with environmental variables were calculated rather than full model construction. Correlations suggest greater cracking in soft soil (Spearman $r_{penetration} = 0.69$; $p = 0.0380$) and under an open canopy ($r_{open} = 0.69$; $p = 0.0382$).

The observed distributions of pavement fractal dimension (D) and lacuniarity (lambda) in bikepath plots were very close to those expected under a normal distribution, so predictive models were constructed as a mixed linear expression (package lme; library lme4). The best fractal model included only pavement width, indicating more degraded pavement in wider pavement sections (Table B3). The best lacuniarity model included only pavement width and curvature (Table B3). Higher lacuniarity (more damaged pavement) [Matlack et al. unpublished b] was observed in wider and straighter pavement sections. MTD was tested assuming a Gamma error distribution in GLMER, however, the procedure did not arrive at a significant model. Evidently the environmental variables recorded here do not predict MTD in bikepath plots.

**Rural Road Plots**

Road plots showed greater variation in most environmental variables than bikepath plots (standard deviations; Table B4) reflecting a greater range of landscape position, traffic loading, and paving history. Bikepath plots declined more on either side than road plots (Adjacent, Opposite) reflecting their position on a re-purposed rail line built on fill above a floodplain. Bikepath plots showed lower values of Curvature, Camber, and Width, as appropriate to a rail line.

Landscape position affected rural roads in their Width, Camber and edge Dropoff. Roads tended to be wider at mid-slope than at low-slope or floodplain positions (Kruskal-Wallis, $\chi^2 = 11.791$, $p = 0.018$); slope sites had a slightly greater drop-off at the pavement edge than uplands or flood plains ($\chi^2 = 13.015$, $p = 0.0112$), and floodplain roads showed substantially less camber than any other landscape position ($\chi^2 = 45.971$, $p = 0.0000$). Landscape position was evident in roadside gradients. Roads cut into hillsides showed positive values of slope on the uphill side whereas land on uplands or floodplains fell away on both sides of the road ($\chi^2 = 12.351$, p =

0.0149). Soil was significantly softer at mid slope than in other landscape positions ($\chi^2$ = 12.238, p=0.01566). However, landscape position did not affect the proximity of roadside trees, nor their size, stem density, or openness of the tree canopy (probabilities > 0.10).

Twenty-two tree species were encountered as "nearest trees", with strong representation of *Acer saccharum* (sugar maple ~ 27 plots), *Juglans nigra* (black walnut ~ 21 plots), and *Carya* spp. (hickory species ~ 18 plots). For convenience, all species represented by fewer than ten plots were combined as "other species" (38 plots). Species identity did not correspond with variation in any other environmental variable (Kruskal-Wallis probabilities > 0.10).

NMDS of plots on the basis of environmental gradients fit two axes. A solution was reached after twenty iterations with a final stress of 0.0312. Vector fitting (R package *envft*) reveals that plots were most strongly separated by Opposite ($r^2$ = 0.998, p = 0.001), Adjacent ($r^2$ = 0.998, p = 0.001), Camber ($r^2$ = 0.108, p = 0.001), Openness ($r^2$ = 0.052, p= 0.015), and Curvature ($r^2$ = 0.032, p = 0.073). Other variables were only weakly correlated with axis scores (probabilities > 0.300). Inclusive polygons based on landscape position overlapped closely (not shown), implying little difference between sites in different positions.

Pavement was significantly more degraded in road plots than bikepath plots in every measure of pavement condition except Crack length (Table B4). In road plots pavement condition differed with landscape position (Kruskal-Wallis $\chi^2$ = 12.847, p = 0.012); Fractal dimension showed the lowest values (suggesting greatest pavement degradation) in high slope positions; and flood plains. MTD contrasted between high values (greatest degradation) in upland road plots and low values in low- and mid-slope positions ($\chi^2$ = 12.562, p = 0.014). Neither the subjective pavement index nor crack presence or length differed with landscape position (p > 0.05).

Pavement condition differed significantly according to nearest tree species. The subjective index was highest near *Quercus alba* (white oak) and lowest near *Acer negundo* (box elder) (Kruskal-Wallis $\chi^2$ = 14.289, p = 0.075) although the median difference was only 0.6 on a scale of 1.0-5.0. Lacuniarity showed the highest median values (greatest degradation) near *Acer saccharum* (sugar maple) and the lowest under *Platanus occidentalis* (sycamore) and "other species" ($\chi^2$ = 15.734, p = 0.046). MTD returned the highest values (greatest degradation) near *Carya* spp. (hickory species) and lowest near *Acer negundo* (box elder) ($\chi^2$ = 19.786, p = 0.011). Curvature, however, did not significantly affect any measure of pavement condition (probabilities > 0.05).

Within road sites, pavement condition differed between canopy openness classes (Table B5). Canopy openness class significantly separated plots on the basis of the normalized subjective index (Subj; Kruskal-Wallis $\chi^2$ = 24.017, p = 0.000) with significantly higher values (more degraded pavement) in Under plots than either Open or Partial plots (Figure B3a). However, the difference was minor (a median difference of 0.2 on a scale of 1.0-5.0). Fractal dimension was higher (less degraded) in Open and Partial plots than in plots under a tree canopy (Figure B3c; $\chi^2$ = 33.665, p = 0.000). Lacuniarity was higher (more degraded) under a canopy than Partial plots and lower in Open plots than Partial ($\chi^2$ = 45.048, p = 0.000; Figure B3d). MTD showed greater depth under a tree canopy implying greater degradation, although the separation of median values between treatments was only 8.5% ($\chi^2$ = 7.652, p = 0.022; Figure B3e). Cracks were more common in Under plots (68%) than in Partial (48%) or Open (59%). Crack length was not significantly distinguishable between canopy treatments.

Best models for each pavement condition metric are listed in Table B6. The subjective index was strongly dependent on canopy openness, with higher values in more open plots suggesting less degraded pavement under a closed tree canopy. Curvature and Opposite slopes also contributed although weakly. "Site" accounted for 46.9% of variation in Subj. However, median values in Under plots are only 6.7% greater than Open plots demonstrating only a minor difference in pavement condition.

Crack presence was positively affected by Penmin, suggesting that a harder substrate is more likely to cause cracking; crack length appeared to respond to edge dropoff (more cracking at plots with a greater drop). Crack length was strongly dependent on environmental variation within sites (only 8.8% attributed to variation between sites). In contrast, Crack presence was strongly influenced by variation between sites (52.5% between).

The best model for fractal dimension showed a positive effect of canopy openness and negative effects of opposite slope and pavement width (Table B6), implying more degraded pavement in road sections above the surrounding land and under open sky. However, this appears to be only a weak effect: 37.2% of variation in pavement quality was determined by variation between sites and the actual difference between Under and Open plots was < 1%.

Lacuniarity was sensitive to the widest range of environmental influence, responding significantly to Openness, Opposite, Dropoff, and Diameter (Table B6). Positive effects of openness, and negative responses to Opposite imply greater pavement degradation under open sky and in sections with slope dropping away from the road.

Mean Texture Depth (MTD) responded only to canopy openness (Table B6), showing deeper crevices under an open sky. It is notable that substantially greater variation was accounted for by site than canopy condition implying a relatively weak canopy contribution (Table B5); the difference between median values in Under and Open plots was only 8.5%.

## Discussion

Overhanging trees appear to have affected pavement condition in rural roads of Athens County. However, the impact of tree canopy does not appear to be a direct effect, as the literature suggest, but requires interactions with traffic loading and landscape position. Two aspects of pavement condition, abrasion of the pavement surface and formation of cracks show contrasting responses, apparently responding to different aspects of pacemen micro-environment. Thus tree canopy cannot be considered unequivocally positive or negative influence on asphalt pavement. Effective road management must consider complex landscape/ engineering/environment interactions.

*Overpass Plots.*

In the Overpass plots, a barrier above the pavement provided a degree of protection and extended service life. Plots shielded by an overpass showed no pavement cracking, in contrast to many of the respective Open plots, and significantly less vertical variation in MTD. In those plots where cracking was observed, Partial plots had shorter total crack length (mean, 46.6 ft (14.20 m)) than Open (127.6 ft (38.88 m)) suggesting that partial cover also conferred some amount of protection. The lack of cracking presumably reflects reduced thermal expansion in plots shielded from solar radiation [McPherson and Muchnick, 2005], whereas the less-degraded pavement texture may be caused by protection from UV radiation and rain wetting [Akbari et al.,

1997; Xiao et al., 2008; Adlinge and Gupta, 2010]. Lacuniarity (lambda) showed higher values in sheltered plots, suggesting that cover causes pavement damage.

The pavement environment was notably homogeneous; environment variables did not differ between openness classes, ruling out indirect effects of the overpass structure on pavement condition (such a high degree of plot similarity is expected in sites shaped by highway construction). Like an overpass, a tree canopy provides a measure of protection from thermal effects, UV, and wetting, but whether pavement protection can be generalized to tree canopies must be tested under a real tree canopy.

*Bikepath Plots.*

Bikepath plots showed little variation in curvature, camber, or elevation, reflecting their location on a re-purposed railroad grade. To the extent that plots differed on environmental gradients, most differences were minor and unrelated to the strong contrasts in canopy openness. Bikepath pavement was in relatively good condition, notwithstanding its age, and showed little effect of canopy openness. Only fractal dimension and lacuniarity responded to canopy class when tested directly, suggesting marginally less degradation in open-sky plots. Cracks were slightly more likely to be present under canopies although there was no significant difference between canopy classes in total crack length. Neither canopy openness nor any other tree-related variable appeared in regressions on any measure of pavement condition, deferring to variables such as pavement width and edge dropoff which can be interpreted in terms of construction methods and roadbed condition.

The results from the plots along the bikepath do not support a tree-canopy effect on pavement condition. Evidently a leafy canopy is sufficiently permeable to light and moisture to obscure the protective effects noted in the Overpass plots, above, and other aspects of the bikepath environment appear to have only a modest effect on pavement integrity. It is notable that pavement cracking was not associated with trees. In other studies, pavement cracking has been associated with mechanical expansion caused by roots from trees very close to the pavement edge [Nicoll and Armstrong, 1998; Wong et al., 2012], and cracking has been linked to tree presence in qualitative studies in the study area However, the presence of cracks in this present study plots was not significantly related to tree size, species, distance, density, or canopy coverage, so root extension seems unlikely as an agent of pavement degradation. Lack of damage is probably due to the distance of trees from the bikepath. All trees in these sites were > 6.6 ft (2 m) from the pavement edge whereas most studies reporting pavement cracking have used trees < 3.3 ft (1 m) from the pavement.

The lack of pavement variation observed in bikepath plots reflects the lack of heavy traffic on a recreational structure designed for bicyclists and pedestrians and the uniform grade and substrate of a repurposed rail line. With traffic and topographic variation removed, microclimatic gradients caused by the presence of trees are not sufficient to affect pavement quality. It is possible, however, that trees may affect pavement condition indirectly through interaction with processes occurring on real roads. To assess indirect effects, it is necessary to extend our analysis to the road plots.

*Road Plots.*

Rural roads included substantially more topographic and environmental variation than bikepath sites. Whereas bikepath sites were all situated on the floodplain of the Hocking River,

each of the five landscape positions was represented by at least seven sites in the Road data set. Road plots showed abundant variation in slope of adjacent land, camber, and curvature. Landscape position was significantly related to a number of road features which potentially affected pavement condition, including exposure of the road edge, soil density, and pavement camber. However, selection of plots for specific degrees of canopy openness ensured that landscape positions did not differ in the size, proximity, or arrangement of adjacent trees.

As expected, road plots were significantly more degraded than bikepath plots, presumably reflecting the heavier traffic loading on roads. Road plots generally showed considerable surface wear, with a substantial proportion of the first layer of aggregate missing. Thus the baseline for road condition is a moderately degraded surface approaching its service lifespan; and can expect these plots to show the maximum effect of all forms of wear.

In general, open-sky plots on rural roads showed a rougher pavement surface (higher values of Subj, MTD, and Fractal D and lower Lambda) than those located under tree canopies. However, there is considerable variation between indices of pavement condition. The subjective index (Subj) was dominated by canopy openness (no other environmental variables appeared in the regression model), and Open plots were statistically distinguishable from Under and Partial plots implying a negative effect of tree canopy on pavement condition. Plots under the canopy had lower values of MTD and Fractal D than Partial or Open plots, which field trials have shown to be consistent with more degraded pavement [Matlack et al., unpublished b]. Whereas MTD and Subj were narrowly influenced by canopy openness, road design, and landscape position also contributed substantially to D and Lambda.

Cracking showed a pattern of environmental response different from the metrics of abrasion discussed above. In the comparison of normalized plots, crack presence varied little (15%), and crack length was equivalent in all canopy classes. This result is contrary to the findings of field studies [McPherson and Muchnick, 2006] and controlled trials from this present study (discussed within this report) which suggest solar exposure as the factor driving pavement cracking. Instead, crack length and presence appeared to respond to edge distance, dropoff at the edge, and soil density implying that cracking is a response to foundation strength and structural weakness at the pavement margin. The importance of foundation strength and edge location is widely accepted as contributors to pavement condition [Seed, Chan, and Lee, 1962; Mallik and El Korchi, 2017], thus, it can be concluded that pavement failure by cracking is caused by mechanisms unrelated to adjacent trees.

Although several measures of surface abrasion agree on the negative effects of a tree canopy, differences between open-sky and canopy-covered plots were modest. The subjective metric differed only 0.20 (median) on a scale of 1.0-5.0, distinguishing between slightly less and slightly more than the “moderately abraded” pavement category [Matlack et al., unpublished b]. A large portion of variation in Subj (46.4%) was determined by unspecified contrasts between sites. Median MTD was only 0.0135 in (0.343 mm) greater under a tree canopy, and environmental variables, including canopy openness, contributed only 43% of variation in MTD. The difference in Fractal D between canopy classes was equivalent to 0.0009 (median values) compared with a standard deviation of 0.0022 observed between “under” plots. Under plots show lacuniarity values only 0.0359 higher than the median value observed in open-sky plots (0.2032), and several other environmental variables also made strong contributions to pavement condition.

*Caveats.*

Canopy openness figured prominently in most regression models related to surface texture, but it is important not to overlook the contributions of other environmental and structural variables. Unlike the other environmental metrics, plots were intentionally selected for extreme values of openness guaranteeing their strength in comparative tests. In addition to openness, measures of slope appear several times implying that the landscape context of a pavement section has a strong influence on surface texture, possibly related to drainage or the potential for foundation slumping on a steep slope. A bank rising from the road was associated with degraded pavement in the subjective index, fractal D, and crack length, it was positively linked to pavement condition, so a definitive statement cannot be made from these results. The influence of slope needs to be investigated in controlled trials.

The subjective index (Subj) of pavement condition and MTD are widely recognized as indices of pavement condition. However, fractal dimension (D) and lacuniarity (Lambda) are new condition metrics, only introduced to the pavement engineering community very recently [Matlack et al., unpublished b] and have not been widely tested. In this study, high values of D (high quality pavement) are significantly associated with open canopies and rising opposite slopes. D shows a fairly direct relationship to pavement quality, and is, thus, relatively easy to interpret. Lambda showed a bimodal response in controlled trials [Matlack et al., unpublished b]. The very frequent significant response of lambda to environmental variables, including unique responses to tree diameter, should be interpreted with caution.

*Tree Canopies and Pavement Condition.*

These results suggest that abrasive degradation of the surface layer in rural roads is caused by an interaction of overhanging foliage, traffic loading, and road engineering. Tree canopy appears to have a negative influence on surface condition measured by MTD, Fractal D, Lacuniarity, and the subjective index, although the mechanism by which canopy operates on pavement is not clear. This result contradicts the expectation based on studies in dry, subtropical climates [McPherson and Muchnick, 2005; Shashua-Bar, et al., 2010; Mascaro, 2012] in which fatigue in response to thermal cycling is assumed to be the primary agent. It also runs against predictions based on controlled trials [Xiao et al., 2008] which emphasized protection from rain wetting and snow accumulation but is consistent with the observation that moisture evaporates more slowly under a tree canopy [Georgi and Zafirdis, 2006]. The strong suggestion is that tree canopy has acted on pavement by extending the presence of moisture on the pavement surface.

Comparison of road plots with overpass and bikepath sites suggests a mechanism of pavement degradation. The relatively good condition of pavement beneath overpasses implies that the agent of pavement degradation comes from above, potentially including rain and sunlight. The lack of canopy effects at bikepath sites demonstrates that exposure to wetting and solar radiation alone is not sufficient to cause surface raveling; it can be inferred that tree cover affects pavement surface layers through interactions with traffic loading and landscape slope both of which are absent or minor on the bike path. Traffic loading, especially by heavy trucks, is widely recognized as an important contributor to pavement degradation [Zafir et al., 1994; Croney and Croney, 1998; Zhongzhi et al., 2002] and may contribute in rural roads by abrading and flexing pavement already made susceptible by water penetration and molecular detachment of binder [Little and Jones, 2003]. Steep slopes may increase road moisture by increasing shading

[Coutts et al., 2016; Sanusi et al., 2016] by funneling moisture onto the road foundation [Ahmed et al., 2018; Sapkota et al., 2019], or by interaction with road construction.

Road cracking appears to proceed by a different mechanism than raveling. Cracks are slightly (15%) more common under a tree canopy, possibly related to the raveling process suggested above. However, crack presence is more strongly linked to soil density and broad-scale differences between sites. Where cracks are present, crack length is best described in regression models by structural features such as edge proximity and dropoff, slope, and soil condition. These results suggest that cracking is controlled by road design, drainage, and soil properties, possibly exacerbated by sub-base moisture in the moderate- to high-rainfall climate of southeast Ohio. These results do not support a link of cracking to tree cover contrary to the findings of McPherson and Muchnick [2005].

Partial plots are most representative of actual tree cover in rural road sections. The > 95% cover in Under plots provides an extreme comparison to test mechanisms of tree impact, but Under plots are not typical of rural roads in general. Indeed, > 95% tree cover is uncommon even in forest sections (GRM personal observation). Thus, from the standpoint of practical road management, it is more important to consider pavement response to partial canopy coverage than to total cover. Observations from controlled trials [Armson et al., 2013; Gillner et al., 2015; Xiao et al., 2008] and including this study, suggest that the degree of pavement heating and wetting is proportional to the size and density of the tree canopy; partial canopies create effects intermediate between completely covered and completely open sites, and we may expect incremental microclimate effects to translate into intermediate levels of pavement degradation.

Partial plots in Overpass and Bikepath sites examined in this study were usually indistinguishable from Under and Open plots reflecting the minimal canopy effects at those sites. However, Road sites showed significant separation between Partial and other plots. In all metrics related to surface abrasion (raveling) Partial plots were significantly different from Under plots and indistinguishable from Open plots (except a slight difference in lacuniarity; crack metrics showed little difference between plots. The similarity between Open and Partial plots can be understood in terms of the rapid pavement drying accomplished by even brief exposure to sunlight. It appears that although tree cover may contribute to abrasion damage, this is only true in the extreme case of near-total canopy coverage. In the more realistic circumstances of partial (0-60%) coverage, roadside trees have no effect on pavement condition.

## Conclusion

Tree cover does control pavement microclimate in our temperate-seasonal study area, but physical effects do not translate into pavement condition as suggested by studies in dry-subtropical studies [McPherson and Muchnick, 2005; Mascaro, 2012]. Instead, pavement condition in rural roads appears to be determined by a combination of tree cover, traffic loading, and road engineering. Surface abrasion is related to tree cover in completely covered sections experiencing traffic loading, an effect probably related to retention of moisture. However, the effect is fairly minor in absolute terms. Cracking is more easily understood in terms of landform and soil condition; canopy coverage seems to be irrelevant. Thus, selective pruning might marginally improve service life in areas with > 95% canopy cover. Such areas are rare, however, even in road sections through forest. Road sections with < 60% tree cover (a much more common situation) are not impact by overhanging trees, and pruning will not improve pavement condition.

## Bibliography.


Adlinge, S.S., A.K. Gupta. 2010. Pavement Deterioration and its Causes. *IOSR Journal of Mechanics and Civil Engineering* 2: pp.6-15.

Ahmed, A., S. Hossain, M.S. Khan, A. Shishani. 2018. Data-Based Real-Time Moisture Modeling in Unsaturated Expansive Subgrade in Texas. *TRR* 2672, pp.86-95.

Akbari, H., A.H. Rosenfeld, H.G. Taha. 1990. Summer Urban Heat Islands, Urban Trees and White Surfaces. ASHRAE Transactions, Atlanta Georgia.

Akbari, H., D.M. Kurn, S.E. Bretz, J.W. Hanford. 1997. Peak Power and Cooling Energy Savings of Shade Trees. *Energy and Buildings* 25: pp.139-148.

Akbari, H., M. Pomerantz, H. Taha. 2001. Cool Surfaces and Shade Trees to Reduce Energy Use and Improve Air Quality in Urban Areas. *Solar Energy* 70: pp.295-310.

Alavi, M., N.E. Morian, E.Y. Hajj, P.E. Sebaaly. 2015. Influence of Asphalt Binder Oxidative Aging on Critical Thermal Cracking Characteristics of Asphalt Mixtures. *Journal of the Association of Asphalt Paving Technologists*, 84: pp.115-142.

Armson, D., M.A. Rahman, A.R. Ennos. 2013. A Comparison of the Shading Effectiveness of Fire Different Street Tree Species in Manchester, UK. *Arboriculture and Urban Forestry*. 39: pp.157-164.

Asphalt Institute 2009. MS-16 Asphalt in Paving, Preservation & Maintenance 4th Edition. Lexington, Ky.

Asphalt Restoration Technology Systems. 2016. Turning Back the Clock on your Asphalt Pavement. Asphalt News, http://www.asphaltnews.com/rejuvenation_pdc.htm

Benjamini Y., Y. Hochberg. 1995. Controlling the False Discovery Rate: A Practical and Powerful Approach to Multiple Testing. *Journal of the Royal Statistical Society*: Series B (Methodological), 57: pp.289-300.

Boyer, B., 1999. Life Cycle Performance. The Asphalt Institute. Available on line at http://www.asphaltmagazine.
com/archives/1999/Summer/Life_Cycle_Performance.pdf.

Chianucci, F., A. Cutini. 2013. Estimation of Canopy Properties in Deciduous Forests with Digital Hemispherical and Cover Photography. *Agricultural and Forest Meteorology* 168: pp.130-139.

Cominsky, R.J., G.A. Huber, T.W. Kennedy, M. Anderson. 1994. The Superpave Mix Design Manual for New Construction and Overlays. SHRP-A-407. National Research Council, Washington.

Coutts, A.M., E.C. White, N.J. Tapper, J. Beringer, S.J. Livesley. 2016. Temperature and Human Thermal Comfort Effects of Street Trees Across Three Contrasting Street Canyon Environments 124: pp.55-68.

Crockford, R.H., D.P. Richardson. 1990. Partitioning of Rainfall in a Eucalypt Forest and Pine Plantation in Southeastern Australia. 1. Throughfall Measurement in a Eucalypt Forest: Effect of Method and Species Composition. *Hydrological Processes* 4: pp.131–144.

Croney, D., P. Croney. 1998. Design and Performance of Road Pavements. (3rd Ed.) Mcgraw Hill.

Dawson, A. 2014. Anticipating and Responding to Pavement Performance as Climate Changes. Pages 127-157 in Climate Change, Energy, Sustainability and Pavements. (eds. K. Gopalakrishnan, W.J. Steyn, J. Harvey) Springer Verlag, Berlin.

Dormann, C., F.J. Elith et al. 2013. Collinearity, A Review of Methods to Deal with it and a Simulation Study Evaluating their Performance. *Ecography* 36: pp.27-46.

Federal Highway Administration. 2015. Public Road Length. https://www.fhwa.dot.gov/policyinformation/statistics/2013/hm12.cfm accessed 12/8/16.

Georgi, N.J., K. Zafiriadis. 2006. The Impact of Park Trees on Microclimate in Urban Areas. *Urban Ecosystems* 9: pp.195-209.

Gillner, S., J. Vogt, A. Tharang, S. Dettmann, A. Roloff. 2015. Role of Street Trees in Mitigating Effects of Heat and Drought at Highly Sealed Urban Sites. *Landscape and Urban Planning* 143: pp.33-42.

Golden, J.S. 2004. The Built Environment Induced Urban Heat Island Effect in Rapidly Urbanizing Arid Regions – A Sustainable Urban Engineering Complexity. *Environmental Science Journal of Integrated Environmental Research* 1: pp.321-349.

Golden, J.S., J. Carlson, K.E. Kaloush, P. Phelan. 2007. A Comparative Study of the Thermal and Raitive Impacts of Photovoltaic Canopies on Pavement Surface Temperatures. *Solar Energy* 81: pp.872-883.

Grote, R. et al. 2016. Functional Traits of Urban Trees: Air Pollution Mitigation Potential. *Frontiers in Ecology and Environment* 14: pp.543-550.

Gui, J., P.E. Phelan, K.E. Kaloush, J.S. Golden. 2007. Impact of Pavement Thermophysical Properties on Surface Temperatures. *ASCE Journal of Materials in Civil Engineering* 19: pp.683-690.

Johansson, E., R. Emmanuel. 2006. The Influence of Urban Design on Outdoor Thermal Comfort in the Hot, Humid City of Colombo, Sri Lanka. *International Journal of Biometeorology* 51: pp.119-133.

Klemm, W., B.G. Heusinkveld, S. Lenzholzer, B. van Hove. 2015. Street Greenery and its Physical and Psychological Impact on Thermal Comfort. *Landscape and Urban Planning* 138: pp.87-98.

Kottek, M., J. Grieser, C. Beck, B. Rudolf, F. Rubel. 2006: World Map of the Köppen-Geiger Climate Classification Updated. Meteorol. Z., 15, 259-263.

Lemmon, P.E. 1956. A Spherical Densiometer for Estimating Forest Overstory Density. *Forest Science* 2(4), pp.314-320.

Little, D.N., D.R. Jones. 2003. Chemical and Mechanical Processes of Moisture Damage in Hot-Mix Asphalt Pavements. National Seminar on Moisture Sensitivity in Asphalt Pavements. 37-70.

Lucht, T.E., D.L. Brown, N.H. Martin. 1985. Soil Survey of Athens County, Ohio. US Department of Agriculture, Soil Conservation Service.

Rajib B. Mallick, Tahar El-Korchi. 2017. Pavement Engineering: Principles and Practice, Third Edition, CRC Press, New York.

Mascaro, J. 2012. Shaded Pavements in the Urban Environment – A Case Study. *Road Materials and Pavement Design* 13 (3), pp.556-565.

Matlack G.R., I. Khoury, B. Naik. 2020a. *Roadside Trees Control Pavement Microclimate in a Moist-Temperate Region*. Unpublished manuscript.

Matlack G.R., A. Horn, A. Aldo, L.F. Walubita, I. Khoury, B. Naik. 2020b. Three Hand-Portable Methods for Assessing Surface Texture of Asphalt Pavement. Unpublished manuscript.

McPherson, E.G., J. Muchnik. 2005. Effects of Street Tree Shade on Asphalt Concrete Pavement Performance. *Journal of Arboriculture* 31, pp.303-310.

Monsted, J. 2017. Forest Regeneration and Land Use History. MS Thesis, Department of Environmental and Plant Biology, Ohio University, Athens.

Nicoll, B., A. Armstrong. 1998. Development of Prunus Root Systems in a City Street: Pavement Damage and Root Architecture. *Arboricultural Journal* 22: pp.259-270.

Ohio Department of Transportation, 2004. Pavement Condition Rating System. Ohio Department of Transportation, Office of Pavement Engineering, Columbus, Ohio.

Ohio Department of Transportation, 2006. Pavement Condition Rating Manual. ODOT, Office of Pavement Engineering, Columbus, Ohio.

Ohio Department of Transportation 2011. Financial and Policy Implications on Assuming Primary Responsibility for all State Routes throughout Ohio Regardless of Local Government Jurisdiction. Ohio Department of Transportation, Columbus, Ohio.

Praticò, F.G., R.Vaiana. 2015. A Study on the Relationship Between Mean Texture Depth and Mean Profile Depth of Asphalt Pavements. *Construction and Building Materials* 101: pp.72-79.

PRISM Climate Group 2015. 30-Year Normals. Northwest Alliance for Computational Science and Engineering, Oregon State University. http://www.prism.oregonstate.edu/normals/

Qiao, Y., G.W. Flintsch, A.R. Dawson, T. Parry. 2013. Examining Effects of Climatic Factors on Flexible Pavement Performance and Service Life. *TRR* 2349: pp.100-107.

R Core Team. 2013. R, A language and environment for statistical computing. R Foundation for Statistical Computing, Vienna, Austria. URL http,//www.R-project.org/.

Sanusi, R., D. Johnstone, P. May, S.J. Livesley. 2016. Street Orientation and Side of the Street Greatly Influence the Microclimate Benefits Street Trees Can Provide in Summer. *Journal of Environmental Quality* 45: pp.167-174.

Sapkota, A., A. Ahmed, P. Pandey, M.S. Hossain, N. Lozano. 2019a. Stabilization of Rainfall-Induced Slope Failure and Pavement Distresses Using Recycled Plastic Pins and Modified Moisture Barrier. In *Eighth International Conference on Case Histories in Geotechnical Engineering* (Geo-Congress 2019), American Society of Civil Engineers, Reston, VA, 237–246.

Schmidt, R.J, P.E. Graf. 1972. Effect of Water on Resilient Modulus of Asphalt-Treated Mixes. *Proceedings of the Association of Asphalt Paving Technologists* 41: pp.118-162.

*Schneider, C.A., W.S. Rasband, K.W. Eliceiri. 2012.* NIH Image to ImageJ: 25 years of image analysis*, Nature methods 9(7): pp.671-675.*

Scott, K.I., J.R. Simpson, E.G. McPherson. 1999. Effects of Tree Cover on Parking Lot Microclimate and Vehicle Emissions. *Journal of Arboriculture* 25: pp.129-142.

Seed, H.B., C.K. Chan, C.E. Lee. 1962. Resilience Characteristics of Subgrade Soils and their Relation to Fatigue Failures in Asphalt Pavements. *International Conference on the Structural Design of Asphalt Pavements*. Supplement, University of Michigan, Ann Arbor, pp.77-113.

Shahrestani, M., R. Yao, Z. Luo, E. Turkbeyler, H. Davies. 2015. A Field Study of Urban Microclimates in London. *Renewable Energy* 73: pp.3-9.

Shashua-Bar, L., O. Potchter, A. Bitan, D. Boltansky, Y. Yaakov. 2010. Microclimate Modelling of Street Tree Species Effects Within the Varied Urban Morphology in the Mediterranean City of Tel Aviv, Israel. *International Journal of Climatology* 30: pp.44-57.

Simpson, J.R. 1998. Urban Forest Impacts on Regional Cooling and Heating Energy Use: Sacramento County Case Study. *Journal of Arboriculture* 24: pp.201-214.

Souch, C.A., C. Souch. 1993. The Effect of Trees on Summertime Below Canopy Urban Climates: A Case Study Bloomington, Indiana. *Journal of Arboriculture* 19: pp.303-312.

Stempihar, J.J., T, Pourshams-Manzouri, K.K. Kaloush, M.C. Rodezono. 2012. Porous Asphalt Pavement Temperature Effects on Overall Urban Heat Island. Annual Meeting of the Transportation Research Board, Washington, D.C.

Stidger, R.W. 2002. Diagnosing Problem Pavements. *Better Roads*, June 2002.

Sturm, M. 1992. Snow Distribution and Heat Flow in the Tiaga. *Artic and Alpine Research* 24: pp.145-152.

Sydnor, T.D., D. Gamstetter, J. Nichols, B. Bishop, J. Favorite, C. Blazer, L. Turpin. 2000. Trees Are Not The Root of Sidewalk Problems. *Journal of Arboriculture* 26, pp.20-29.

Tabatabaee, H.A., R. Velasquez, H.U. Bahia. 2012. Predicting Low Temperature Physical Hardening in Asphalt Binders. *Journal of Construction and Building Materials* 34: pp.162-169.

Timm, D.H., V.R. Voller. 2003. Field Validation and Parametric Study of a Thermal Crack Spacing Model. Association of Asphalt Paving Technologists – *Proceedings of the Technical Sessions* 72, pp.356-387.

Vailshery, L.S., M. Jaganmohan, H. Nagendra. 2013. Effect of Street Trees on Microclimate and Air Pollution in a Tropical City. *Urban Forestry and Urban Greening* 12: pp.408-415.

Willway, T., S. Reeves, L. Baldachin. 2008. Maintaining Pavements in a Changing Climate, The Stationary Office, London.

Wolters, R.O. 2003. Raveling of Hot-Mixed Asphalt. Minnesota Asphalt Pavement Association. http://www.asphaltisbest.com/PDFs/Raveling_of_HMA_Oct03.pdf

Xiao, Q., E.G. McPherson, S.L. Ustin, M.E. Grismer, J.R. Simpson. 2000. Winter Rainfall Intercption by Two Mature Open-Grown Trees in Davis, California. *Hydrological Processes* 14: pp.763-784.

Xiao, Q., E.G. McPherson. 2002. Rainfall Interception by Santa Monica's Municipal Urban Forest. *Urban Ecosystems* 6: pp.291-2002.

Xiao, Q., E.G. McPherson. 2011. Rainfall Interception of Three Trees in Oakland, California. *Urban Ecosystems* 14: pp.755-769.

Yaacob, H., A.H. Norhidayah, M.R. Hainin, F.R. Muhammad. 2012. Comparison of Sand Patch Test and Multi Laser Profiler in Pavement Surface Measurement. *Jurnal Teknolgi* 70: pp.103-106.

Yilmaz, H., S. Toy, M.A. Irmak, S. Yilmaz, Y. Bulut. 2008. Determination of Temperature Differences Between Asphalt Concrete, Soil and Grass Surfaces of the City of Erzurum, Turkey. *Atmosfera* 21: pp.135-146.

Yu, X., J. Wei, Y. Lin, Y. Luo, Y. Wang, L. Yin. 2013. Effects of Moisture on Rheological Properties of PAV Aged Asphalt Binders. China Petroleum and Petrochemical Technology, 15: pp.38-44.

Wong , T.W., J.E.G. Good, M.P. Denne. 2018. Tree Root Damage to Pavements and Kerbs in the City of Manchester, *Arboriculture Journal* 12: pp.17-34.

Zafir, Z.R., R. Siddhartan, P.E. Sebaaly. 1994. Dynamic Pavement Strains from Moving Traffic Loads. *ASCE Journal of Transportation Engineering* 120 (5): pp. 821–842.

Zanon, S.A. 2014. Landscaping with Trees in the Midwest. A Guide for Residential and Commerical Property Owners. Ohio University Press, Athens.

Zhongzhi, L., K.C. Kinha, P.S. McCarthy. 2002. A Determination of Load and Non-Load Shares of Highway Pavement Routine Maintenance Expenditures. *Road and Transport Research*, June 2002.

Zuur, A., E.N. Leno, N. Walker, A.A. Saveliev, G.M. Smith. 2009. Mixed Effects Models and Extensions in Ecology with R. Springer Verlag, New York.

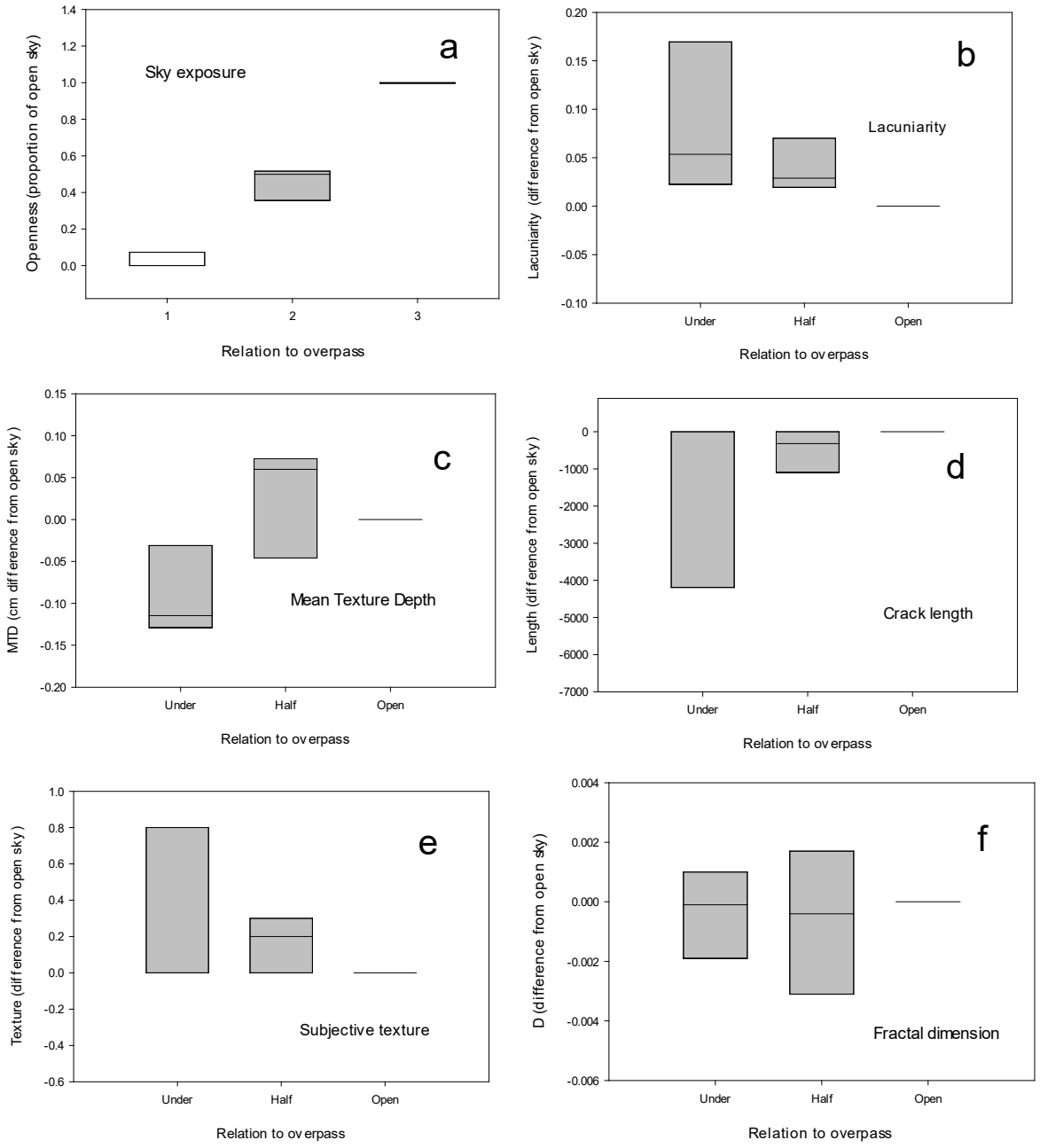


***Figure B1. Pavement Condition and Canopy Openness Under, Partial Under, and Adjacent to Seven Highway Overpasses in Athens County, Ohio. Note: all values are normalized to the respective Open plot. a. Canopy openness above each plot assessed by hemispherical photography; b. Lacuniarity of pavement texture (lambda); c. Mean texture depth assessed by the volumetric method (MTD); d. Total crack length (Length); e. Subjective texture rating (SUBJ); f. Fractal dimension of pavement texture (D). Shaded blocks indicate interquartile range. (1 cm = 0.4 in).***

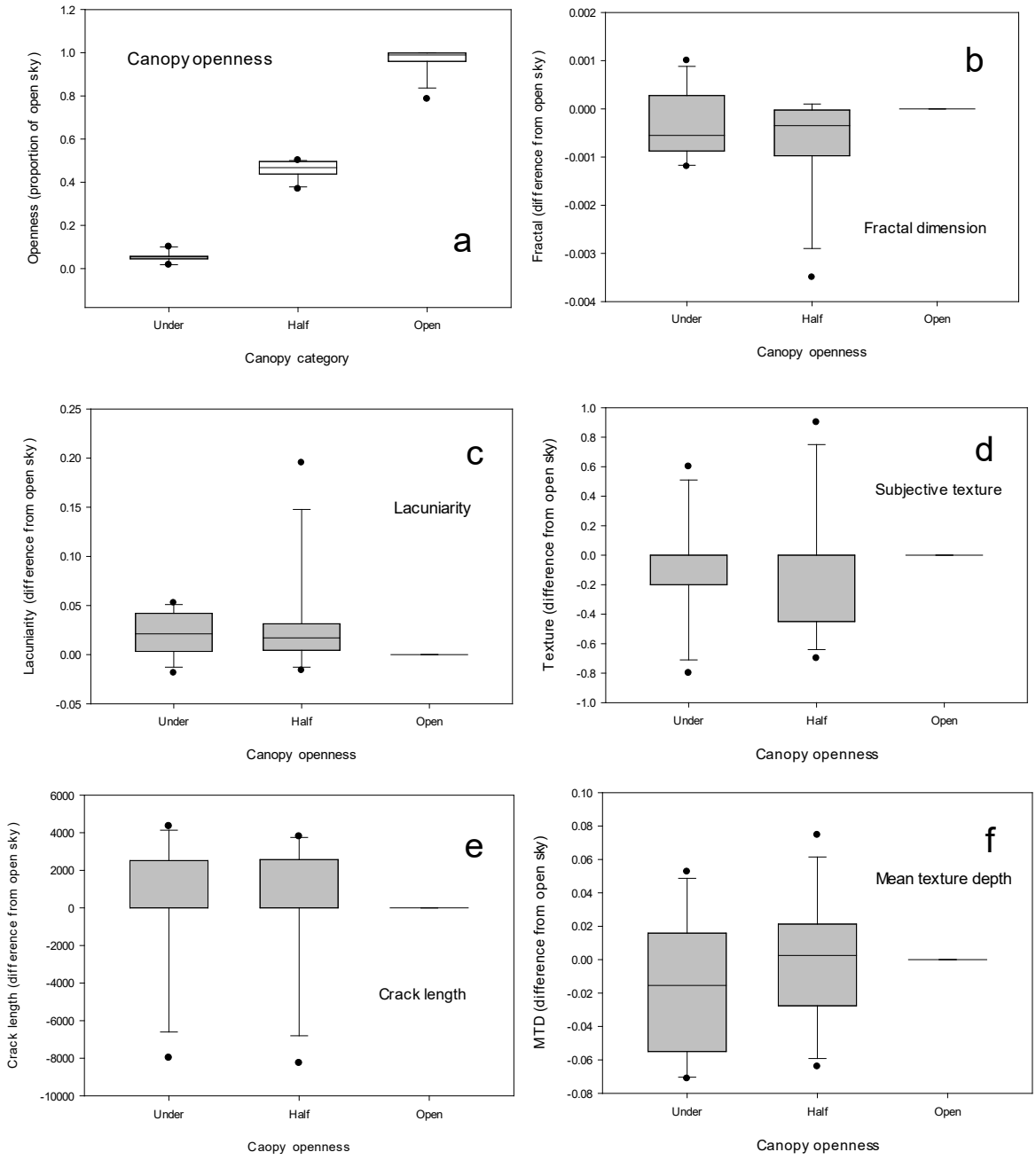


***Figure B2. Pavement Condition and Canopy Openness Under, Partial Under, and Adjacent to Trees on a Bike Path in Athens County, Ohio. Note: all values are normalized to the respective Open plot. a. Canopy openness above each plot assessed by hemispherical photography; b. Lacuniarity of pavement texture (lambda); c. Mean texture depth assessed by the volumetric method (MTD); d. Total crack length (Length); e. Subjective texture rating (SUBJ); f. Fractal dimension of pavement texture (D). (1 cm = 0.4 in).***

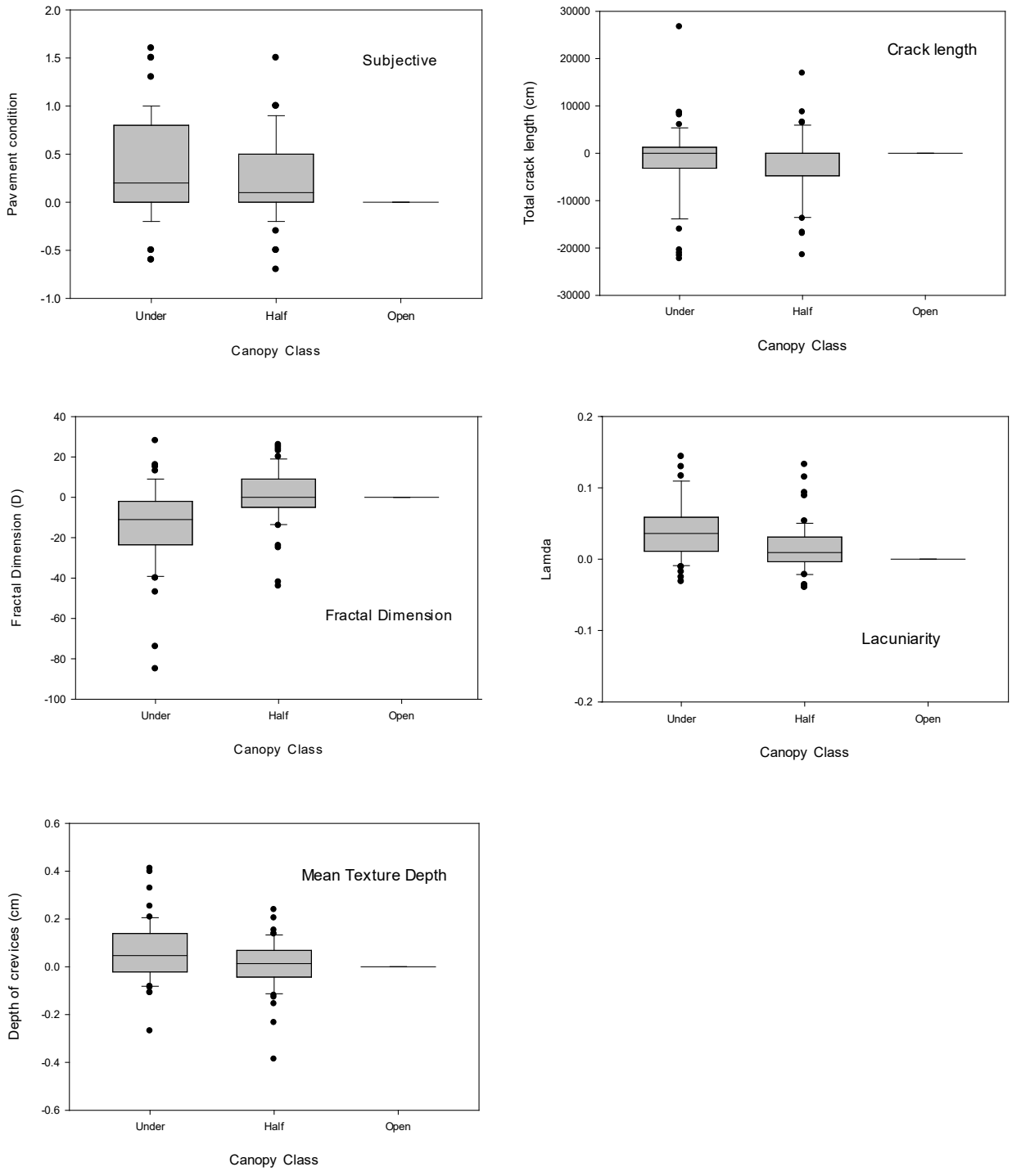


***Figure B3. Pavement Condition and Canopy Openness Under, Partial Under, and Adjacent to Trees on Rural Roads in Athens County, Ohio. Note: all values are normalized to the respective Open plot. a. Subjective texture rating; b. Total crack length (Length); c. Fractal dimension of pavement texture (D).; d. Lacuniarity of pavement texture (lambda); e. Mean texture depth assessed by the volumetric method (MTD). (1 cm = 0.4 in).***

***Table B1. Environment at road and bike path sites in Athens County, Ohio. Environment at road and bike path sites in Athens County, Ohio. Road and bike path values are compared by Wilcoxon nonparametric tests; χ2 and probability are shown here. Values are mean, standard deviation, and median, listed vertically. Highlighting indicates higher value in significant comparisons. Bold text indicates significance at α 0.050.***

| Environment | | Road (168 plots) | | Bikepath (36) | | $\chi^2$ | p |
|---|---|---|---|---|---|---|---|
| | mean | 113.18 | 4.456 | 23.61 | 0.930 | | |
| Camber (mm \| in) | std. dev. | 67.61 | 2.662 | 25.76 | 1.014 | 57.702 | **0** |
| | median | 100 | 3.9 | 20 | 0.8 | | |
| | mean | 6.231 | 20.443 | 3.607 | 11.834 | | |
| Width (m \| ft) | std. dev. | 0.561 | 1.841 | 0.371 | 1.217 | 89.652 | **0** |
| | median | 6.1 | 20.0 | 3.6 | 11.8 | | |
| | mean | -167.05 | -6.577 | -68.61 | -2.701 | | |
| Dropoff (mm \| in) | std. dev. | 137.00 | 5.394 | 61.79 | 2.433 | 23.009 | **0** |
| | median | -170 | -6.7 | -70 | -2.8 | | |
| | mean | 1576.24 | 62.057 | 1448.61 | 57.032 | | |
| Edge (mm \| in) | std. dev. | 263.97 | 10.393 | 130.06 | 5.120 | 10.519 | **0.0012** |
| | median | 1540 | 60.6 | 1490 | 58.7 | | |
| | mean | 109.45 | 4.309 | -743.06 | -29.254 | | |
| Opposite (mm \| in) | std. dev. | 1315.96 | 51.809 | 778.38 | 30.645 | 13.733 | **0.0002** |
| | median | 100 | 3.9 | -550 | -21.7 | | |
| | mean | -118.18 | -4.653 | -827.78 | -32.590 | | |
| Adjacent (mm \| in) | std. dev. | 1313.05 | 51.695 | 885.55 | 34.864 | 8.777 | **0.0031** |
| | median | -350 | -13.8 | -750 | -29.5 | | |
| | mean | 12.218 | 12.218 | 11.29 | 11.29 | | |
| Nearest (m \| ft) | std. dev. | 9.897 | 9.897 | 10.371 | 10.371 | 1.55 | 0.2239 |
| | median | 9.3 | 9.3 | 7.1 | 7.1 | | |
| | mean | 1.288 | | 2.056 | | | |
| Number (trees) | std. dev. | 1.759 | | 2.242 | | 2.9619 | **0.0853** |
| | median | 1 | | 1 | | | |
| | mean | 338.47 | 111.047 | 275.56 | 90.407 | | |
| Diameter (mm \| in) | std. dev. | 187.06 | 61.371 | 143.71 | 47.149 | 3.515 | **0.0608** |
| | median | 320 | 105.0 | 250 | 82.0 | | |
| | mean | 1.095 | | 2.029 | | | |
| Penmin (units) | std. dev. | 1.098 | | 1.056 | | 27.364 | **0** |
| | median | 0.75 | | 1.8 | | | |
| | mean | 4.083 | | 4.478 | | | |
| Penmax (units) | std. dev. | 0.859 | | 0.133 | | 11.696 | **0.0006** |
| | median | 4.5 | | 4.5 | | | |
| | mean | 5.505 | | 1.738 | | | |
| Curve (degrees) | std. dev. | 9.613 | | 4.82 | | 5.108 | **0.0238** |
| | median | 0 | | 0 | | | |

***Table B2. Pavement condition under tree canopies at 36 bike path plots in Athens County, Ohio. Plots are >95% covered by leafy foliage ("Under"), 45-55% covered ("Partial"), and 0-5% covered ("Open"). Numbers show (top to bottom) mean value, standard deviation, and median, except in the case of Crack Presence/Absence.***

| Pavement | Under | Partial | Open |
|---|---|---|---|
| **Subjective** | | | |
| Mean | 2.09 | 2.28 | 2.16 |
| Std dev | 0.373 | 0.354 | 0.32 |
| Median | 2 | 2 | 2.05 |
| CV | 0.178 | 0.155 | 0.148 |
| **Crack length (mm)** | | | |
| Mean | 10080 | 6010 | 9720 |
| Std dev | 16560 | 14070 | 24960 |
| Median | 0 | 0 | 0 |
| CV | 1.643 | 2.341 | 2.57 |
| **Crack length (in)** | | | |
| Mean | 396.85 | 236.61 | 382.68 |
| Std dev | 651.97 | 553.94 | 982.68 |
| Median | 0 | 0 | 0 |
| CV | 1.643 | 2.341 | 2.57 |
| **Crack presence (proportion)** | | | |
| Present | 0.417 | 0.167 | 0.167 |
| **Fractal D** | | | |
| Mean | 1.87 | 1.87 | 1.87 |
| Std dev | 0.001 | 0.001 | 0.001 |
| Median | 1.87 | 1.87 | 1.87 |
| CV | 0 | 0.001 | 0 |
| **Lacuniarity** | | | |
| Mean | 0.211 | 0.22 | 0.19 |
| Std dev | 0.014 | 0.05 | 0.019 |
| Median | 0.21 | 0.205 | 0.185 |
| CV | 0.066 | 0.228 | 0.098 |
| **MTD** | | | |
| Mean | 0.267 | 0.281 | 0.282 |
| Std dev | 0.025 | 0.041 | 0.032 |
| Median | 0.266 | 0.276 | 0.274 |
| CV | 0.093 | 0.147 | 0.115 |

***Table B3. Best-fit models for six metrics of pavement condition at bike path sites in Athens County, Ohio. Best-fit models for six metrics of pavement condition at bike path sites in Athens County, Ohio. Mixed models with "site" as a random effect. Predictor variables are centered and scaled, allowing comparison of coefficients. Note fractal D and lacuniarity were best fit with linear mixed effects models with error normal distributions (proc LME) rather than generalized mixed effect models.***

| Pavement | Predictor | Coefficient | Test statistic | Probability |
|---|---|---|---|---|
| **Crack presence** | | | | |
| | Intercept | -2.3950 | -2.814 | 0.0049 |
| Binomial | Dropoff | -0.1590 | -1.956 | 0.0505 |
| **Fractal D** | | | | |
| | Intercept | 1.876 | 1436 | 0.0000 |
| | Width | -0.0007 | -2.736 | 0.0118 |
| **Lacuniarity** | | | | |
| | Intercept | -0.0932 | -1.824 | 0.0818 |
| | Width | 0.0607 | 5.876 | 0.0000 |
| | Curvature | -0.0036 | -3.241 | 0.0037 |
| **Subjective** | | | | |
| | Intercept | 0.4910 | 21.278 | 0.0000 |
| Gamma | Dropoff | 0.0038 | 2.099 | 0.0358 |

***Table B4. Comparison of pavement conditions at road and bike path sites in Athens County, Ohio. Numbers indicate mean, standard deviation, and median. Comparison by Kruskal Wallis test except in the case of Crack presence/absence, which is compared to pavement type by a χ2 test.***

| Pavement measure | | Road sites | Bike path sites | $\chi^2$ | p |
|---|---|---|---|---|---|
| | mean | 3.114 | 2.164 | | |
| **Subjective** | std.dev. | 0.461 | 0.347 | 72.33 | 0 |
| | median | 3 | 2 | | |
| | mean | 1.871 | 1.873 | | |
| **Fractal dimension (D)** | std.dev. | 0.002 | 0.001 | 37.987 | 0 |
| | median | 1.871 | 1.873 | | |
| | mean | 0.23 | 0.207 | | |
| **Lacuniarity (lambda)** | std.dev. | 0.046 | 0.035 | 11.564 | 0.0007 |
| | median | 0.216 | 0.202 | | |
| | mean | 4.37 | 2.78 | | |
| **Mean Texture Depth (mm)** | std.dev. | 1.35 | 0.34 | 53.592 | 0 |
| | median | 4.04 | 2.74 | | |
| | mean | 0.172 | 0.109 | | |
| **Mean Texture Depth (in)** | std.dev. | 0.053 | 0.013 | 53.592 | 0 |
| | median | 0.159 | 0.108 | | |
| **Crack presence (%)** | | 58.3 | 24.2 | 10.553 | 0.0012 |
| | mean | 2502.02 | 33.29 | | |
| **Crack length (m)** | std.dev. | 23528.83 | 24.15 | 0.559 | 0.3856 |
| | median | 38.32 | 34.07 | | |
| | mean | 8208.73 | 109.22 | | |
| **Crack length (ft)** | std.dev. | 77194.32 | 79.23 | 0.559 | 0.3856 |
| | median | 125.72 | 111.78 | | |

***Table B5. Pavement condition under tree canopies at 162 rural road plots in Athens County, Ohio. Plots are >95% covered by leafy foliage (Under), 45-55% covered (Partial), and 0-5% covered (Open). Numbers show (top to bottom) mean value, standard deviation, and median, except in the case of Crack Presence/Absence. Highest values in each category are highlighted.***

| Pavement | Under | Partial | Open |
|---|---|---|---|
| **Subjective** | | | |
| Mean | 3.260 | 3.166 | 2.921 |
| Std dev | 0.457 | 0.457 | 0.408 |
| Median | 3.2 | 3.0 | 3.0 |
| CV | 0.140 | 0.144 | 0.140 |
| **Crack length (m)** | | | |
| Mean | 48.88 | 57.06 | 89.67 |
| Std dev | 57.97 | 48.58 | 83.27 |
| Median | 28.66 | 47.96 | 60.53 |
| CV | 1.186 | 0.851 | 0.929 |
| **Crack length (ft)** | | | |
| Mean | 160.37 | 187.20 | 294.19 |
| Std dev | 190.19 | 159.38 | 273.20 |
| Median | 94.03 | 157.35 | 198.59 |
| CV | 1.186 | 0.851 | 0.929 |
| **Crack presence (percent)** | | | |
| Present | 66.7 | 47.3 | 55.8 |
| **Fractal D** | | | |
| Mean | 1.8696 | 1.871 | 1.8709 |
| Std dev | 0.0022 | 0.0018 | 0.0015 |
| Median | 1.8702 | 1.8714 | 1.8711 |
| CV | 0.0012 | 0.0010 | 0.0008 |
| **Lacuniarity (lamda)** | | | |
| Mean | 0.2543 | 0.2243 | 0.2104 |
| Std dev | 0.0578 | 0.0392 | 0.0237 |
| Median | 0.2426 | 0.2138 | 0.2032 |
| CV | 0.2273 | 0.1748 | 0.1126 |
| **Mean Texture Depth (mm)** | | | |
| Mean | 4.726 | 4.212 | 4.158 |
| Std dev | 1.494 | 1.249 | 1.137 |
| Median | 4.366 | 4.033 | 4.023 |
| CV | 0.3161 | 0.2965 | 0.2734 |
| **Mean Texture Depth (in)** | | | |
| Mean | 0.1861 | 0.1658 | 0.1637 |
| Std dev | 0.0588 | 0.0492 | 0.0448 |
| Median | 0.1719 | 0.1588 | 0.1584 |
| CV | 0.3161 | 0.2965 | 0.2734 |

***Table B6. Best fit models for six metrics of pavement condition at rural road sites in Athens County, Ohio. Mixed models with "site" as a random effect. Predictor variables are centered and scaled, allowing comparison of coefficients. Only predictor variables with coefficients > the respective standard errors are shown. Significance of predictor variables is tested by likelihood comparisons.***

| Pavement | Predictor | Coefficient | Test statistic | Probability |
|---|---|---|---|---|
| **MTD** | **Intercept** | 0.437 | | |
| Site 56.9% of variance | **Open** | -0.0232 | $\chi^2 = 6.858$ | 0.0088 |
| **Crack length (log)** | **Intercept** | 8.069 | | |
| Site 8.8% | Edge | -0.23 | $\chi^2 = 2.469$ | 0.1161 |
| | **Dropoff** | -0.25 | 3.098 | 0.0784 |
| | Penmin | 0.177 | 1.938 | 0.1639 |
| | Opposite | 1.097 | 1.097 | 0.295 |
| | Diameter | -1.889 | 1.688 | 0.1878 |
| **Crack presence** | Intercept | 0.393 | t = 1.617 | 0.1059 |
| Site 52.5% | Open | -0.357 | 1.61 | 0.1073 |
| Binomial | Edge | 0.164 | 0.725 | 0.4683 |
| | **Penmin** | 0.473 | 1.985 | 0.0471 |
| | Dropoff | -0.273 | 1.207 | 0.2275 |
| | Diameter | -0.195 | 0.902 | 0.3669 |
| **Fractal D** | **Intercept** | 1.871 | | |
| Site 37.2% | **Open** | $5.560 \times 10^{-4}$ | $\chi^2 = 15.974$ | 0 |
| | **Width** | $-3.695 \times 10^{-4}$ | 4.021 | 0.045 |
| | Penmax | $1.990 \times 10^{-4}$ | 1.953 | 0.1623 |
| | **Opposite** | $-4.353 \times 10^{-4}$ | 8.342 | 0.0154 |
| | Adjacent | $-1.767 \times 10^{-4}$ | 1.334 | 0.2481 |
| | Curvature | $-1.929 \times 10^{-4}$ | 1.946 | 0.163 |
| | Camber | $2.736 \times 10^{-4}$ | 2.681 | 0.1016 |
| **Lacuniarity** | **Intercept** | -1.4881 | | |
| Site 31.1% | Camber | -0.0214 | $\chi^2 = 2.118$ | 0.1456 |
| | **Open** | -0.0673 | 26.464 | 0 |
| | **Opposite** | 0.0352 | 5.8163 | 0.0159 |
| | **Dropoff** | -0.0177 | 1.933 | 0.1645 |
| | **Diameter** | 0.0293 | 5.8 | 0.002 |
| | Penmax | -0.0159 | 1.5343 | 0.2155 |
| **Subjective** | **Intercept** | 3.133 | | |
| Site 46.4% | **Open** | -0.104 | $\chi^2 = 11.596$ | 0.0007 |
| | Curvature | 0.045 | 2.085 | 0.1488 |
| | Opposite | 0.048 | 1.617 | 0.2035 |
| | Adjacent | 0.038 | 1.225 | 0.2684 |
| | Edge | -0.054 | 2.577 | 0.1084 |

## APPENDIX C: ROAD SECTION ANALYSIS ON EFFECTS OF TREE CANOPY ON PAVEMENT MICROCLIMATE, CONDITION AND SAFETY.

## Site Selection, Description, and Locations

The selection of test road sections was confined to the eastern part of the state of Ohio and specifically to Ohio DOT districts 4, 5, 9, 10, 11, and 12 as depicted in Figure C1. These Ohio DOT districts were selected due to (i) the climatic variations and precipitation levels, (ii) their proximity to the Ohio University Athens campus, and (iii) the perceived abundance of tree canopied roads.

An initial list of canopied roadway segments was developed using a Geographic Information Systems (GIS) based enquiry that involved overlapping of roadway and canopy datafiles. This initial list was then shared with Ohio DOT personnel (Highway Management Administrators, Pavement Engineers, etc.) within each of the six districts identified above. The Ohio DOT personnel (based on their experience of routes in their respective jurisdictions) further edited (i.e., added to/deleted from) the initial list in order to narrow down to a potential set of roadways with canopy overtop the pavement surface. The set of potential sites was then used in combination with "PathWeb" – a digital photolog maintained by Ohio DOT [2018]. The roadway imagery (front view, left shoulder, right shoulder, and rear view) are obtained using a vehicle that is instrumented with four digital cameras that are each set to take a picture at a rate of 200 pictures per mile [Ohio DOT, 2018]. These pictures are "stitched" together and stored to allow for a seamless visual of the roadway. Additionally, a GPS unit on the vehicle allows for accurate location data (latitude and longitude) to be tagged to the video as well as accurate County, Route, and Milepost information.

Each potential canopied roadway segment provided by Ohio DOT was then manually "skimmed" within PathWeb to identify the presence of canopy coverage overtop a roadway. Figure C2 depicts the PathWeb screen as a roadway segment was "skimmed" for canopy. In Figure C2, the top image depicts the driver view of roadway whereas the bottom right image depicts the rear view of the roadway. On the bottom left, an interactive map shows the selected roadway (red line), exact location on roadway that is being viewed (blue dot), and includes information such as latitude/longitude, route number, county, and mile marker. When a roadway segment with canopy was observed in PathWeb its details (latitude/longitude, mile marker, county) were noted. Lastly, a field inspection was then completed to verify the presence of canopy overtop the roadway on the segments identified using PathWeb.

Using the process described above, a total of 39 roadway segments were selected as test sites. Table C1 presents information for the 39 test sites including: location, route #, and milepost. Each test site comprised a roadway segment with portions that had no canopy, had partial canopy, and had full canopy. Note that test segments were of different lengths and depended on the amount of tree canopy present. Figure C3 depicts the Ohio DOT districts considered in this research study and information on the selected test segments including number of sites, total mileage, full canopy mileage, partial canopy mileage and no canopy mileage.

## Data Collection Methods

### Tree Canopy Coverage

At each test roadway segment, there was need to quantify the amount of canopy that was present overtop the pavement surface. This was done using a convex spherical densiometer shown in Figure C4. The densiometer is a small wooden box with a spherical convex shaped mirror inside that is engraved with twenty-four ¼" (6.4 mm) squares. The density of canopy cover is estimated by holding the densiometer in a level position with mirror facing upwards and under trees; then the operator/user will count the number of corners where there are openings in the canopy [Forestry Suppliers, 2008]. The number open squares are multiplied by a constant of 1.04 to obtain the percentage of canopy coverage that is open; and that number is subtracted from 100 to obtain the percentage of canopy coverage above. Therefore, at 25-ft (7.6 m) intervals along centerline of each roadway test segment, the densiometer was used to take four readings (facing North, East, South, West) and an average value computed as a measure of canopy coverage [Forestry Suppliers, 2008]. Coverage values were categorized as follows: 75 to 100% (Full Canopy); 25 to 75% (Partial Canopy); and 0 to 25% (No Canopy).

The measurements of tree canopy coverage assisted in determining where, along a test roadway segment, there was no canopy, partial canopy, and full canopy. Figure C5 shows graphical representation of the estimated canopy coverage along SR 124 in Jackson County, Ohio. Similar graphs for all 39 sites are provided in Appendix G). The three different colors visually depict between canopy coverage – dark green (full canopy), a light green (partial canopy), and white (no canopy). That is, no canopy (0 to 275 ft (0 to 84 m)), partial canopy (275 to 375 ft (84 to 114 m), full canopy (375 to 900 ft (114 to 274 m), partial canopy (900 to 1150 ft (274 to 350 m), and no canopy (1150 to 1200 ft (350 to 366 m)). A visual image of the SR 124 test segment, obtained from a GoPro camera at the time of the field visit, is shown in Figure C6.

### Pavement Surface

This section presents details related to data and methods of collecting data on the pavement surface and in particular to the moisture, temperature, and condition of pavement.

*Condition Rating Data*

The pavement condition data was collected in accordance with the Ohio DOT PCR Manual [Ohio DOT, 2006]. The manual's flexible pavement condition rating (PCR) form considers thirteen different types of distresses, described in detail in the manual's appendices. Each distress type was rated to have a severity of low, medium or high and an extent of either occasional, frequent or extensive. The severity and extent values were multiplied by a distress weight to then obtain a deduction value. Once all distresses were accounted for, the total deduction value is subtracted from 100 to get the PCR value.

For each test segment, the pavement was rated by direction and by canopy coverage level. Therefore, at each test location, a PCR value (by direction) was assessed for the no canopy, partial canopy, and full canopy portions. Using a GoPro camera, video of the pavement surface was captured, and the pavement rated (in accordance with Ohio DOT PCR manual) in the lab. The GoPro images have sufficiently high resolution to make a valid PCR and preserves a record for later review and comparison. Table C2 presents the PCR values for 38 of the site locations.

*Moisture Data*

Moisture data were collected from 21 roadway segments in order to examine the moisture related effects of tree canopy and in particular to provide answers to the question that trees overtop the roadway "shelter" rainfall from reaching the pavement surface (light rain conditions) but also prevent sunlight from drying the roadway and subsequently causing prolonged moisture damage to the pavement. The amount of moisture on the pavement surface was measured using the Mobile Advanced Road Weather Information Sensor (MARWIS) manufactured by Lufft. The MARWIS is a device consisting of multiple sensors that provide reliable road condition and environmental data in a safe and easy manner [Lufft, 2019]. The device is attached to a vehicle (as shown in Figure C7) with its sensors facing the pavement surface. The vehicle is then driven at a steady and constant speed along the roadway with the data being logged at 100 times per second.

For this research study, the "instrumented" vehicle was driven along each test roadway segment at a speed of approximately 15 mph (24 km/h) or below and data were collected every second in both directions of travel. The data were collected within 24 hours after a rain event. A sample data log file that was made available from the MARWIS is presented in Figure C8. The data includes the following; date and time information; location information (latitude/longitude); condition of roadway (i.e., dry, wet, icy); pavement surface temperature (in °C at an accuracy of ±0.8°C (±1.4°F) at 0°C (32°F)); presence of moisture (film height) to an accuracy of 10%; and coefficient of friction of the pavement surface.

Using a combination of latitude/longitude information (MARWIS), exact test segment location data (Google Earth), and the estimated canopy coverage information; it was possible to "match" the moisture to the exact location(s) along each test roadway segment and subsequently to canopy level overtop the pavement surface. Figure C9 is an example plot depicting the water film height in µm (1 µm = 0.39 mil) under different canopy coverage levels on SR 124 (WB); and similar graphs for all the other test locations are provided in Appendix H. As expected, for this specific test segment, it can be observed that there is relatively more moisture on the pavement surface under canopy than that under open-sky. Tables C3 and C4 present descriptive summary statistics of the moisture levels by canopy coverge level at each test site.

*Temperature Data*

In addition to moisture on pavement surface, temperature data were also collected and examined to determine the temperature related effects of tree canopy. While it is common knowledge that trees overtop the roadway put a shade on the pavement surface there was a need to answer additional questions such as; are the temperature differences that exist between open and canopied roadway sections statistically significantly different and what are the magnitude of these temperature differences? The temperature (°F at an accuracy of ±3.6°F (±2.0°C)) data were collected using a FLIR E6 infrared camera shown in Figure C10. This was in addition to the temperature data available from the MARWIS system described above.

The MARWIS based temperature data were "matched" to the exact location(s) on each roadway segment and subsequently to canopy level overtop the pavement surface. Figure C11 depicts an example plot depicting the MARWIS pavement surface temperature (converted from °C to °F) under different canopy coverage levels at the SR 124 (WB) location; and similar graphs for all the other test locations are provided in Appendix I. As expected, for this specific segment,

it can be obeserved that the pavement surface in the open (no canopy) portion is relatively warmer than under canopy cover. There is, on average, a 10°F (5.6°C) observed difference in temperature between pavement surface in open and canopied portions. Tables C5-C7 present descriptive summary statistics of the pavement surface temperature (MARWIS) by canopy coverage level at each test site.

Pavement surface temperature was also measured using the FLIR E6 camera and along the center of each lane and at 25 ft (7.6 m) intervals for each study location. Each infrared image has a legend showing the maximum, minimum, and average temperature of the picture as well as a colored temperature scale. The average temperature was used for all data analysis. Figure C12 depicts an example graph of pavement surface temperature under different canopy coverage levels at the SR 124 (EB and WB) test site; and similar graphs for all the other test locations are presented in Appendix J. Tables C8-C10 present descriptive summary statistics of the pavement surface temperature (FLIR) by canopy coverage level at each test site.

**Safety Analysis Data**

In order to assess the safety related effects of tree canopy, the research team performed a before-after evaluation of the effectiveness of tree trimming operations. Primarily, crash and traffic volume data were obtained. In addition, surrogate safety data were also collected.

*Crash and Traffic Volume Data*

As an initial step, it was fundamental that low volume roadways where tree trimming operations had been performed were identified. With assistance from Ohio DOT, the research team were provided with a comprehensive list of locations in all 12 Ohio DOT districts where tree maintenance was performed in the last four years. Information on the specific county, route type and number, beginning and ending mile marker (of maintenance work), date on which work was performed, and the specific work activity conducted were included. For the safety analysis performed for this project, the comprehensive list was narrowed to include only segments in Districts 4, 5, 9, 11, and 12. Additional criteria adopted were;

- Must be a state route (SR);
- Maintenance activity was coded as: M666-001 - Pruning existing trees;
- Segment length was less than or equal to 5 mi (8 km); and
- Any maintenance performed was before the year 2018.

Traffic crash data from 2009 to 2018 (i.e., for the segments identified in the narrowed list above) were obtained from Ohio DOTs GIS Crash Analysis (GCAT) system. GCAT is a crash database that is maintained by Ohio DOT and includes every crash record that is police reported in the state of Ohio [Ohio DOT, 2019a]. At most, crash data were gathered for five years, with a minimum of three years before tree trimming occurred. During the after period, crash data was collected for three years (excluding the year in which tree trimming was performed) with a minimum of one year after being collected.

Traffic volume data (per year) for the entire before-after study period were obtained from the Traffic Monitoring Management System (TMMS) which is a traffic count database maintained by Ohio DOT [2019b]. In addition, geometric design features for segments in the analysis such as lane widths, shoulder widths, horizontal/vertical alignments parameters etc. were obtained using a combination of Google Earth and a geolocation tool available in AutoCAD Civil 3D.

Features such as grade, driveway density, presence of passing lanes, etc. were determined by "skimming" the segments within PathWeb. It was assumed that there were no centerline rumble strips, and there was no automated speed enforcement on all segments in the analysis.

*Surrogate Measures of Safety*

Before-After road safety analysis are in many cases performed using direct measures of crash frequency and severity. However, with crashes being rare and random events, many analyses are (i) lacking in the use of a "rich" crash database, and (ii) lacking in details to improve crash failure mechanism and avoidance behavior [Tarko, et al., 2009]. Using non-crash traffic events and other surrogate data is an option to safety analysis in the absence of crashes. Examples of some surrogate measures that have been used in the literature include: traffic conflicts [Chin, Quek, and Cheu, 1992; Chin and Quek, 1997; Naik, Appiah, and Rilett, 2018]; aggressive lane merging, speeding, and running-on-red [Kloeden and McLean, 1997; Porter and Berry, 1999]; acceleration noise [Shoarian-Sattari and Powell, 1987]; post-encroachment time [Naik, Appiah, and Rilett, 2018]; and time-integrated time-to-collision [Minderhoud and Bovy, 2001]. For this research study, driver's behavior – travel speeds and also braking operations – as they travelled through a test segment were observed.

Drivers travel speeds within full canopy and also no canopy (open) sections were collected at three test sites and compared. It was anticipated the results would provide insight on any potential "tunneling" effect that may be due to tree canopy. The speed data were collected using road tube counters, more specifically JAMAR Technologies products – TRAX Flex HS Counter/Classifier and the TRAX Apollyon II.

In addition to the speed data, braking operations for drivers were also observed. That is, observations of whether a driver braked or not as he/she traversed a full canopied segment were monitored. Trail cameras (see Figure C13) that begin recording when motion is detected were used. These cameras have a 20-megapixel resolution, an Illumi-Night 2 Sensor for clear and bright night vision videos and pictures, a 100 ft (30.5 m) range for infrared flash, 80 ft (24 m) range during the night, and a trigger speed of 0.3 seconds [Moultrie Feeders, 2018].

A trail camera was attached to a wooden stake and placed near the edge of pavement facing the direction of travel. At a single test location and in each direction, two cameras were placed at approximately 200 ft (61 m) and 400 ft (122 m) from the center of a full canopy segment. The cameras were set up to face the direction of travel of the nearest lane so when a vehicle passed, the camera would begin recording and capture the rear end of each vehicle for up to 10 seconds. These recorded videos were later post-processed and analyzed in the lab.

## Data Analysis

The overall objective of this part of the work was to provide data-driven empirical insights on the impact of tree canopy overtop the roadway pavement along low-volume two-lane roadways in Ohio. A variety of observed data – moisture, temperature, pavement condition – that are related to the pavement surface were analyzed. In addition, a safety related analysis was also performed. Specific details regarding the data collection methods and site selection were presented in the previous section; and this section outlines the statistical approach used to analyze the data.

**Comparisons of Pavement Surface Data**

For comparing the pavement surface data, the analysis methodology adopted a number of statistical tests to determine from the data a more definite answer on the effect of tree canopies on low volume roadways. Figure C14 is a flowchart of the process for obtaining statistical inference to the hypotheses regarding the effects of tree canopy overtop the pavement. The statistical tests were all performed using IBM's Statistical Package for the Social Sciences (SPSS v25) software – a common tool used by researchers for performing interactive or batched statistical analyses on large datasets [IBM, 2007]. Details and background information about each statistical test used (normality, Levene's test for homogeneity of variances, Welch's F ratio, ANOVA, Tukey, Kruskal-Wallis H, Mann Whitney U, and Games Howell) are discussed at length by Horn [2019] in Chapter 4.

**Safety Analysis – Predictive Method**

To examine the safety benefits (if any) of tree trimming along canopied rural roadways, a before-after safety analysis using the Highway Safety Manual (HSM) predictive method was adopted. The predictive method, can be used to quantitatively estimate the safety of a transportation facility [AASHTO, 2010]. The HSM predictive method includes the use of statistically derived equations known as safety performance functions (SPFs) and crash modification factors (CMFs). Essentially, an SPF predicts the crash frequency for a set of base conditions unique to each facility type; and then a set of CMFs modify the base condition estimates to help account for various changes in non-base conditions. A calibration factor (CF) further modifies the base estimate to account for changes in local conditions. The HSM provides SPFs and CMFs for segments and intersections for the following transportation facility types including: Rural Two-Lane, Two-Way Roads; Rural Multilane Highways; and Urban and Suburban Arterials [AASHTO, 2010]. For the purpose of this study, the predictive method for rural two-lane, two-way (TLTW) roadways was adopted [AASHTO, 2010]. Therefore, the general mathematical formulation to compute the predicted number of crashes on a rural 2-lane 2-way road segment is presented in Equation 1.

$$N_{\text{pred},rs} = N_{spf,rs} * C_r * (CMF_{1r} * CMF_{2r} * \ldots * CMF_{12r}) \quad (1)$$

Where:

$N_{\text{pred},rs}$ = predicted average crash frequency for an individual roadway segment for a specific year,
$N_{spf\,rs}$ = predicted average crash frequency for base conditions for an individual roadway segment,
$C_r$ = calibration factor developed for a particular jurisdiction or geographical area, and
$CMF_{1r} \ldots CMF_{12r}$ = crash modification factors.

The base condition SPF for rural 2-lane 2-way segments as specified in the HSM is shown in Equation 2. This SPF provides an estimate of the average crashes per year as a function of AADT and length of roadway segment.

$$N_{spf\,rs} = AADT * L * 365 * 10^{-6} * e^{(-0.312)} \quad (2)$$

Where:

$N_{spf\,rs}$ = predicted total crashes per year for roadway segment under base conditions,
$AADT$ = average annual daily traffic volume (vehicles per day), and

*L* = length of roadway segment (miles) (1 mi = 1.6 km).

The base condition estimate obtained from Equation 2 is then modified using a total of 12 different CMFs. The specific CMF and their details are available in Volume 2 Chapter 10 of the HSM [AASHTO, 2010]. The modification factors are multiplied by the SPF in order to account for site specific geometric design features. The specific CMFs and the typical range of values that were calculated for the segments that were analyzed are given in Table C11. Note: where a CMF could not be calculated due to lack of data, the suggested base value was adopted.

The Empirical Bayes (EB) method was used to compare the predicted average crash frequency to the observed crash frequency to generate a corrected predicted frequency of crashes if tree trimming had not been performed. This is divided into the difference between this corrected prediction (without trimming) and the actual observed rate after trimming to generate an "index of safety". A bias factor is used to determine a composite safety value, and a Z test is used to determine if the change in crash rates is statistically significant at the 90% ($|Z| \geq 1.70$) or 95% ($|Z| \geq 2.0$) level.

### Surrogate Measure of Safety

Surrogate measures of safety (SMOS) are generally, "…an observed non-crash event that is physically related in a predictable and reliable way to crashes…" [Tarko, 2018]. SMOS are indirect safety measures that allow safety performance assessments to be made when crash frequencies are very low or altogether not available. A variety of SMOS have been used in past research such as traffic conflicts, running on red; acceleration noise; post-encroachment time; speed profile variation; and near crashes.

In this research, the SMOS were those of driver speeds and braking behaviors. These were compared between full canopy and open canopy segments at a couple of test locations. These SMOS will be aimed at determining if drivers behave differently under varying canopy levels. The observed speeds were quantitatively analyzed, whereas the braking data were analyzed as simple descriptive statistics.

## Results

### Before-After Crash Analysis

An analysis to determine the safety related benefits (if any) of tree trimming operations was undertaken using data from 46 roadway segments. The results from a naïve analysis (i.e., basic comparison of observed crashes in before and after periods), showed an overall decrease in average crashes – approximately 23% for all crash types – attributed to tree trimming/pruning. In addition, a more detailed safety analysis using methods described in the highway safety manual [AASHTO, 2010] was also performed.

Results from the Empirical Bayes based method indicated mixed findings with 39 locations exhibiting safety improvements and seven locations indicating no improvement in safety. Detailed results from these analyses are provided in Tables C12-C16. The composite (project level) results indicated that there was an overall 11% deterioration in safety at locations where tree maintenance operations (trimming/pruning) were performed. However, at 95% confidence,

this composite decrease in safety was not significant (Z-score = -1.43) and thus, these safety related results must be viewed with caution.

**Surrogate Measures of Safety**

*Speed Data*

Table C17 presents the results from Kruskal-Wallis H tests on the speed data by time of day (day/night). Overall, there were statistically significant differences under specific canopy levels for day and night conditions. Despite the statistically significant differences, no conclusive interpretations can be made due to the mixed results. That is,

- The average speed for drivers is higher during the night under full canopy for two site locations and lower during the night for one site location.
- The average speed for drivers is higher during the night under open canopy for one site location and lower during the night for one site location.

## Conclusion

Based on results from the study of large pavement segments – "road section study", the following conclusions can be made:

- There were no statistically significant differences between pavement condition ratings (PCR) under various canopy coverage levels. Based on the specified classification ranges, all of the test sections can be rated as "GOOD".
- Tree canopy causes moisture to remain on the pavement surface underneath for a longer time than is the case for open sky pavement (no canopy overtop). This is based on observed differences in water film height; on average +4.42 μm (0.17 mil) of additional moisture under canopied sections of roadway than open sky pavement. In practice, with moisture levels well below 0.1 inches (2.5 mm), there is a very small likelihood of drivers hydroplaning and subsequently impacting safety.
- Tree canopy overtop the pavement surface does affect the microclimate beneath and the shading (of sunlight) does cause temperature differentials. The analyses on observed data indicate that pavement surface exposed to direct sunlight was warmer – on average +5.09°F (+2.83°C) – than the pavement surface beneath tree canopy. This is expected; however, the temperature differential is minimal.
- Based on the safety analysis performed in this research, roadside maintenance activities (i.e., trimming/pruning of trees) provided safety benefits on a site-by-site basis. A further analysis of surrogate measures of safety (speed and braking operations) did not provide any conclusive findings. Observed speed data showed that drivers were traveling at high speeds under canopied road sections. Similarly, observed braking data suggest that the presence of tree canopies does not impact driver behavior.

## Bibliography


American Association of State Highway and Transportation Officials (AASHTO), 2010. *Highway Safety Manual*, American Association of State Highway and Transportation Officials, Washington, D.C.

Chin, H.C., S.T. Quek, and R.L., Cheu, 199. Quantitative Examination of Traffic Conflicts, *TRR* 1376, 1992.

Chin, H.C., and S.T. Quek, 1997. Measurement of Traffic Conflicts, *Safety Science*, vol. 26, no. 3, pp. 169–185.

FLIR Systems, Inc. 2019. FLIR E6 Infrared Camera with MSX|FLIR Systems. Available online at https://www.flir.com/products/e6/, Accessed March 22, 2019.

Forestry Suppliers, Inc. 2019. "Forestry Suppliers Spherical Crown Densiometers," *Forestry Suppliers, Inc.* Available online at http://www.forestry-suppliers.com/product_pages/products.php?mi=13971&itemnum=43887, Accessed March 22, 2019.

Hauer, E., 1997. *Observational Before/After Studies in Road Safety*. Emerald Group Publishing Limited.

Horn, A.L., 2019. *Assessment of Tree Canopy Effects Overtop Low Volume Roadways*, Master of Science Thesis (Unpublished), Department of Civil Engineering, Ohio University, Athens, OH, August 2019.

International Business Machines (IBM), 2017. IBM SPSS Statistics 25 Core System User's Guide.

JAMAR Technologies. 2019. "JAMAR TECHNOLOGIES: Traffic Data Collection & DMI Devices, Hatfield, PA. Available online at https://www.jamartech.com/, Accessed June 22, 2019.

Kloeden, C.N., and V.M. McLean, 1997. *Traveling Speed and the Risk of Crash Involvement*, p. 69, 1997.

G. Lufft Mess- und Regeltechnik GmbH (Lufft). 2019. MARWIS - Mobile Advanced Road Weather Information Sensor. Available online at https://www.lufft.com/products/road-runway-sensors-292/marwis-umb-mobile-advanced-road-weather-information-sensor-2308/, Accessed June 21, 2019.

Minderhoud, M.M., and P.H.L. Bovy, 2001. Extended Time-to-Collision Measures for Road Traffic Safety Assessment, *Accident Analysis & Prevention*, vol. 33, no. 1, pp. 89–97.

Moultrie Feeders. 2018. Instructions for M-Series Game Cameras. Available online at https://smhttp-ssl-79917.nexcesscdn.net/media/downloads/1989/M-SERIES%20(2018)%20manual_ENGLISH_7-20-18_web.pdf, Accessed December 17, 2019.

Naik, B., J. Appiah, and L.R. Rilett, 2018. Are Dilemma Zone Protection Systems Useful on High-Speed Arterials with Signal Coordination? A Case Study, presented at the Transportation Research Board 97th Annual Meeting, Washington DC.

Ohio DOT, 2006. *Pavement Condition Rating Manual*. Ohio Department of Transportation, Office of Pavement Engineering, Columbus, Ohio.

Ohio DOT, 2018. "Pages - Digital Photolog.". Available online at http://www.dot.state.oh.us/Divisions/Planning/TechServ/infrastructure/Pages/DigitalPhotolog.aspx, Accessed: August 14, 2018.

Ohio DOT, 2019a. “Pages - GIS Crash Analysis Tool (GCAT).” Available online at http://www.dot.state.oh.us/Divisions/Planning/ProgramManagement/HighwaySafety/HSIP/Pages/GCAT.aspx, Accessed June 21, 2019.

Ohio DOT, 2019b. “Transportation Data Management System.” Available online at https://odot.ms2soft.com/tcds/tsearch.asp?loc=Odot&mod=, Accessed June 21, 2019.

Porter, B.E., and T.D. Berry, 1999. A Nationwide Survey of Red Light Running: Measuring Driver Behaviors for the ‘Stop Red Light Running’ Program”.

Shoarian-Sattari, K., and D. Powell, 1987. Measured Vehicle Flow Parameters as Predictors in Road Traffic Accident Studies, *Traffic engineering and control*, vol. 28, no. 6, pp. 328–329.

Tarko, A.P., 2018. Chapter 17. Surrogate Measures of Safety, in *Safe Mobility: Challenges, Methodology and Solutions*, vol. 11, 0 vols., Emerald Publishing Limited, 2018, pp. 383–405.

Tarko, A. et al., 2009. Surrogate Measures of Safety, 28-Apr-2009. Available online at http://n.saunier.free.fr/saunier/stock/tarko09surrogate.pdf, Accessed June 21, 2019.

Trailacampro.com. 2019. Moultrie M-50, *Trailcampro.com*. Available online at https://www.trailcampro.com/products/moultrie-m-50, Accessed March 22, 2019.


***Figure C1. State of Ohio Map Showing ODOT Districts 4, 5, 9, 10, 11, and 12.***

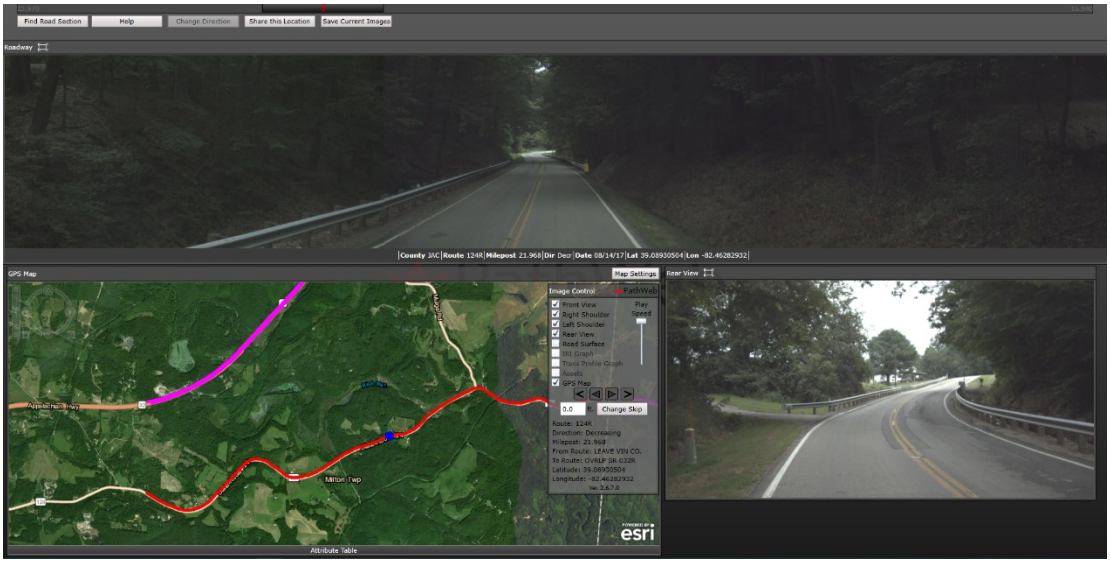


***Figure C2. Pathweb Screen [Ohio DOT, 2018].***

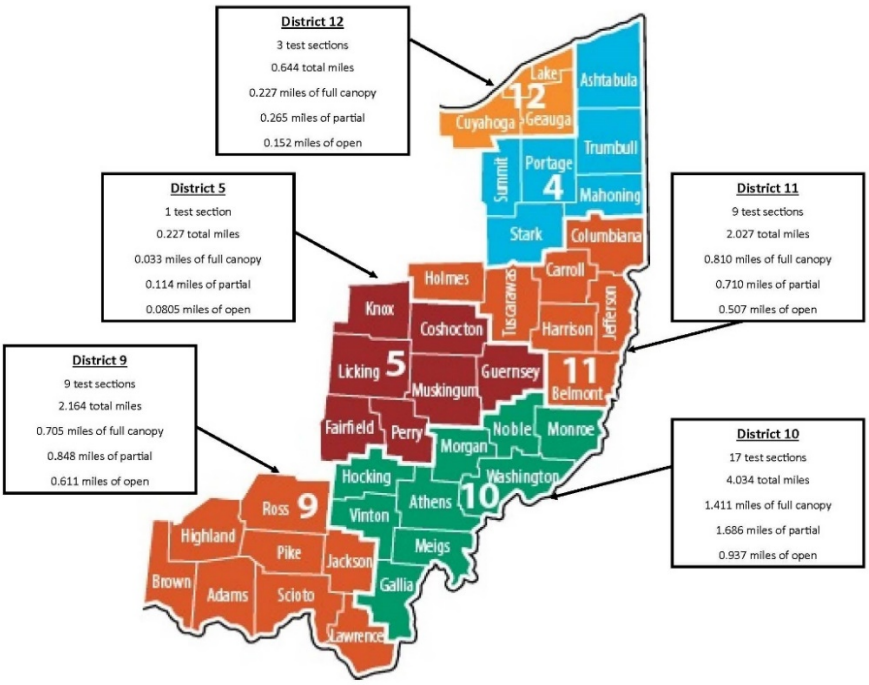


***Figure C3. Summary of Selected Test Locations in Ohio DOT Districts 5, 9, 10, 11, and 12.***


***Figure C4. Convex Spherical Forestry Densiometer [Forestry Suppliers, 2019].***

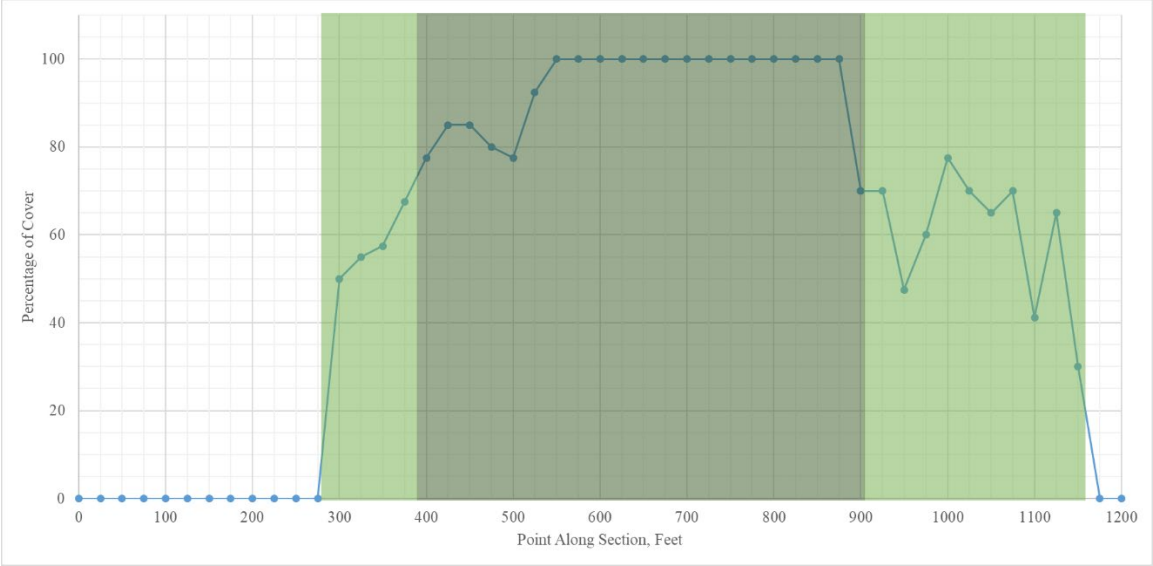


***Figure C5. Measured Canopy Coverage - SR 124 (2) in Jackson County, Ohio.***

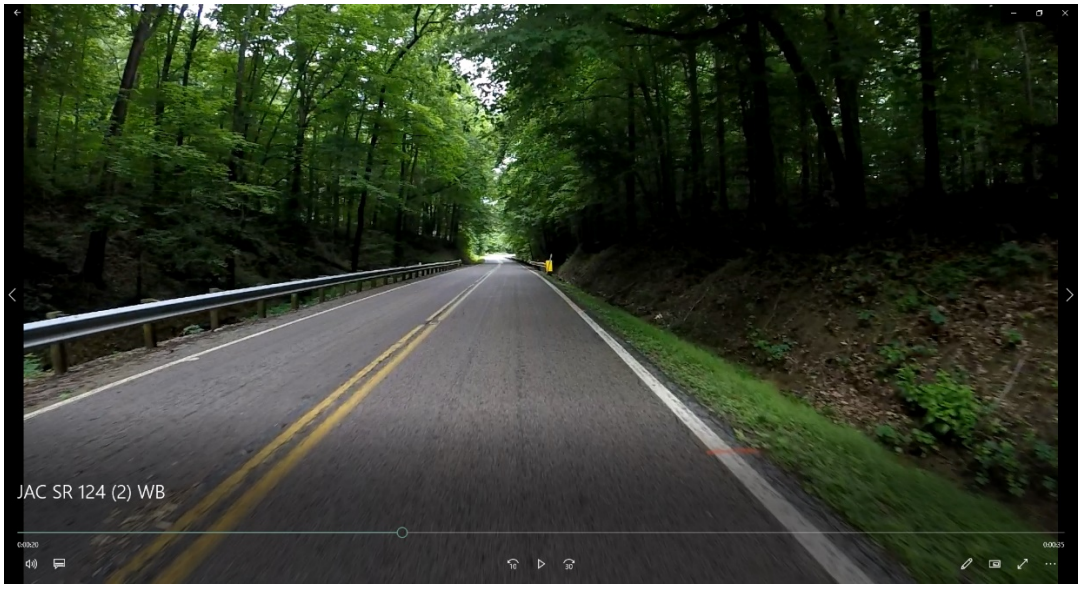


***Figure C6. Snapshot of Video – SR 124 (2) (WB) in Jackson County, Ohio.***


*Figure C7. Lufft MARWIS Sensor.*

| 1 | date | time | latitude | longitude | altitude | course | speed | Dew Point [°C] | Surface Temperature [°C] | Road Condition Lufft [logic] | Friction [] | Ice Percent [%] | Water Film Height [µm] |
|---|---|---|---|---|---|---|---|---|---|---|---|---|---|
| 2 | 9/10/2018 | 11:07:19 AM | 39.13436189 | -82.57489426 | 226.26 | 182 | 33 | 16.02 | 21.77 | 0 | 0.82 | 0 | 0 |
| 3 | 9/10/2018 | 11:07:20 AM | 39.1342424 | -82.57489803 | 227.03 | 182 | 32 | 16.02 | 22.02 | 0 | 0.82 | 0 | 0 |
| 4 | 9/10/2018 | 11:07:21 AM | 39.13410938 | -82.57490013 | 226.65 | 181 | 32 | 16.02 | 21.99 | 0 | 0.82 | 0 | 0 |
| 5 | 9/10/2018 | 11:07:22 AM | 39.13398437 | -82.57490465 | 227.63 | 182 | 32 | 16.02 | 22.16 | 0 | 0.82 | 0 | 0 |
| 6 | 9/10/2018 | 11:07:23 AM | 39.13384954 | -82.57491396 | 223.98 | 181 | 32 | 16.02 | 22.56 | 0 | 0.82 | 0 | 0 |
| 7 | 9/10/2018 | 11:07:24 AM | 39.13370915 | -82.57492184 | 224.15 | 182 | 33 | 16.03 | 23.2 | 0 | 0.82 | 0 | 0 |
| 8 | 9/10/2018 | 11:07:25 AM | 39.13345547 | -82.57494304 | 225.07 | 185 | 32 | 16.03 | 22.45 | 0 | 0.82 | 0 | 0 |
| 9 | 9/10/2018 | 11:07:26 AM | 39.13332723 | -82.574964 | 226.1 | 188 | 32 | 16.04 | 21.73 | 0 | 0.82 | 0 | 0 |
| 10 | 9/10/2018 | 11:07:27 AM | 39.13332723 | -82.574964 | 226.1 | 188 | 32 | 16.04 | 21.35 | 0 | 0.82 | 0 | 0 |
| 11 | 9/10/2018 | 11:07:28 AM | 39.13318851 | -82.5749951 | 225.9 | 189 | 34 | 16.04 | 20.5 | 0 | 0.82 | 0 | 0 |
| 12 | 9/10/2018 | 11:07:29 AM | 39.13305507 | -82.57504212 | 225.76 | 192 | 34 | 16.04 | 19.54 | 0 | 0.82 | 0 | 8.96 |
| 13 | 9/10/2018 | 11:07:30 AM | 39.13292037 | -82.57508311 | 225.74 | 193 | 34 | 16.04 | 20.46 | 1 | 0.81 | 0 | 29.61 |
| 14 | 9/10/2018 | 11:07:31 AM | 39.13266719 | -82.57518847 | 225.56 | 200 | 34 | 16.05 | 20.6 | 0 | 0.82 | 0 | 4.27 |
| 15 | 9/10/2018 | 11:07:32 AM | 39.13266719 | -82.57518847 | 225.56 | 200 | 34 | 16.05 | 19.63 | 0 | 0.82 | 0 | 0 |
| 16 | 9/10/2018 | 11:07:34 AM | 39.13240509 | -82.5753577 | 226.42 | 208 | 36 | 16.05 | 19.43 | 0 | 0.82 | 0 | 0 |
| 17 | 9/10/2018 | 11:07:35 AM | 39.13217974 | -82.57557127 | 227.21 | 215 | 36 | 16.06 | 20.02 | 0 | 0.82 | 0 | 0 |
| 18 | 9/10/2018 | 11:07:36 AM | 39.13217974 | -82.57557127 | 227.21 | 215 | 36 | 16.06 | 19.69 | 0 | 0.82 | 0 | 0 |
| 19 | 9/10/2018 | 11:07:37 AM | 39.1320795 | -82.57567219 | 227.48 | 215 | 35 | 16.07 | 19.07 | 0 | 0.82 | 0 | 0 |
| 20 | 9/10/2018 | 11:07:38 AM | 39.13196311 | -82.57577017 | 227.71 | 216 | 34 | 16.08 | 19.47 | 0 | 0.82 | 0 | 0 |
| 21 | 9/10/2018 | 11:07:39 AM | 39.13171845 | -82.57600386 | 228.02 | 217 | 36 | 16.09 | 20.18 | 0 | 0.82 | 0 | 0 |
| 22 | 9/10/2018 | 11:07:40 AM | 39.13171845 | -82.57600386 | 228.02 | 217 | 36 | 16.09 | 20.19 | 0 | 0.82 | 0 | 0 |
| 23 | 9/10/2018 | 11:07:41 AM | 39.13150538 | -82.57621843 | 229.97 | 217 | 36 | 16.11 | 20.33 | 0 | 0.82 | 0 | 0 |
| 24 | 9/10/2018 | 11:07:43 AM | 39.13140094 | -82.57632379 | 230.3 | 217 | 36 | 16.11 | 22.57 | 0 | 0.82 | 0 | 0 |

*Figure C8. Sample MARWIS Data Log File from SR 124 (2) in Jackson County, OH.*

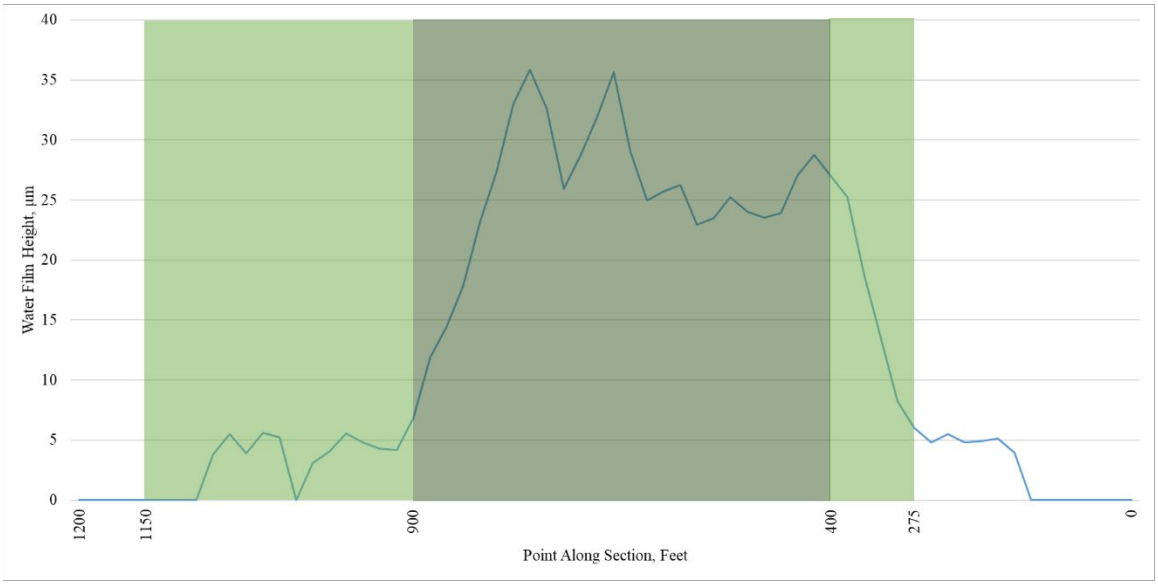


***Figure C9. Measured Moisture Levels – SR 124 (2) (WB) in Jackson County, OH.***


***Figure C10. FLIR E6 Infrared Camera [FLIR Systems, Inc., 2019].***

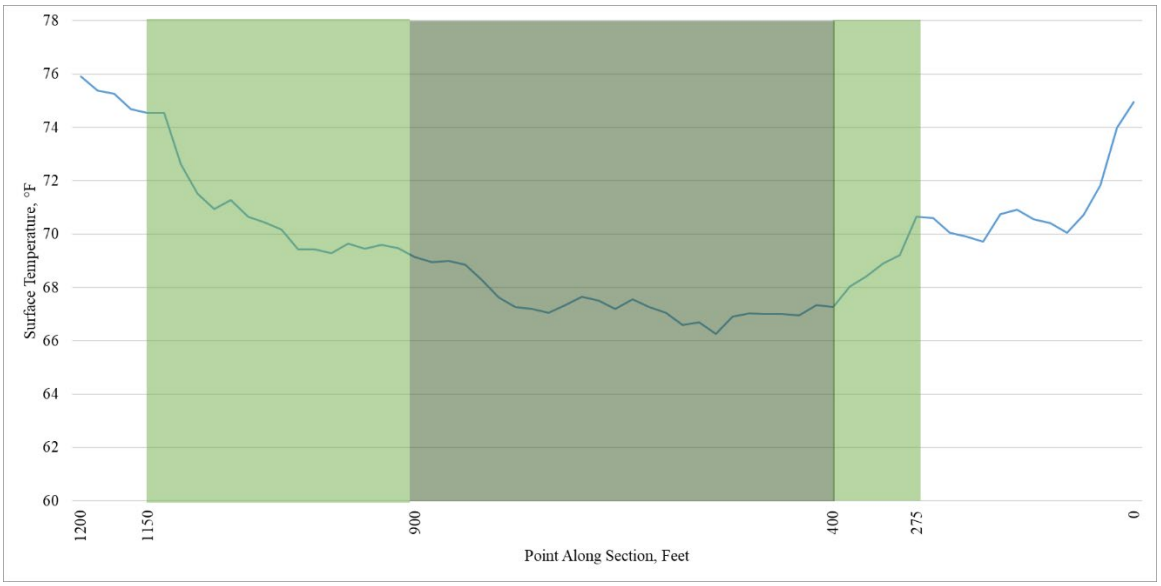


***Figure C11. Measured Pavement Temperatures – SR 124 (2) (WB) in Jackson County, OH. (1 ft = 0.305 m, Temperature range is 15.6°C to 25.6°C)***

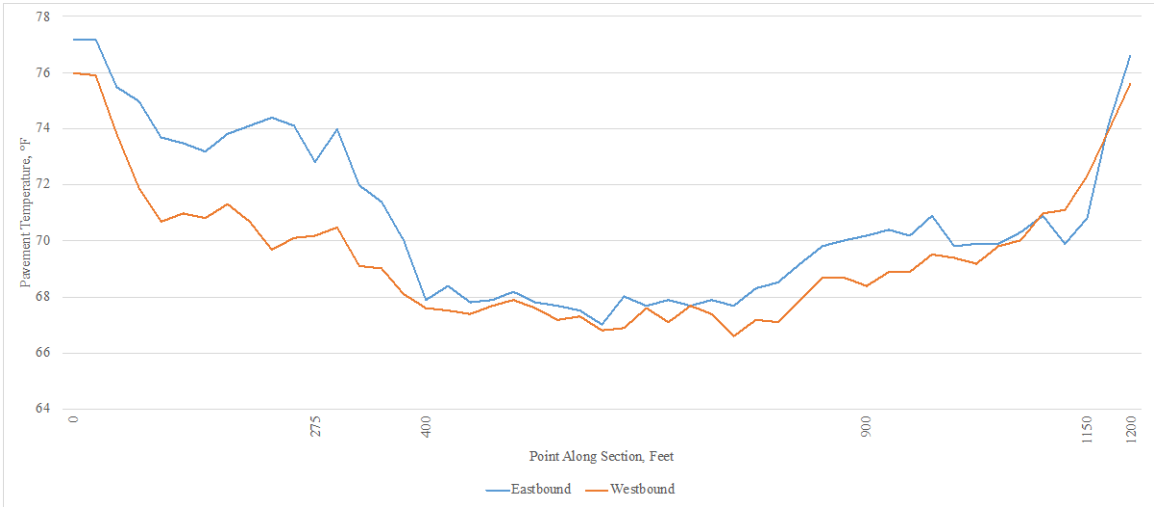


***Figure C12. Measured Temperature Levels on SR 124 (2) (EB, WB) in Jackson County, Ohio (1 ft = 0.305 m, Temperature range 17.8°C to 25.6°C)***


***Figure C13. Moultrie M-50 Trail Camera [Moultrie Feeders, 2019].***

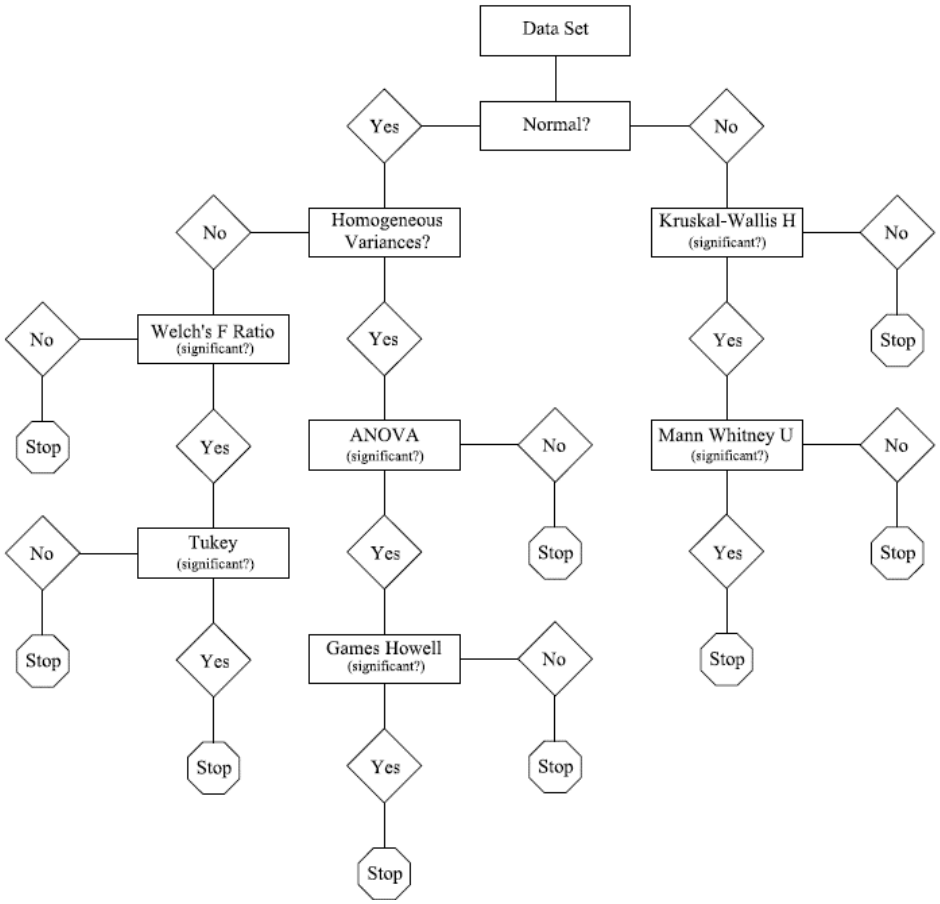


***Figure C14. Statistical Analysis Flowchart [Horn, 2019].***

***Table C1. Location of tree canopied test sites.***

| ODOT District | County | Route | Milepost | |
|---|---|---|---|---|
| | | | Canopy Start | Canopy End |
| 5 | Muskingum | SR 284 | 7.665 | 7.91 |
| 9 | Scioto | SR 139 | 14.084 | 14.35 |
| | | SR 125 | 5.484 | 5.259 |
| | Pike | SR 335 (1) | 14.578 | 14.967 |
| | | SR 335 (2) | 11.541 | 11.686 |
| | Jackson | SR 139 | 7.396 | 7.63 |
| | | SR 327 (1) | 14.924 | 14.714 |
| | | SR 327 (2) | 14.924 | 15.244 |
| | | SR 124 (1) | 23.161 | 23.431 |
| | | SR 124 (2) | 21.818 | 22.023 |
| 10 | Vinton | SR 356 | 0.302 | 0.478 |
| | | SR 124 | 4.605 | 4.84 |
| | | SR 56 | 1.705 | 1.218 |
| | | SR 327 (1) | 2.926 | 2.816 |
| | | SR 327 (2) | 4.918 | 4.614 |
| | Hocking | SR 56 | 13.196 | 12.97 |
| | | SR 374 (1) | 0 | 0.244 |
| | | SR 374 (2) | 1.505 | 1.897 |
| | | SR 374 (3) | 2.817 | 3.118 |
| | | SR 278 | 5.187 | 5.398 |
| | | SR 595 | 7.076 | 6.846 |
| | Athens | SR 13 | 14.86 | 14.67 |
| | | SR 685 | 0.856 | 0.59 |
| | Washington | SR 260 | 10.25 | 10.039 |
| | | SR 555 | 15.26 | 15.475 |
| | | SR 676 (1) | 10.496 | 10.606 |
| | | SR 676 (2) | 10.357 | 10.131 |
| 11 | Belmont | SR 26 | 6.649 | 6.865 |
| | | SR 148 | 3.4 | 3.155 |
| | Harrison | SR 258 (1) | 1.793 | 1.984 |
| | | SR 258 (2) | 0.325 | 0.516 |
| | | SR 258 (3) | 1.021 | 1.248 |
| | Tuscarawas | SR 258 (1) | 19.654 | 19.836 |
| | | SR 258 (2) | 20.653 | 20.467 |
| | | SR 800 (1) | 24.924 | 25.213 |
| | | SR 800 (2) | 0.814 | 0.63 |
| 12 | Cuyahoga | SR 87 | 16.176 | 15.941 |
| | | SR 174 | 3.067 | 2.807 |
| | Lake | SR 608 | 0.669 | 0.432 |

Note: Routes with numbers in parenthesis correspond to multiple locations on the same route

***Table C2. Estimated directional PCR values at study sites.***

| ODOT District | County | Route | Northbound/Eastbound | | | Southbound/Westbound | | |
|---|---|---|---|---|---|---|---|---|
| | | | Full | Partial | Open | Full | Partial | Open |
| 5 | Muskingum | SR 284 | 78.35 | 68.75 | 73.98 | 92.95 | 91.63 | 83.78 |
| 9 | Scioto | SR 139 | 96.85 | 98.50 | 98.50 | 96.35 | 97.05 | 97.50 |
| | | SR 125 | 93.35 | 92.80 | 93.00 | 94.40 | 91.00 | 91.00 |
| | Pike | SR 335 (1) | 88.33 | 89.05 | 89.28 | 88.88 | 87.95 | 90.68 |
| | | SR 335 (2) | 84.33 | 89.63 | 87.65 | 83.23 | 86.03 | 85.88 |
| | Jackson | SR 139 | 91.35 | 94.93 | 95.50 | 93.53 | 93.65 | 94.50 |
| | | SR 327 (1) | 69.38 | 69.75 | 78.85 | 68.20 | 62.70 | 74.73 |
| | | SR 327 (2) | 80.50 | 72.90 | 79.93 | 73.48 | 69.90 | 82.13 |
| | | SR 124 (2) | 80.30 | 75.40 | 77.15 | 70.03 | 73.80 | 83.73 |
| | | SR 124 (1) | 74.95 | 75.85 | 81.65 | 75.75 | 77.05 | 86.75 |
| 10 | Vinton | SR 356 | 90.00 | 87.20 | 85.10 | 83.70 | 82.30 | 84.50 |
| | | SR 124 | 87.30 | 88.95 | 90.35 | 82.70 | 90.60 | 90.35 |
| | | SR 56 | 96.50 | 98.50 | 98.50 | 96.50 | 96.50 | 98.50 |
| | | SR 327 (2) | 87.10 | 87.10 | 84.10 | 88.50 | 90.10 | 84.10 |
| | | SR 327 (1) | 91.50 | 84.00 | 98.50 | 91.50 | 85.75 | 98.50 |
| | Hocking | SR 56 | 98.50 | 98.50 | 98.50 | 98.50 | 98.50 | 98.50 |
| | | SR 374 (3) | 88.10 | 89.10 | 91.20 | 89.50 | 89.10 | 90.20 |
| | | SR 374 (2) | 88.15 | 90.50 | 92.50 | 88.15 | 89.50 | 92.50 |
| | | SR 278 | 84.25 | 87.25 | 90.60 | 83.80 | 87.25 | 91.50 |
| | | SR 595 | 72.00 | 70.80 | 63.45 | 65.65 | 64.30 | 63.45 |
| | Athens | SR 13 | 73.65 | 83.45 | 77.15 | 68.60 | 74.35 | 78.05 |
| | | SR 685 | 67.25 | 73.25 | 73.00 | 67.25 | 70.95 | 75.30 |
| | Washington | SR 260 | 79.35 | 85.20 | 83.95 | 80.95 | 85.20 | 85.95 |
| | | SR 555 | 98.50 | 98.50 | 98.50 | 98.50 | 98.50 | 98.50 |
| | | SR 676 (1) | 83.55 | 82.85 | 84.95 | 82.85 | 80.60 | 84.95 |
| | | SR 676 (2) | 81.20 | 80.45 | 86.95 | 81.95 | 80.45 | 87.70 |
| 11 | Harrison | SR 26 | 85.95 | 80.08 | 85.05 | 86.88 | 91.75 | 89.03 |
| | | SR 148 | 80.93 | 79.53 | 87.53 | 84.65 | 84.53 | 78.93 |
| | | SR 258 (1) | 72.45 | 78.13 | 78.10 | 73.05 | 80.33 | 84.80 |
| | | SR 258 (2) | 66.90 | 73.83 | 76.20 | 68.53 | 72.93 | 72.63 |
| | | SR 258 (3) | 68.68 | 79.93 | 77.28 | 72.80 | 67.05 | 70.75 |
| | Tuscarawas | SR 258 (1) | 77.90 | 80.18 | 77.18 | 80.88 | 80.78 | 78.05 |
| | | SR 258 (2) | 83.00 | 82.00 | 85.30 | 76.85 | 79.20 | 81.38 |
| | | SR 800 (1) | 76.00 | 78.05 | 79.03 | 71.33 | 78.28 | 80.20 |
| | | SR 800 (2) | 94.65 | 95.40 | 95.40 | 93.65 | 96.80 | 95.30 |
| 12 | Cuyahoga | SR 87 | 88.40 | 92.35 | 95.35 | 91.85 | 92.35 | 95.45 |
| | | SR 608 | 75.15 | 73.28 | 80.90 | 72.20 | 70.78 | 80.28 |
| | | SR 174 | 93.85 | 93.50 | 94.15 | 93.35 | 93.20 | 93.15 |

**Note**: Routes with numbers in parenthesis correspond to multiple locations on the same route.
Canopy definitions: "Open" = 0-25% coverage, "Partial" = 25-75% coverage, "Full" = 75-100% coverage.
PCR ratings are on a scale of 0 to 100, with 100 being best.

***Table C3. Descriptive statistics of moisture film height on pavement surface.***

| County (ODOT District) | Route | Canopy | N | Mean | | Median | | Std. Deviation | |
|---|---|---|---|---|---|---|---|---|---|
| | | | | (µm) | (mil) | (µm) | (mil) | (µm) | (mil) |
| Athens (District 10) | SR 13 | Open | 23 | 0 | 0 | 0 | 0 | 0 | 0 |
| | | Partial | 39 | 1.24 | 0.049 | 0 | 0 | 3.63 | 0.143 |
| | | Full | 26 | 1.23 | 0.048 | 0 | 0 | 3.51 | 0.138 |
| Hocking (District 10) | SR 56 | Open | 48 | 1.52 | 0.06 | 0 | 0 | 2.77 | 0.109 |
| | | Partial | 31 | 0.27 | 0.011 | 0 | 0 | 0.85 | 0.033 |
| | | Full | 70 | 6.15 | 0.242 | 0 | 0 | 14.86 | 0.585 |
| | SR 374 (1) | Open | 38 | 25.52 | 1.005 | 16.79 | 0.661 | 33.04 | 1.301 |
| | | Partial | 27 | 13.85 | 0.545 | 12.74 | 0.502 | 4.04 | 0.159 |
| | | Full | 74 | 15.3 | 0.602 | 15.12 | 0.595 | 3.37 | 0.133 |
| | SR 374 (2) | Open | 66 | 16.29 | 0.641 | 16.95 | 0.667 | 6.77 | 0.267 |
| | | Partial | 218 | 8.89 | 0.35 | 8.08 | 0.318 | 4.46 | 0.176 |
| | | Full | 129 | 12.07 | 0.475 | 11.62 | 0.457 | 7.43 | 0.293 |
| | SR 374 (3) | Open | 29 | 108.45 | 4.27 | 94.02 | 3.702 | 58.57 | 2.306 |
| | | Partial | 51 | 76.79 | 3.023 | 52.34 | 2.061 | 64.69 | 2.547 |
| | | Full | 115 | 43.34 | 1.706 | 23.06 | 0.908 | 49.19 | 1.937 |
| Vinton (District 10) | SR 356 | Open | 56 | 0 | 0 | 0 | 0 | 0 | 0 |
| | | Partial | 87 | 0.31 | 0.012 | 0 | 0 | 1.08 | 0.043 |
| | | Full | 29 | 0.99 | 0.039 | 0 | 0 | 2.09 | 0.082 |
| | SR 124 | Open | 7 | 0.51 | 0.02 | 0 | 0 | 1.35 | 0.053 |
| | | Partial | 33 | 0.35 | 0.014 | 0 | 0 | 0.98 | 0.039 |
| | | Full | 50 | 2.97 | 0.117 | 3.17 | 0.125 | 2.65 | 0.104 |
| | SR 56 | Open | 86 | 13.44 | 0.529 | 13.09 | 0.515 | 2.91 | 0.115 |
| | | Partial | 251 | 10.04 | 0.395 | 9.99 | 0.393 | 3.04 | 0.12 |
| | | Full | 94 | 6.78 | 0.267 | 6.6 | 0.26 | 2.21 | 0.087 |
| | SR 327 (1) | Open | 5 | 0 | 0 | 0 | 0 | 0 | 0 |
| | | Partial | 54 | 7.73 | 0.304 | 7.04 | 0.277 | 6.76 | 0.266 |
| | | Full | 9 | 13.1 | 0.516 | 5.98 | 0.235 | 9.69 | 0.381 |
| | SR 327 (2) | Open | 43 | 2.77 | 0.109 | 0 | 0 | 4.16 | 0.164 |
| | | Partial | 69 | 6.84 | 0.269 | 6.64 | 0.261 | 3.93 | 0.155 |
| | | Full | 17 | 12.93 | 0.509 | 13.54 | 0.533 | 2.18 | 0.086 |
| Washington (District 10) | SR 260 | Open | 35 | 68.91 | 2.713 | 46.11 | 1.815 | 56.77 | 2.235 |
| | | Partial | 33 | 38.83 | 1.529 | 42.7 | 1.681 | 10.16 | 0.4 |
| | | Full | 50 | 33.76 | 1.329 | 30.81 | 1.213 | 13.81 | 0.544 |
| | SR 555 | Open | 28 | 0.39 | 0.015 | 0 | 0 | 1.24 | 0.049 |
| | | Partial | 47 | 2.51 | 0.099 | 0 | 0 | 4 | 0.157 |
| | | Full | 43 | 1.71 | 0.067 | 0 | 0 | 3.14 | 0.124 |
| | SR 676 (1) | Open | 19 | 0.89 | 0.035 | 0 | 0 | 1.2 | 0.047 |
| | | Partial | 33 | 2.17 | 0.085 | 0 | 0 | 3.73 | 0.147 |
| | | Full | 20 | 4.32 | 0.17 | 4.5 | 0.177 | 3.5 | 0.138 |
| | SR 676 (2) | Open | 17 | 8.2 | 0.323 | 4.54 | 0.179 | 7.45 | 0.293 |
| | | Partial | 54 | 13.86 | 0.546 | 14.77 | 0.581 | 8.34 | 0.328 |
| | | Full | 37 | 13.85 | 0.545 | 14.61 | 0.575 | 7.15 | 0.281 |

***Table C4. Descriptive statistics of moisture film height on pavement surface.***

| County (ODOT District) | Route | Canopy | N | Mean | | Median | | Std. Deviation | |
|---|---|---|---|---|---|---|---|---|---|
| | | | | (µm) | (mil) | (µm) | (mil) | (µm) | (mil) |
| Harrison (District 11) | SR 258 (4) | Open | 21 | 79.08 | 3.113 | 57.37 | 2.259 | 56.82 | 2.237 |
| | | Partial | 30 | 47.34 | 1.864 | 33.24 | 1.309 | 34.11 | 1.343 |
| | | Full | 60 | 25.54 | 1.006 | 24.48 | 0.964 | 12.57 | 0.495 |
| Tuscarawas (District 11) | SR 800 (1) | Open | 28 | 15.83 | 0.623 | 16.14 | 0.635 | 4.86 | 0.191 |
| | | Partial | 44 | 18.84 | 0.742 | 17.64 | 0.694 | 6.54 | 0.257 |
| | | Full | 43 | 17.8 | 0.701 | 16.64 | 0.655 | 6.96 | 0.274 |

***Table C5. Descriptive statistics of pavement surface temperature – MARWIS.***

| County (ODOT District) | Route | Canopy | N | Mean | | Median | | Std. Deviation | |
|---|---|---|---|---|---|---|---|---|---|
| | | | | (°F) | (°C) | (°F) | (°C) | (°F) | (°C) |
| Jackson (District 9) | SR 124 (1) | Open | 45 | 72.14 | 22.3 | 72.07 | 22.26 | 0.89 | 0.49 |
| | | Partial | 38 | 68.83 | 20.46 | 68.66 | 20.37 | 0.74 | 0.41 |
| | | Full | 58 | 68.1 | 20.06 | 68.07 | 20.04 | 0.59 | 0.33 |
| | SR 124 (2) | Open | 36 | 72.16 | 22.31 | 71.18 | 21.77 | 2.14 | 1.19 |
| | | Partial | 43 | 70.16 | 21.2 | 69.66 | 20.92 | 1.43 | 0.79 |
| | | Full | 53 | 67.57 | 19.76 | 67.48 | 19.71 | 0.67 | 0.37 |
| Pike (District 9) | SR 335 (1) | Open | 47 | 67.71 | 19.84 | 67.57 | 19.76 | 0.94 | 0.52 |
| | | Partial | 108 | 67.6 | 19.78 | 67.56 | 19.76 | 0.73 | 0.41 |
| | | Full | 58 | 67.33 | 19.63 | 67.44 | 19.69 | 0.82 | 0.46 |
| | SR 335 (2) | Open | 40 | 69.18 | 20.66 | 69.13 | 20.63 | 1.55 | 0.86 |
| | | Partial | 28 | 66.65 | 19.25 | 66.41 | 19.12 | 1.04 | 0.58 |
| | | Full | 51 | 67.08 | 19.49 | 66.87 | 19.37 | 0.94 | 0.52 |
| Scioto (District 9) | SR 139 | Open | 46 | 70.9 | 21.61 | 71.4 | 21.89 | 1.27 | 0.71 |
| | | Partial | 54 | 68.38 | 20.21 | 68.29 | 20.16 | 0.53 | 0.29 |
| | | Full | 64 | 68.03 | 20.02 | 68.01 | 20.01 | 0.42 | 0.23 |

***Table C6. Descriptive statistics of pavement surface temperature – MARWIS.***

| County (ODOT District) | Route | Canopy | N | Mean | | Median | | Std. Deviation | |
|---|---|---|---|---|---|---|---|---|---|
| | | | | (°F) | (°C) | (°F) | (°C) | (°F) | (°C) |
| Harrison (District 11) | SR 258 (4) | Open | 21 | 81.37 | 27.43 | 81.32 | 27.4 | 1.17 | 0.65 |
| | | Partial | 30 | 81.22 | 27.34 | 80.9 | 27.17 | 2.26 | 1.26 |
| | | Full | 60 | 77.29 | 25.16 | 76.9 | 24.94 | 1.28 | 0.71 |
| Tuscarawas (District 11) | SR 800 (1) | Open | 28 | 79.12 | 26.18 | 79.2 | 26.22 | 1.03 | 0.57 |
| | | Partial | 44 | 76.96 | 24.98 | 76.92 | 24.96 | 0.93 | 0.52 |
| | | Full | 43 | 76.11 | 24.51 | 76.17 | 24.54 | 1.12 | 0.62 |

***Table C7. Descriptive statistics of pavement surface temperature – MARWIS.***

| County (ODOT District) | Route | Canopy | N | Mean | | Median | | Std. Deviation | |
|---|---|---|---|---|---|---|---|---|---|
| | | | | (°F) | (°C) | (°F) | (°C) | (°F) | (°C) |
| Athens (District 10) | SR 13 | Open | 22 | 94.25 | 34.58 | 93.27 | 34.04 | 7.03 | 3.91 |
| | | Partial | 34 | 85.31 | 29.62 | 85.87 | 29.93 | 4.71 | 2.62 |
| | | Full | 26 | 81.35 | 27.42 | 80.47 | 26.93 | 2.74 | 1.52 |
| Hocking (District 10) | SR 56 | Open | 34 | 80.98 | 27.21 | 80.66 | 27.04 | 2.12 | 1.18 |
| | | Partial | 20 | 78.25 | 25.69 | 78.94 | 26.08 | 2.75 | 1.53 |
| | | Full | 48 | 75.36 | 24.09 | 75.2 | 24 | 1.5 | 0.83 |
| | SR 374 (1) | Open | 28 | 76.72 | 24.84 | 77.16 | 25.09 | 1.71 | 0.95 |
| | | Partial | 22 | 73.69 | 23.16 | 73.54 | 23.08 | 1.51 | 0.84 |
| | | Full | 48 | 72.97 | 22.76 | 72.73 | 22.63 | 1.25 | 0.69 |
| | SR 374 (2) | Open | 32 | 61.52 | 16.4 | 60.81 | 16.01 | 1.15 | 0.64 |
| | | Partial | 80 | 60.59 | 15.88 | 60.4 | 15.78 | 0.74 | 0.41 |
| | | Full | 50 | 60.35 | 15.75 | 60.21 | 15.67 | 0.73 | 0.41 |
| | SR 374 (3) | Open | 20 | 62 | 16.67 | 62.02 | 16.68 | 0.21 | 0.12 |
| | | Partial | 36 | 61.62 | 16.46 | 61.66 | 16.48 | 0.6 | 0.33 |
| | | Full | 74 | 61.2 | 16.22 | 61.12 | 16.18 | 0.52 | 0.29 |
| Vinton (District 10) | SR 356 | Open | 38 | 78.55 | 25.86 | 78.59 | 25.89 | 2.17 | 1.28 |
| | | Partial | 54 | 71.66 | 22.04 | 71.02 | 21.68 | 3.34 | 2.13 |
| | | Full | 22 | 70 | 21.11 | 69.69 | 20.94 | 2.19 | 1.74 |
| | SR 124 | Open | 4 | 72.01 | 22.23 | 72.3 | 22.39 | 0.25 | 0.7 |
| | | Partial | 22 | 70.82 | 21.56 | 70.93 | 21.63 | 0.51 | 0.79 |
| | | Full | 32 | 69.11 | 20.62 | 69.07 | 20.6 | 1.3 | 0.46 |
| | SR 56 | Open | 40 | 62.07 | 16.7 | 62 | 16.67 | 1.1 | 0.68 |
| | | Partial | 120 | 61.25 | 16.25 | 61.14 | 16.19 | 0.68 | 0.75 |
| | | Full | 42 | 60.81 | 16.01 | 60.81 | 16.01 | 0.67 | 0.6 |
| | SR 327 (1) | Open | 4 | 68.86 | 20.48 | 68.92 | 20.51 | 0.21 | 0.66 |
| | | Partial | 40 | 67.65 | 19.8 | 67.7 | 19.84 | 0.78 | 0.61 |
| | | Full | 6 | 66.85 | 19.36 | 66.87 | 19.37 | 0.11 | 0.37 |
| | SR 327 (2) | Open | 36 | 70.28 | 21.27 | 70.47 | 21.37 | 1.34 | 0.8 |
| | | Partial | 64 | 67.95 | 19.97 | 67.84 | 19.91 | 0.66 | 0.87 |
| | | Full | 22 | 66.63 | 19.24 | 66.7 | 19.28 | 0.56 | 0.36 |
| Washington (District 10) | SR 260 | Open | 35 | 81.65 | 27.58 | 81.82 | 27.68 | 1.22 | 0.68 |
| | | Partial | 33 | 77.89 | 25.49 | 78.04 | 25.58 | 1.1 | 0.61 |
| | | Full | 50 | 75.85 | 24.36 | 75.7 | 24.28 | 0.92 | 0.51 |
| | SR 555 | Open | 28 | 87.48 | 30.82 | 83.78 | 28.77 | 7.56 | 4.2 |
| | | Partial | 47 | 83.44 | 28.58 | 80.91 | 27.17 | 5.8 | 3.22 |
| | | Full | 43 | 79.92 | 26.62 | 79.03 | 26.13 | 3.03 | 1.68 |
| | SR 676 (1) | Open | 19 | 94.58 | 34.77 | 94.84 | 34.91 | 1.45 | 0.81 |
| | | Partial | 33 | 87.83 | 31.02 | 87.93 | 31.07 | 2.81 | 1.56 |
| | | Full | 20 | 81.61 | 27.56 | 81.1 | 27.28 | 3.18 | 1.77 |
| | SR 676 (2) | Open | 17 | 84.96 | 29.42 | 84.29 | 29.05 | 2.03 | 1.13 |
| | | Partial | 54 | 82.15 | 27.86 | 81.87 | 27.71 | 2.22 | 1.23 |
| | | Full | 37 | 81.21 | 27.34 | 81.12 | 27.29 | 2.72 | 1.51 |

***Table C8. Descriptive statistics of pavement surface temperature – FLIR.***

| County (ODOT District) | Route | Canopy | N | Mean | | Median | | Std. Deviation | |
|---|---|---|---|---|---|---|---|---|---|
| | | | | (°F) | (°C) | (°F) | (°C) | (°F) | (°C) |
| Athens (District 10) | SR 13 | Open | 22 | 99.74 | 37.63 | 99.95 | 37.75 | 5.13 | 2.85 |
| | | Partial | 34 | 90.89 | 32.72 | 90.45 | 32.47 | 3.55 | 1.97 |
| | | Full | 26 | 83.94 | 28.86 | 83.35 | 28.53 | 2.2 | 1.22 |
| Hocking (District 10) | SR 56 | Open | 34 | 86.45 | 30.25 | 86.55 | 30.31 | 2.21 | 1.23 |
| | | Partial | 20 | 82.67 | 28.15 | 83.25 | 28.47 | 2.21 | 1.23 |
| | | Full | 48 | 79.38 | 26.32 | 79.25 | 26.25 | 2.13 | 1.18 |
| | SR 374 (1) | Open | 28 | 82.13 | 27.85 | 80.9 | 27.17 | 1.51 | 0.84 |
| | | Partial | 22 | 78.35 | 25.75 | 78.5 | 25.83 | 3.31 | 1.84 |
| | | Full | 48 | 76.87 | 24.93 | 76.7 | 24.83 | 1.36 | 0.76 |
| | SR 374 (2) | Open | 32 | 62.82 | 17.12 | 63 | 17.22 | 1.25 | 0.69 |
| | | Partial | 80 | 61.32 | 16.29 | 61.55 | 16.42 | 1.48 | 0.82 |
| | | Full | 50 | 60.85 | 16.03 | 61.1 | 16.17 | 0.87 | 0.48 |
| | SR 374 (3) | Open | 20 | 62.7 | 17.06 | 62.85 | 17.14 | 0.91 | 0.51 |
| | | Partial | 36 | 61.88 | 16.6 | 61.75 | 16.53 | 0.51 | 0.28 |
| | | Full | 74 | 61.07 | 16.15 | 61 | 16.11 | 0.68 | 0.38 |
| Vinton (District 10) | SR 356 | Open | 38 | 82.56 | 28.09 | 82.75 | 28.19 | 2.17 | 1.21 |
| | | Partial | 54 | 74.83 | 23.79 | 73.4 | 23 | 3.34 | 1.86 |
| | | Full | 22 | 71.81 | 22.12 | 71.1 | 21.72 | 2.19 | 1.22 |
| | SR 124 | Open | 4 | 70.88 | 21.6 | 70.85 | 21.58 | 0.25 | 0.14 |
| | | Partial | 22 | 70.45 | 21.36 | 70.3 | 21.28 | 0.51 | 0.28 |
| | | Full | 32 | 73.03 | 22.79 | 72.7 | 22.61 | 1.3 | 0.72 |
| | SR 56 | Open | 40 | 61.72 | 16.51 | 61.65 | 16.47 | 1.1 | 0.61 |
| | | Partial | 120 | 60.94 | 16.08 | 61 | 16.11 | 0.68 | 0.38 |
| | | Full | 42 | 60.13 | 15.63 | 60.15 | 15.64 | 0.67 | 0.37 |
| | SR 327 (1) | Open | 4 | 72.93 | 22.74 | 72.9 | 22.72 | 0.21 | 0.12 |
| | | Partial | 40 | 69.43 | 20.79 | 69.4 | 20.78 | 0.78 | 0.43 |
| | | Full | 6 | 68.3 | 20.17 | 68.3 | 20.17 | 0.11 | 0.06 |
| | SR 327 (2) | Open | 36 | 70.86 | 21.59 | 70.7 | 21.5 | 1.34 | 0.74 |
| | | Partial | 64 | 67.78 | 19.88 | 67.7 | 19.83 | 0.66 | 0.37 |
| | | Full | 22 | 66.84 | 19.36 | 66.85 | 19.36 | 0.56 | 0.31 |
| Washington (District 10) | SR 260 | Open | 26 | 81.43 | 27.46 | 80.6 | 27 | 1.22 | 2.05 |
| | | Partial | 24 | 77.18 | 25.1 | 77.45 | 25.25 | 1.1 | 1.59 |
| | | Full | 40 | 74.72 | 23.73 | 74.7 | 23.72 | 0.92 | 1.1 |
| | SR 555 | Open | 20 | 86.22 | 30.12 | 86.4 | 30.22 | 7.56 | 2.36 |
| | | Partial | 38 | 80.82 | 27.12 | 80.8 | 27.11 | 5.8 | 3.45 |
| | | Full | 36 | 78.52 | 25.84 | 78.55 | 25.86 | 3.03 | 2.33 |
| | SR 676 (1) | Open | 16 | 90.96 | 32.76 | 91 | 32.78 | 1.45 | 2.71 |
| | | Partial | 30 | 87.9 | 31.06 | 86.95 | 30.53 | 2.81 | 3.98 |
| | | Full | 16 | 81.17 | 27.32 | 81.05 | 27.25 | 3.18 | 1.41 |
| | SR 676 (2) | Open | 12 | 93.19 | 33.99 | 94.55 | 34.75 | 2.03 | 4.47 |
| | | Partial | 46 | 87.67 | 30.93 | 88.4 | 31.33 | 2.22 | 4.26 |
| | | Full | 32 | 85.73 | 29.85 | 87.15 | 30.64 | 2.72 | 4.66 |

***Table C9. Descriptive statistics of pavement surface temperature – FLIR.***

| County (ODOT District) | Route | Canopy | N | Mean | | Median | | Std. Deviation | |
|---|---|---|---|---|---|---|---|---|---|
| | | | | (°F) | (°C) | (°F) | (°C) | (°F) | (°C) |
| Jackson (District 9) | SR 124 (1) | Open | 34 | 76.01 | 24.45 | 75.85 | 24.36 | 1.31 | 0.73 |
| | | Partial | 30 | 71.21 | 21.78 | 71.35 | 21.86 | 0.83 | 0.46 |
| | | Full | 42 | 70.52 | 21.4 | 70.35 | 21.31 | 0.8 | 0.44 |
| | SR 124 (2) | Open | 28 | 73.46 | 23.03 | 73.8 | 23.22 | 2.24 | 1.25 |
| | | Partial | 30 | 70.19 | 21.22 | 70 | 21.11 | 1.22 | 0.68 |
| | | Full | 40 | 67.82 | 19.9 | 67.7 | 19.83 | 0.72 | 0.4 |
| Pike (District 9) | SR 335 (1) | Open | 34 | 69.53 | 20.85 | 69.53 | 20.85 | 1.16 | 0.64 |
| | | Partial | 62 | 69.16 | 20.65 | 69.15 | 20.64 | 0.73 | 0.41 |
| | | Full | 34 | 69.33 | 20.74 | 69.2 | 20.67 | 0.72 | 0.4 |
| | SR 335 (2) | Open | 26 | 71.48 | 21.93 | 71.5 | 21.94 | 1.94 | 1.08 |
| | | Partial | 14 | 68.96 | 20.53 | 68.6 | 20.33 | 1.38 | 0.77 |
| | | Full | 26 | 68.76 | 20.42 | 68.65 | 20.36 | 0.7 | 0.39 |
| Scioto (District 9) | SR 139 | Open | 28 | 72.22 | 22.35 | 72.9 | 22.72 | 1.68 | 0.93 |
| | | Partial | 40 | 69.11 | 20.62 | 69.3 | 20.72 | 1.02 | 0.56 |
| | | Full | 46 | 68.72 | 20.4 | 69 | 20.56 | 1.12 | 0.62 |

***Table C10. Descriptive statistics of pavement surface temperature – FLIR.***

| County (ODOT District) | Route | Canopy | N | Mean | | Median | | Std. Deviation | |
|---|---|---|---|---|---|---|---|---|---|
| | | | | (°F) | (°C) | (°F) | (°C) | (°F) | (°C) |
| Harrison (District 11) | SR 258 (4) | Open | 16 | 82.69 | 28.16 | 82.95 | 28.31 | 1.35 | 0.75 |
| | | Partial | 24 | 79.69 | 26.49 | 79.35 | 26.31 | 1.97 | 1.09 |
| | | Full | 50 | 76.14 | 24.52 | 76.15 | 24.53 | 0.93 | 0.52 |
| Tuscarawas (District 11) | SR 800 (1) | Open | 30 | 80.3 | 26.83 | 80.4 | 26.89 | 1.3 | 0.72 |
| | | Partial | 48 | 76.88 | 24.93 | 76.85 | 24.92 | 1.01 | 0.56 |
| | | Full | 44 | 75.45 | 24.14 | 75.3 | 24.06 | 1.18 | 0.66 |

***Table C11. CMF description, minimum and maximum values.***

| CMF | Description | Minimum Value | Maximum Value |
|---|---|---|---|
| 1 | Lane Width | 1.00 | 1.31 |
| 2 | Shoulder Width/Type | 1.00 | 1.01 |
| 3 | Roadside Hazard Rating | 1.00 | 1.00 |
| 4 | Driveway Density | 0.86 | 2.38 |
| 5 | Horizontal Curve | 1.00 | 27.55 |
| 6 | Vertical Curve | 1.00 | 1.24 |
| 7 | Centerline Rumble Strips | 1.00 | 1.00 |
| 8 | Passing Lanes | 1.00 | 1.00 |
| 9 | Two-way left-turn lanes | 1.00 | 1.00 |
| 10 | Lighting | 1.00 | 1.00 |
| 11 | Automated speed enforcement | 1.00 | 1.00 |
| 12 | Grade Level | 1.00 | 1.10 |

***Table C12. HSM predictive method results – District 4.***

**District 4**

| County | Route | $x_b$ | $x_a$ | $P_o$ | $\pi_a$ | var(m) | var($\pi_a$) | $\theta_a$ | % Change | Std Dev θ |
|---|---|---|---|---|---|---|---|---|---|---|
| ATB | 193 | 14 | 15 | 3.69 | 4.79 | 2.59 | 0.74 | 1.33 | -33.33 | 0.41 |
| | 534 | 19 | 10 | 6.29 | 9.23 | 6.66 | 2.88 | 0.8 | 19.61 | 0.28 |
| MAH | 630 | 14 | 3 | 3.42 | 3.1 | 9.14 | 0.39 | 0.27 | 72.76 | 0.16 |
| POR | 282 | 20 | 12 | 2.47 | 4.84 | 2.62 | 0.75 | 1.06 | -5.97 | 0.35 |
| STA | 21 | 10 | 2 | 1.25 | 2.01 | 5.34 | 0.31 | 0.24 | 76.18 | 0.17 |
| | 173 | 13 | 1 | 2 | 2.58 | 8.12 | 0.39 | 0.11 | 89.17 | 0.11 |
| SUM | 303 (1) | 13 | 5 | 8.34 | 5.71 | 11.79 | 1.81 | 0.56 | 43.64 | 0.27 |
| | 303 (2) | 9 | 5 | 5.46 | 5.13 | 6.48 | 1.99 | 0.78 | 22.17 | 0.36 |
| TRU | 46 | 13 | 12 | 10.54 | 8.27 | 10.67 | 3.53 | 1.13 | -13.1 | 0.4 |
| | 82 | 23 | 9 | 8.34 | 9.55 | 13.23 | 2.65 | 0.68 | 31.58 | 0.25 |
| Total | | | 74 | | 55.21 | | 15.44 | 1.26 | -25.88 | 0.17 |

Note: Routes with numbers in parenthesis correspond to multiple locations on the same route

Counties: ATB = Ashtabula County
MAH = Mahoning County
POR = Portage County
STA = Stark County
SUM = Summit County
TRU = Trumbull County

***Table C13. HSM predictive method results – District 5.***

**District 5**

| County | Route | $x_b$ | $x_a$ | P | π | var(m) | var(π) | θ | % Change | Std Dev θ |
|---|---|---|---|---|---|---|---|---|---|---|
| COS | 16 (1) | 8 | 8 | 5.925 | 5.92 | 7.05 | 2.19 | 0.93 | 7.34 | 0.38 |
| | 16 (2) | 9 | 2 | 4.377 | 4.38 | 6.23 | 1.81 | 0.29 | 70.59 | 0.21 |
| | 60 | 7 | 3 | 2.782 | 2.78 | 0.34 | 0.39 | 0.3 | 69.6 | 0.18 |
| | 541 | 3 | 3 | 1.359 | 1.36 | 0.38 | 0.16 | 0.31 | 69.39 | 0.18 |
| Total | | | 16 | | 14.44 | | 4.55 | 0.91 | 9.19 | 0.26 |

Note: Routes with numbers in parenthesis correspond to multiple locations on the same route

Counties: COS = Coshocton County

***Table C14. HSM predictive method results – District 12.***

**District 12**

| County | Route | $x_b$ | $x_a$ | $P_o$ | $\pi_a$ | var(m) | var($\pi_a$) | $\theta_a$ | % Change | Std Dev θ |
|---|---|---|---|---|---|---|---|---|---|---|
| GEA | 87 | 24 | 3 | 5.4 | 4.83 | 18.01 | 0.66 | 0.25 | 75.23 | 0.14 |

Note: Routes with numbers in parenthesis correspond to multiple locations on the same route

Counties: GEA = Geauga County

***Table C15. HSM predictive method results – District 9.***

**District 9**

| County | Route | $x_b$ | $x_a$ | $P_o$ | $\pi_a$ | var(m) | var($\pi_a$) | $\theta_a$ | % Change | Std Dev θ |
|---|---|---|---|---|---|---|---|---|---|---|
| ADA | 770 | 3 | 2 | 0.07 | 0.12 | 0.02 | 0 | 0.03 | 96.79 | 0.02 |
| BRO | 221 | 10 | 2 | 0.42 | 0.7 | 0.11 | 0.02 | 0.06 | 93.99 | 0.04 |
| | 505 (1) | 12 | 3 | 1.73 | 3.42 | 4 | 0.73 | 0.37 | 63.04 | 0.22 |
| | 505 (2) | 6 | 2 | 0.2 | 0.19 | 3 | 0 | 0.03 | 96.88 | 0.02 |
| | 756 | 11 | 2 | 7.39 | 2.97 | 12.16 | 0.56 | 0.24 | 75.82 | 0.17 |
| | 763 | 6 | 1 | 0.11 | 0.24 | 0.11 | 0.01 | 0.02 | 97.65 | 0.02 |
| | 774 | 26 | 12 | 30 | 12.26 | 29.02 | 3.88 | 0.78 | 22.18 | 0.25 |
| HIG | 124 | 9 | 2 | 13.4 | 4.11 | 14.61 | 0.78 | 0.21 | 78.7 | 0.15 |
| | 138 (1) | 10 | 7 | 2.85 | 2.38 | 7.08 | 0.31 | 0.7 | 30.28 | 0.29 |
| | 138 (2) | 15 | 3 | 1.29 | 2.59 | 2.05 | 0.29 | 0.26 | 73.91 | 0.15 |
| | 785 | 22 | 2 | 1.72 | 3.63 | 3.51 | 0.41 | 0.16 | 84 | 0.11 |
| JAC | 776 | 13 | 11 | 4.76 | 6.31 | 4.89 | 1.85 | 1.13 | -13.27 | 0.4 |
| LAW | 93 (1) | 14 | 9 | 2.66 | 4.64 | 9.57 | 1.34 | 1.11 | -10.92 | 0.43 |
| | 93 (2) | 6 | 1 | 0.92 | 1.02 | 3.04 | 0.1 | 0.09 | 90.97 | 0.09 |
| | 243 | 35 | 11 | 23.81 | 21.57 | 31.93 | 11.86 | 0.47 | 52.98 | 0.16 |
| | 522 | 6 | 7 | 7.32 | 6.15 | 3.29 | 1.65 | 0.71 | 29.17 | 0.29 |
| | 650 | 16 | 3 | 5.85 | 4.38 | 13.41 | 0.79 | 0.3 | 69.9 | 0.18 |
| PIK | 104 | 13 | 1 | 1.18 | 2.08 | 6.63 | 0.26 | 0.1 | 89.96 | 0.1 |
| | 124 | 4 | 2 | 2.72 | 2.52 | 2.25 | 0.77 | 0.35 | 65.45 | 0.24 |
| | 335 (1) | 12 | 2 | 0.94 | 1.47 | 2.56 | 0.11 | 0.13 | 86.98 | 0.09 |
| | 335 (2) | 5 | 5 | 1.1 | 2.28 | 1.04 | 0.73 | 0.93 | 7.43 | 0.47 |
| | 772 | 11 | 2 | 1.54 | 1.85 | 2.97 | 0.14 | 0.14 | 86.35 | 0.1 |
| SCI | 104 | 33 | 24 | 15.31 | 19.05 | 23.47 | 8.84 | 1.13 | -13.19 | 0.28 |
| Total | | | 116 | | 105.96 | | 35.44 | 1.06 | -6.47 | 0.12 |

Note: Routes with numbers in parenthesis correspond to multiple locations on the same route

Counties: BRO = Brown County
HIG = Highland County
JAC = Jackson County
LAW = Lawrence County
PIK = Pike County
SCI = Scioto County

***Table C16. HSM predictive method results – District 11.***

**District 11**

| County | Route | $x_b$ | $x_a$ | $P_o$ | $\pi_a$ | var(m) | var($\pi_a$) | $\theta_a$ | % Change | Std Dev θ |
|---|---|---|---|---|---|---|---|---|---|---|
| COL | 39 (1) | 11 | 8 | 4.14 | 5.74 | 6.96 | 2.36 | 0.98 | 2.09 | 0.41 |
| | 39 (2) | 18 | 10 | 2.29 | 5.09 | 7.25 | 1.16 | 1.06 | -5.54 | 0.38 |
| | 164 | 6 | 1 | 0.24 | 0.57 | 0.74 | 0.04 | 0.06 | 93.54 | 0.06 |
| | 517 | 3 | 1 | 0.52 | 0.86 | 1.55 | 0.19 | 0.19 | 81.2 | 0.17 |
| | 558 | 8 | 4 | 0.4 | 1.05 | 0.54 | 0.1 | 0.34 | 66.34 | 0.18 |
| HAS | 646 (1) | 4 | 2 | 15.35 | 1.69 | 7.33 | 0.35 | 0.3 | 69.5 | 0.21 |
| | 646 (2) | 5 | 3 | 2.66 | 2.07 | 3.81 | 0.47 | 0.46 | 54.05 | 0.28 |
| TUS | 751 | 18 | 1 | 0.56 | 1.22 | 1.7 | 0.05 | 0.04 | 95.76 | 0.04 |
| Total | | | 30 | | 18.3 | | 4.71 | 1.35 | -35.22 | 0.29 |

Note: Routes with numbers in parenthesis correspond to multiple locations on the same route

Counties: COL = Columbiana County
HAS = Harrison County
TUS = Tuscarawas County

***Table C17. Kruskal-Wallis H test results (speed by canopy level and time of day).***

| County | Route | Canopy | Time of Day | N | Mean Rank | Kruskal-Wallis H | Asymp. Sig. (p-value) |
|---|---|---|---|---|---|---|---|
| Vinton | SR 356 | Open | Night | 10 | 88.05 | 2.497 | 0.114 |
| | | | Day | 127 | 67.05 | | |
| | | Full | Night | 38 | 330.17 | 0.96 | 0.327 |
| | | | Day | 686 | 364.29 | | |
| Hocking | SR 56 | Open | Night | 174 | 1707.5 | 17.17 | 0.000* |
| | | | Day | 2730 | 1436.25 | | |
| | | Full | Night | 173 | 1795.12 | 31.806 | 0.000* |
| | | | Day | 2722 | 1425.94 | | |
| Hocking | SR 374 (3) | Open | Night | 245 | 3681.23 | 1.732 | 0.188 |
| | | | Day | 7485 | 3871.53 | | |
| | | Full | Night | 1060 | 4495.73 | 181.371 | 0.000* |
| | | | Day | 6305 | 3546.36 | | |

Note: Routes with numbers in parenthesis correspond to multiple locations on the same route
*statistically significant (α=0.05)

## APPENDIX D: SUPPLEMENTAL ASSESMENTS – PAVEMENT CORE SAMPLING TO ANALYZE EFFECT OF TREE CANOPY ON PAVEMENT CONDITION.

To supplement findings from the small plot and road section studies mentioned above, the research team performed additional work on the SR374 and SR56 test sites including pavement texture measurements and coring. Also, an investigation of root infiltration from trees with canopies overtop roadways was performed. The findings from core testing and investigation of root infiltration are aimed at providing preliminary answers to questions pertaining to observed raveling on the pavement surface with canopy coverage.

## Data Collection Methods

A forensic investigation was performed to study the effect of tree canopy on pavement performance. Time lapse images at sites in question showed a significantly longer time (approximately 6 to 7 hours) until the pavement surface is dry after a rain event relative to areas without a tree canopy. The pavement engineering literature shows when asphalt pavement is exposed to moisture for prolonged periods of time, damage (stripping) can occur. Moisture can damage asphalt mixes in three ways: "loss of cohesion within the asphalt binder or mastic; loss of adhesion between the asphalt binder and the aggregate; and aggregate degradation particularly when freezing occurs in the mixture" [Bonaquist, 2014]. If a mix is susceptible to moisture damage, it may be prone to localized distress or defects, such as raveling. When raveling occurs, aggregate from the mix becomes dislodged from the surface. This results in increased voids at the surface, making the asphalt less impermeable. By increasing the voids, more opportunities exist for water to infiltrate the structure from the surface down which further exacerbates raveling at the surface and stripping within the asphalt surface layer and the underlying asphalt layers.

To evaluate if the prolonged exposure of moisture due to the existence of a tree canopy has an effect on pavement performance, pavement cores were extracted from two site locations on SR374 (Hocking County) to make visual observations of the pavement structure, and to conduct laboratory testing. From extracted pavement cores in areas under a full tree canopy, and areas without a tree canopy (open), the following properties of the existing asphalt layers can be determined: density (air voids), mass loss by Cantabro testing, and tensile strength ratio. Areas at the same site without a tree canopy served as the control for comparison with results from areas under a full canopy. It was assumed that at each site, the same pavement structure (mix type for each layer and approximate layer thickness) exists under areas of full and open tree canopy. Figure D1 is a flow chart depicting the testing procedure and the following subsections provide details on the specific tests that were conducted.

### Tensile Strength Ratio

The susceptibility to moisture damage is often assessed during the mix design process, in which the tensile strength ratio (TSR) is determined. To determine TSR, Ohio DOT specifies AASHTO T283 test method and Ohio DOT's Supplement 1051 (S1051). TSR is determined by taking the ratio of the average indirect tensile strength of conditioned specimens to the average indirect tensile strength of unconditioned specimens. Three asphalt pills are conditioned by saturating them under a vacuum to 80 to 90% for Item 442 mixes or 70 to 80% for all other mixes,

subjecting them to a freeze-thaw cycle of 16 hours at -0.4°F (-18°C), followed by 24 hours in a water bath at 140°F (60°C) and then 2 hours in a 77°F (25°C) water bath. Three unconditioned samples remain dry and are brought to a temperature of 77°F (25°C) for 2 hours prior to applying the compressive load along the diameter of the sample. As part of the mix design phase, Ohio DOT requires asphalt mixes have a minimum TSR value of 0.80 for Item 442 mixes and 0.70 for all other mixes. After breaking the specimen under the compressive load, the presence of stripping is then evaluated through visual observations.

For this study, the presence of moisture damage or greater propensity towards moisture damage was sought. The pavements included in this study are in-service and have been exposed to climatic conditions for several years, therefore, the TSR threshold values of 0.70 or 0.80 used for mix design may not be applicable. While comparisons of TSR values to these thresholds may not be fruitful, relative comparisons of TSR values among the samples from each tree canopy condition at a site will be. A mix that is already experiencing moisture damage may experience accelerated damage when subjected to the extreme freeze-thaw cycles under the TSR test and thus have lower TSR values than under an open canopy.

Comparisons of the indirect tensile strength of unconditioned specimens between samples from a full tree canopy and those under an open canopy at the same site provide insights into the effect of the prolonged exposure to moisture experienced up to this point in the pavement's life. It is expected the indirect tensile strength of unconditioned specimens is greater where prolonged exposure to moisture has been minimized (i.e. under the open canopy). Additionally, visual observations of the unconditioned specimens under each tree canopy condition after indirect tensile testing helps determine if stripping has occurred and the approximate degree of severity of stripping.

**Cantabro Mass Loss**

According to AASHTO TP 108, the Cantabro mass loss test is used to evaluate cohesion, bonding, and effects of traffic abrasion on asphalt mixes. All of which are related to the susceptibility of a mix to experience raveling. The Cantabro mass loss is determined by weighing the specimens prior to and after subjecting asphalt specimens to 300 revolutions in the L.A. Abrasion machine (without the steel charges) and calculating the percent mass loss. This test has historically been used to evaluate open-graded asphalt mixes during the mix design phase in which threshold values of 20% mass loss has typically been used. For this study, relative comparisons of the percent mass loss among the different tree canopy conditions provides insight to how susceptible these pavement areas are to raveling or disintegration. It is expected areas under full tree canopies which have been subjected to prolonged exposure to moisture have greater mass loss than those under an open canopy.

**Density (Air Voids)**

When combined with texture measurements made previously, visual observations for stripping of unconditioned TSR samples, and Cantabro mass loss results, measuring density in areas of full tree canopy and comparing with density of the same layer under an open (no) tree canopy may provide insights into the extent of raveling or loss of mix that may be occurring. Determination of existing density of each specimen is also required for TSR testing as samples are grouped into unconditioned and conditioned sample sets based on density.

To determine density (air voids) following AASHTO T269 and Ohio DOT S1036, two tests are required: bulk specific gravity of the mix (Gmb), and maximum specific gravity of the mix (Gmm). For each sample, Gmb will be determined following AASHTO T166 and Ohio DOT S1036. It is assumed the same pavement structure (mix type for each layer and approximate layer thickness) exists within a site regardless of the tree canopy condition, therefore the Gmm will be determined from one sample taken from the open canopy where the likelihood of stripping is lowest. The Gmm will be determined following AASHTO T209 and Ohio DOT S1036.

## Data Analysis

As described above, full-depth pavement cores under open and full tree canopy were extracted from two locations along SR374. The pavement surface layer is of primary concern as it is directly impacted by the prolonged exposure to moisture, and as such laboratory testing will be conducted on the surface layer. However, if stripping is observed on field cores at layer interfaces below the surface layer, other pavement layers may also be tested.

Ohio DOT routinely places surface layers between 1 and 1.5 in (25 and 38 mm) thick, while intermediate layers are typically 0.5 to 1.75 in (25 to 44 mm) thick on the two-lane system. AASHTO T283 specifies 4 in (100 mm) cores be used when layer thickness is less than or equal to 2.5 in (63 mm). Although core diameter is not specified for Cantabro testing in AASHTO TP108, maintaining a height to diameter ratio closest to that of specimens prepared in the laboratory is desired. Therefore, 4 in (100 mm) diameter cores were extracted.

To achieve the minimum sample size required for surface courses and assuming a 1 in (25 mm) surface layer, three cores will be required to determine Gmm of the mix following AASHTO T209 and Ohio DOT S1036. Since the extracted cores will have cut faces, the procedure for saturated surface dry (SSD) in Ohio DOT S1036 will be followed. These cores will be taken in an area of an open tree canopy at each site. To conduct TSR testing following AASHTO T283 and Ohio DOT S1051, six samples are required, therefore, six cores were taken under each tree canopy condition (open and full) at each site. Two test methods exist at the national level for Cantabro testing, AASHTO TP108 and ASTM D7064. Although the AASHTO TP108 test method has some guidance on field cores, it is limited, as noted previously core diameter is not specified, nor is the height to diameter ratio, and three specimens are required. ASTM D7064 is applicable to open graded mixes, requires four specimens and provides no guidance for testing field cores. Some agencies have developed their own test method. Texas Department of Transportation (TxDOT) has a test method, Tex-245-F, and although it does not include provisions for field cores, it is very similar to AASHTO TP108 in terms of procedure and only requires two specimens. To minimize the number of cores taken, it is recommended Tex-245-F be applied to the extracted cores to determine Cantabro mass loss. As such, two cores were collected from each tree canopy condition at each site. The cores were photographed and their layer thickness measured prior to separating the samples by sawcutting at the layer interfaces. Density (air voids) of the surface layer were determined for each core following AASHTO T166, AASHTO T269 and Ohio DOT S1036. The number of cores extracted at each site is summarized in Table D1; 20 cores (6 in (150 mm) diameter) were extracted from random locations on SR374 where at least two tree canopy sections were located.

## Results

Overall, the cores from pavement sections under canopy were found to have lower density (higher air voids) and be more susceptible to moisture damage (showing lower TSR values and more signs of stripping in the mixture) and degradation (showing larger percentage of Cantabro mass loss) than cores from pavement sections in no canopy (open) conditions. More specific results are presented below.

### Tensile Strength Ratio

To evaluate the moisture susceptibility of the mixture under both, canopy and no-canopy conditions, the AASHTO T283 test was performed. All values of the tensile strength, average conditioned (dry) and unconditioned (wet) tensile strength and TSR values for the canopy and no-canopy sections are summarized in Table D2. As anticipated, cores from pavement under canopy exhibited higher susceptibility to moisture damage (TSR = 0.71) than the cores from pavement under no-canopy conditions (TSR = 0.85). Figure D2 depicts the unconditioned indirect tensile strength which was found, as expected, to be on average higher where exposure to moisture was minimized (i.e. no-canopy sections). Additionally, visual inspection on the specimens revealed the presence of stripping where tree canopy is present.

### Cantabro Mass Loss

Since the Cantabro Mass Loss (M.L.%) has been found to be sensitive to mixture density, the two surface specimens for each canopy condition were selected so their average densities were representative (relatively close to) of the average density obtained for each condition. After 300 revolutions in the L.A. abrasion machine (without the steel charges), the M.L.% for the specimens was calculated. The individual and average M.L.% are presented in Table D3. In addition, Figure D3 depicts a comparison of the M.L.% against test duration for both canopy conditions. After 100 revolutions, the samples from canopy sections began to disintegrate much faster than samples from the no-canopy (open) sections. After 300 revolutions, the average mass loss was larger (69.8%) for the mixture under tree canopy than for the mixture in the no-canopy (open) section (33%). Figure D3 also shows the core remnant from the canopy section (residual) is much less than that from the no-canopy (open) section.

### Density (Air Voids)

The density (air void) content was determined for all 20 surface core samples by measuring their bulk specific gravity (Gmb) and relating it to the maximum specific gravity of the mix (Gmm) as reported on the job mix formula (JMF). It was assumed the same pavement structure (mix type for each layer and approximate layer thickness) exists within the site, therefore the Gmm should apply to the whole section regardless of the tree canopy condition. The average density and air voids for both canopy and no-canopy sections are shown in Table D4. As shown, the average density under canopy condition was found to be lower and more consistent, 92.5%, than for no canopy, 94.1%.

These results suggest that lower density, found in sections of the road under canopy condition, correspond to a lower tensile strength ratio (TSR) value and higher Cantabro mass loss

(CML%). Other researchers have found the same relationships. For instance, Cox et al. [2017] found that for dense graded mixes compacted at different air void levels (1% to 13%) (density 87% to 99%), the CML% increased with the decrease in density; even for the same mixes, increases in CML% were larger with aging. On the other hand, a consensus of several researchers presented by Alderson [2011] suggest that the increase in density will increase the resistance to moisture damage. Recently, Green et al. [2018] reported TSR values decreasing as the in-place density decreased for several asphalt concrete base mixtures studied in the state of Ohio. This trend was also reported by Masad et al. [2009] in their study of the compactability of asphalt mixes and its influence on mechanical properties. It should be kept in mind however, that percent density (air voids) is not the only influencing factor in TSR and ML. Asphalt binder content is likely to have the same or greater effect on TSR and ML than density. Given that only one road was sampled, it is difficult determine if the difference is due to raveling, field compaction, or both. More research covering a greater number of pavements will be needed to reach a definite conclusion.

## Bibliography


Alderson, A. *Influence of Compaction on the Performance of Dense-Graded Asphalt*. Austroads report APT194-11, Sydney, Australia, 2011.

Bonaquist, R., 2014. Impact of Mix Design on Asphalt Pavement Durability, *Transportation Research Circular Number EC-186, Enhancing the Durability of Asphalt Pavements: Papers from a Workshop January 13, 2013*, Transportation Research Board, Washington, D.C., pp. 9-17.

Cox, B.C, Smith, B.T., Howard, I.L., and James, R.S., 2017. State of Knowledge for Cantabro Testing of Dense Graded Asphalt. *Journal of Materials in Civil Engineering*. 29 (10)

Green, R., Robbins, M., Von Quintus, H., Brink, W., and Garcia-Ruiz, J., 2018. *Evaluation of Asphalt Base Course Construction and Acceptance Requirements, Phase I*. Report No. FHWA/OH-2018/13. ORITE, Athens, OH.

Masad, E., Kassem, E., Chowdhury, A., and Zhanping, Y., 2017. *A Method for Predicting Asphalt Mixture Compatibility and Its Influence on Mechanical Properties*. Report FHWA/TX-09/0-5261-2. Texas Transportation Institute, Austin, TX.

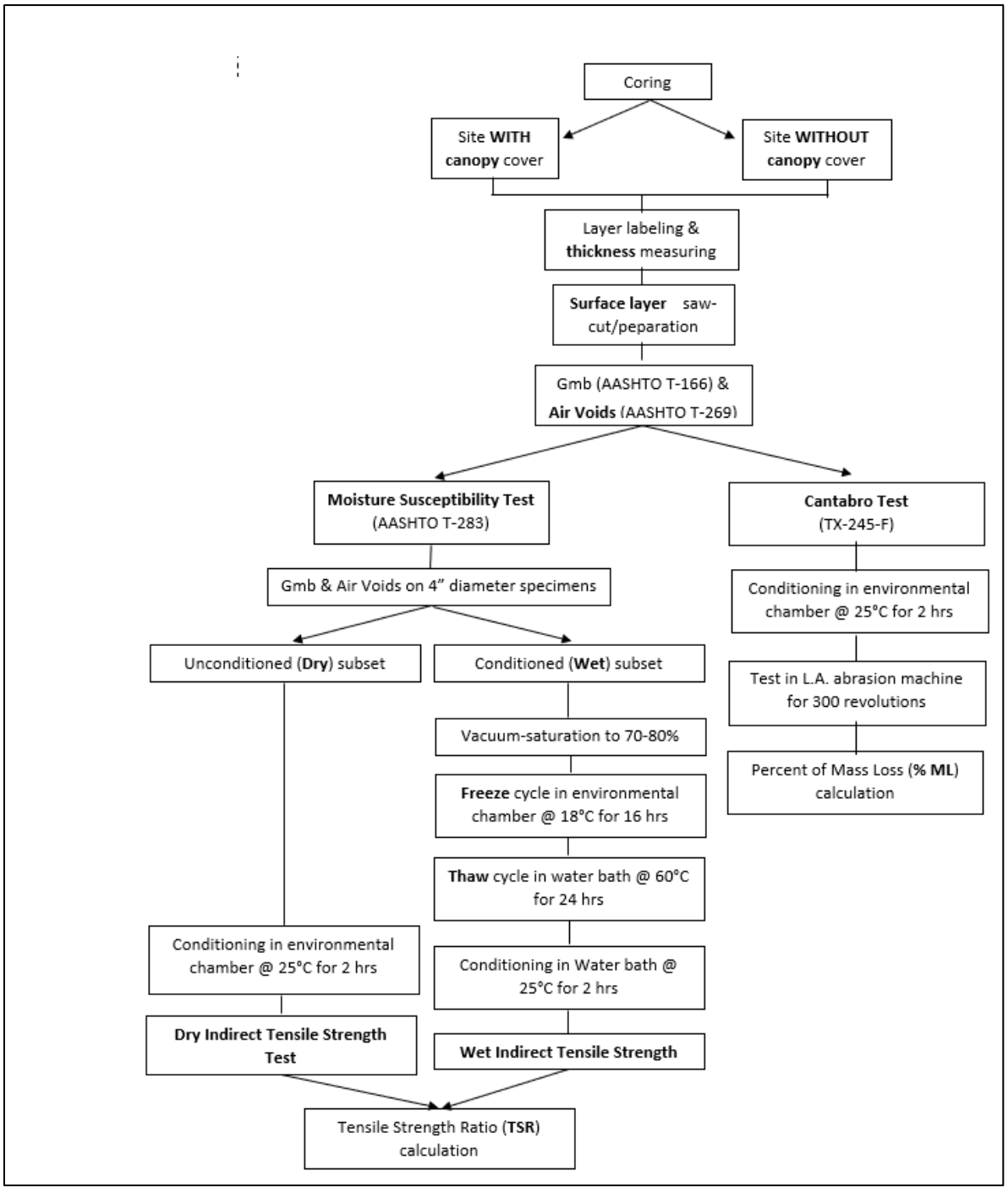


***Figure D1. Flow Chart Depicting Pavement Core Testing Procedure.***

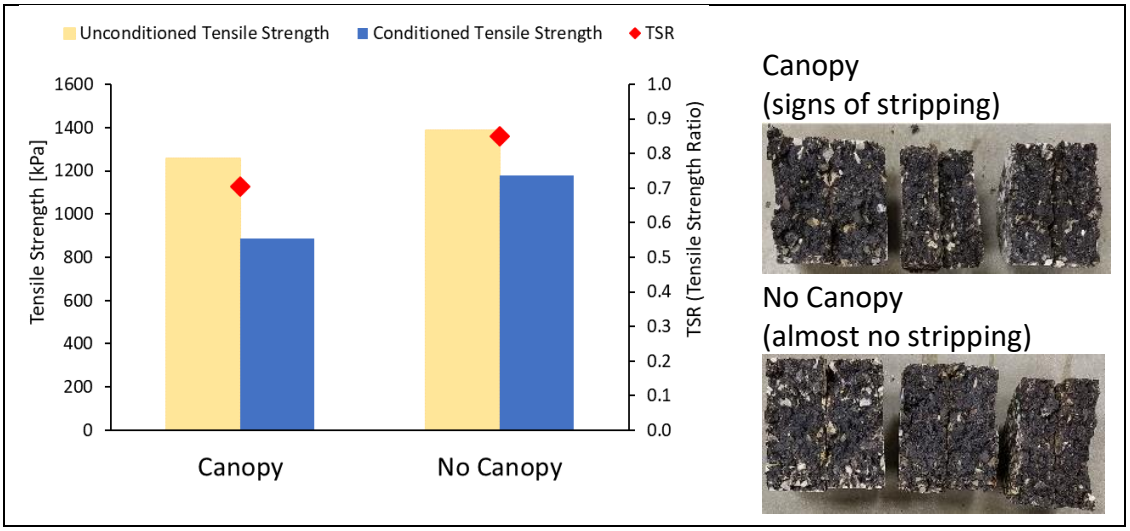


***Figure D2. Tensile Strength and TSR Values for Canopy and No-canopy Conditions.***

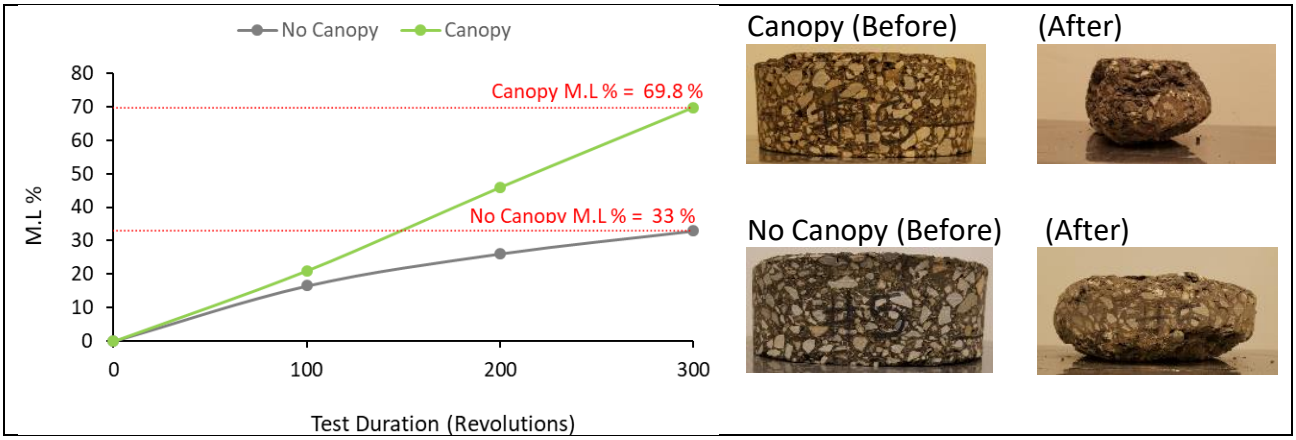


***Figure D3. Cantabro Mass Loss (M.L.%) for Canopy and No-canopy Conditions.***

***Table D1. Summary of cores collected for testing at each site.***

| Test | Location | Test specification | Samples | Cores |
|---|---|---|---|---|
| Gmm | Open canopy (control) | AASHTO T209 and ODOT S1036 - follow SSD | 1 | 3 |
| Gmb and density (air voids) | all cores | AASHTO T166, AASHTO T269, and ODOT S1036 | | |
| Cantabro mass loss | Open canopy (control) | Tex-245-F | 2 | 2 |
| Cantabro mass loss | Full canopy (experimental) | Tex-245-F | 2 | 2 |
| (TSR) | Open canopy (control) | AASHTO T283 | 6 | 6 |
| (TSR) | Full canopy (experimental) | AASHTO T283 | 6 | 6 |
| Extra | To be determined | | | 1 |
| **Total Cores Needed:** | | | | **20** |

***Table D2. Moisture susceptibility test results.***

| | Moisture condition | Sample ID | Density (%) | Average density (%) | Air voids (%) | Average air voids (%) | Thickness (mm) | Diameter (mm) | Maximum Load (N) | Tensile strength (kPa) | Average tensile strength (kPa) | TSR |
|---|---|---|---|---|---|---|---|---|---|---|---|---|
| Canopy | Dry | 7 | 92.8 | 93.3 | 7.2 | 6.7 | 33.1 | 100.4 | 7784.7 | 1490.6 | 1255.7 | 0.71 |
| | | 11 | 94.6 | | 5.4 | | 39.2 | 100.4 | 6142.3 | 992.9 | | |
| | | 16 | 92.5 | | 7.5 | | 33.1 | 100.3 | 6691.1 | 1283.5 | | |
| | Wet | 4 | 94.5 | 93.6 | 5.5 | 6.4 | 43.4 | 100.4 | 7126.5 | 1042.7 | 885.9 | |
| | | 10 | 91.2 | | 8.8 | | 29.3 | 100.4 | 2970.1 | 642.2 | | |
| | | 12 | 95.1 | | 4.9 | | 32.4 | 100.2 | 4965.7 | 972.9 | | |
| No canopy | Dry | 1 | 97.2 | 95.0 | 2.8 | 5.0 | 33.5 | 100.4 | 9242.8 | 1751.9 | 1386.7 | 0.85 |
| | | 8 | 90.8 | | 9.2 | | 30.8 | 100.1 | 6255.7 | 1293.1 | | |
| | | 14 | 97.1 | | 2.9 | | 34.9 | 100.5 | 6146.4 | 1115.2 | | |
| | Wet | 2 | 98.6 | 94.5 | 1.4 | 5.5 | 42.6 | 100.2 | 11560.1 | 1722 | 1177.6 | |
| | | 17 | 91.5 | | 8.5 | | 36.3 | 100.8 | 6375.2 | 1109.3 | | |
| | | 18 | 93.5 | | 6.5 | | 28.9 | 100.3 | 3192.5 | 701.5 | | |

| | Moisture condition | Sample ID | Density (%) | Average density (%) | Air voids (%) | Average air voids (%) | Thickness (in) | Diameter (in) | Maximum Load (lb) | Tensile strength (kPa) | Average tensile strength (kPa) | TSR |
|---|---|---|---|---|---|---|---|---|---|---|---|---|
| Canopy | Dry | 7 | 92.8 | 93.3 | 7.2 | 6.7 | 1.30 | 3.95 | 1750 | 216.2 | 182.1 | 0.71 |
| | | 11 | 94.6 | | 5.4 | | 1.54 | 3.95 | 1381 | 144.0 | | |
| | | 16 | 92.5 | | 7.5 | | 1.30 | 3.95 | 1504 | 186.2 | | |
| | Wet | 4 | 94.5 | 93.6 | 5.5 | 6.4 | 1.71 | 3.95 | 1602 | 151.2 | 128.5 | |
| | | 10 | 91.2 | | 8.8 | | 1.15 | 3.95 | 668 | 93.1 | | |
| | | 12 | 95.1 | | 4.9 | | 1.28 | 3.94 | 1116 | 141.1 | | |
| No canopy | Dry | 1 | 97.2 | 95.0 | 2.8 | 5.0 | 1.32 | 3.95 | 2078 | 254.1 | 201.1 | 0.85 |
| | | 8 | 90.8 | | 9.2 | | 1.21 | 3.94 | 1406 | 187.5 | | |
| | | 14 | 97.1 | | 2.9 | | 1.37 | 3.96 | 1382 | 161.7 | | |
| | Wet | 2 | 98.6 | 94.5 | 1.4 | 5.5 | 1.68 | 3.94 | 2599 | 249.8 | 170.8 | |
| | | 17 | 91.5 | | 8.5 | | 1.43 | 3.97 | 1433 | 160.9 | | |
| | | 18 | 93.5 | | 6.5 | | 1.14 | 3.95 | 718 | 101.7 | | |

***Table D3. Cantabro mass loss test results.***

| Type | Sample ID | Density (%) | Average Density (%) | Air Voids (%) | Average Air Voids (%) | Thickness (mm) | Number of Revolutions | | | Average Mass Loss (%) |
|---|---|---|---|---|---|---|---|---|---|---|
| | | | | | | | 100 | 200 | 300 | |
| | | | | | | | Mass Loss (%) | | | |
| Canopy | 15 | 92.2 | 92.2 | 7.8 | 7.8 | 55.4 | 9.1 | 27.1 | 65.5 | 69.8 |
| | 9 | 92.2 | | 7.8 | | 46.9 | 33.0 | 64.7 | 74.1 | |
| No Canopy | 5 | 94.3 | 95.8 | 5.7 | 6.2 | 55 | 8.4 | 19.4 | 29.3 | 33.0 |
| | 19 | 93.2 | | 6.8 | | 41.4 | 24.7 | 32.9 | 36.6 | |

***Table D4. Density (air voids) test results.***

| Type | Number of Samples | Density (%) | Average Air Voids (%) | Std Dev (%) | Std Error | CoV (%) |
|---|---|---|---|---|---|---|
| Canopy | 9 | 92.5 | 7.5 | 1.4 | 0.5 | 19.2 |
| No Canopy | 11 | 94.1 | 5.9 | 2.6 | 0.8 | 43.1 |

## APPENDIX E: SUPPLEMENTAL ASSESMENTS – ROAD SECTION INVESTIGATION OF POTENTIAL ROOT INFILTRATION.

The goal here was to gain further understanding on the effects of tree canopy on pavement performance and to specifically isolate the effects (if any) of root infiltration beneath the pavement surface. Essentially, to (i) identify if there are any roots under the pavement surface along canopied roadways, and (ii) identify how deep the roots are (if any). A preliminary investigation using a Falling Weight Deflectometer (FWD) on sites located along SR 374 did not provide any conclusive results – no statistically significant differences in the data were found between canopy and open sections. This indicated that the overall structure of the pavement was sound, and there was a low probability of having root infiltration or otherwise under the pavement sections. While it would have been "best" to trench alongside the select canopied road sections and observe the presence of any roots, this was not an option.

Therefore, the research team (after consulting the TAC) settled on soliciting information on the presence/absence of roots from Oho DOT county engineers in the five districts where study sites were located. The information was solicited via a telephone interview that lasted 15-20 minutes. During each interview, the discussion was guided using the following set of questions.

Question 1: What/How much clearance (in feet) is maintained between the road edge and trees along the listed routes?

Question 2: Have you performed (or have knowledge of) trenching/pavement excavations alongside or across any of the listed routes?

a. If **YES**, then move to next question (3).

b. If the answer is **NO**, what do they do?

Question 3: Have you noticed (are aware of) any root infiltration?

a. If **YES**, then ask next series of questions (3.1-3.3).

b. If **NO**, what do they do?

Question 3.1: What were the size of roots?

Question 3.2: At what depth were roots present?

Question 3.2: What was the extent of root infiltration?

Question 4: Have you seen tree roots contributing to pavement distress? What factors or conditions affect such damage (e.g. type of tree, distance, etc.)

Question 5: How where you made aware the damage to the pavement was caused by tree roots?

Question 6: Do you have any other comments regarding tree roots and pavement condition?

### Results

Of the 13 counties in the five Ohio DOT districts where the test sites were located responses were collected from eight Ohio DOT engineers (62 percent). All respondents had no

knowledge/experience of root infiltration below the pavement surface in areas where canopy was present (or was previously present) overtop the roadway. In fact, respondents were "convinced/sure" that it was the canopy overtop the road surface that was responsible for pavement distress rather than any root infiltration.

It was also a consensus among respondents that a minimum clearance of 30 ft (0.9 m) from the centerline on both sides (i.e., available ROW) was maintained. Some respondents mentioned removing all trees within the ROW, whereas other respondents mentioned the removal of all trees except those trees having a trunk diameter of more than 12 in (300 mm). In conditions where the ROW is limited such as embankments, hills, curves and dips, and residential areas; the edge of the roadway (white line) was used. No specifics were provided on the extent (top-bottom) of the clearance, which was dependent on the reach of available trimming equipment – bucket truck or "sky trimmer".

## APPENDIX F: ARBORIST PERSPECTIVE.

Trees along roadways can be assets or liabilities; and is often directly correlated with how they have been managed. Trees with a good structure, form and vigor can often live decades and even centuries. Roadside trees can provide economic and ecological value to our communities by cleaning the air; filtering dust from the air; and they soften and absorb rain runoff which protects culverts, slip prone areas, and valuable real estate. Roadside trees also reduce glare and can act as snow fence, all the while adding to the rural beauty of our state. Ohio DOT and other road managers in Southeast Ohio have expressed that there are have been an unprecedented number of landslides/road slips in the last two years. Many of these landslides/road slips occurred after numerous trees were removed. But trees can also obstruct signage, clog ditches, hide deer and fall onto the roadway.

With informed leadership, good planning, and sound management, public land managers will help protect and grow the benefits of roadside trees while minimizing the problems associated with poorly maintained trees. Modern tools and techniques have the potential to make our roads less labor intensive to care for, but the mechanization of right of way management can be only as effective as the knowledge and experience of the operators and management. With more than 100,000 miles (160,000 km) of highways to maintain in Ohio, the task may seem daunting, but with long-term goals and training roadside trees and forest can be purposefully managed for wide-reaching benefits.

According to Shigo, “Pruning is one of the best things an arborist can do for a tree, but [it] can also be one of the worst things we do to a tree" [Shigo, 1991]. Pruning is the most common tree maintenance work; when performed in a proper manner it helps to selectively remove defective or undesirable parts of a tree and direct growth in the remaining tree branches. Ideally, this improves the structure of a tree, contributes to overall tree health and structure and reduces a tree’s predisposition to failure which could threaten people or property. By contrast, improper pruning can change tree form and architecture and subsequently become detrimental to the health and structure of a tree in the short and long term. The improper work is often visible to the trained eye for years or even decades after. Pruning/trimming trees with equipment such as felling heads, boom grapples, and Jarraff that process more tree material can be less precise and detrimental. Technological advances in modern machinery have made tree and forest management quicker and possibly safer, however there is need to exercise professionalism in their use. Using modern tree trimming standards on roadway right-of-way will show professionalism with a culture of safety, education, and training.

“Topping” is the practice of removing whole tops of trees or large branches and/or trunks from the tops of trees, leaving stubs or lateral branches that are too small to assume the role of a terminal leader. Although once an acceptable widespread practice of tree trimmers, topping has a number of detrimental effects on the structure and health of trees. The main drawback to topping as it pertains to trimming along roadsides is that the resulting re-growth of tissue in the form of vigorous shoots will grow quickly from a latent bud. Moreover, the strength and resilience of a tree stem can be related to its taper in a manner as a fishing rod can absorb the forces of line pull. The stress and weight of a trunk or stem can be incrementally distributed along the even taper of the stem. The vigorous growth of suckers will be unnaturally long with little taper and will place a heavy load on its attachment point at the site of the topping cut.

Overall, with a growth rate of up to 10 ft (3 m) per year, a tree can quickly replace the amount of foliage that was removed and unfortunately that regrowth will now be attached to the decayed stub of the previously injured limb. If the trimming is not repeated on a regular basis then the structural integrity of the canopy is ruined and may present a more hazardous tree than before.

The concept of Compartmentalization of Decay in Trees (CODIT) expresses deeper knowledge of how a woody plant reacts to different types of injury and pruning wounds [Shigo, 1991]. CODIT maps how a woody plants vascular system responds to limit an infection or injury. In terms of pruning/trimming along roadsides, CODIT highlights the importance of resistance to decay that was found to be weakest in a lengthwise direction. When a tree is topped, it opens the end of a stem and thus creates a pathway that may proceed all the way down the inside of a trunk. Whenever a limb is severely topped, the compartmentalization process also makes the nutrients stored in the sapwood unavailable for appropriation. Combined with trimming that might remove a large percentage of the leaf area, this can put a tree under an enormous amount of stress.

Other situations to avoid during tree trimming/pruning are “lion-gating” and potential transmission of disease. The former arises when all the lower, bottom, or interior branches are removed leaving all the new growth to occur at the top or tips. This will upset the balance of taper to length, encourage epicormic branching, and grow more precarious as time grows on. Fungal or bacterial pathogens could rapidly spread from a cutting blade through any new topping wound. For example, Oak and Elm should not be pruned during the growing season due to the presence of disease vectors present under favorable conditions. As well, insect populations may even be chemically attracted to wounded tree tissue.

Competent tree trimming/pruning is an attainable goal for any person or organization and once put into practice should not take too long to implement and reap benefits. A tree can often be reduced or reshaped to a suitable size or redirected using a variety of techniques. Examples of physical mechanisms include performing “reduction cuts”, “thinning cuts”, and/or “crown lifting”. A “reduction cut” should cut a limb back to a lateral branch that is at least one third of the diameter of the stem being removed. This could reduce the overall height or weight of a tree or reduce the length of a horizontal limb. A “thinning cut” removes an entire limb back to the parent trunk or leader that originates from. This cut should be made beyond the branch collar of the trunk so as not to injure or open up the trunk to disease or decay. With crown lifting, lower lateral branches are removed systematically; this works well on roadside trees as it directs tree growth upwards and away from the road while retaining the natural architecture of the tree.

The American National Standards Institute (ANSI) maintains the ANSI A300 (part 1) which the widely accepted standards for tree pruning in the US. Also available are the ANSI Z133 – Standards for Safe Arboricultural Operations. In addition, the International Society of Arboriculture (ISA) has developed a series of Best Management Practices (BMPs) for the purpose of interpreting tree care standards and providing guidelines of practice for arborists, tree workers, and the people who employ their services. This updated BMP booklet provides reasons why pruning should be undertaken, explains pruning types, provides background on pruning cuts, reviews sample pruning specifications, and comments on the timing and necessity of these operations. Additionally, ISA funds research, provides education, and accreditation with the goal of advancing the field. Within Ohio, the Ohio Department of Natural Resources (ODNR) Urban Forestry program has right-of-way tree management resources including: tree pruning, removal,

and risk mitigation; contracts; specifications; cost estimation; tree risk assessment training; management planning; and inventorying vegetation. These resources are taught either through ODNR's "Tree Commission Academy" at various workshops held throughout the year, or at their six annual urban forestry conferences. Additional resources are also available on the ODNR website http://forestry.ohiodnr.gov/urbanforestrytoolbox.

Regardless, whether the work planner is a certified arborist, urban forester, or utility forester, proficiency is the goal. A certified/trained arborist or forester can quickly perform quantified risk assessment on a tree by tree basis.

As far as considering different tree species and their function along roadways, value must be placed on the slower growing and longer living species over more rapidly growing, weaker wooded, and shorter-lived species. Native dominant hardwoods such as Oak, Hickory, Locust, Hackberry, Catalpa, and hard Maples would be most resilient and beneficial. Medium sized natives such as Osage Orange, Kentucky Coffee Tree, Hawthornes, and Red Cedar would be beneficial where shorter trees are required. Fast growing, softer wooded tree species such as Silver Maple, Poplar, Tulip, White Pine and Box Elder would be not without uses but less desirable where they would present a hazard by dropping material on roadways. Use of any non-proven natives should be discouraged as well. Trees such as Bradford Pear, Honeysuckle, Ailanthus, and Russian Olive are examples of plants once encouraged in public works projects that are invasive and should be avoided. Perhaps having dense forest cover would retard the establishment of exotic invasives.

Overall, roadside trees have the potential to be beneficial; and careful management has the potential to retain these trees as an asset to the state instead of a nuisance. It is also pertinent to plan tree planting along new highway systems and interchanges in order to mitigate the environmental impact of new projects.

After reviewing the second draft of this report, the arborist added these comments:

It looks like you did a good job planning and researching this extensive project. You have appeared to validate the positive effects of tree canopy on road surfaces as well as opened up new areas to research further. I agree with your recommendations that tree canopy generally extends the life of roadways, is valued by the public and adds beauty to the state's roadways. It seems to be your recommendation that removing canopies from large swaths of roadway did not have a beneficial effect on road longevity or safety. It is not surprising that road degradation tends to be more about the substrate and which is built as opposed to tree proximity.

As far as my recommendations for maintaining or removing trees above roadways, I think that there are many cases where indiscriminate limbing up of trees with a sky trimmer wastes resources and creates more of an eyesore than actually removing hazards. Down the road you are either producing diseased trees and/or unsightly pruning cuts while producing no benefit. I agree with your decision to focus on removing dead trees as they present the largest hazard of falling onto roadways. Otherwise trees may be culled if they are excavated around, have a presence of decay in the main trunk, or in instances where two trees are growing against each other (called codominant trunks). In the long term it is better to favor tree species which would be stronger and longer lived as opposed to weaker fast-growing species. It is senseless to rashly hack up limbs on an ancient white oak and leave long stubs. Proper pruning technique, if

trimming is necessary, would be to finish all cuts back to a suitable lateral branch or just outside of the branch collar on the trunk. There is a good example of this near the Radford Road intersection with US 50/SR 32 in Athens, OH heading towards Albany, OH. Another example in Athens, OH is on SR 550 at the intersection with Peach Ridge Road.

Another problem I often see along township roads in Athens County is the destruction of a root zone of trees for purposes of widening or increasing the drainage. I see many cases of root balls being excavated around large stately trees which are then left to slowly decline. The basic rule of thumb is to measure the trunk diameter and then try not to disturb the soil within three diameters. Often these are the ancient "wolf trees" that have been delineating a country roadway for hundreds of years. This is much to the chagrin of residents and adjacent property owners who love those trees but have to fight with townships or other authorities to protect them.

## Bibliography

Shigo, A. L. 1991. Modern Arboriculture: A Systems Approach to the Care of Trees and their Associates. Shigo and Trees, Associates.

## APPENDIX G: MEASURED CANOPY COVERAGE AT TEST SITES

- These graphs are listed in order by county name and state route (SR) number.
- White portions indicate densiometer measurements of tree coverage 0-25% (no canopy); light green portions indicate coverage 25-75% (partial canopy); dark green portions indicate coverage 75-100% (full canopy)
- Horizontal axis indicates distance along road section (1 ft = 0.305 m)

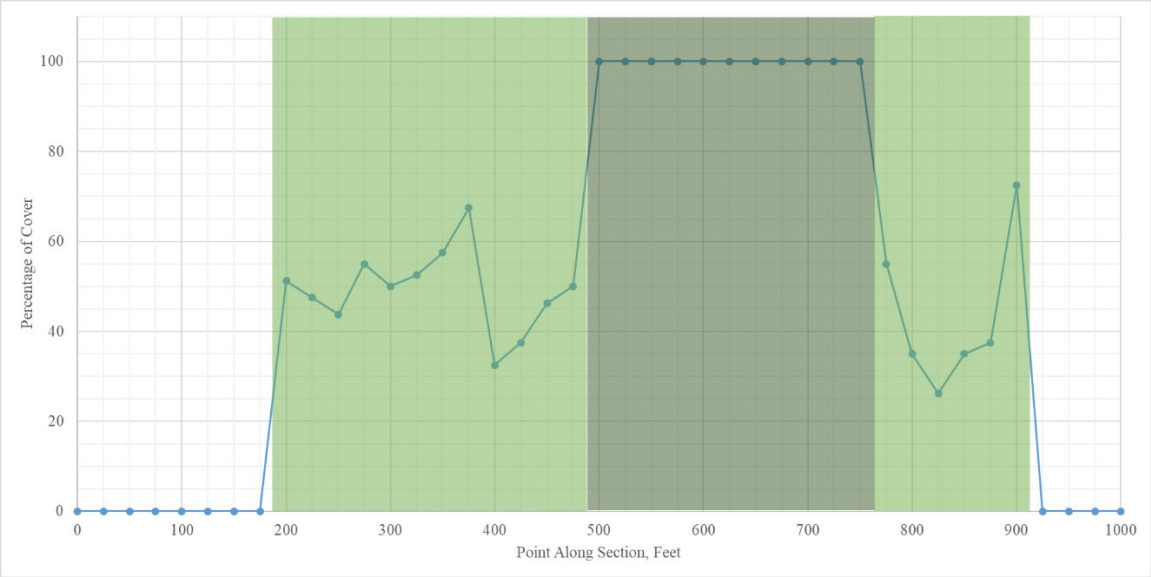


SR 13 in Athens County, Ohio

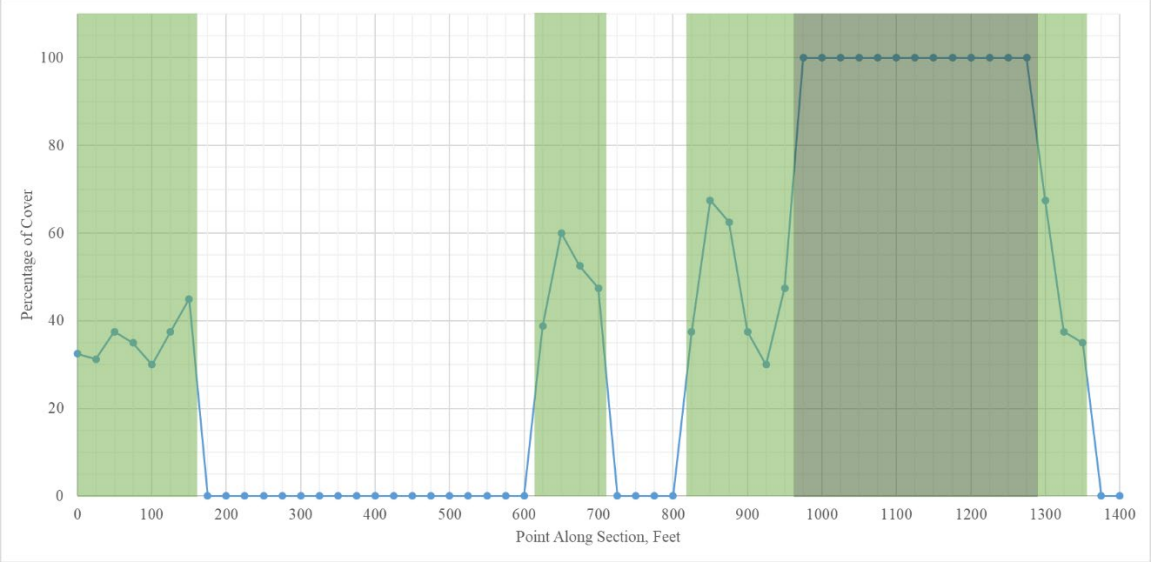


SR 685 in Athens County, Ohio

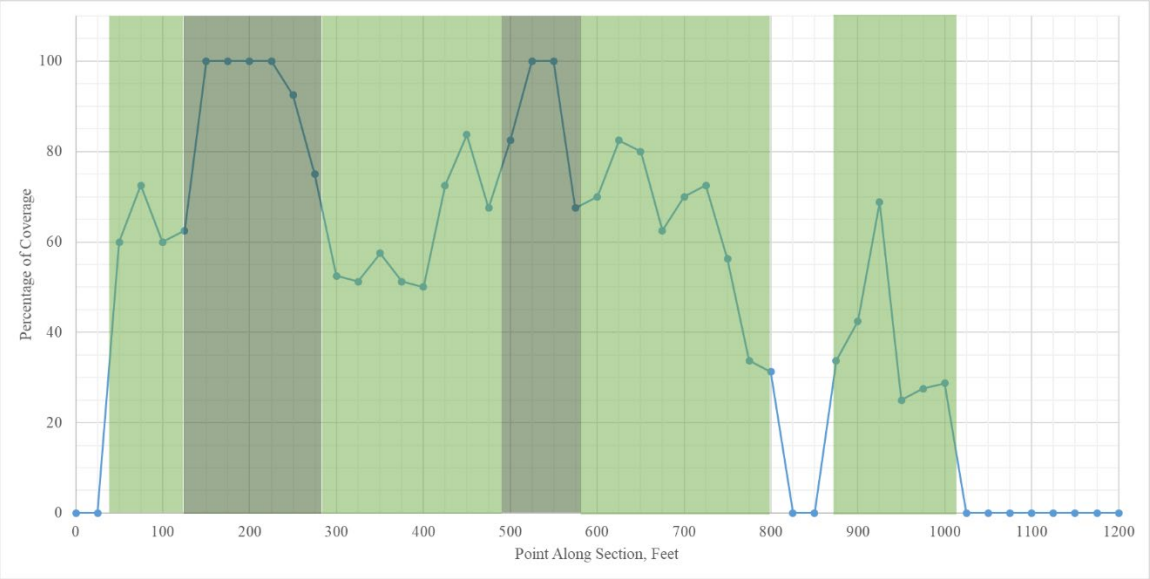


SR 26 in Belmont County, Ohio

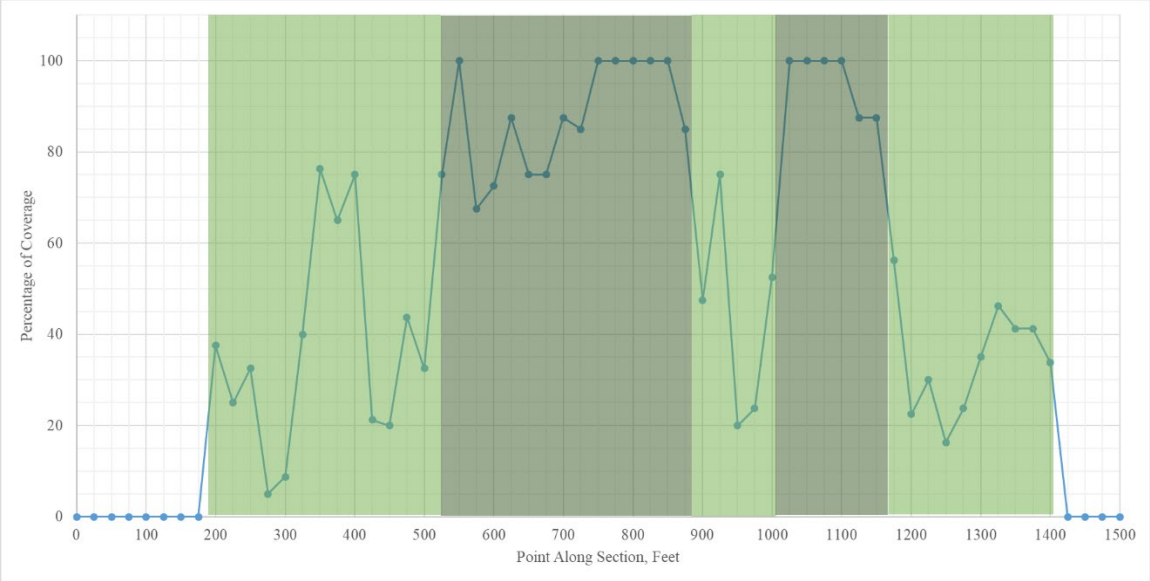


SR 148 in Belmont County, Ohio

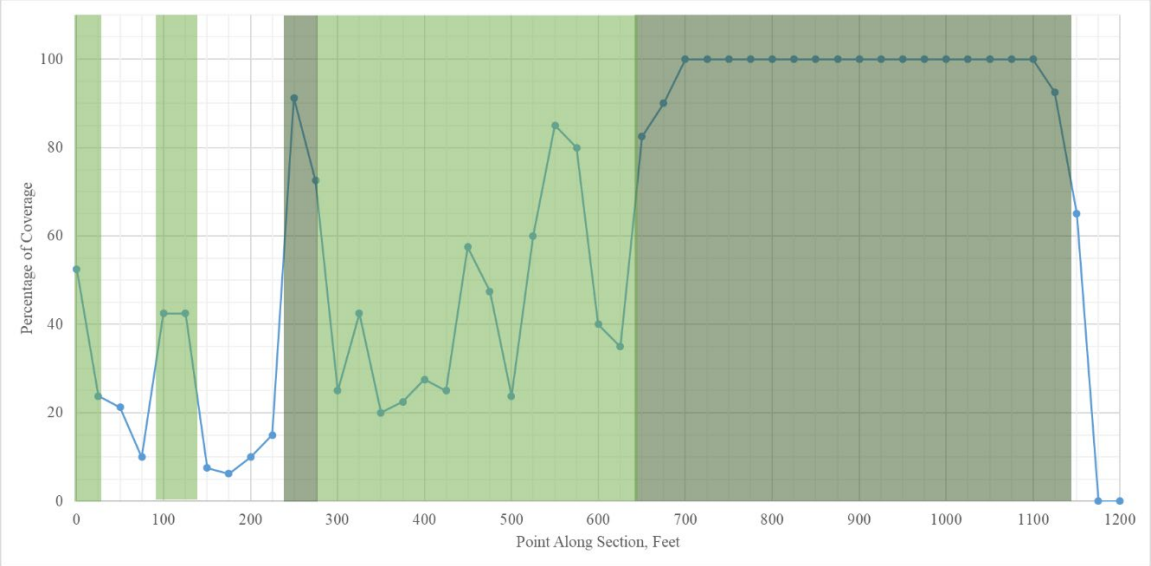


SR 87 in Cuyahoga County, Ohio

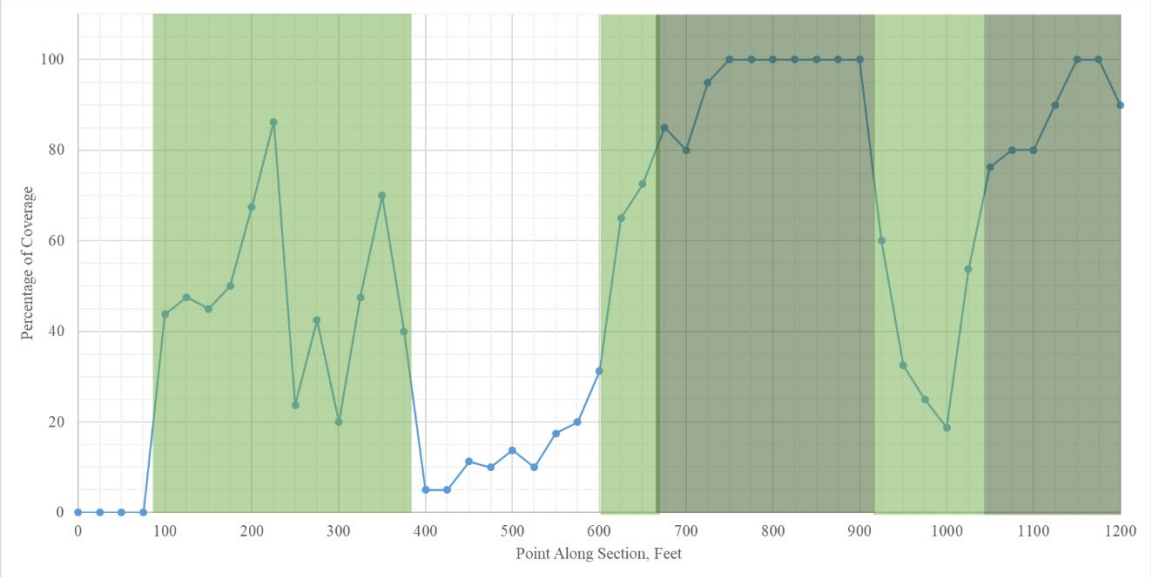


SR 174 in Cuyahoga County, Ohio

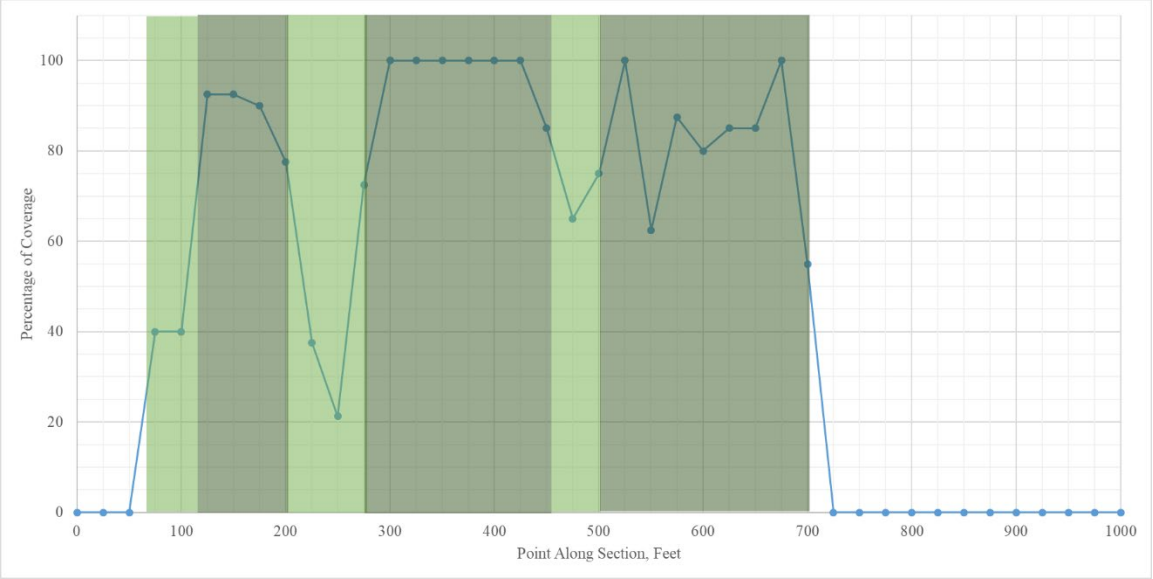


SR 258 (1) in Harrison County, Ohio

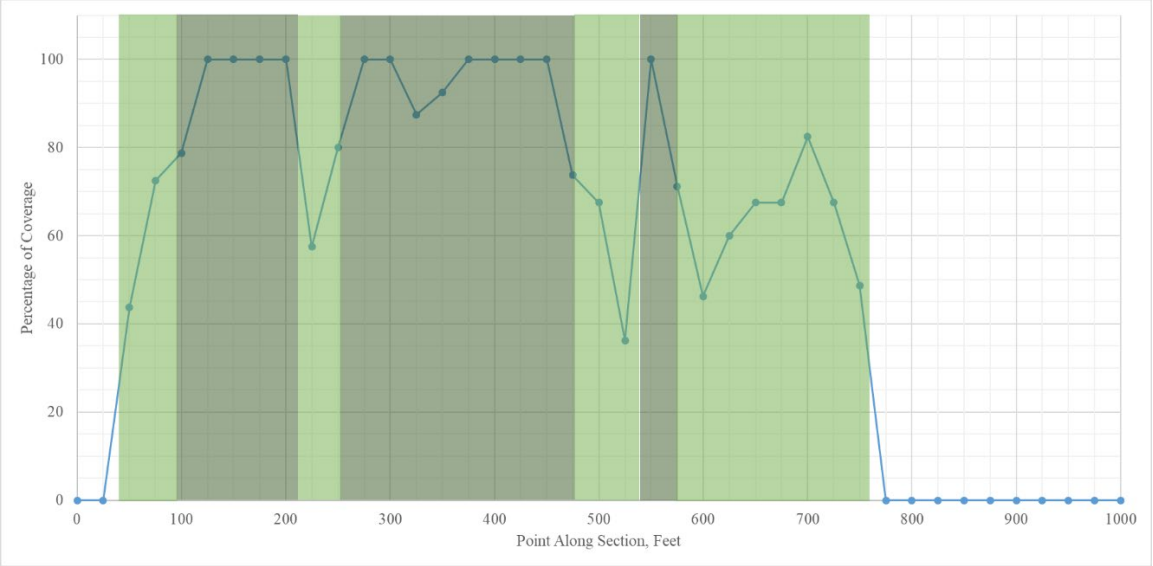


SR 258 (2) in Harrison County, Ohio

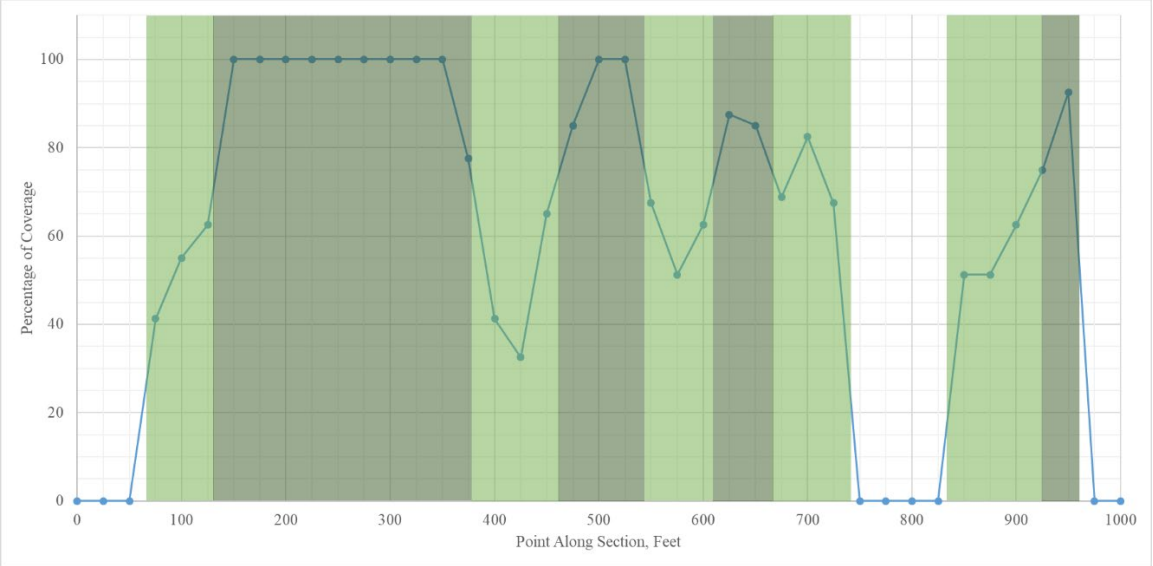


SR 258 (3) in Harrison County, Ohio

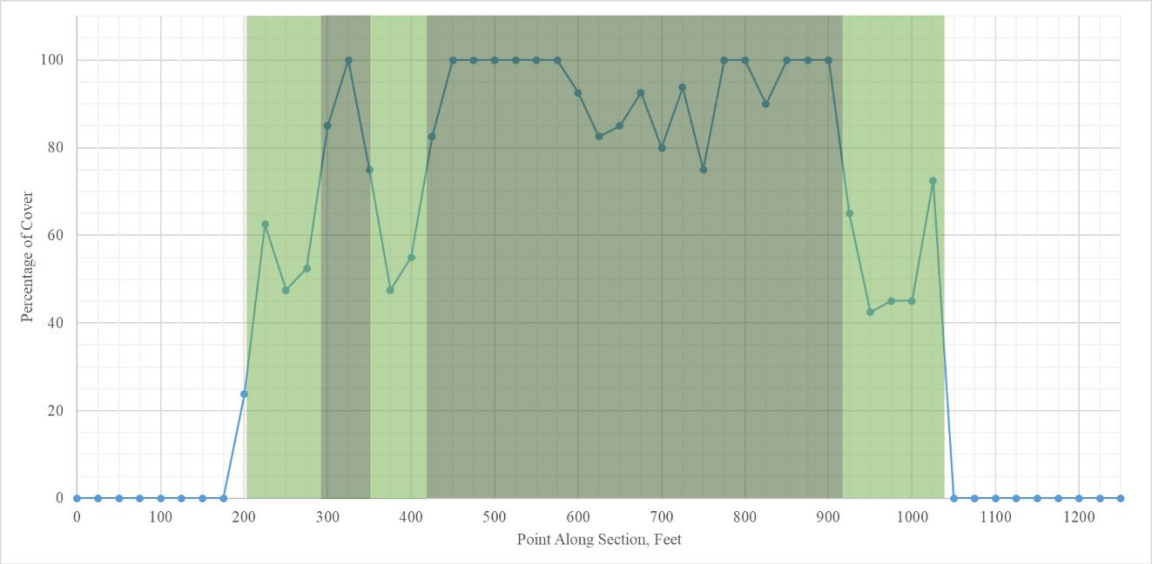


SR 56 in Hocking County, Ohio

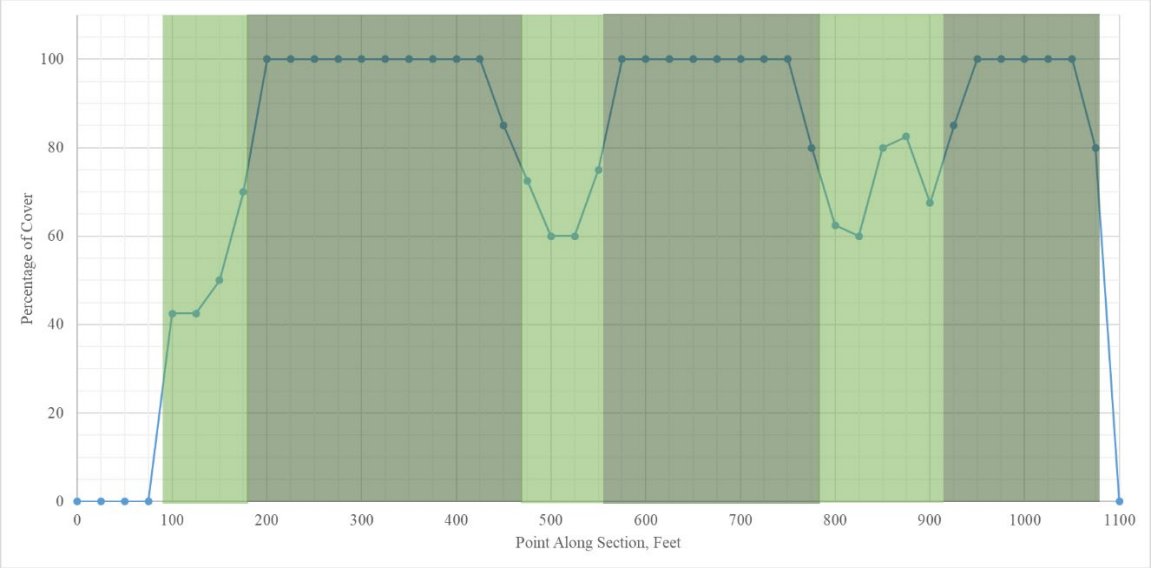


SR 278 in Hocking County, Ohio

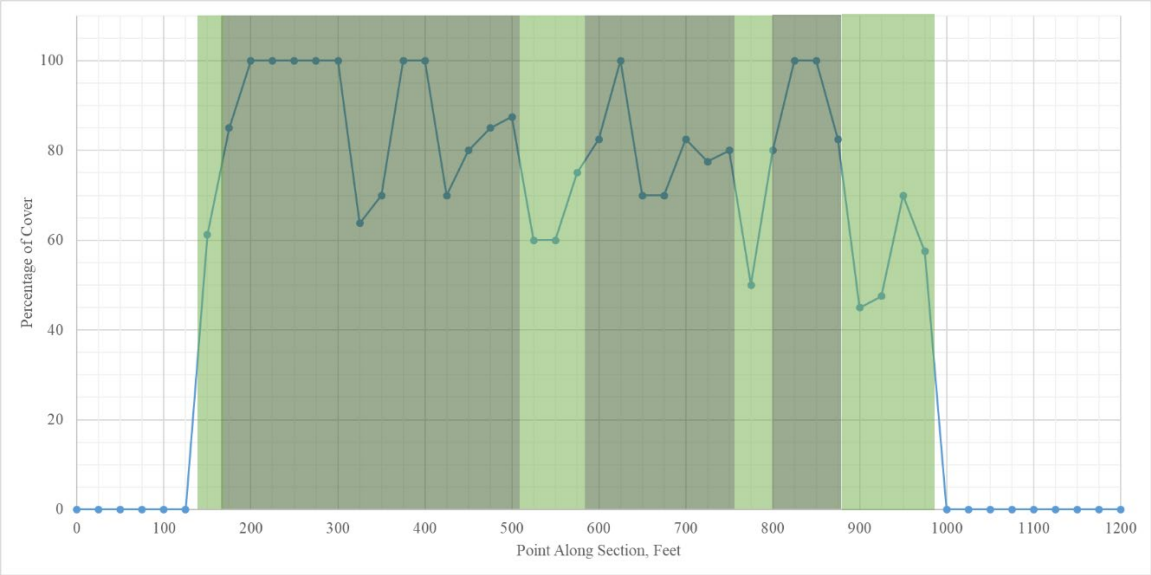


SR 374 (1) in Hocking County, Ohio

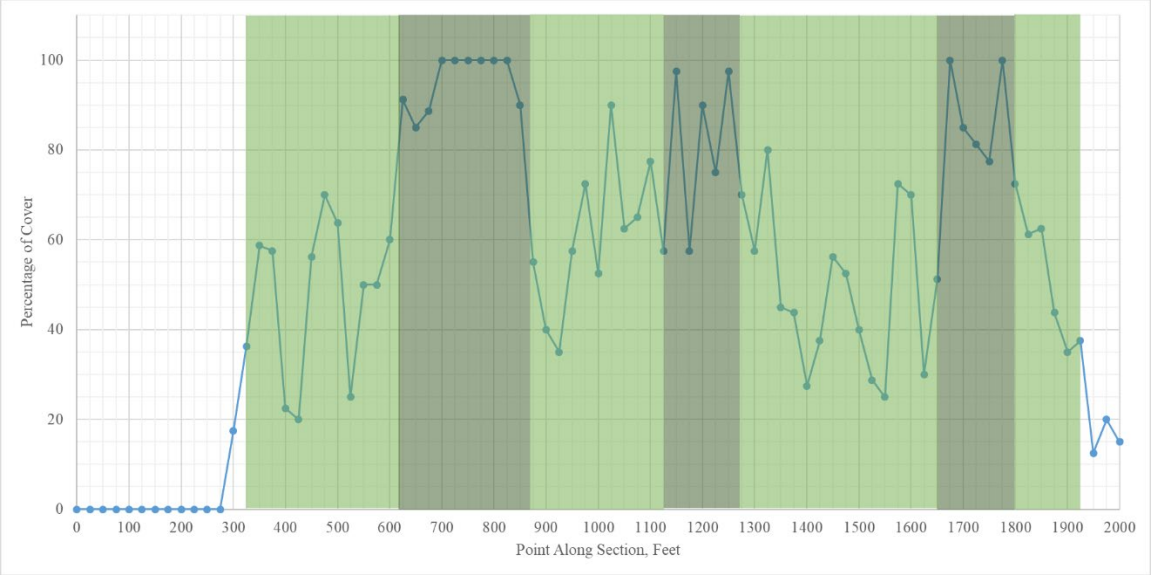


SR 374 (2) in Hocking County, Ohio

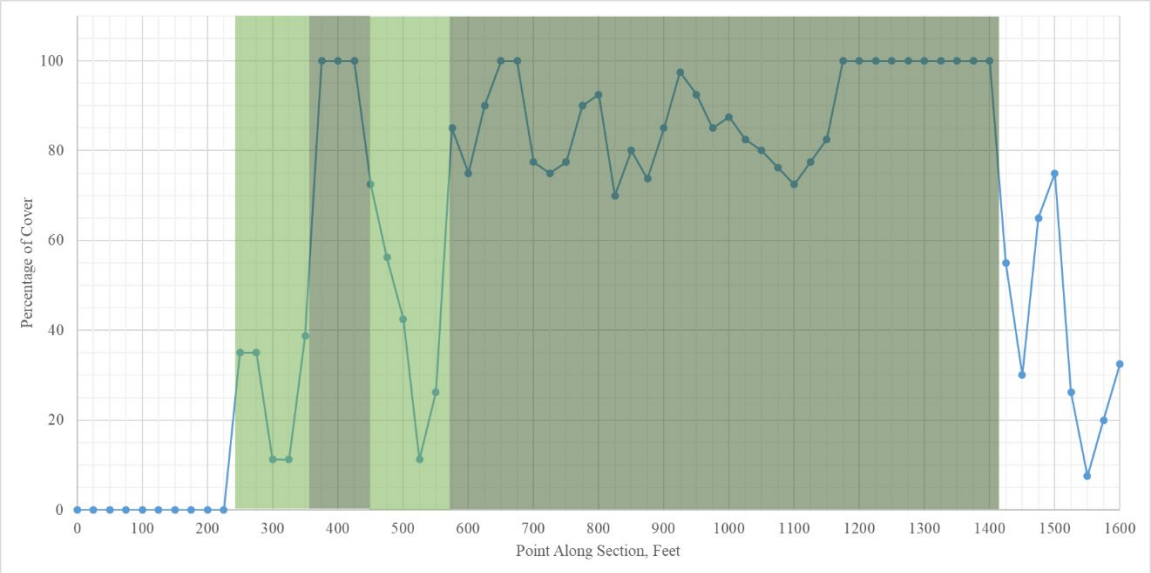


SR 374 (3) in Hocking County, Ohio

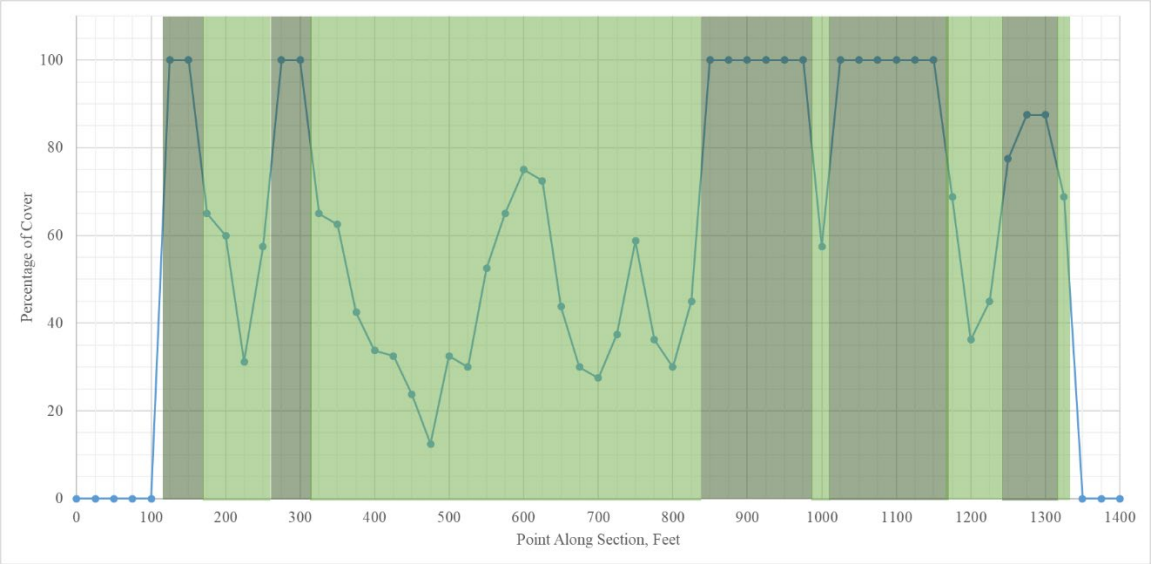

SR 595 in Hocking County, Ohio

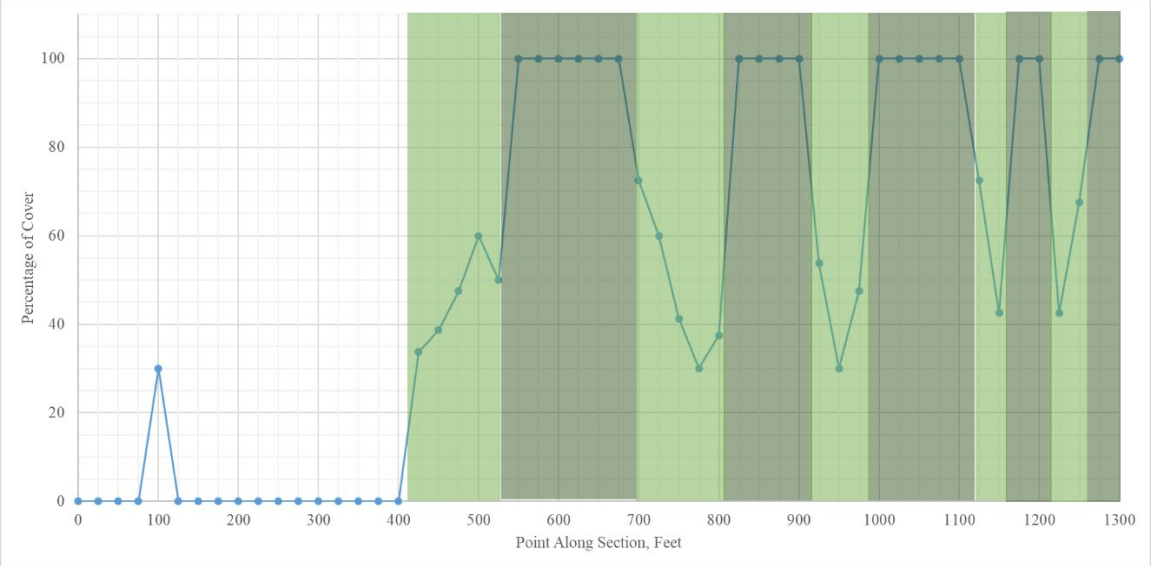

SR 124 (1) in Jackson County, Ohio

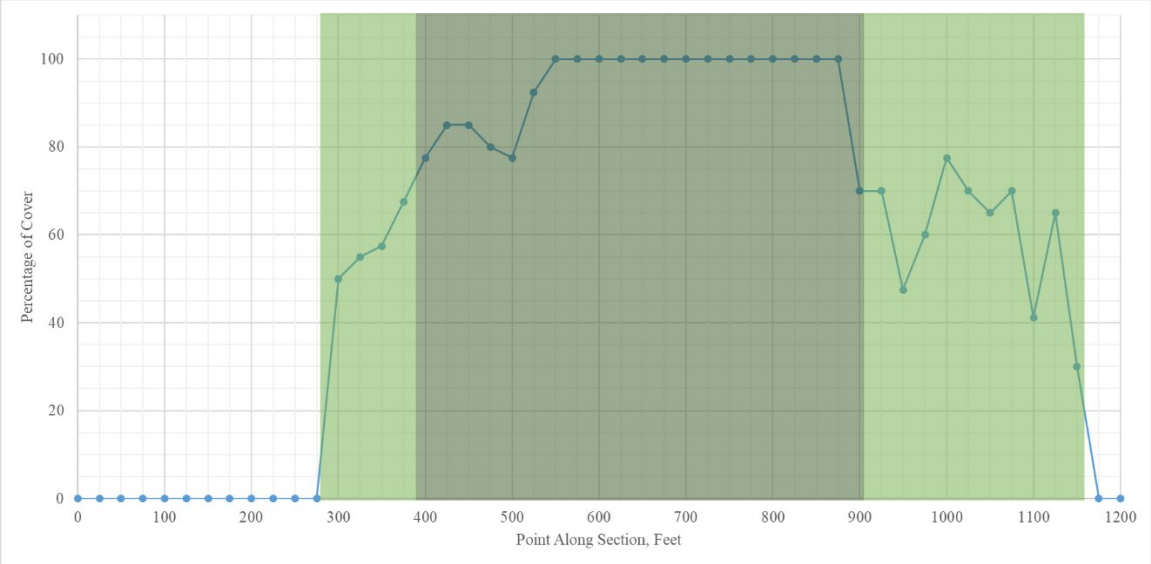


SR 124 (2) in Jackson County, Ohio

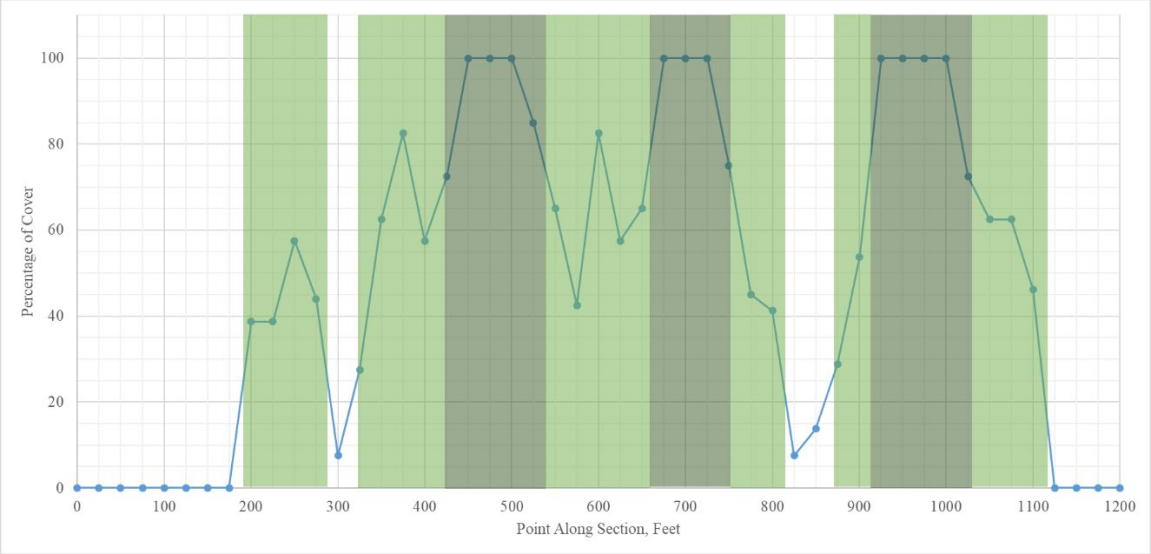


SR 139 in Jackson County, Ohio

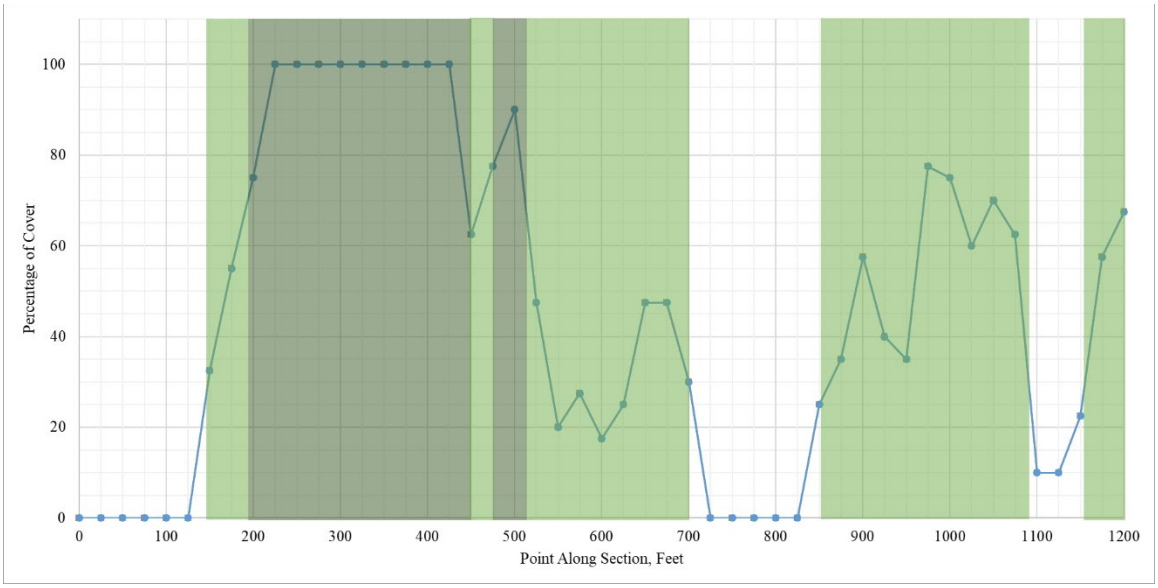


SR 327 (1) in Jackson County, Ohio

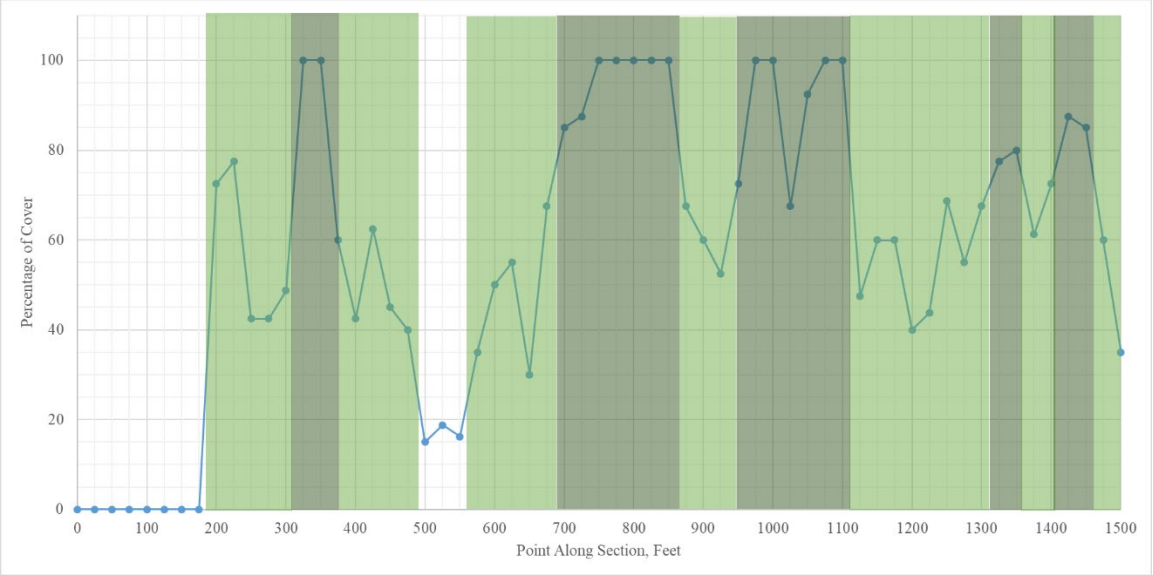


SR 327 (2) in Jackson County, Ohio

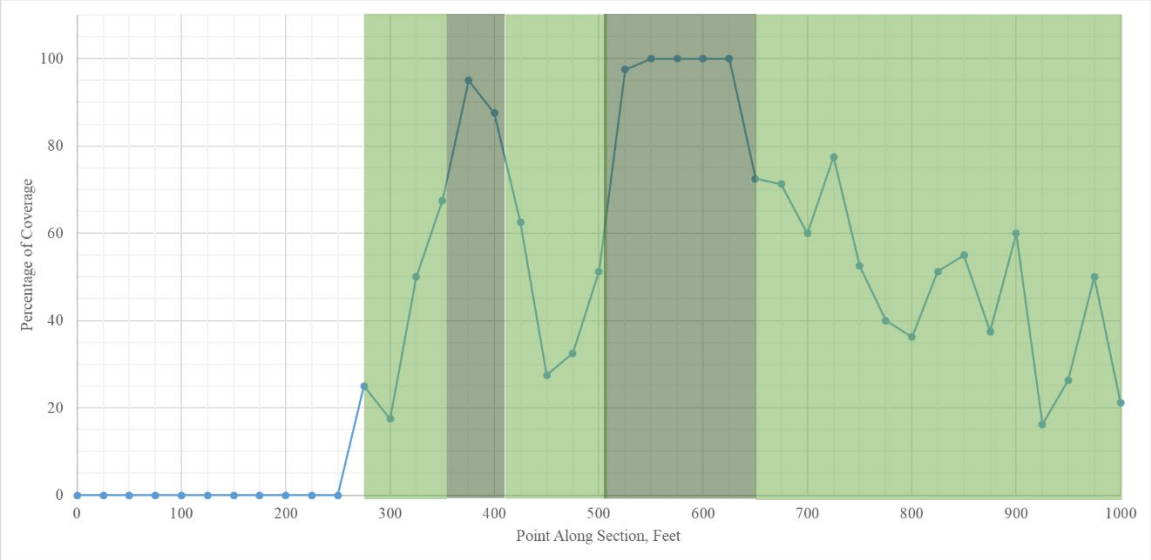


SR 608 in Lake County, Ohio

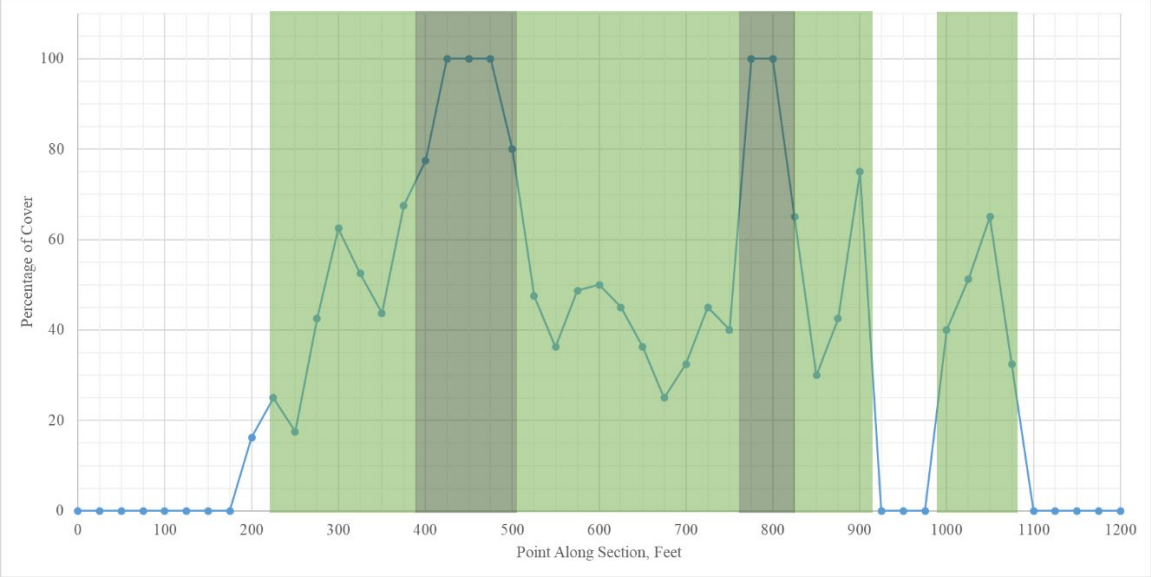


SR 284 in Muskingum County, Ohio

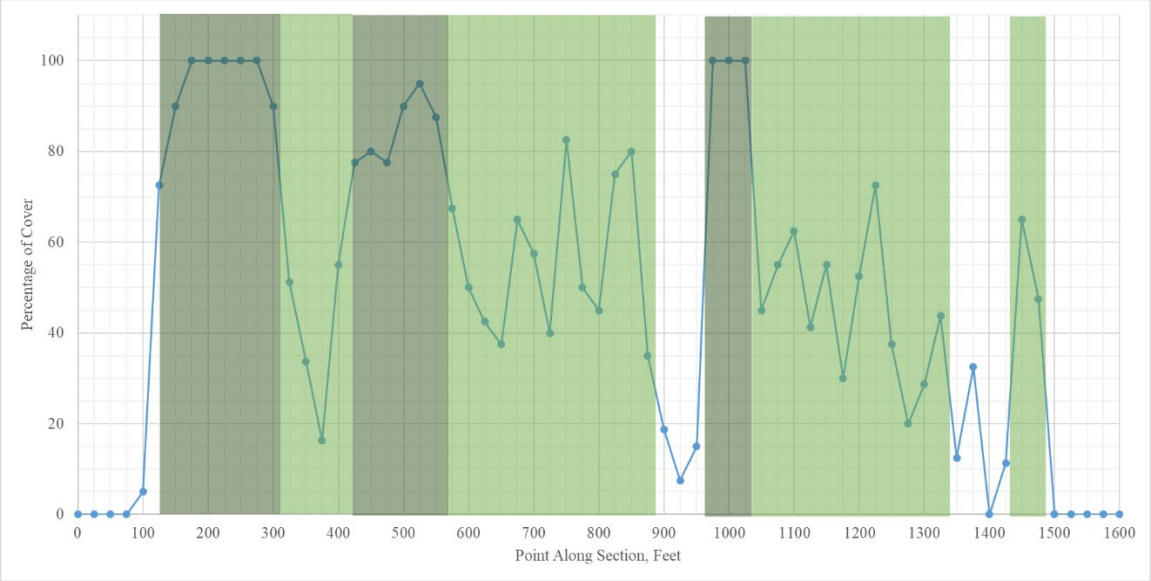


SR 335 (1) in Pike County, Ohio

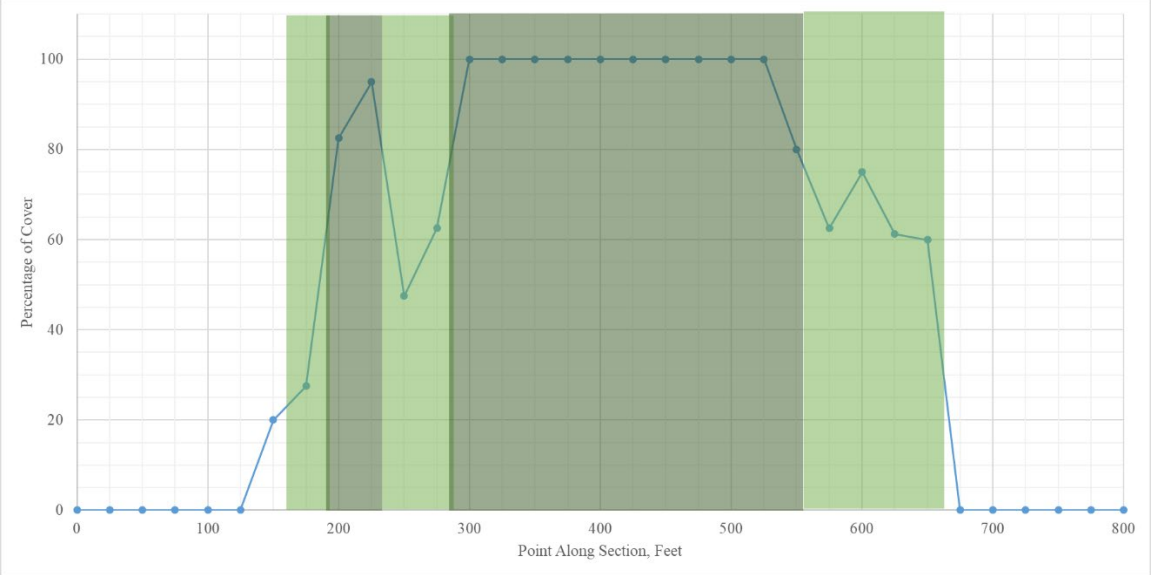


SR 335 (2) in Pike County, Ohio

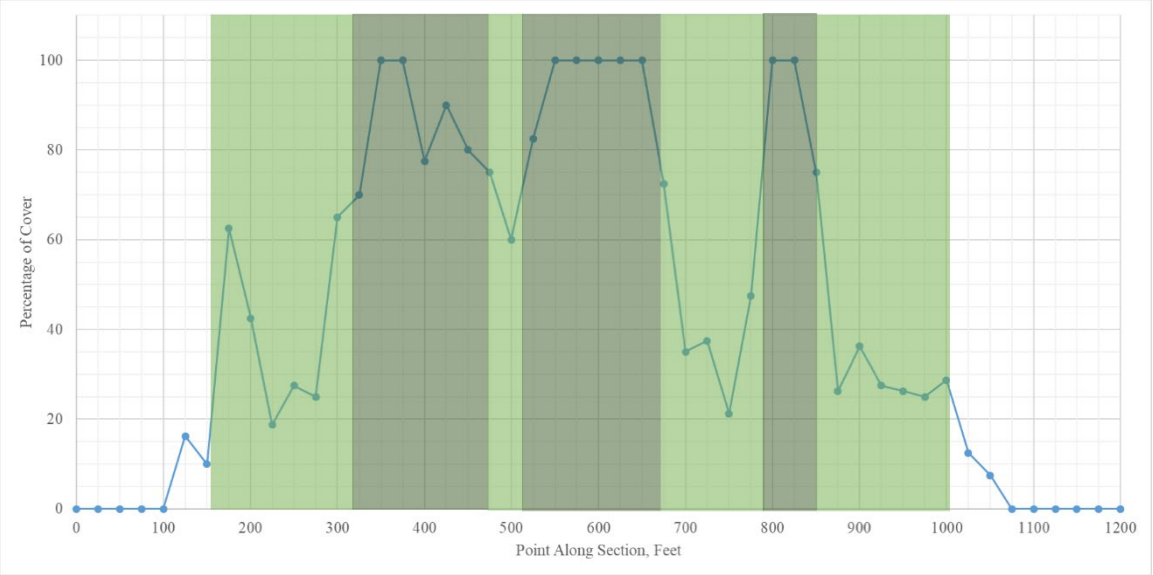


SR 125 in Scioto County, Ohio

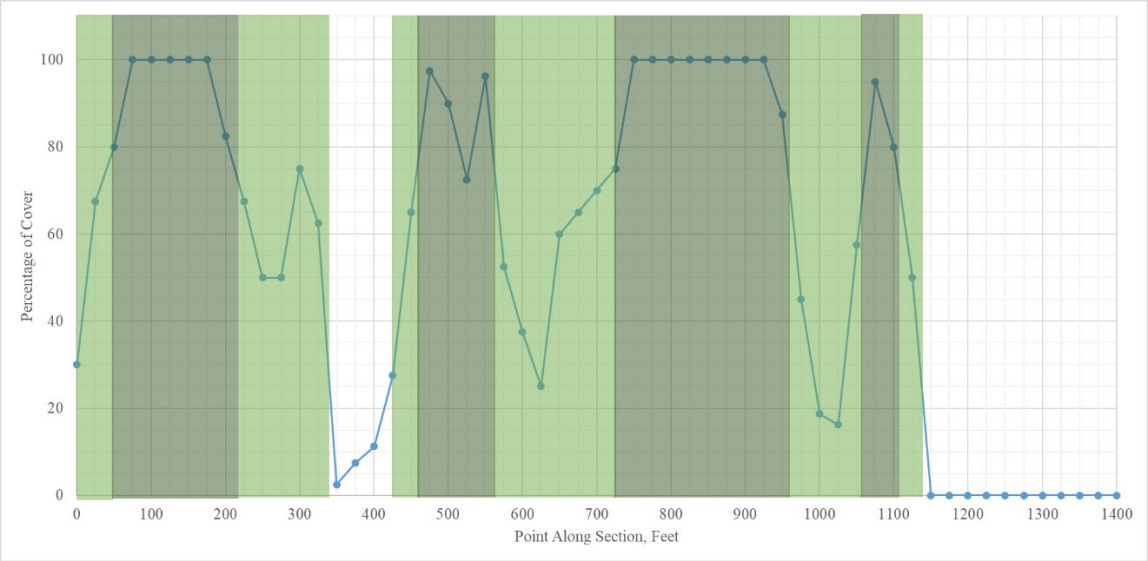


SR 139 in Scioto County, Ohio

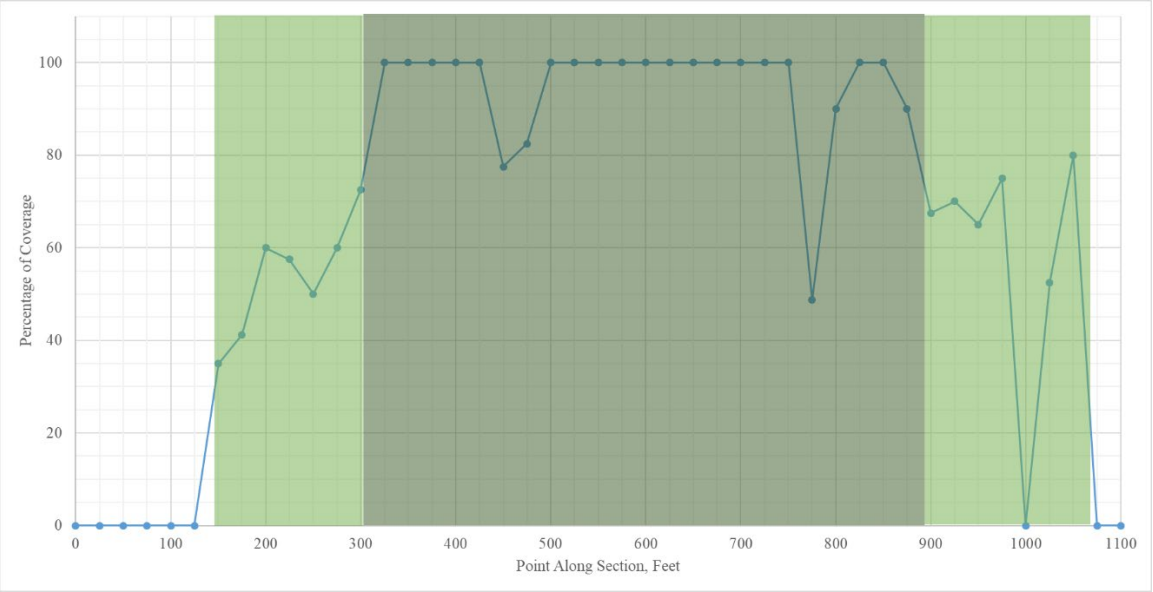


SR 258 (1) in Tuscarawas County, Ohio

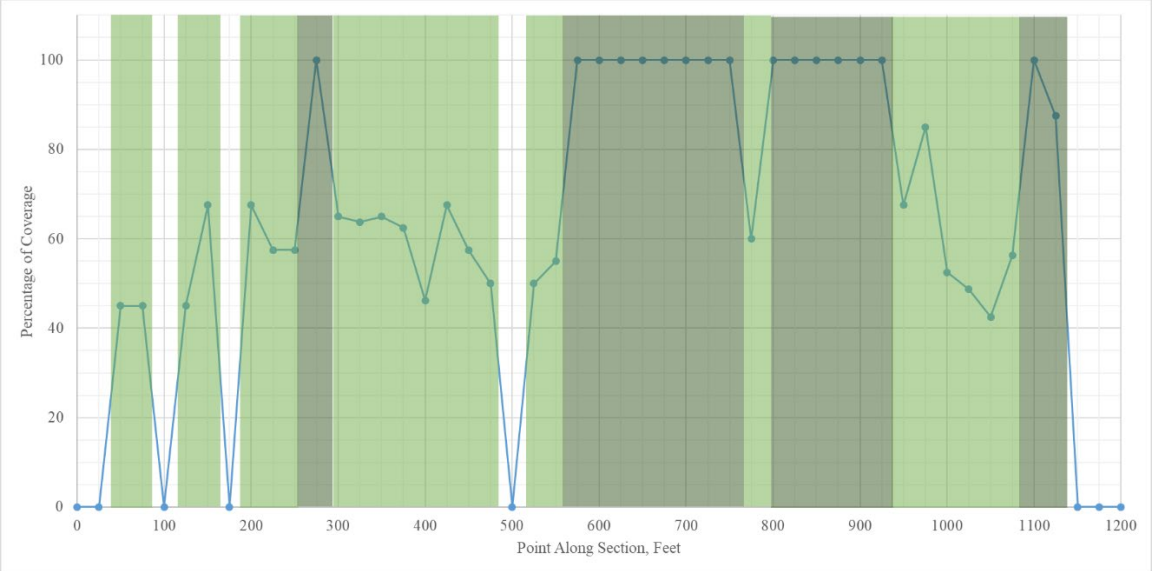


SR 258 (2) in Tuscarawas County, Ohio

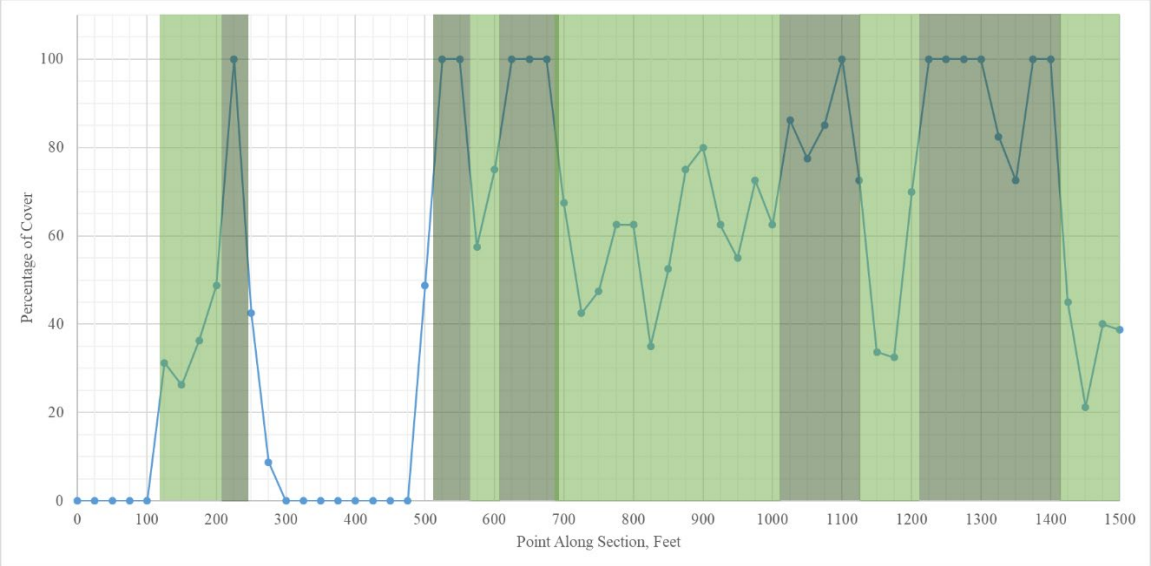


SR 800 (1) in Tuscarawas County, Ohio

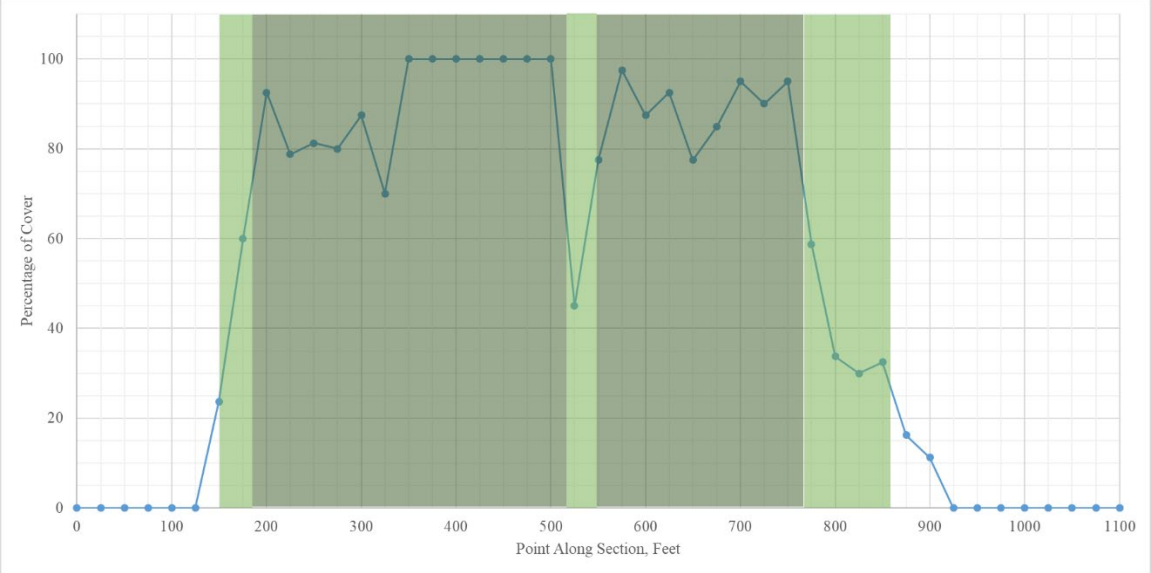


SR 800 (2) in Tuscarawas County, Ohio

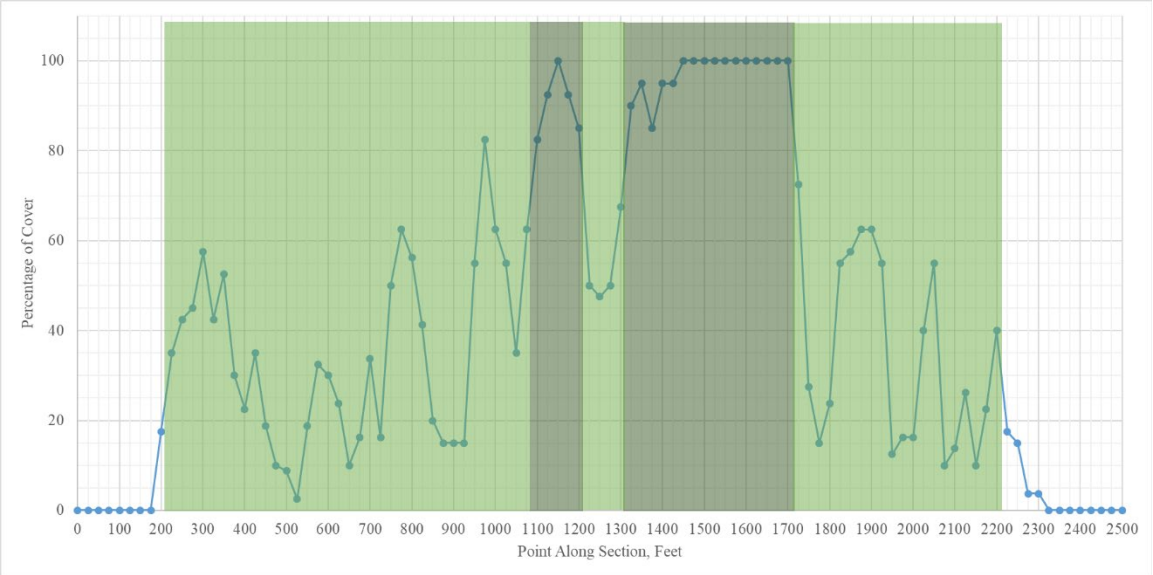


SR 56 in Vinton County, Ohio

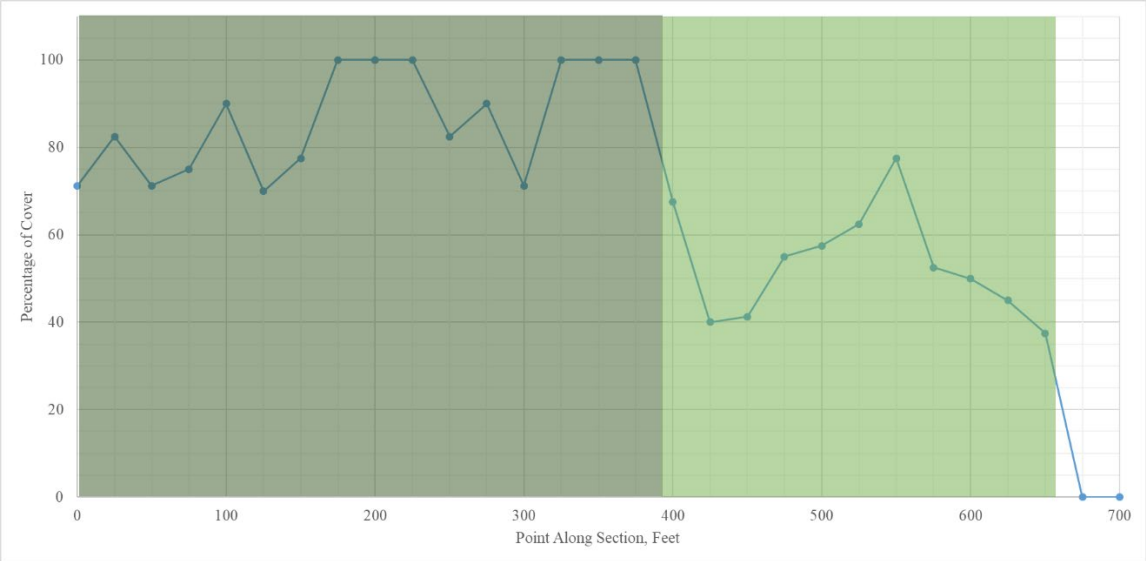


SR 124 in Vinton County, Ohio

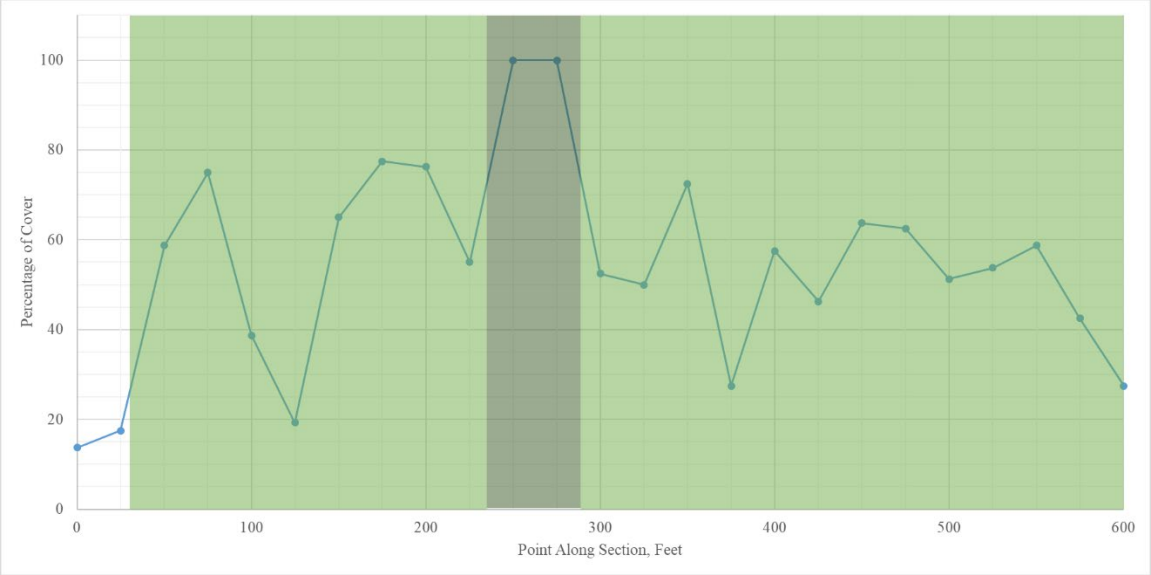


SR 327 (1) in Vinton County, Ohio

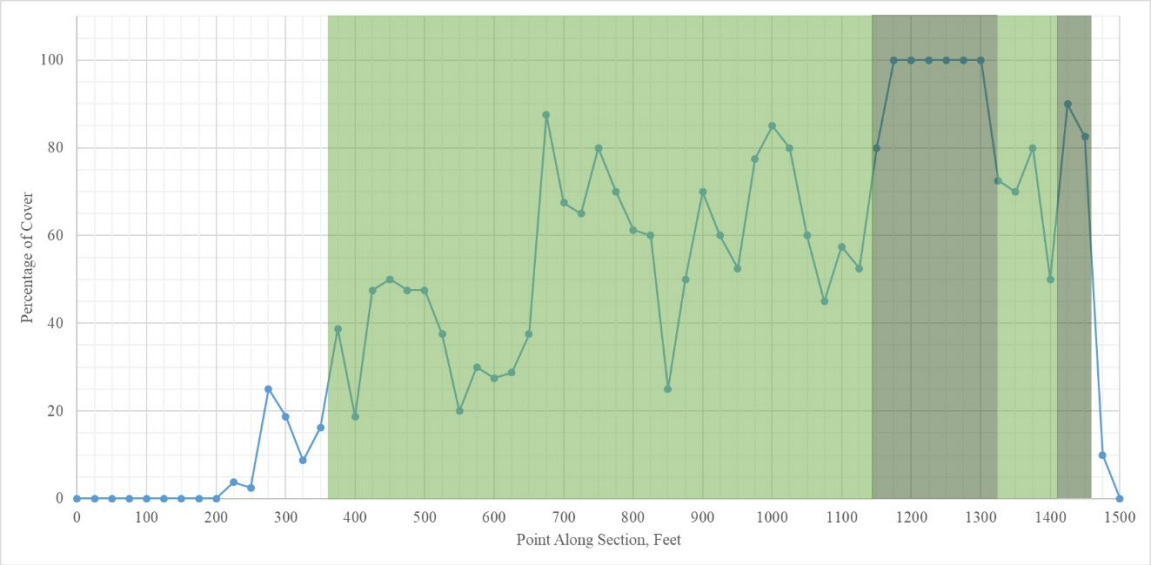


SR 327 (2) in Vinton County, Ohio

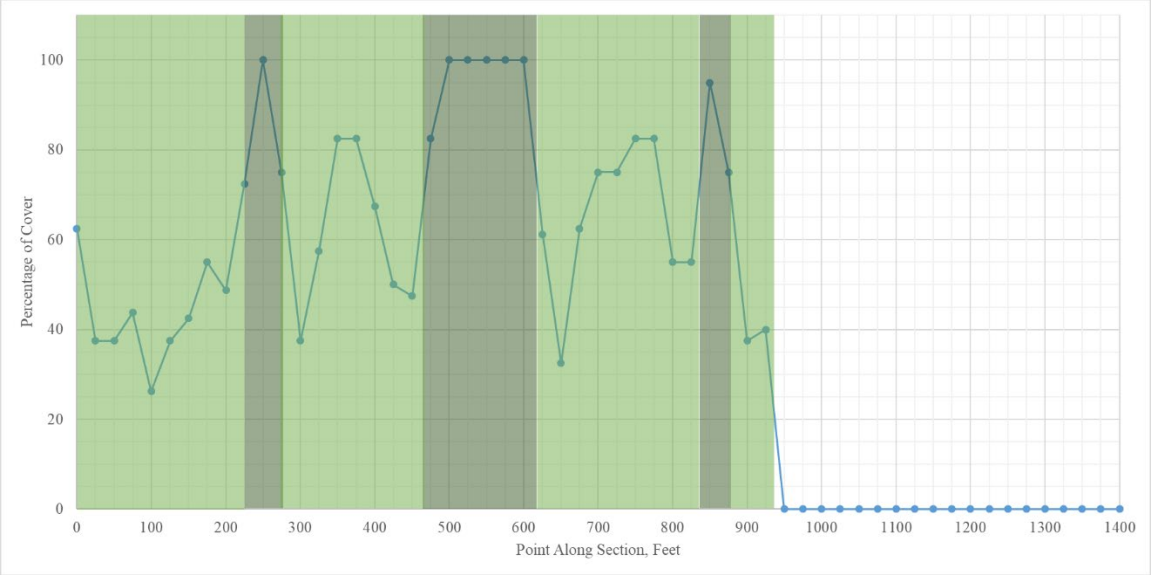


SR 356 in Vinton County, Ohio

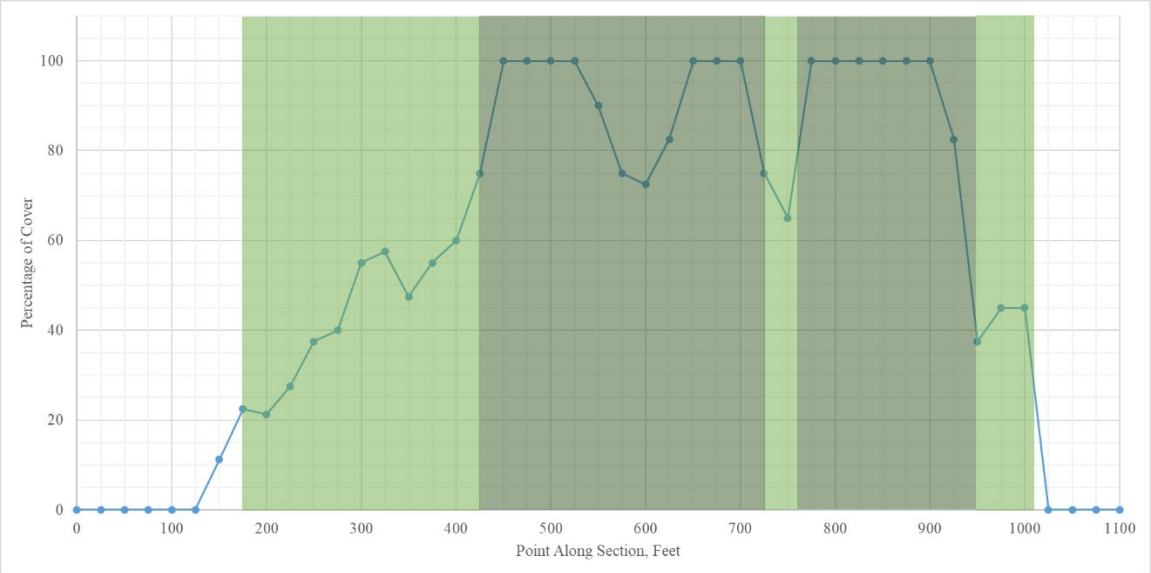


SR 260 in Washington County, Ohio

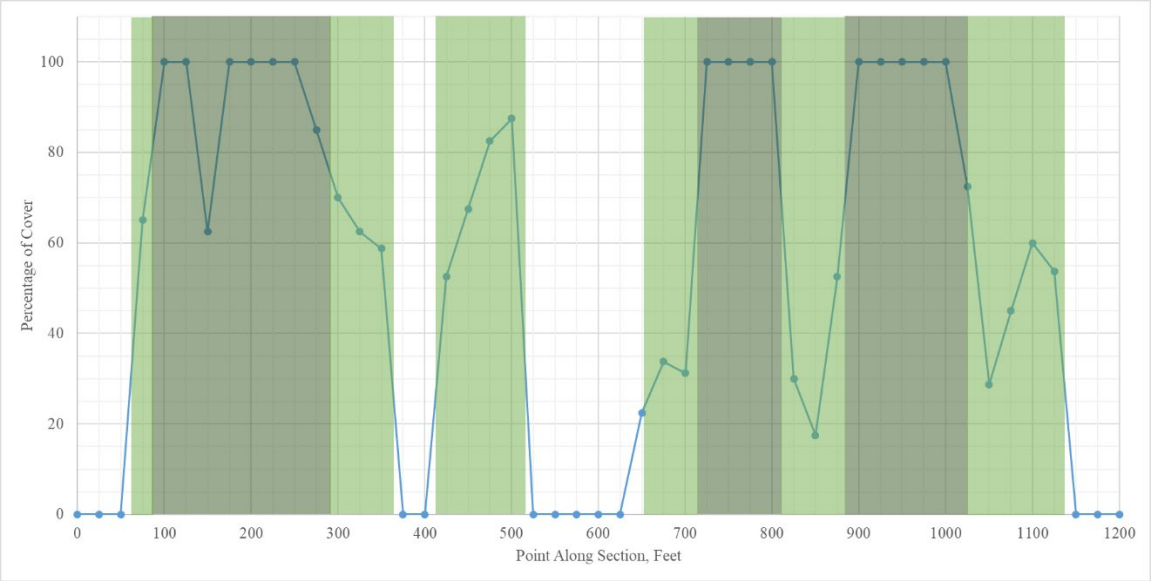


SR 555 in Washington County – Ohio

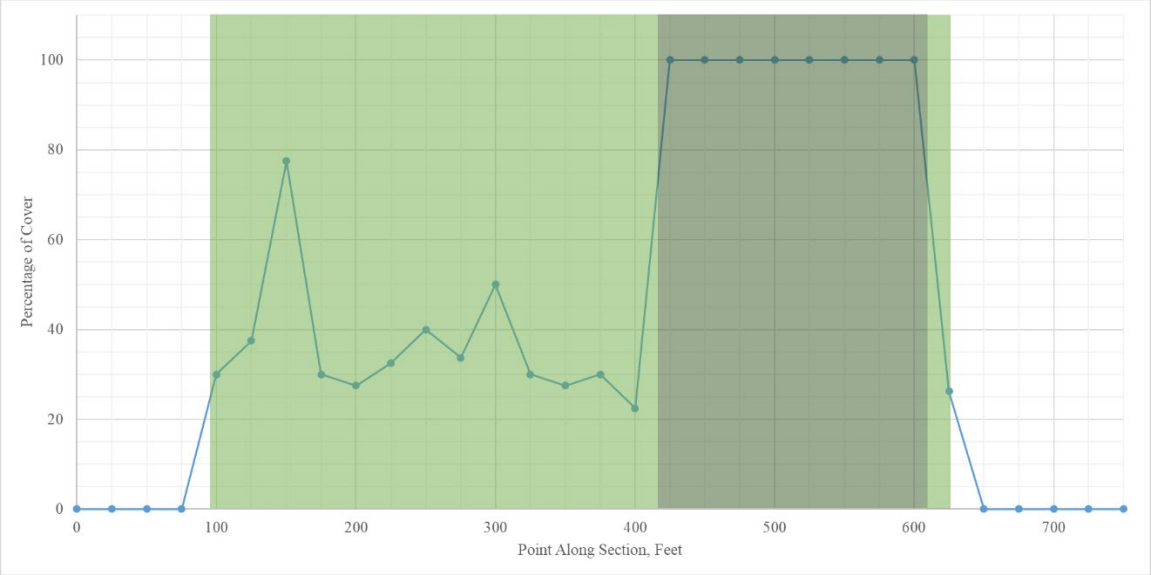


SR 676 (1) in Washington County, Ohio

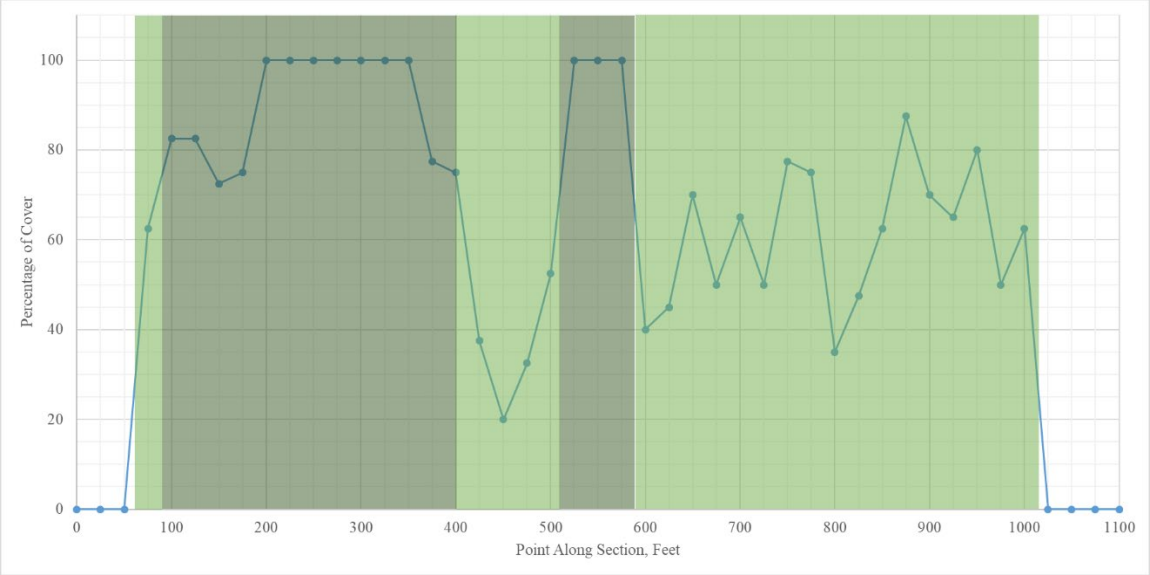

SR 676 (2) in Washington County, Ohio

## APPENDIX H: MARWIS PAVEMENT MOISTURE MEASUREMENTS

- These graphs are listed in order by county name and state route (SR) number.
- White portions indicate densiometer measurements of tree coverage 0-25% (no canopy); light green portions indicate coverage 25-75% (partial canopy); dark green portions indicate coverage 75-100% (full canopy)
- Horizontal axis indicates distance in feet along road section (1 ft = 0.305 m)
- Vertical axis indicates moisture level as water film height in µm (1 µm = 0.4 mil)

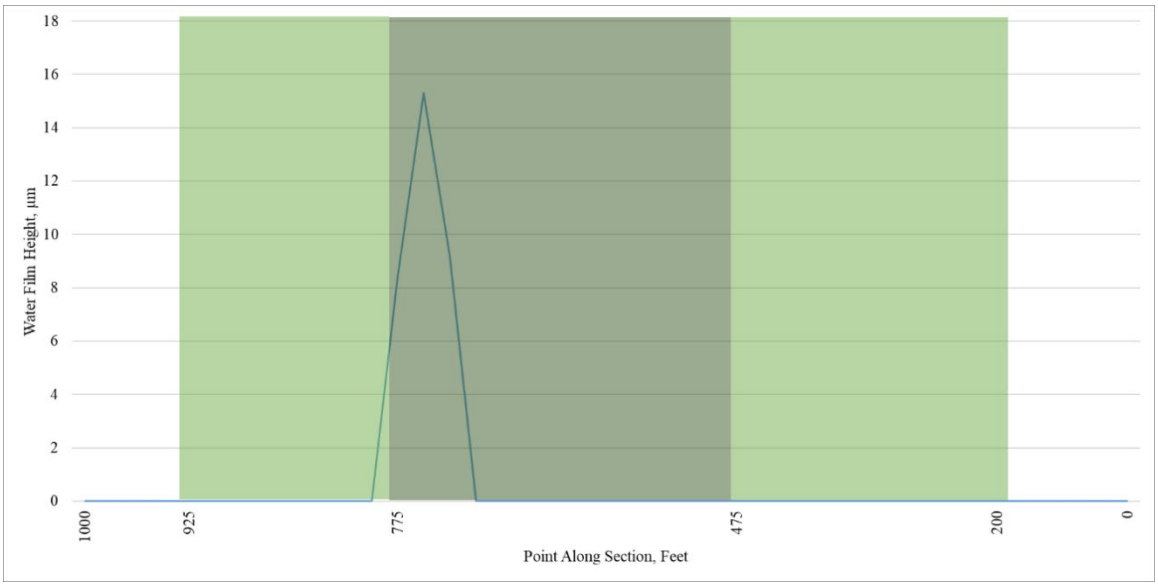


Measured moisture level - SR 13 (NB) in Athens County, Ohio

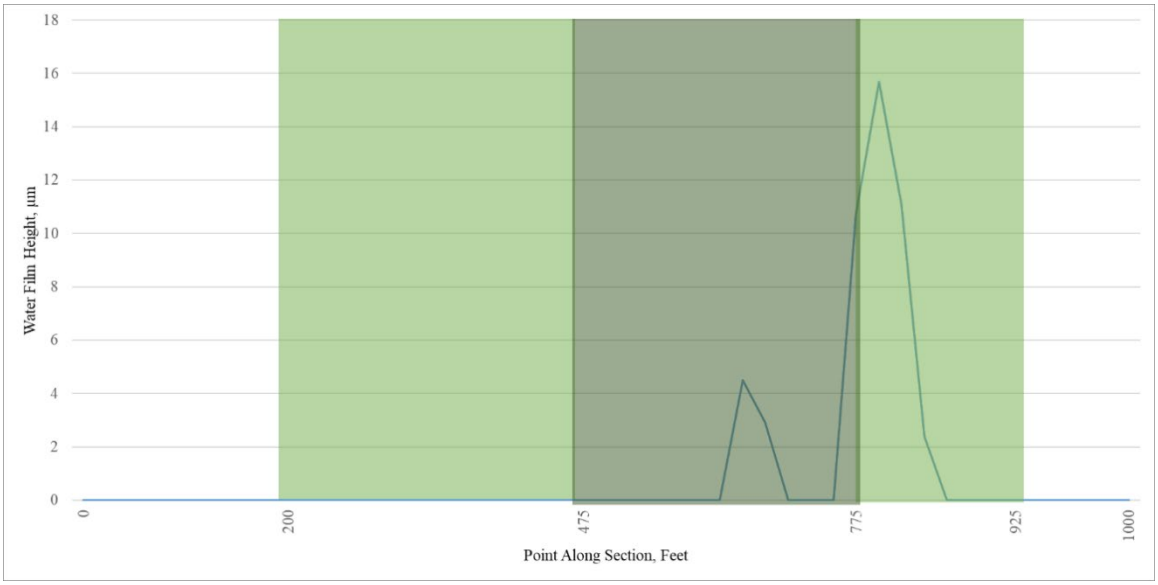


Measured moisture level - SR 13 (SB) in Athens County, Ohio

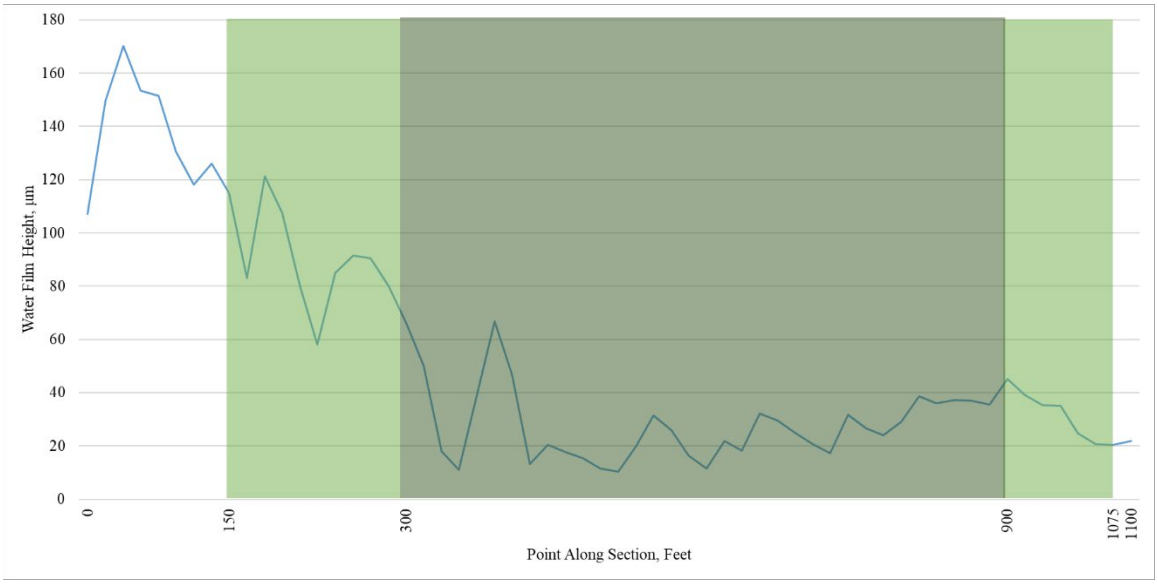


Measured moisture level - SR 258 (2) (NB) in Harrison County, Ohio

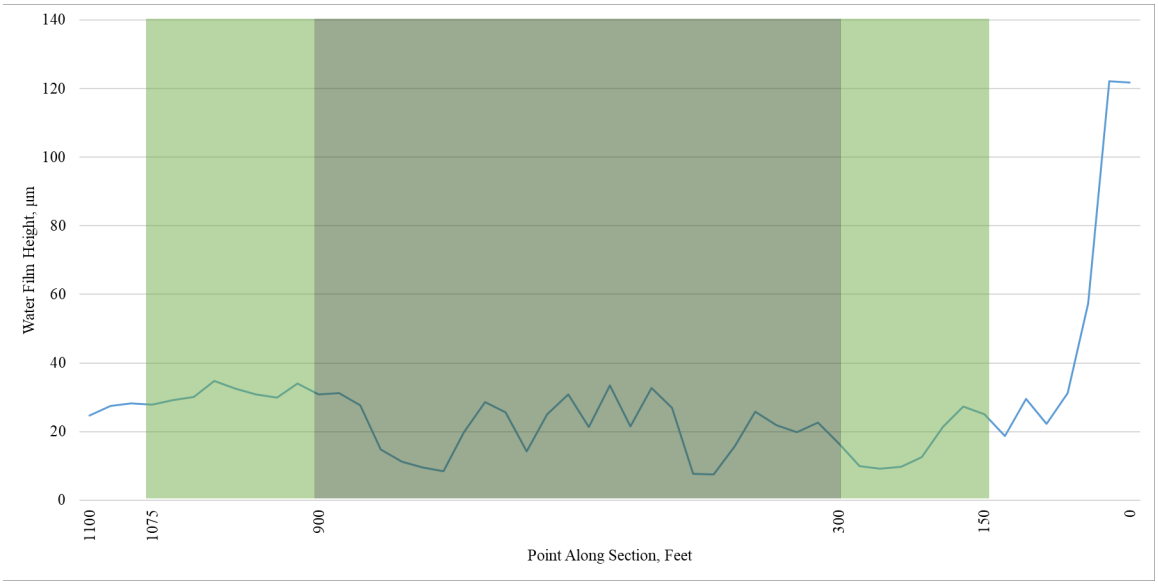


Measured moisture level - SR 258 (2) (SB) in Harrison County, Ohio

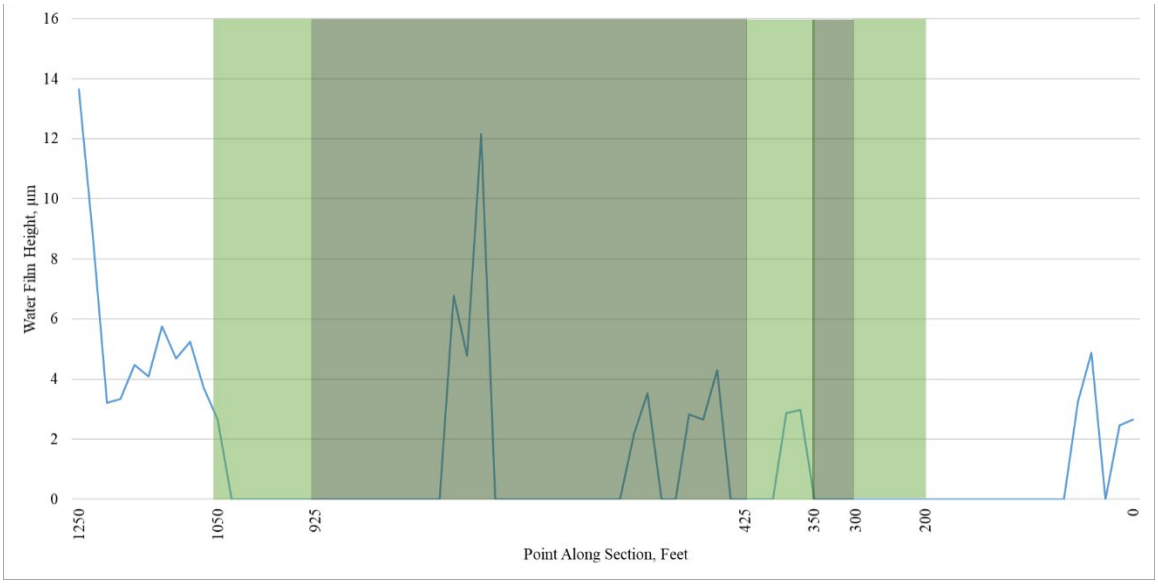


Measured moisture level - SR 56 (EB) in Hocking County, Ohio

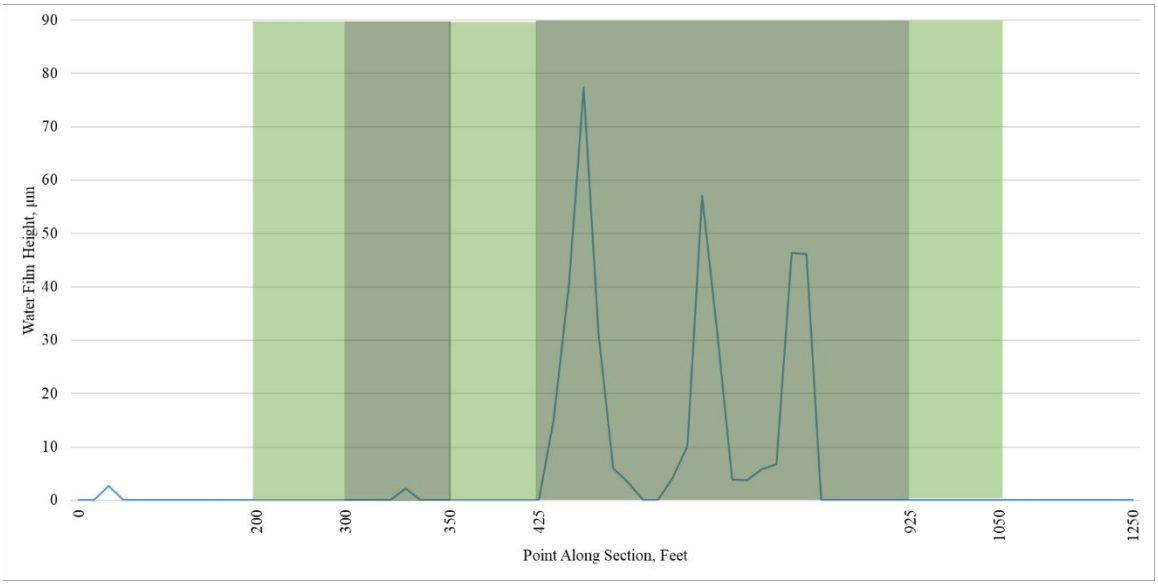


Measured moisture level - SR 56 (WB) in Hocking County, Ohio

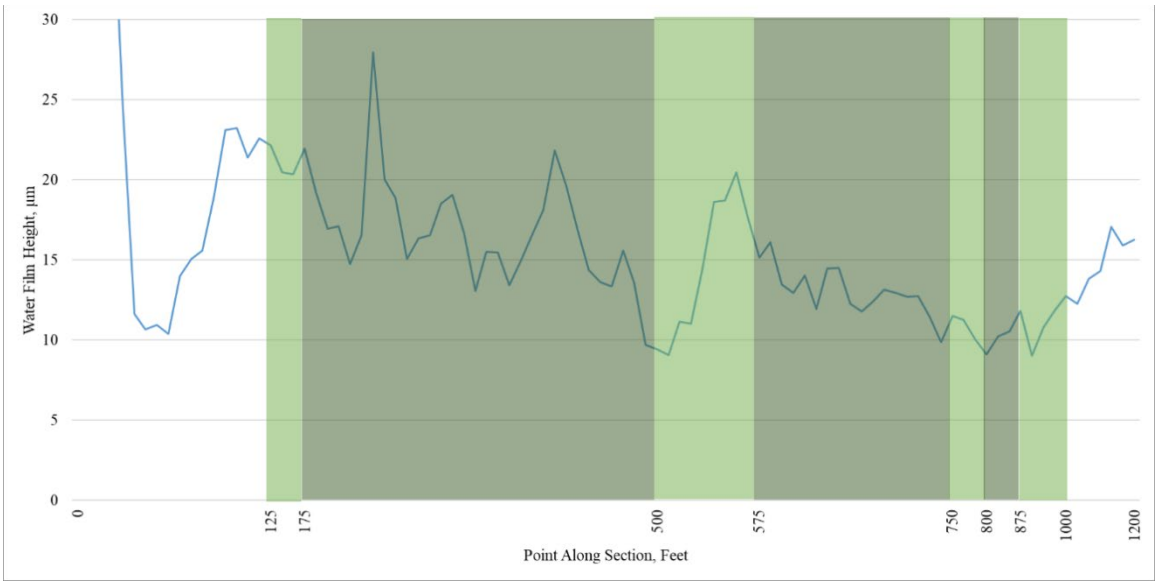


Measured moisture level - SR 374 (1) (NB) in Hocking County, Ohio

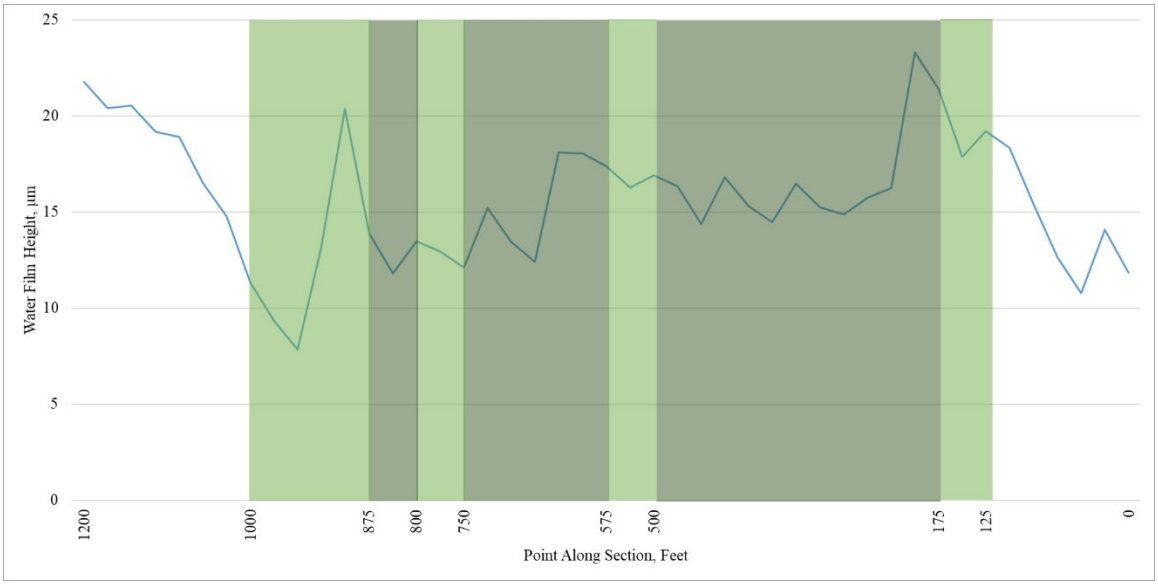


Measured moisture level - SR 374 (1) (SB) in Hocking County, Ohio

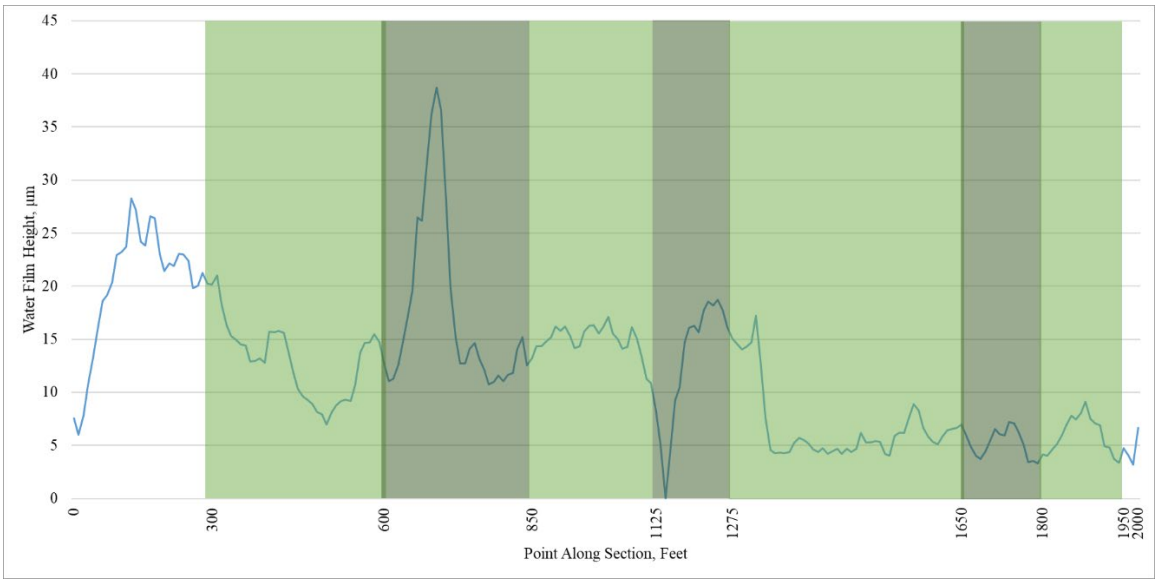

Measured moisture level - SR 374 (2) (NB) in Hocking County, Ohio

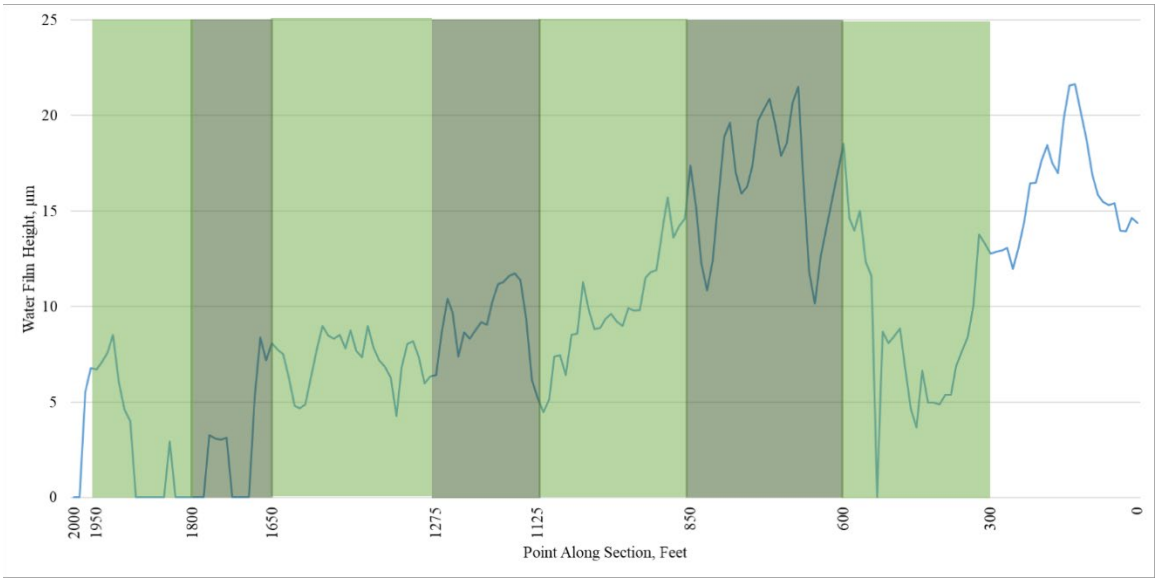

Measured moisture level - SR 374 (2) SB in Hocking County, Ohio

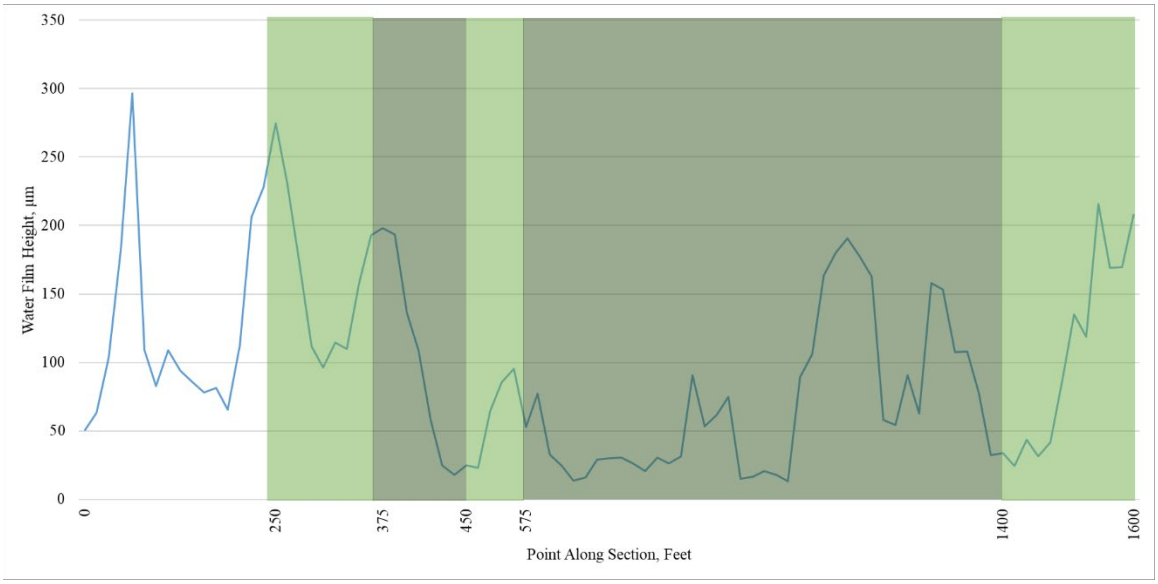


Measured moisture level - SR 374 (3) (NB) in Hocking County, Ohio

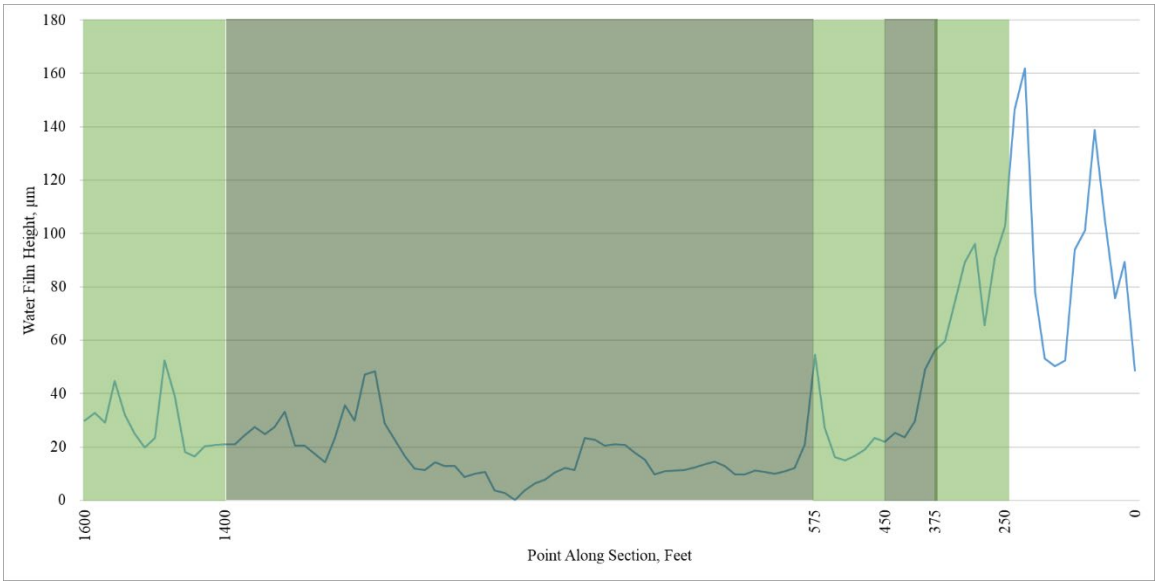


Measured moisture level - SR 374 (3) (SB) in Hocking County, Ohio

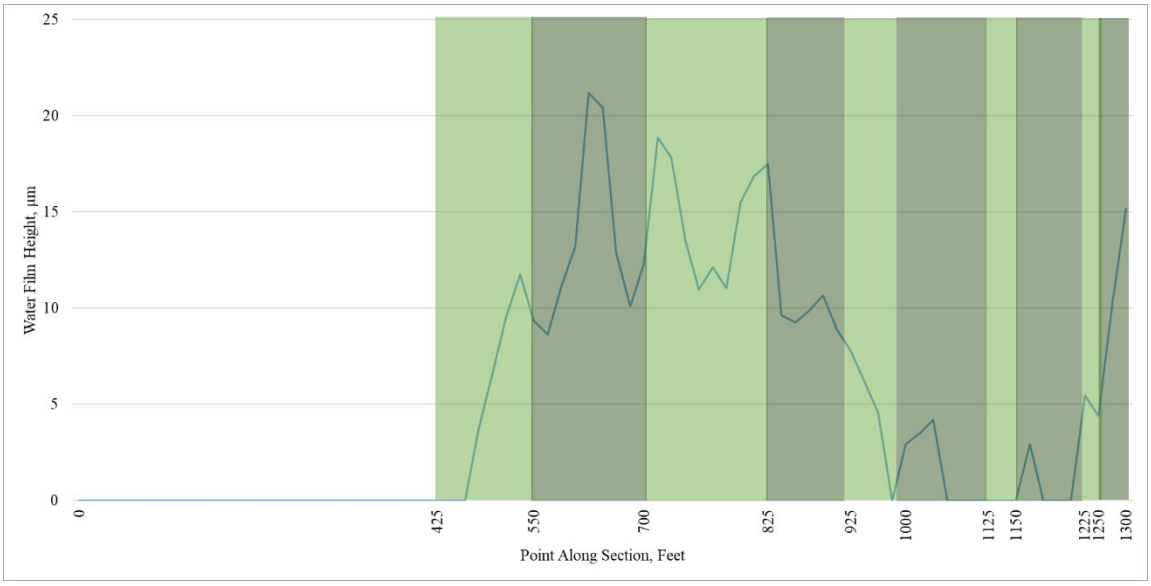

Measured moisture level - SR 124 (1) (EB) in Jackson County, Ohio

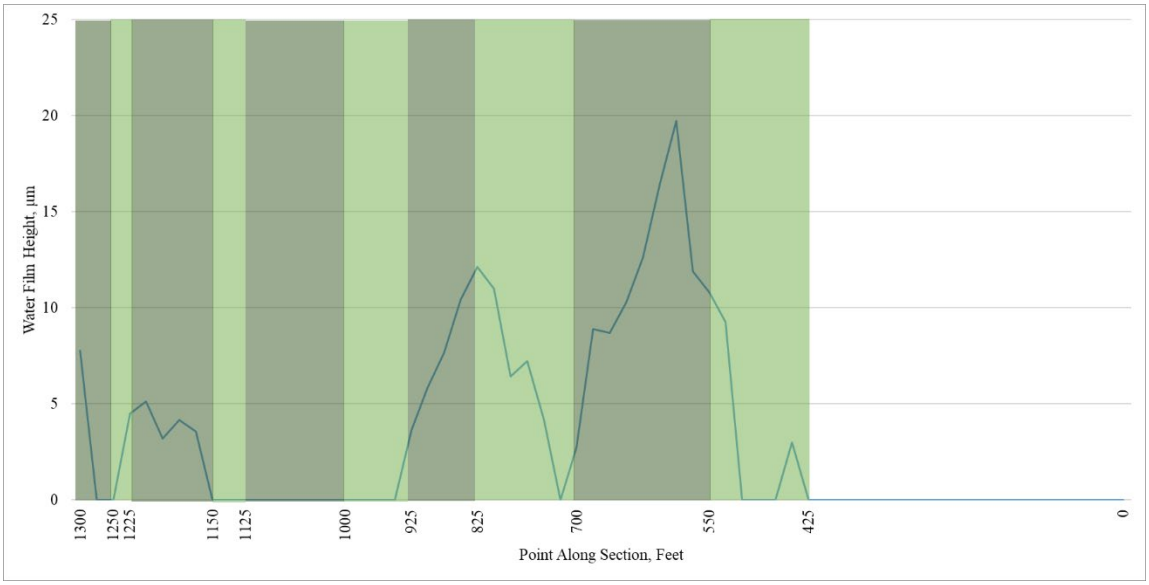

Measured moisture level - SR 124 (1) WB in Jackson County, Ohio

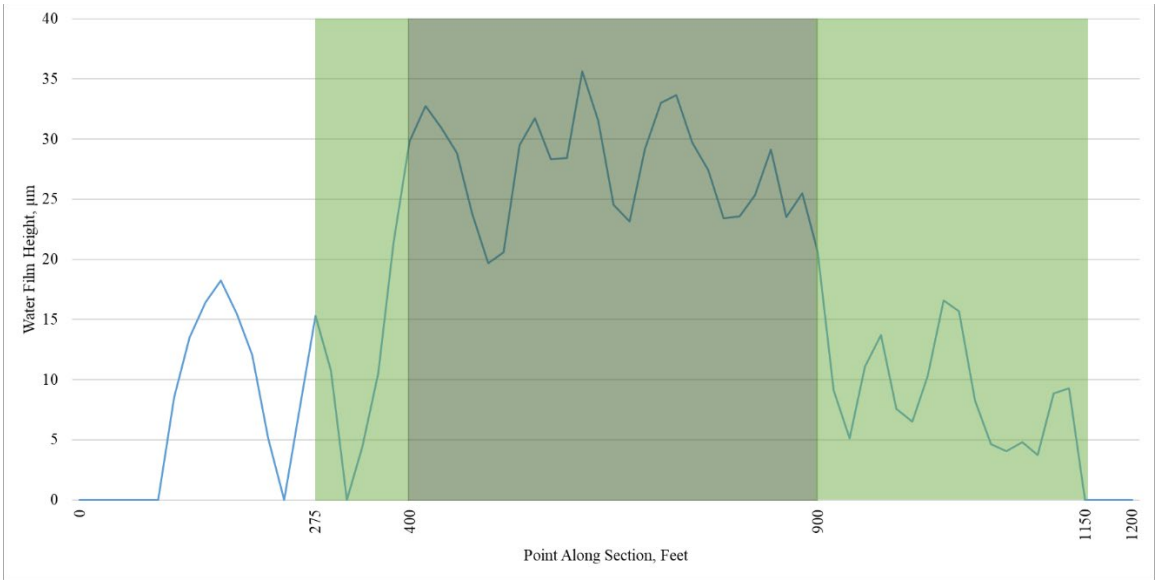


Measured moisture level - SR 124 (2) EB in Jackson County Ohio

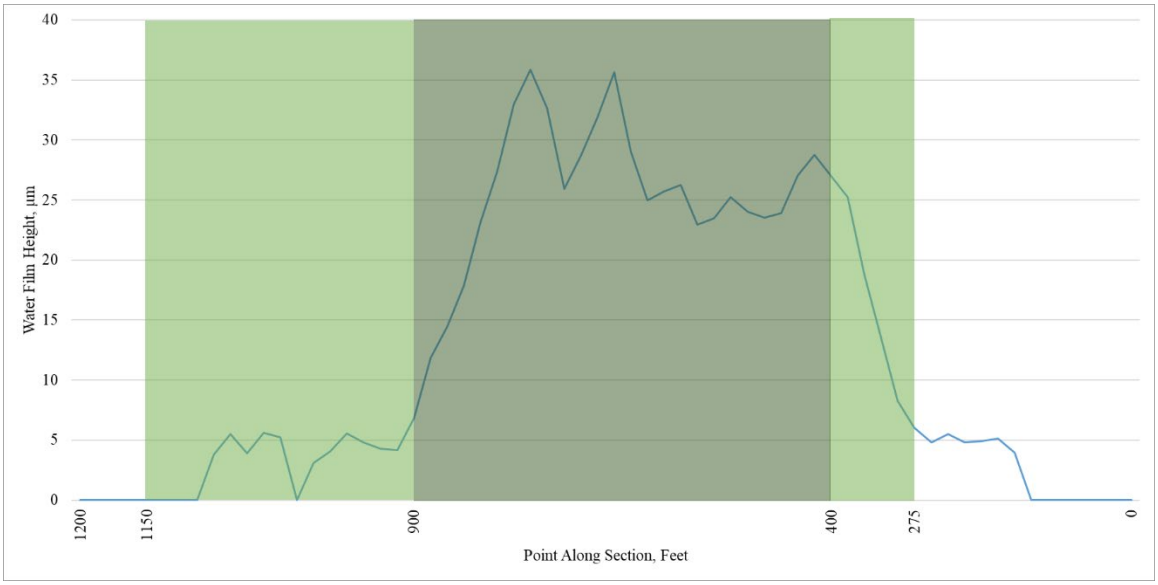


Measured moisture level - SR 124 (2) (WB) in Jackson County, Ohio

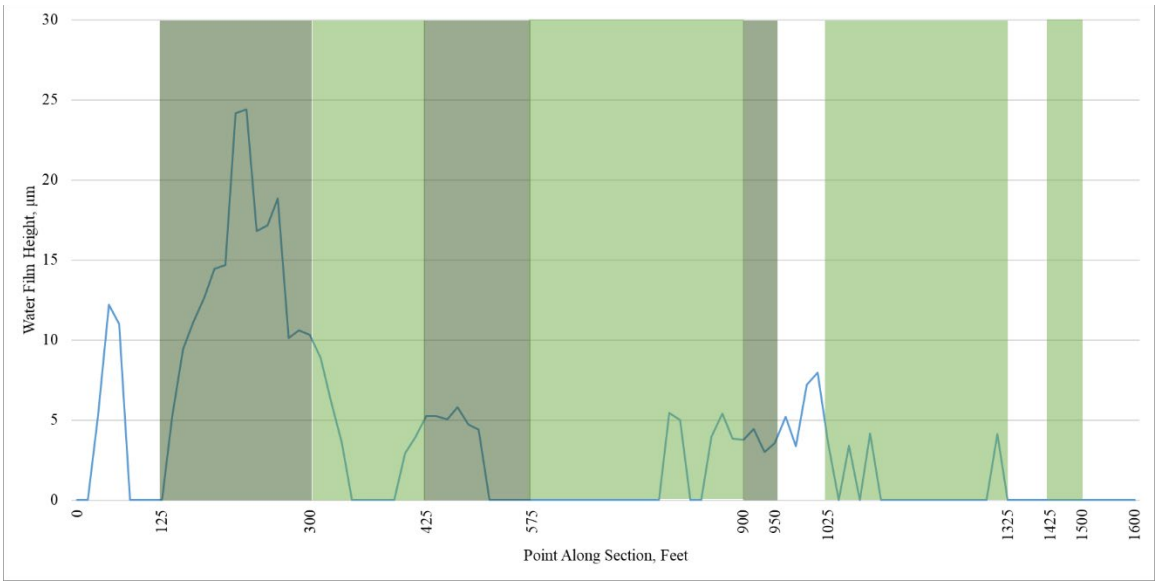

Measured moisture level - SR 335 (1) (EB) in Pike County, Ohio

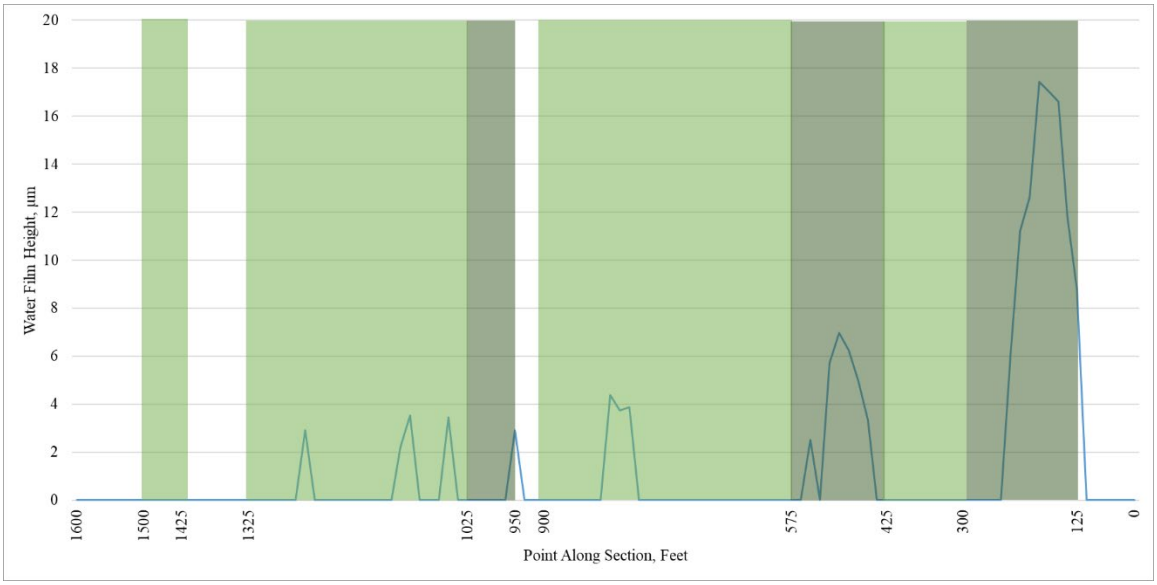

Measured moisture level - SR 335 (1) (WB) in Pike County, Ohio

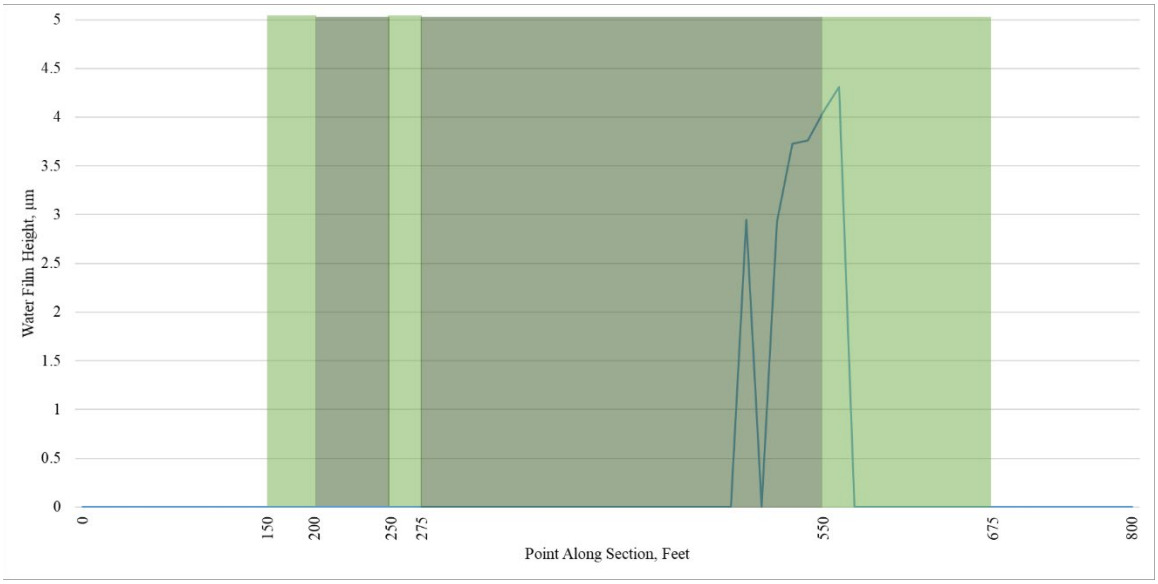


Measured moisture level - SR 335 (2) (NB) in Pike County, Ohio

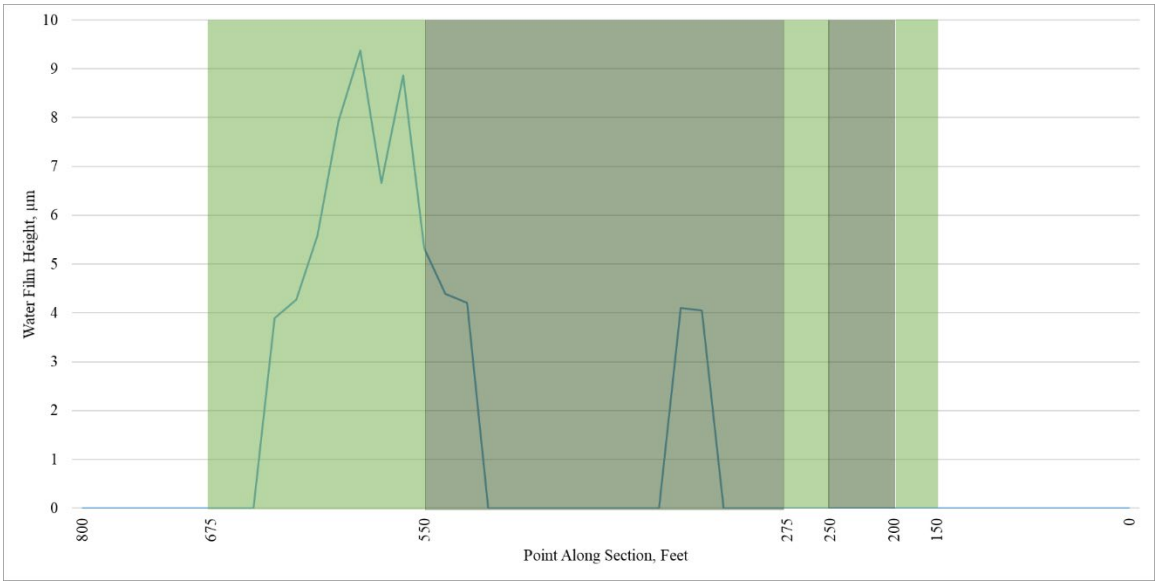


Measured moisture level - SR 335 (2) (SB) in Pike County, Ohio

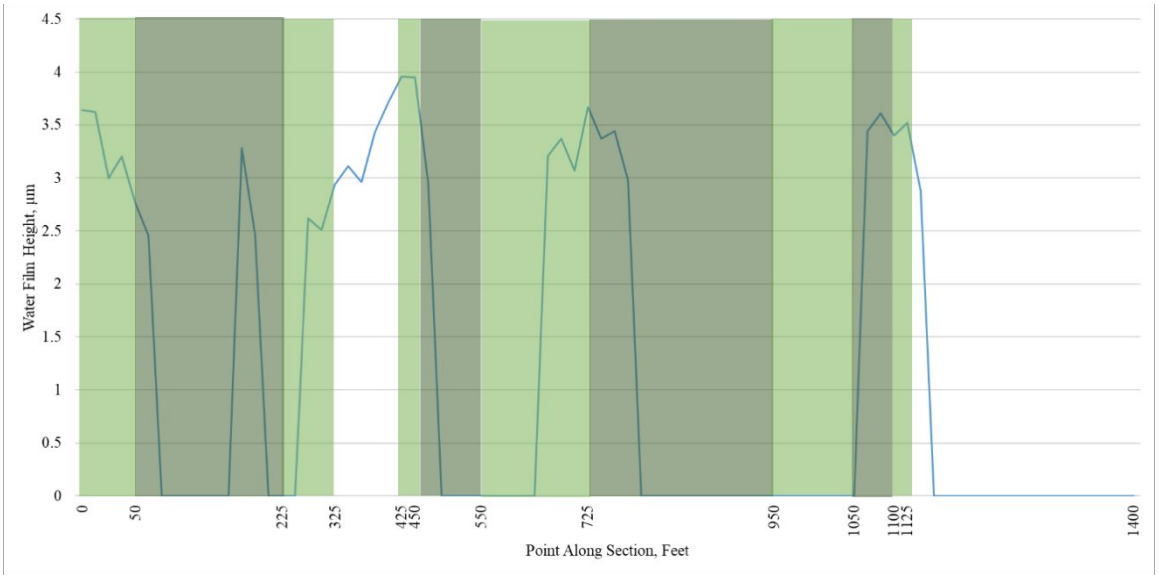


Measured moisture level - SR 139 (EB) in Scioto County, Ohio

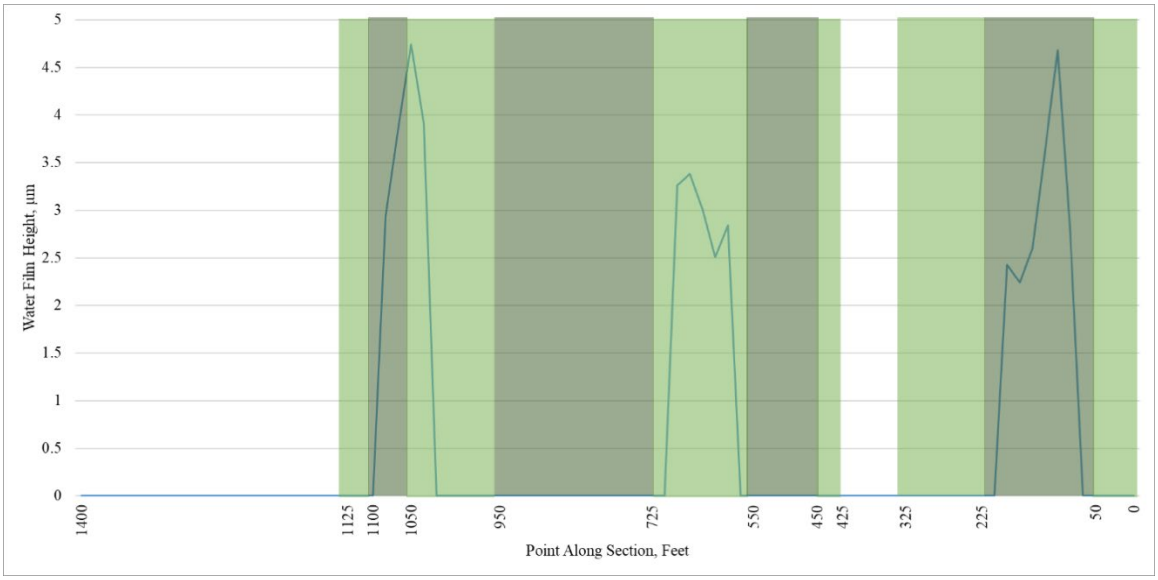


Measured moisture level - SR 139 (WB) in Scioto County, Ohio

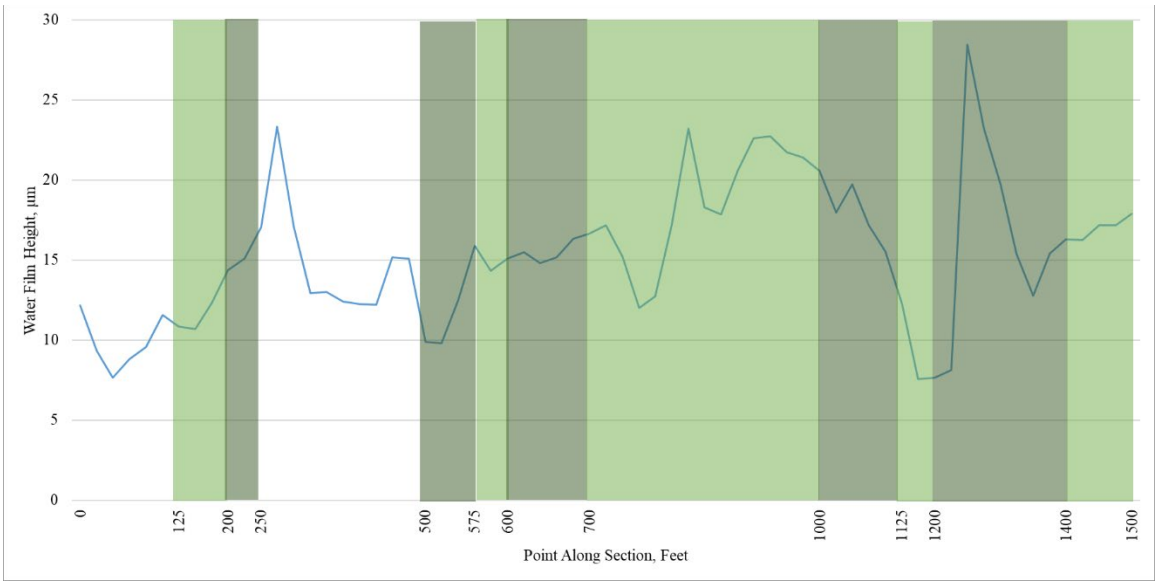

Measured moisture level - SR 800 (1) (NB) in Tuscarawas County, Ohio

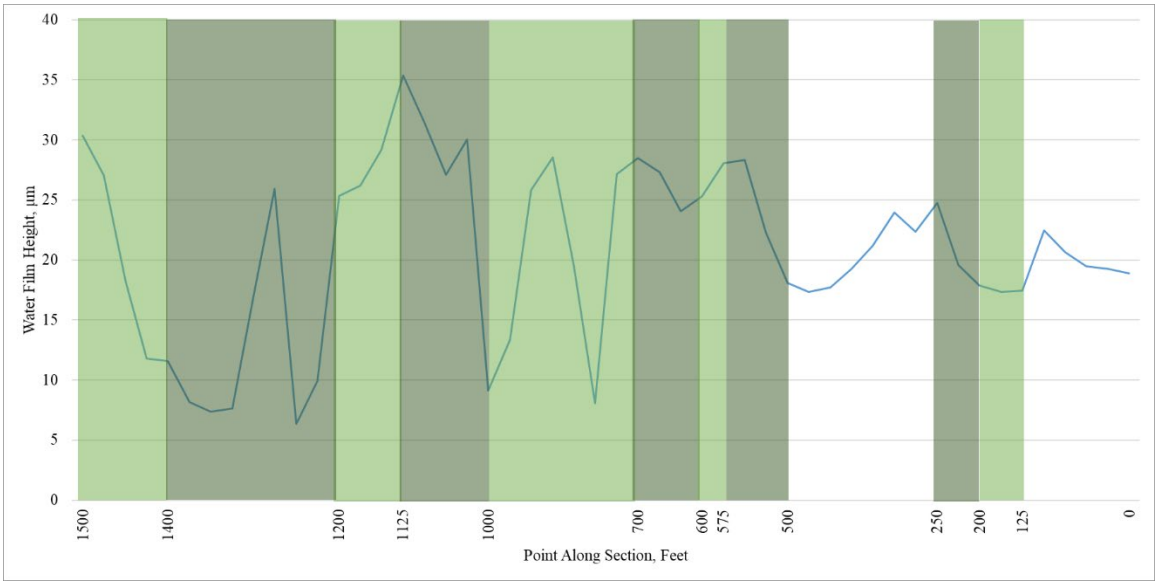

Measured moisture level - SR 800 (1) (SB) in Tuscarawas County, Ohio

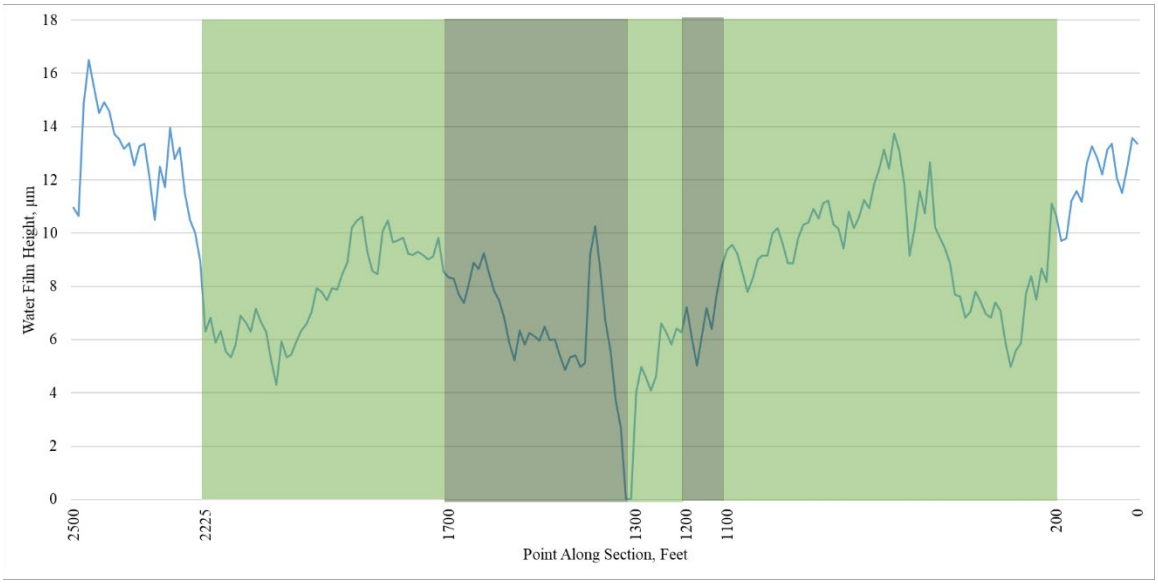


Measured moisture level - SR 56 (EB) in Vinton County, Ohio

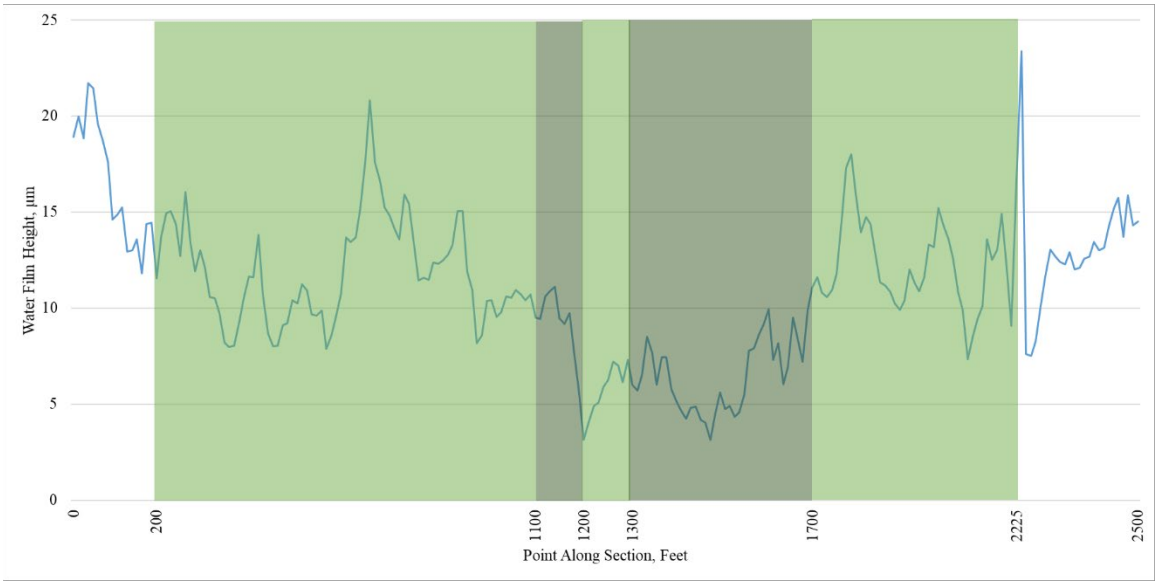


Measured moisture level - SR 56 (WB) in Vinton County, Ohio

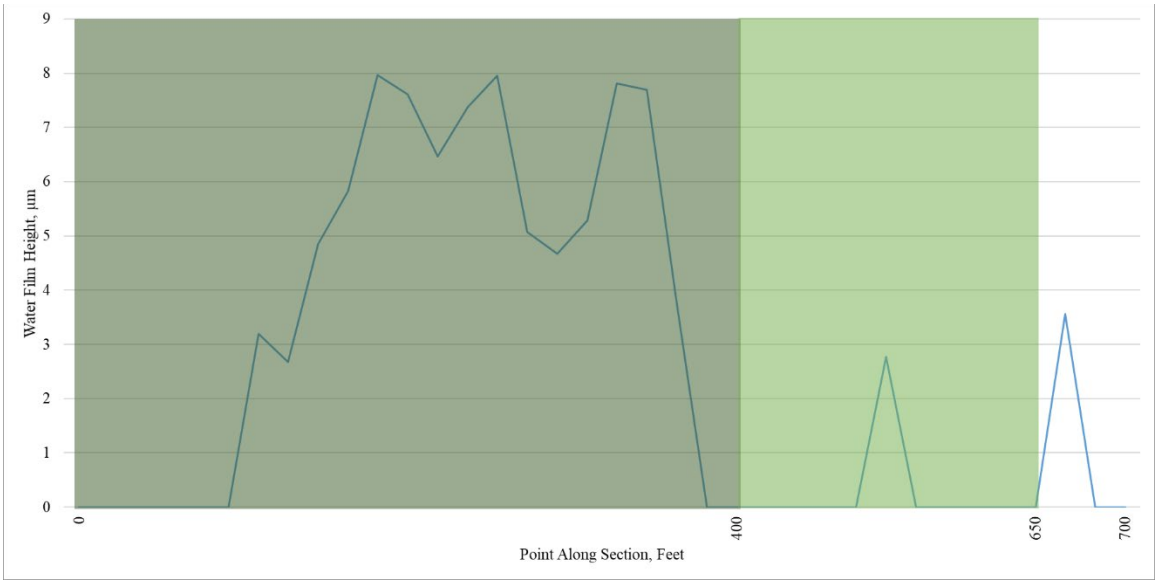

Measured moisture level - SR 124 (EB) in Vinton County, Ohio

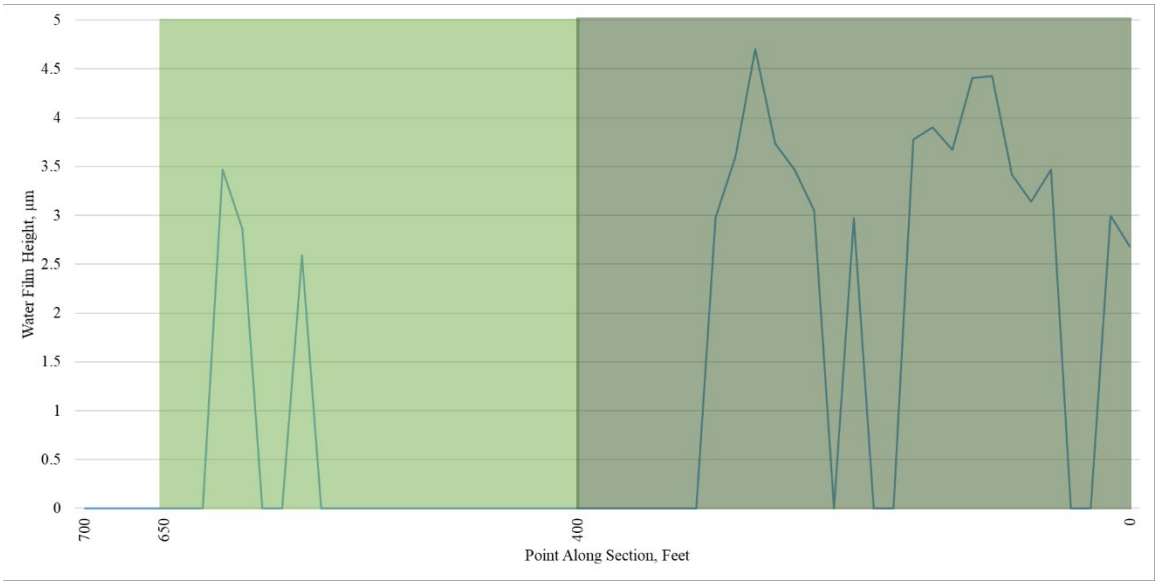

Measured moisture level - SR 124 (WB) in Vinton County, Ohio

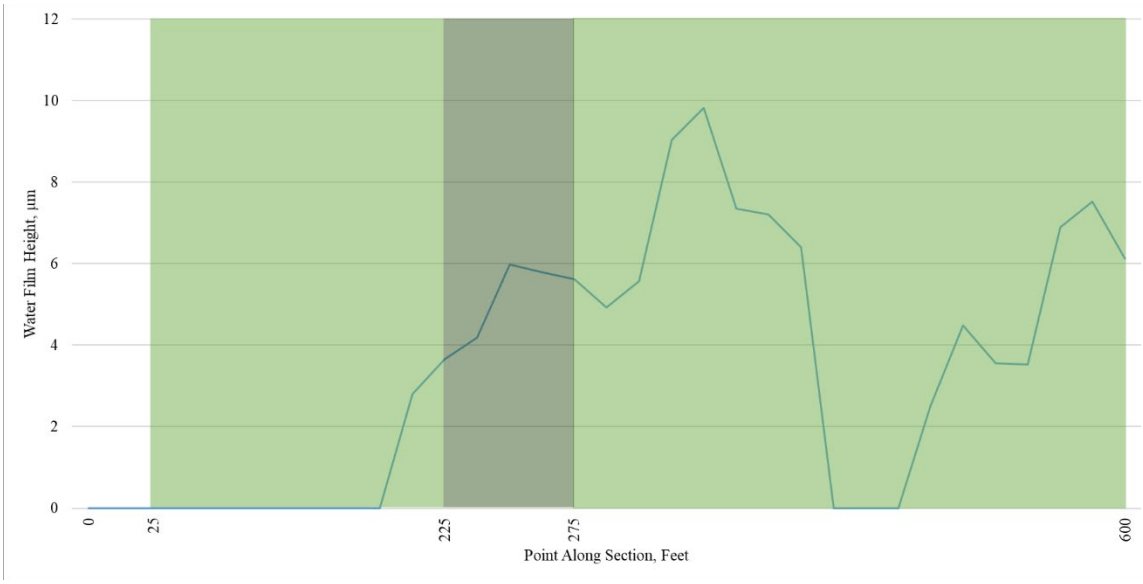


Measured moisture level - SR 327 (1) (NB) in Vinton County, Ohio

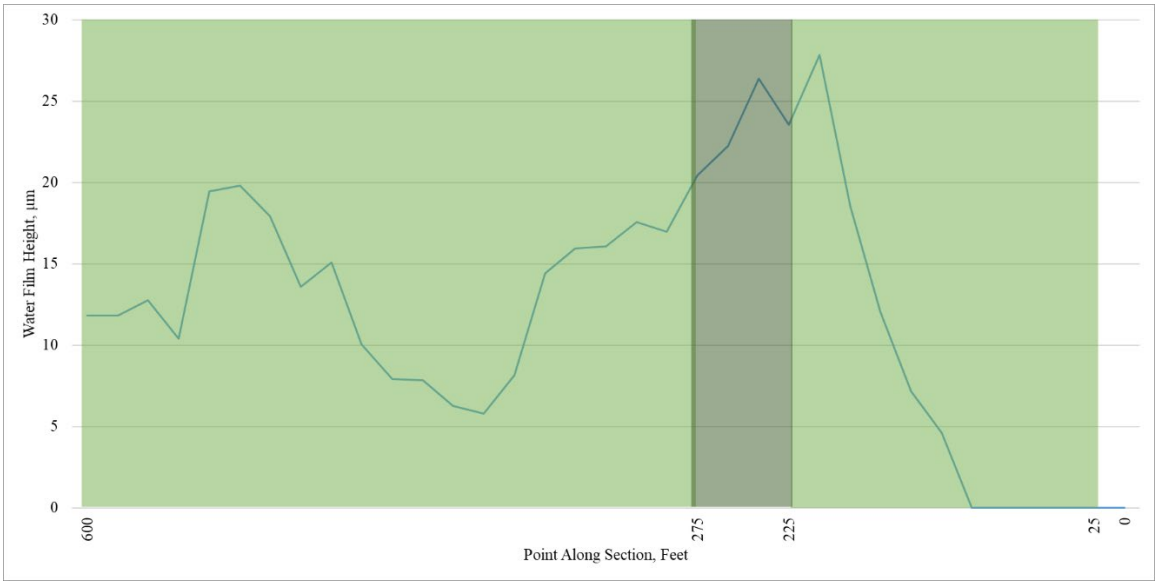


Measured moisture level - SR 327 (1) (SB) in Vinton County, Ohio

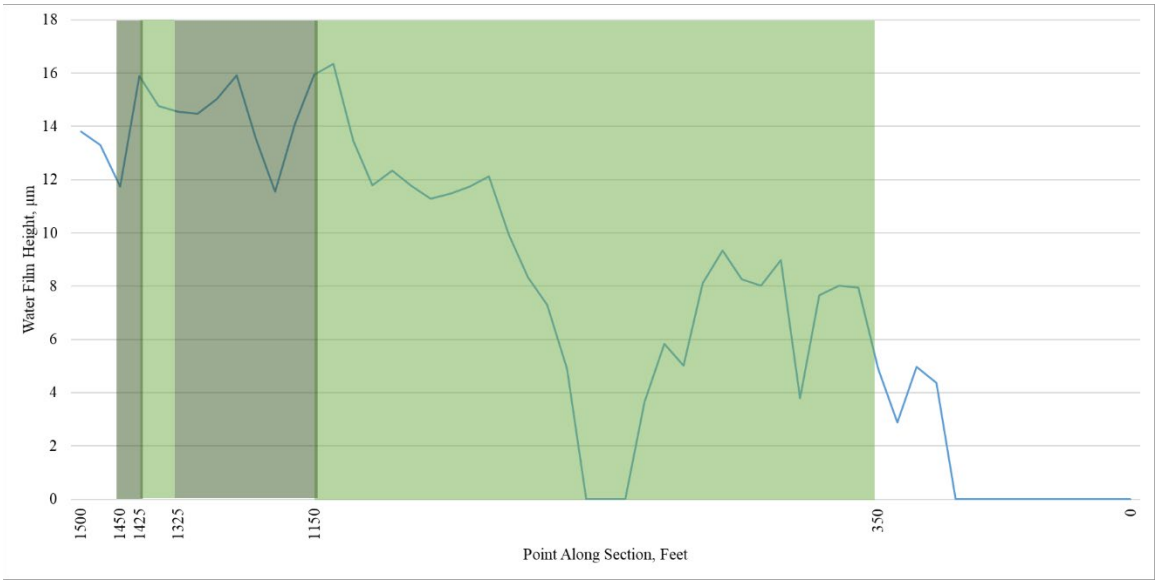

Measured moisture level - SR 327 (2) (NB) in Vinton County, Ohio

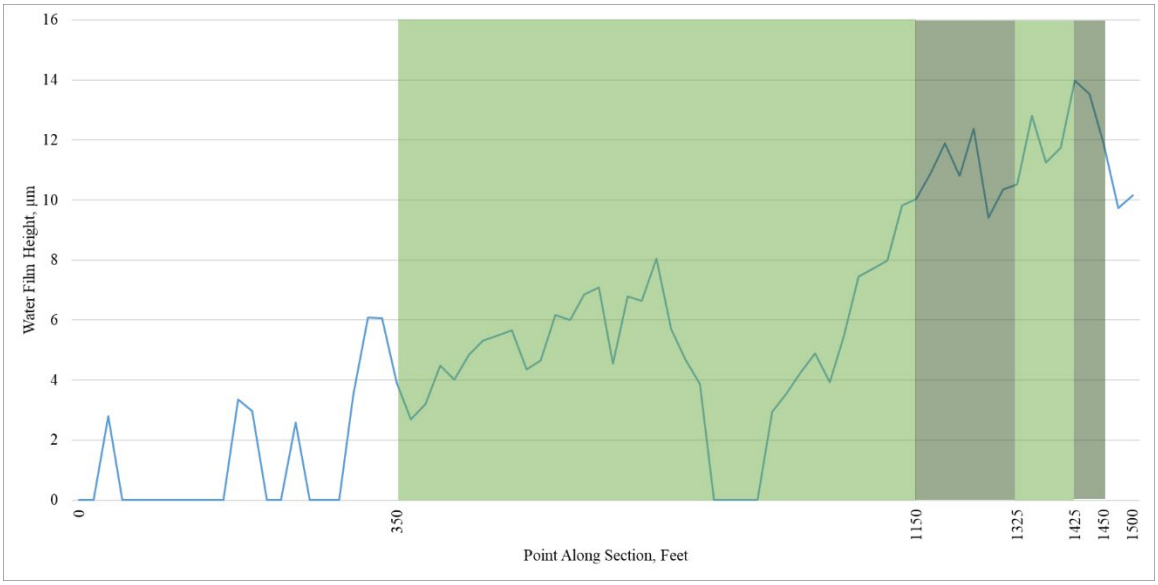

Measured moisture level - SR 327 (2) (SB) in Vinton County, Ohio

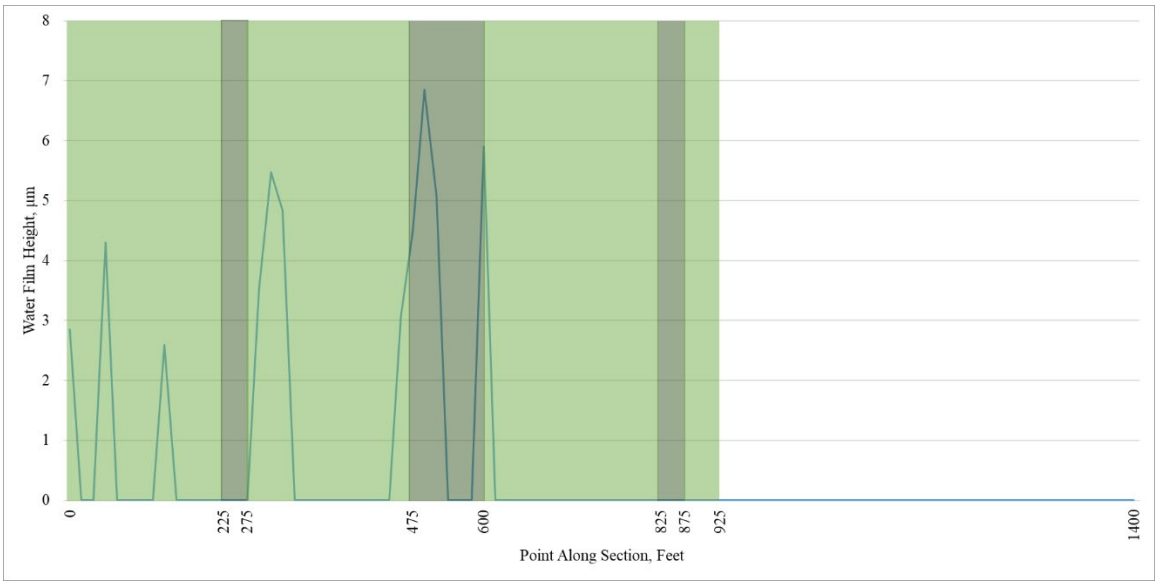

Measured moisture level - SR 356 (NB) in Vinton County

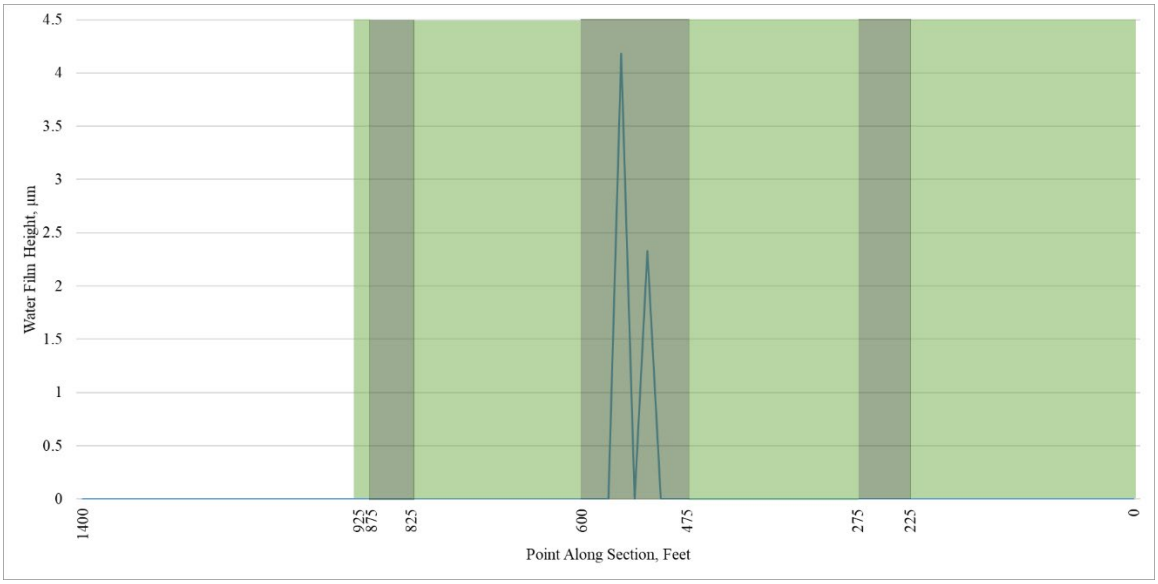

Measured moisture level - SR 356 (SB) in Vinton County, Ohio

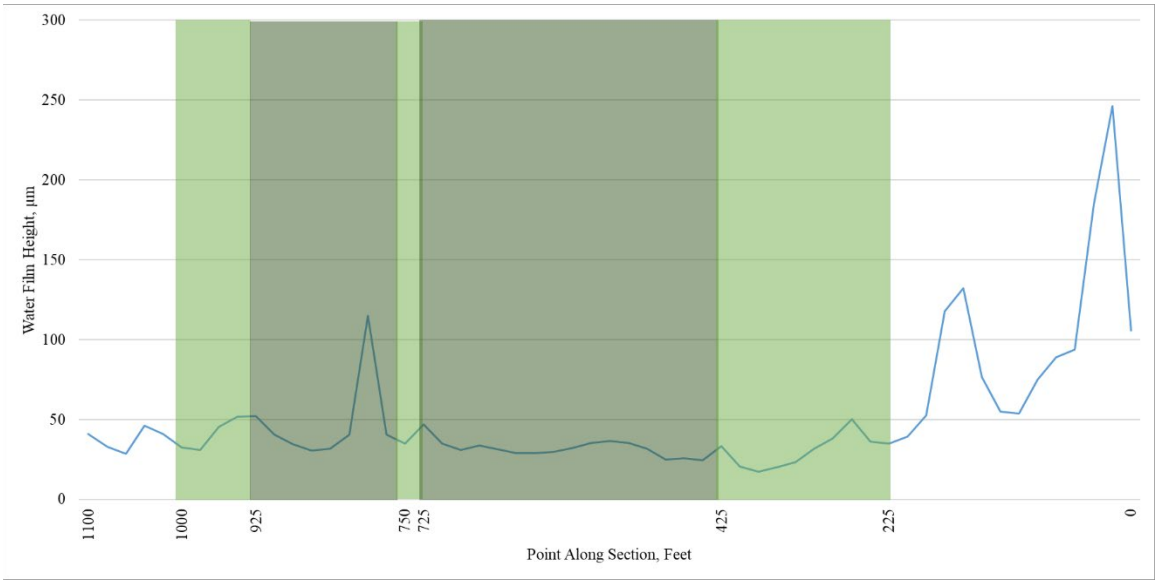

Measured moisture level - SR 260 (NB) in Washington County, Ohio

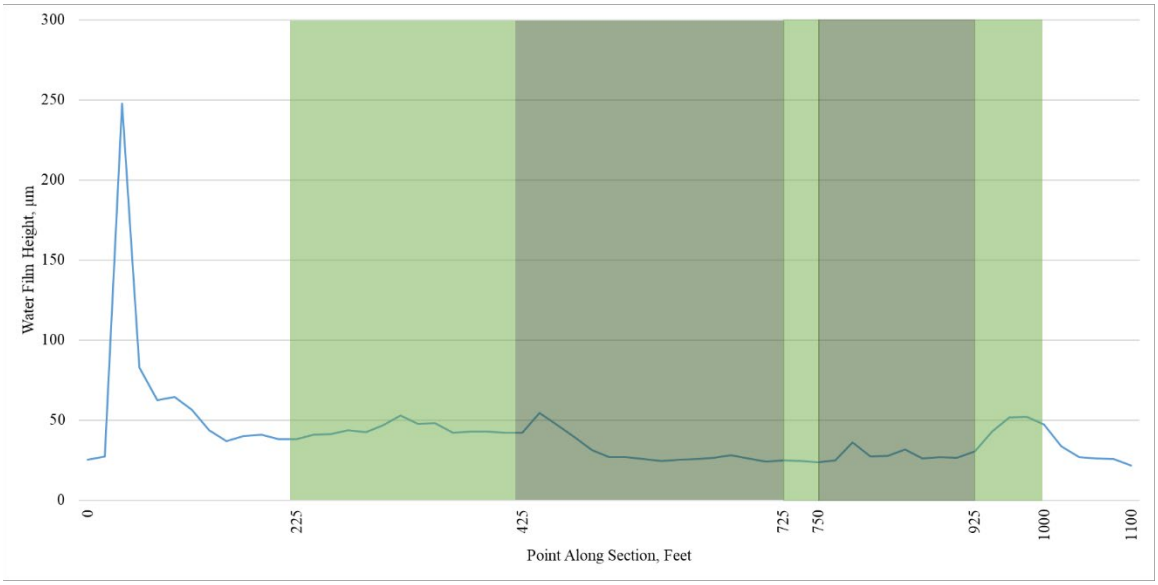

Measured moisture level - SR 260 (SB) in Washington County, Ohio

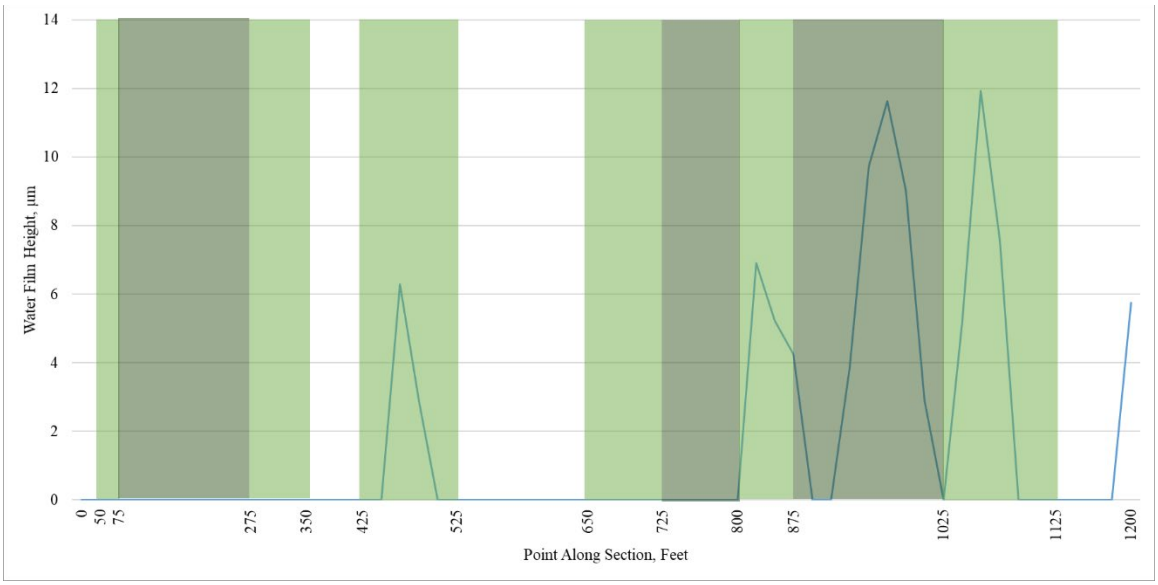

Measured moisture level - SR 555 (NB) in Washington County, Ohio

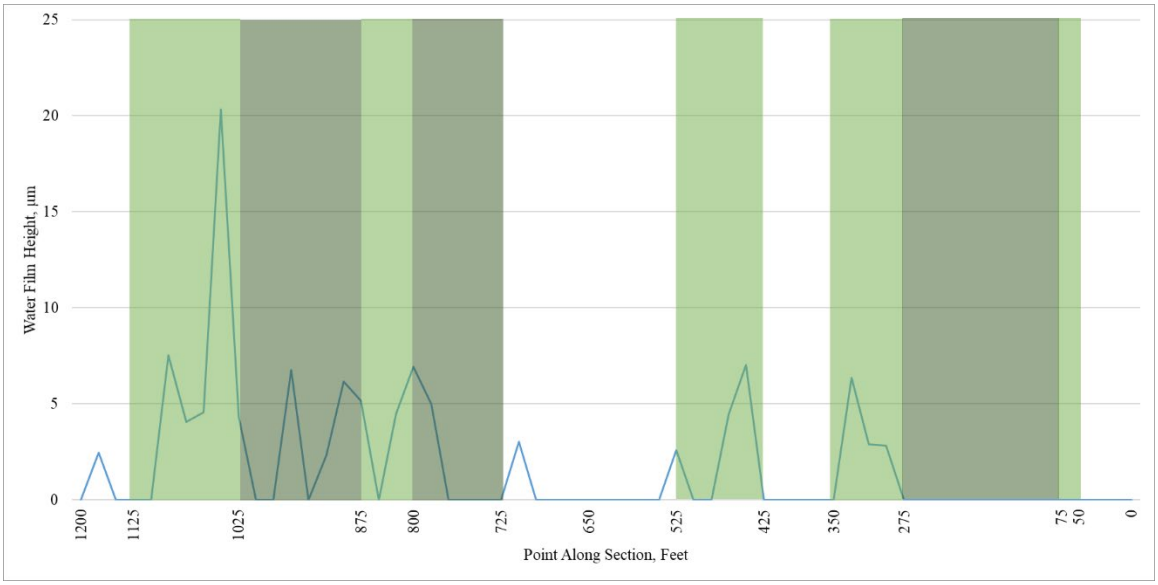

Measured moisture level - SR 555 (SB) in Washington County, Ohio

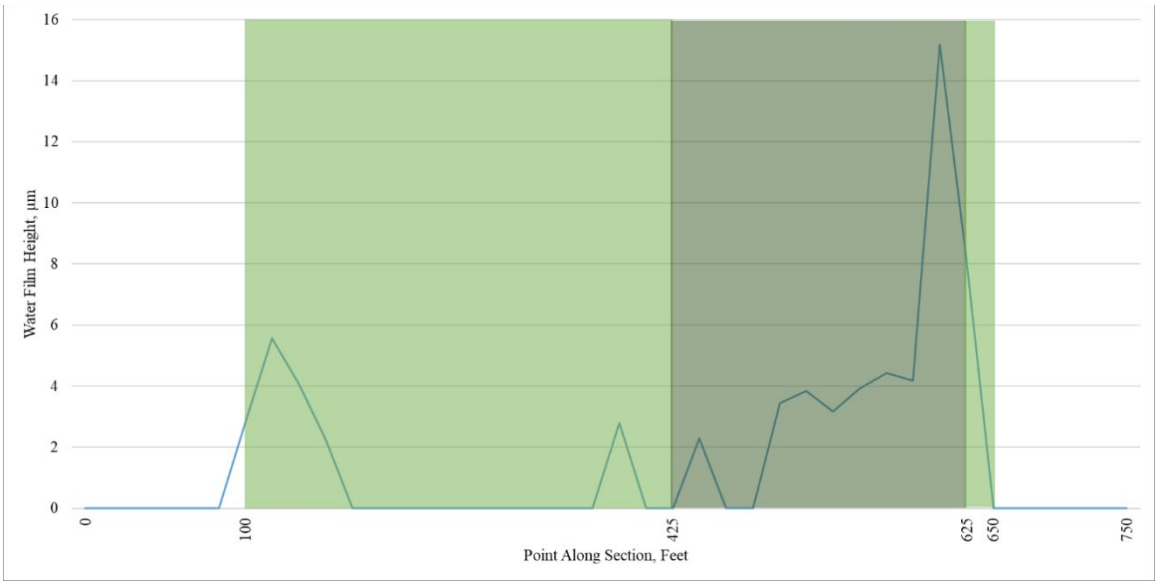

Measured moisture level - SR 676 (1) (EB) in Washington County, Ohio

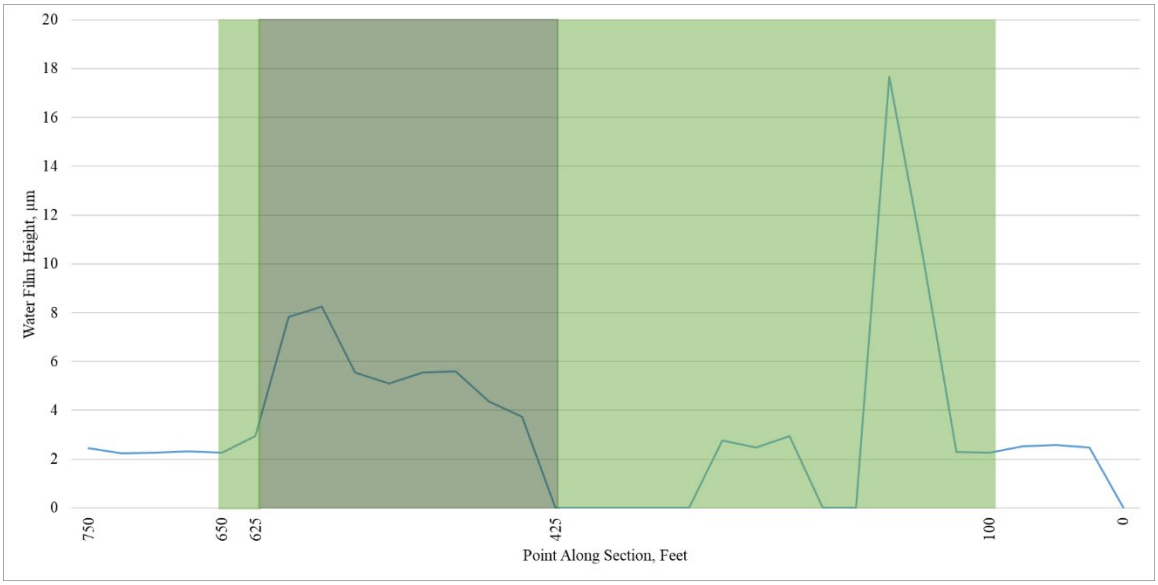

Measured moisture level - SR 676 (1) (WB) in Washington County, Ohio

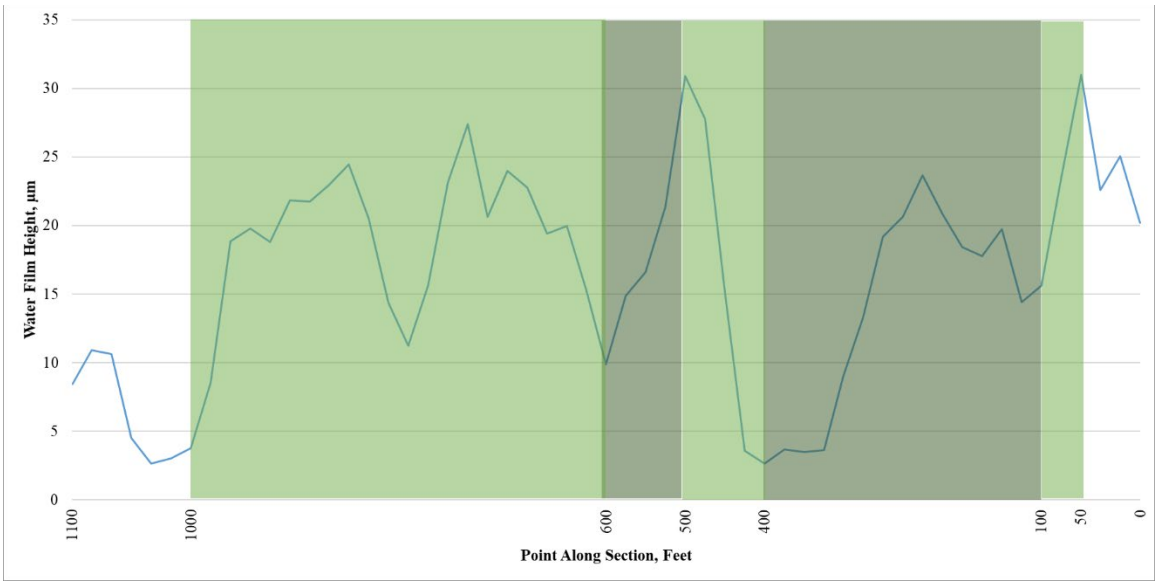

Measured moisture level - SR 676 (2) (EB) in Washington County, Ohio

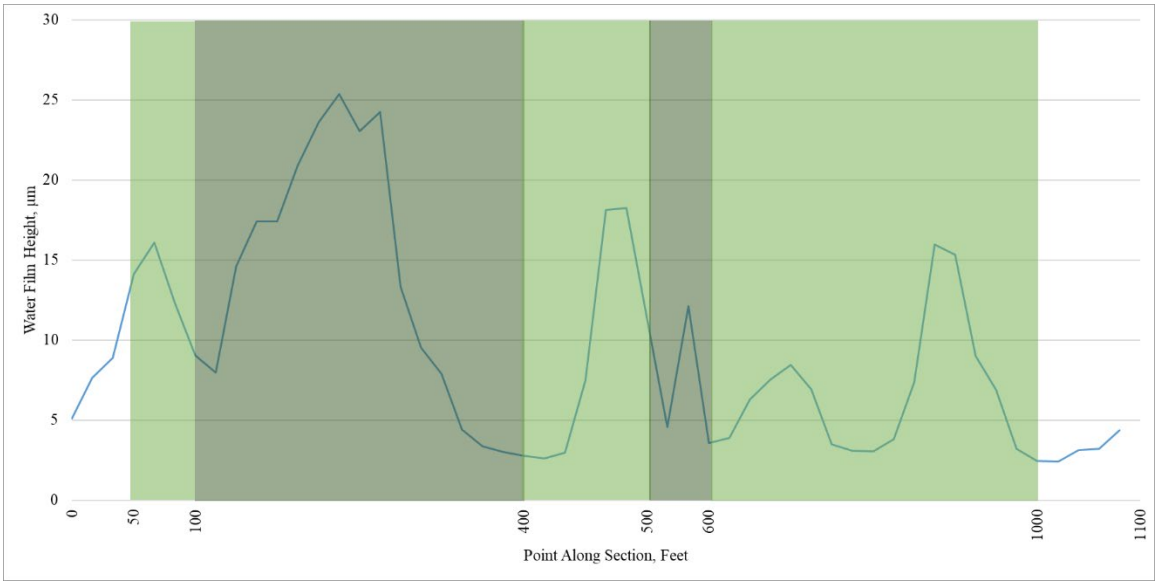

Measured moisture level - SR 676 (2) (WB) in Washington County, Ohio

## APPENDIX I: MARWIS PAVEMENT TEMPERATURE

- These graphs are listed in order by county name and state route (SR) number.
- White portions indicate densiometer measurements of tree coverage 0-25% (no canopy); light green portions indicate coverage 25-75% (partial canopy); dark green portions indicate coverage 75-100% (full canopy)
- Horizontal axis indicates distance in feet along road section (1 ft = 0.305 m)
- Vertical axis indicates surface temperature in degrees F (68°F = 20°C; 113°F = 45°C)

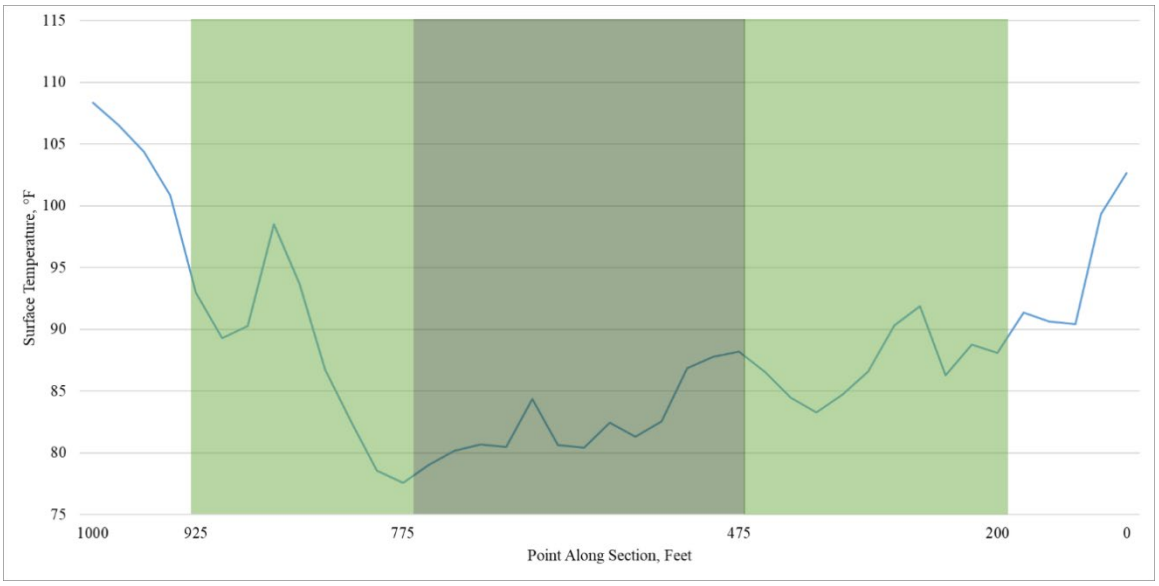


Surface temperature levels measured by MARWIS – SR 13 (NB) in Athens County, Ohio

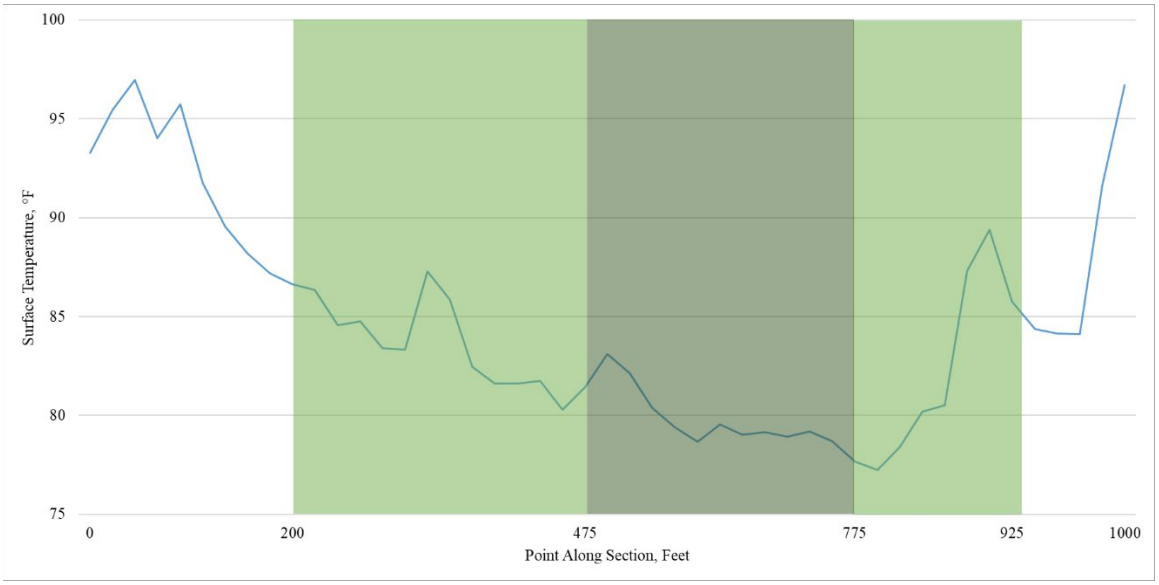


Surface temperature levels measured by MARWIS – SR 13 (SB) in Athens County, Ohio

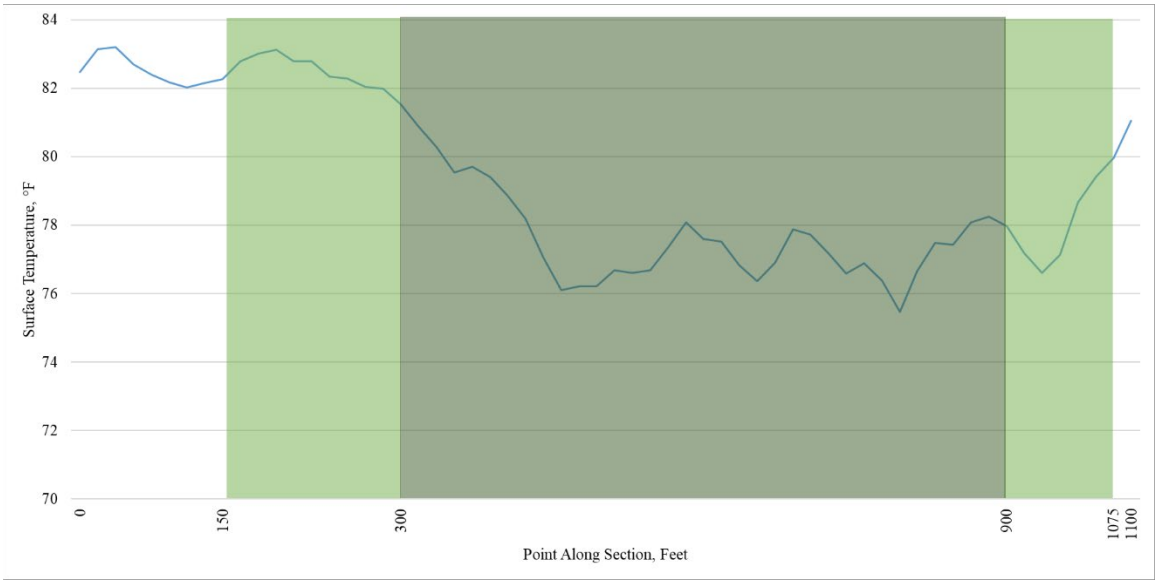

Surface temperature levels measured by MARWIS – SR 258 (2) (NB) in Harrison County, Ohio

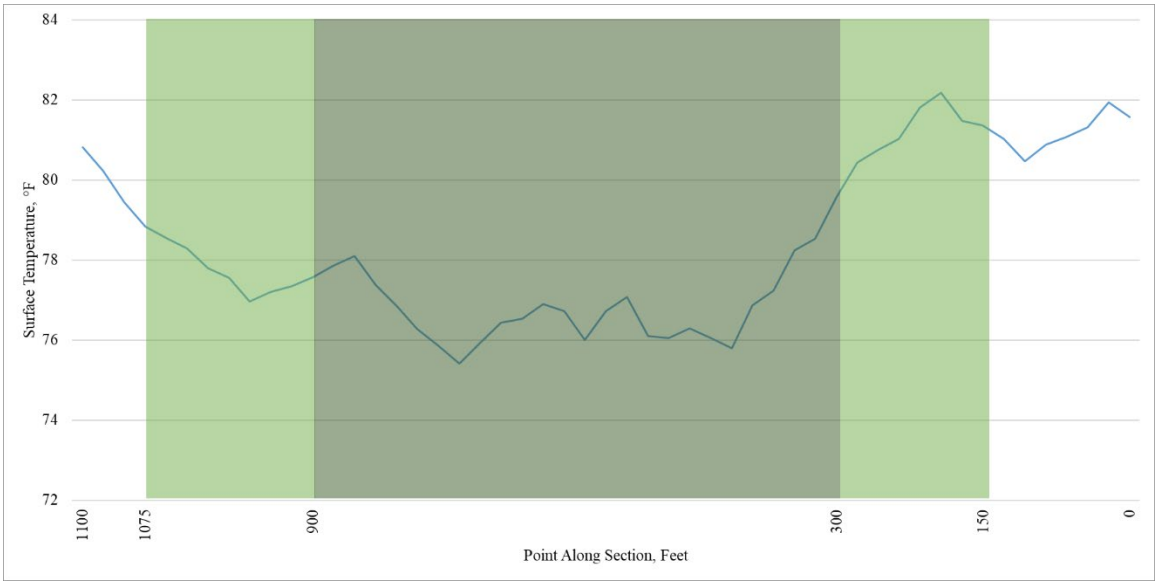

Surface temperature levels measured by MARWIS – SR 258 (2) (SB) in Harrison County, Ohio

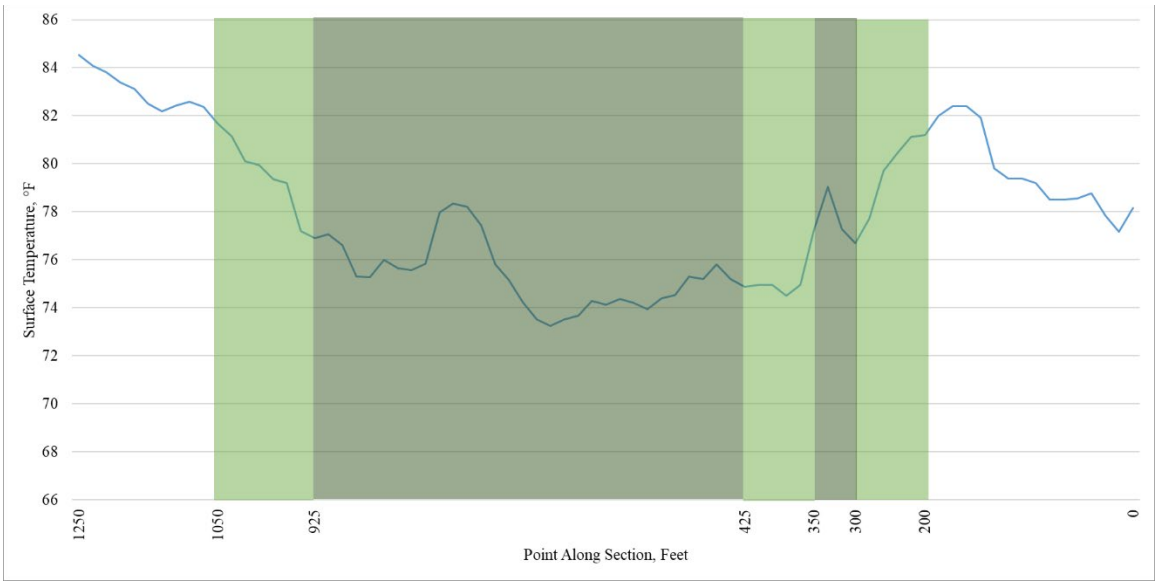

Surface temperature levels measured by MARWIS – SR 56 (EB) in Hocking County, Ohio

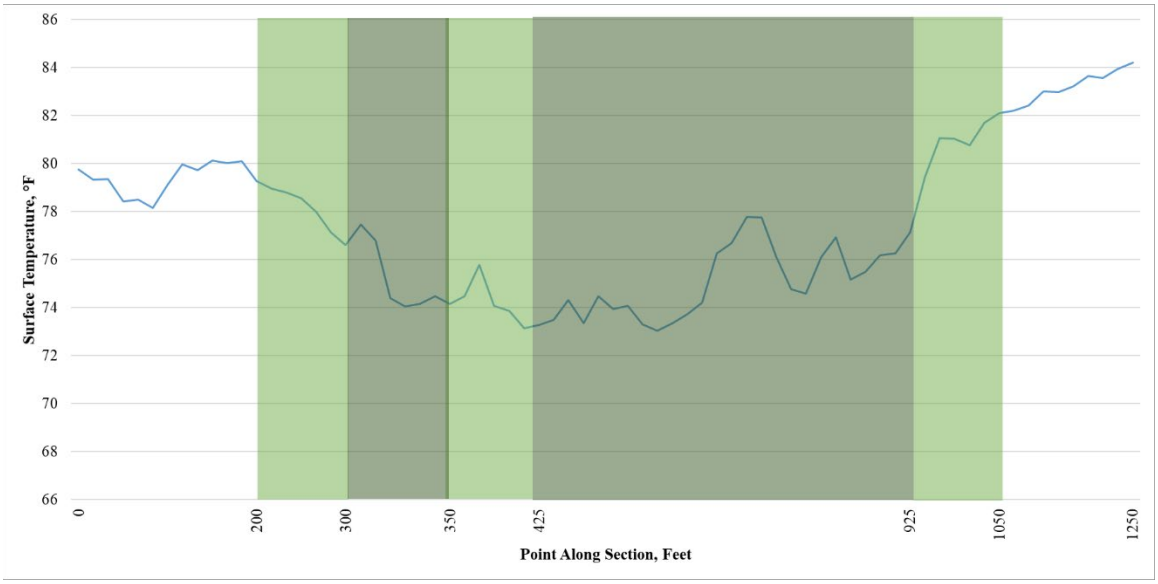

Surface temperature levels measured by MARWIS – SR 56 (WB) in Hocking County, Ohio

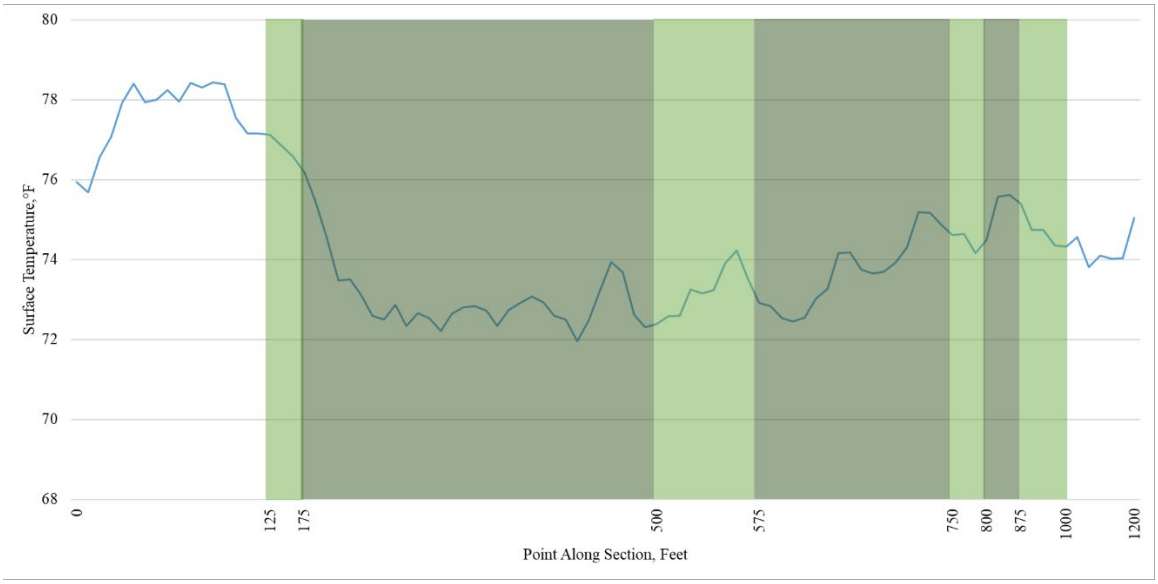

Surface temperature levels measured by MARWIS – SR 374 (1) (NB) in Hocking County, Ohio

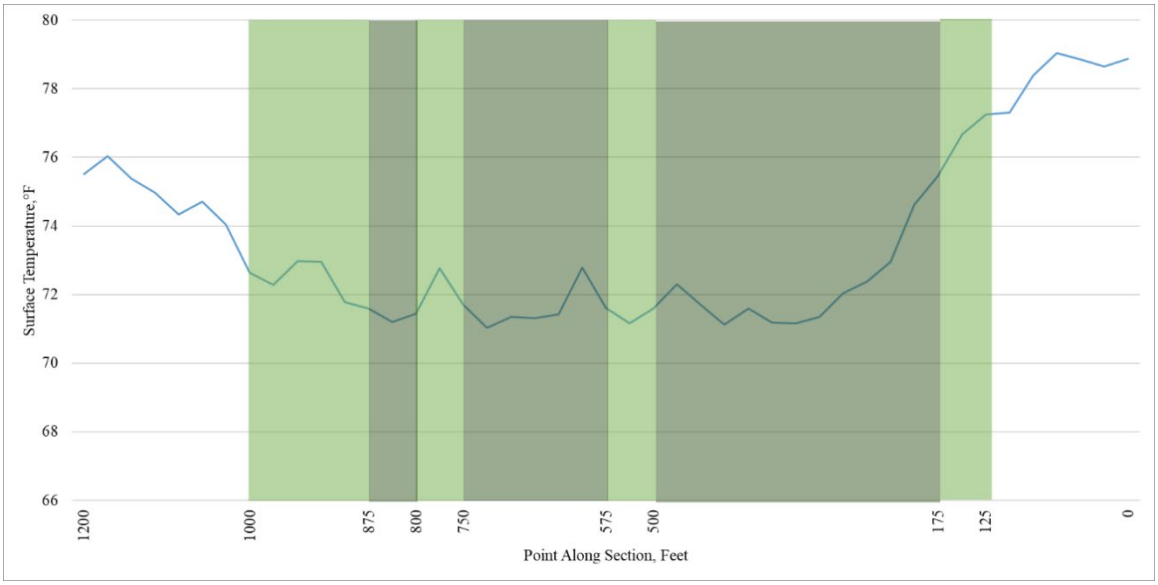

Surface temperature levels measured by MARWIS – SR 374 (1) (SB) in Hocking County, Ohio

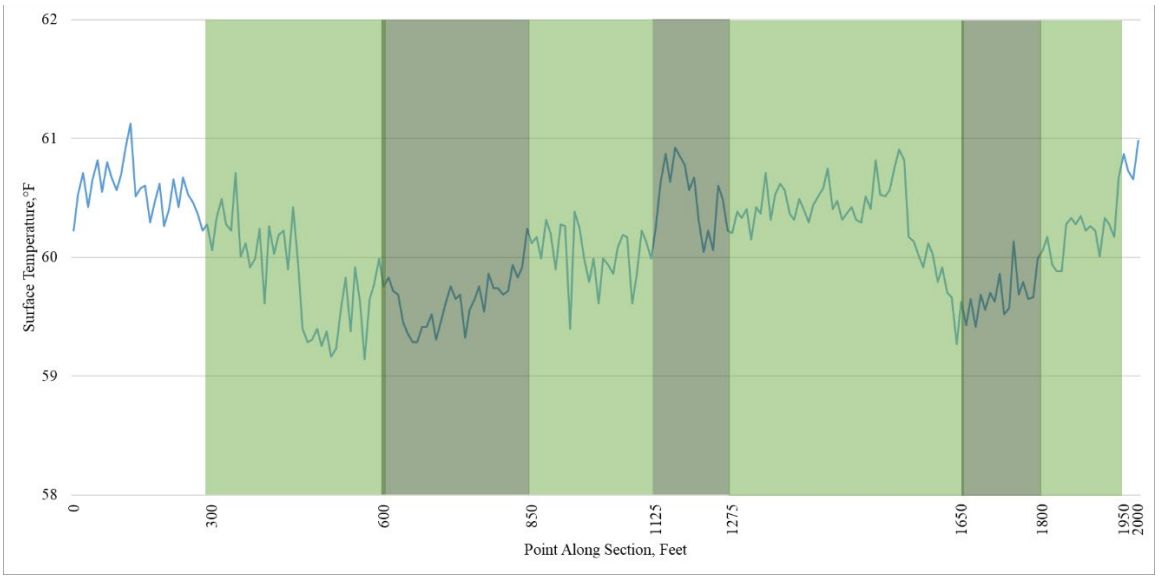

Surface temperature levels measured by MARWIS – SR 374 (2) (NB) in Hocking County, Ohio

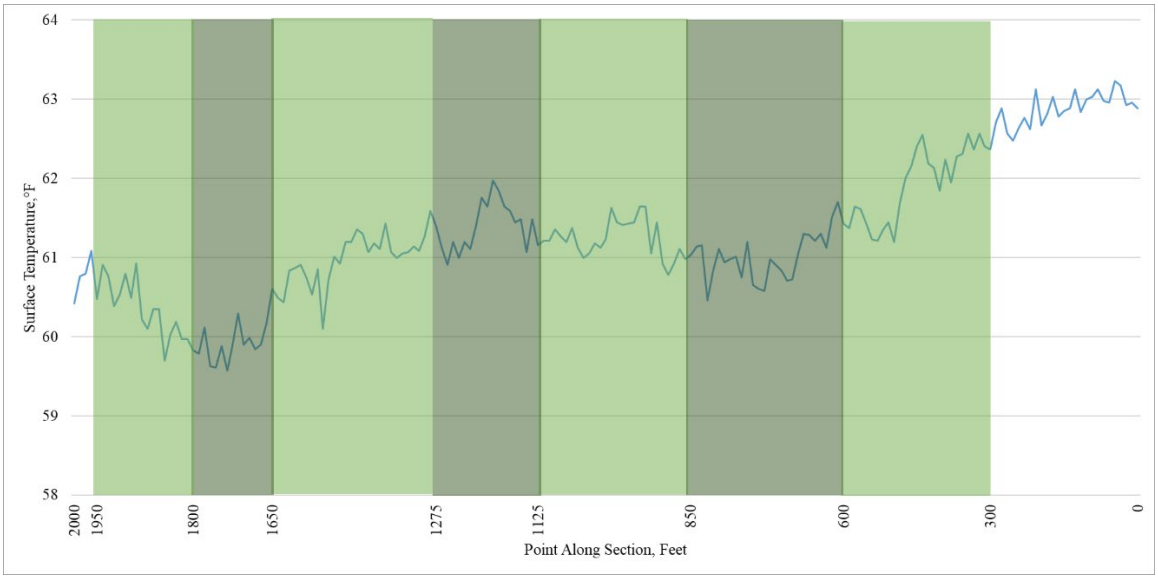

Surface temperature levels measured by MARWIS – SR 374 (2) (SB) in Hocking County, Ohio

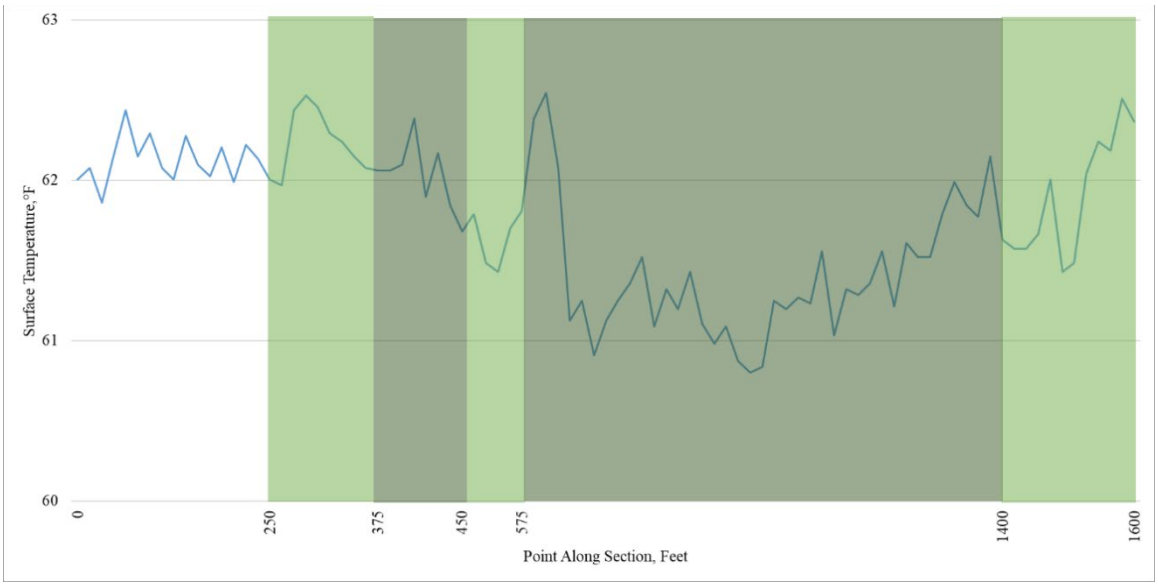

Surface temperature levels measured by MARWIS – SR 374 (3) (NB) in Hocking County, Ohio

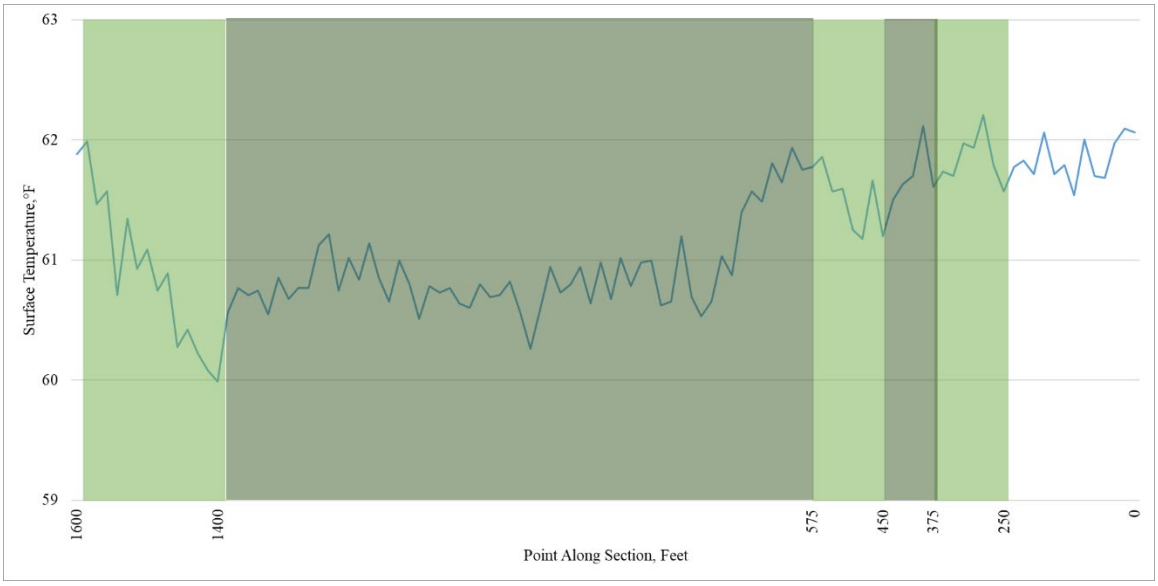

Surface temperature levels measured by MARWIS – SR 374 (3) (SB) in Hocking County, Ohio

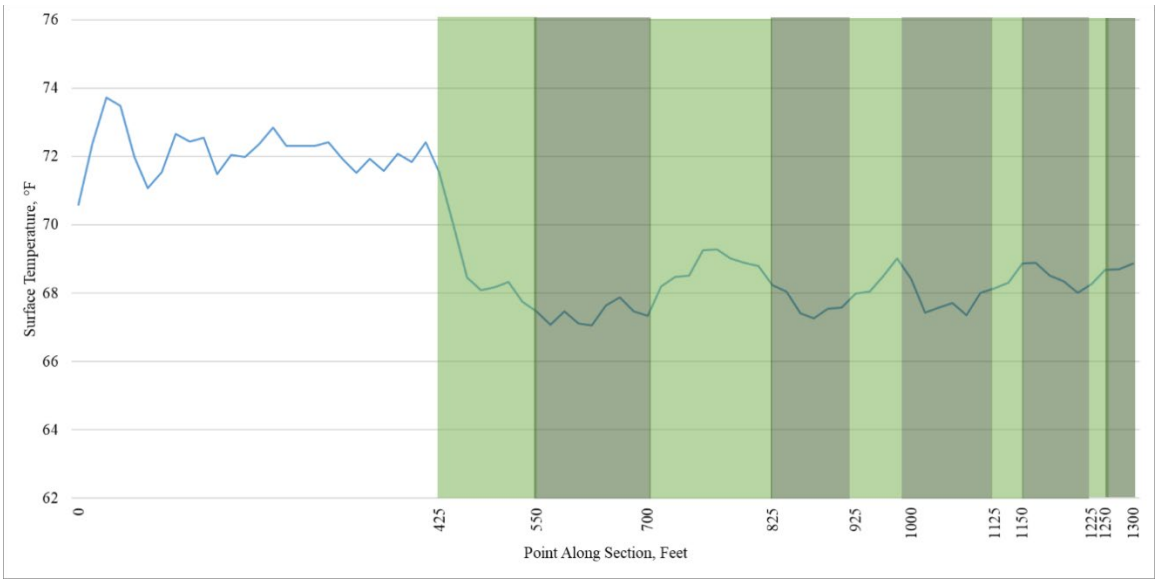

Surface temperature levels measured by MARWIS – SR 124 (1) (EB) in Jackson County, Ohio

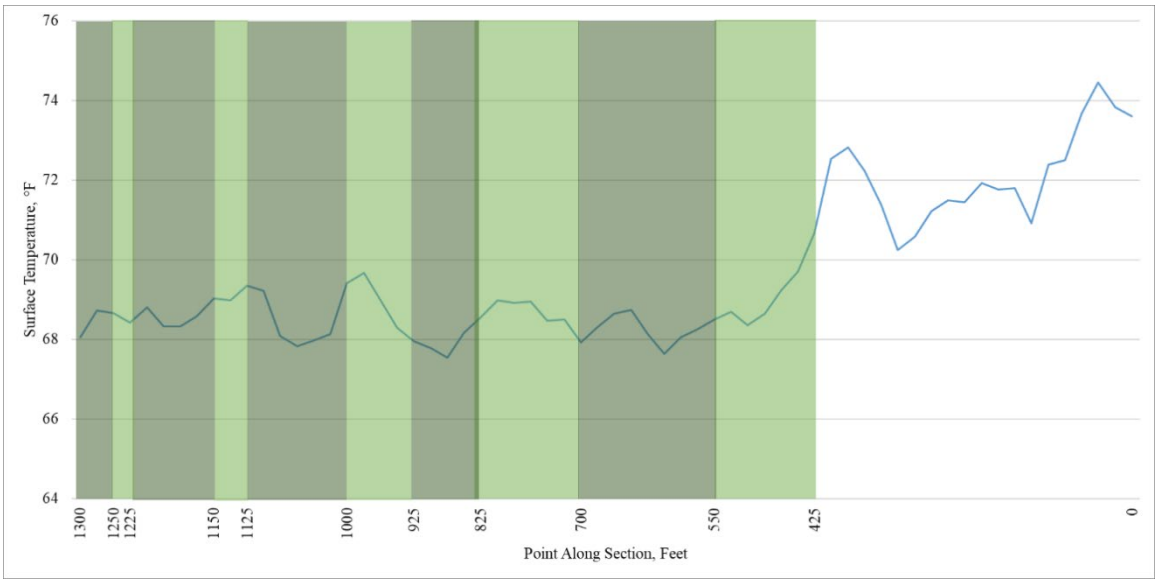

Surface temperature levels measured by MARWIS – SR 124 (1) (WB) in Jackson County, Ohio

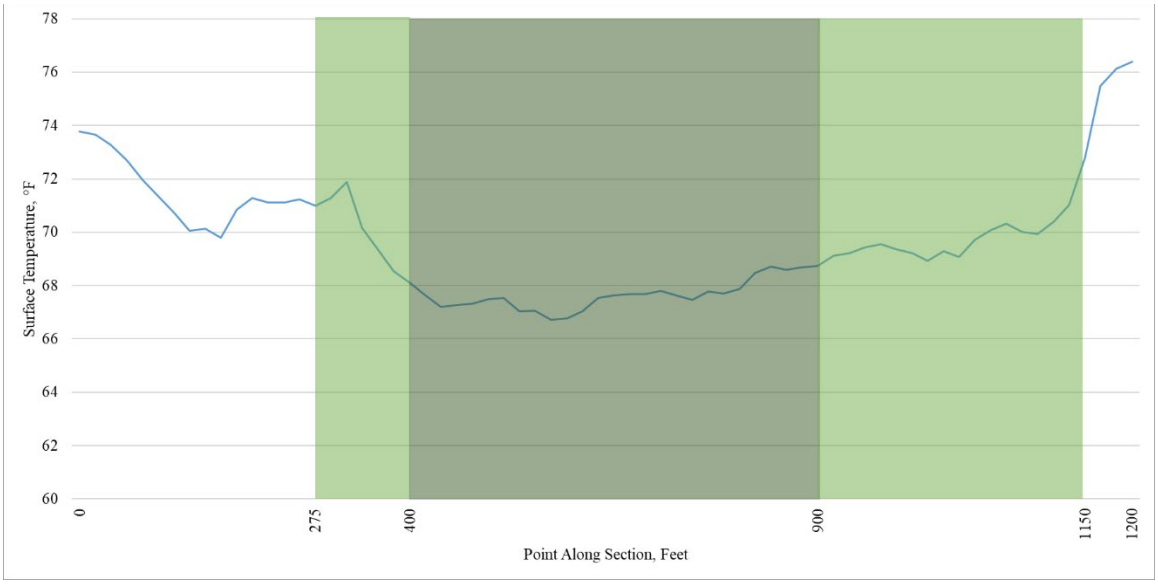

Surface temperature levels measured by MARWIS – SR 124 (2) (EB) in Jackson County, Ohio

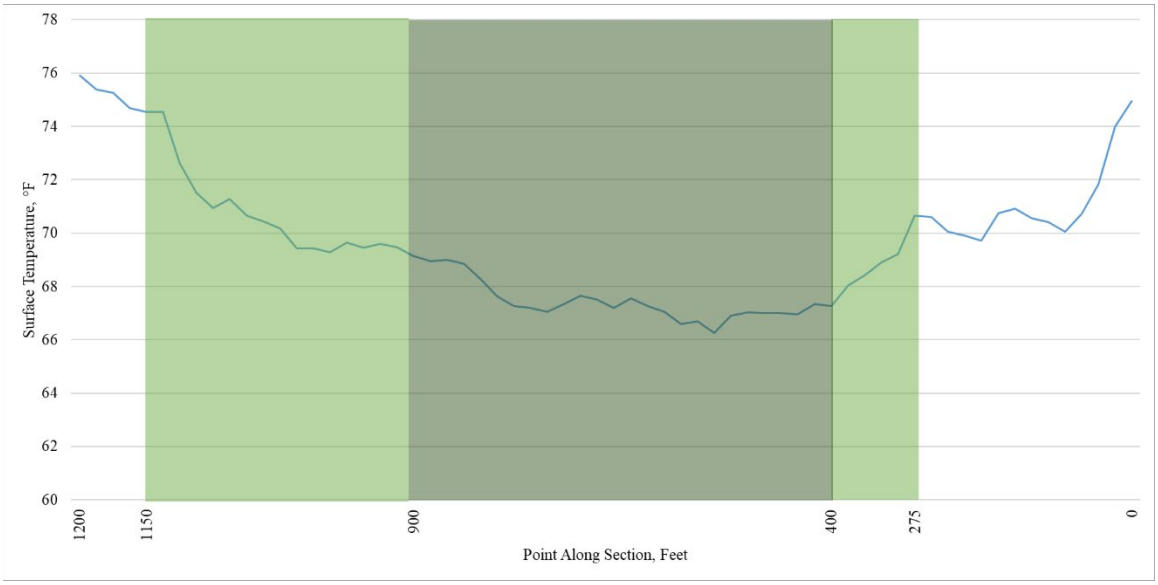

Surface temperature levels measured by MARWIS – SR 124 (2) (WB) in Jackson County, Ohio

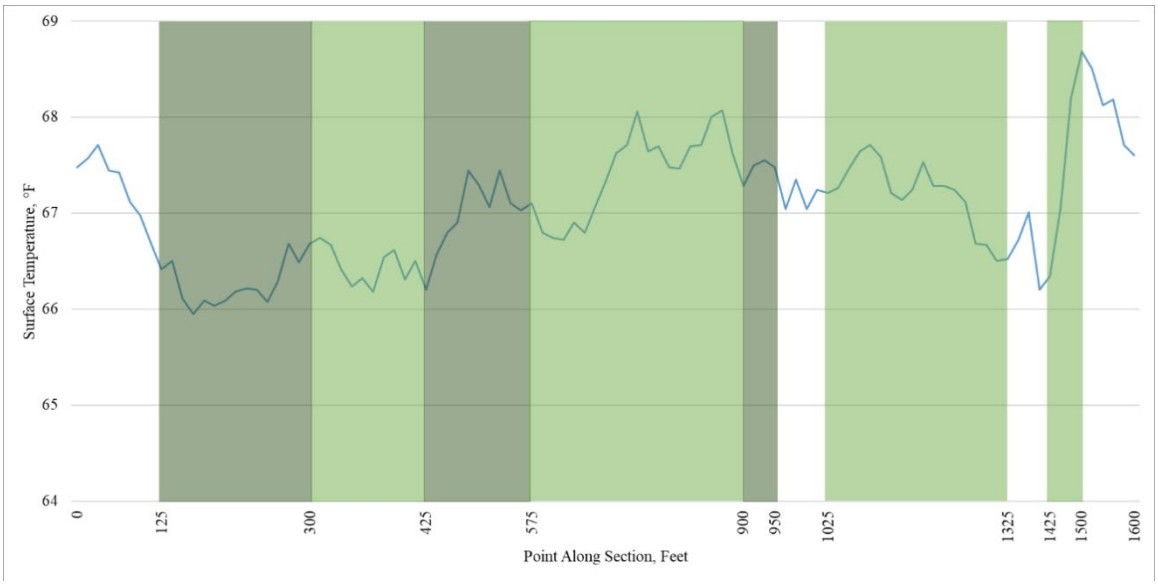

Surface temperature levels measured by MARWIS – SR 335 (1) (EB) in Pike County, Ohio

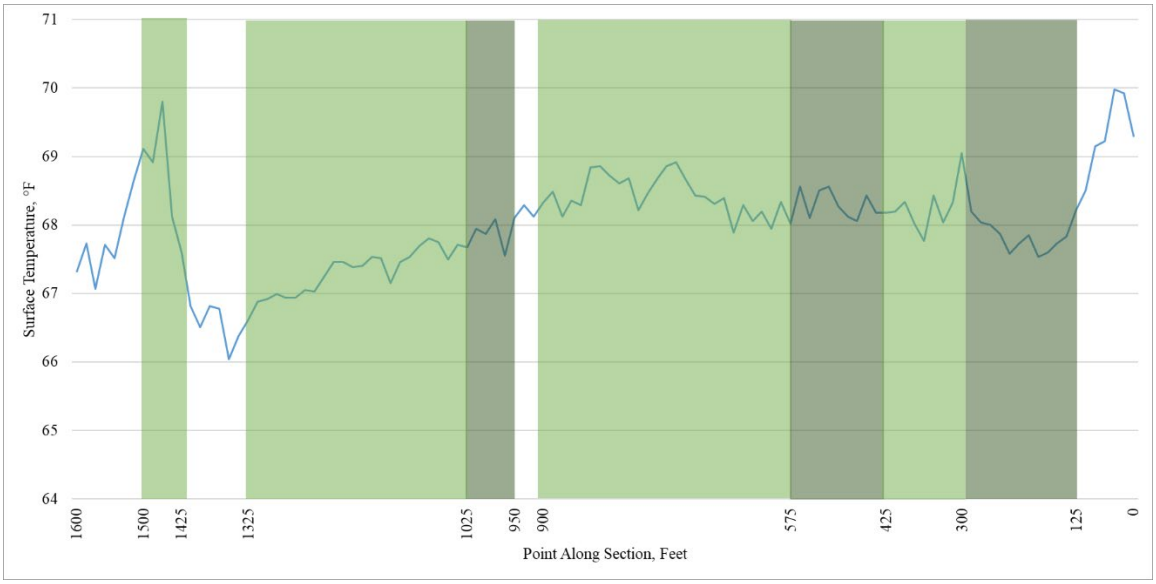

Surface temperature levels measured by MARWIS – SR 335 (1) (WB) in Pike County, Ohio

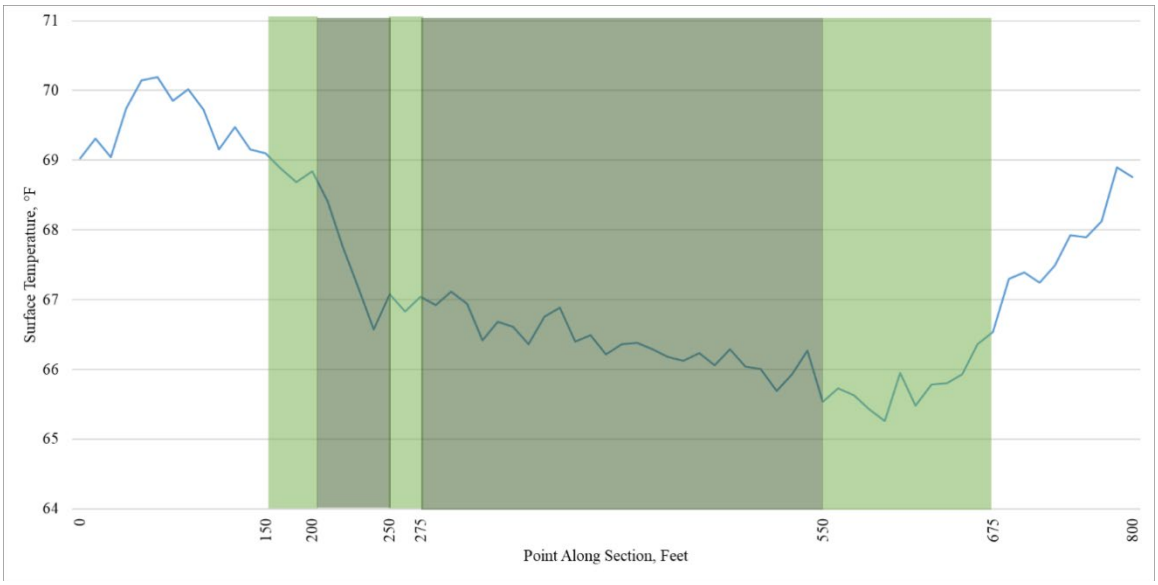

Surface temperature levels measured by MARWIS – SR 335 (2) (NB) in Pike County, Ohio

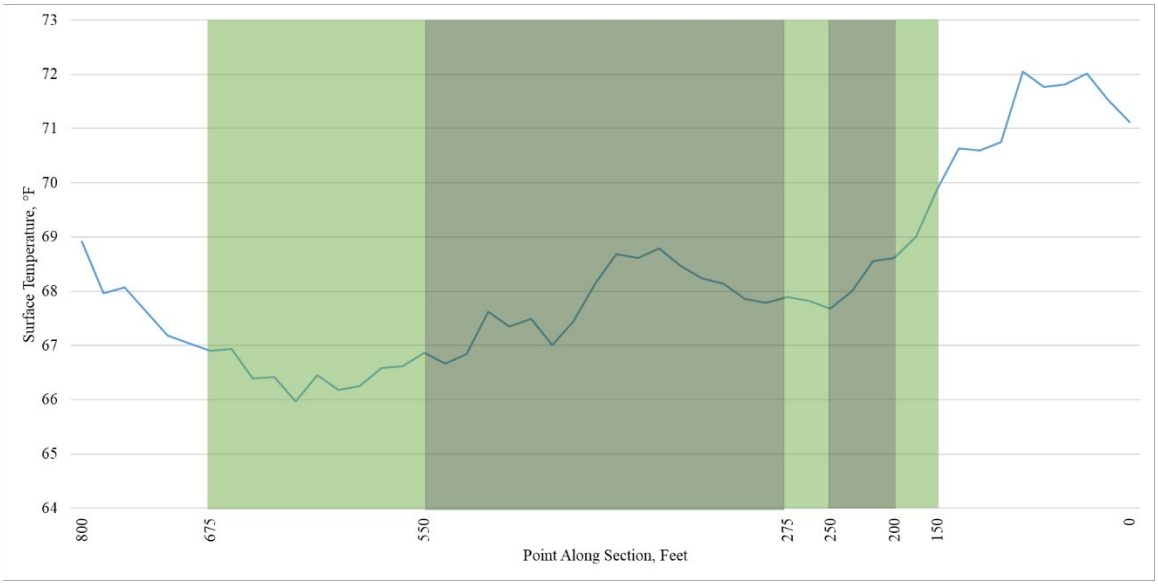

Surface temperature levels measured by MARWIS – SR 335 (2) (SB) in Pike County, Ohio

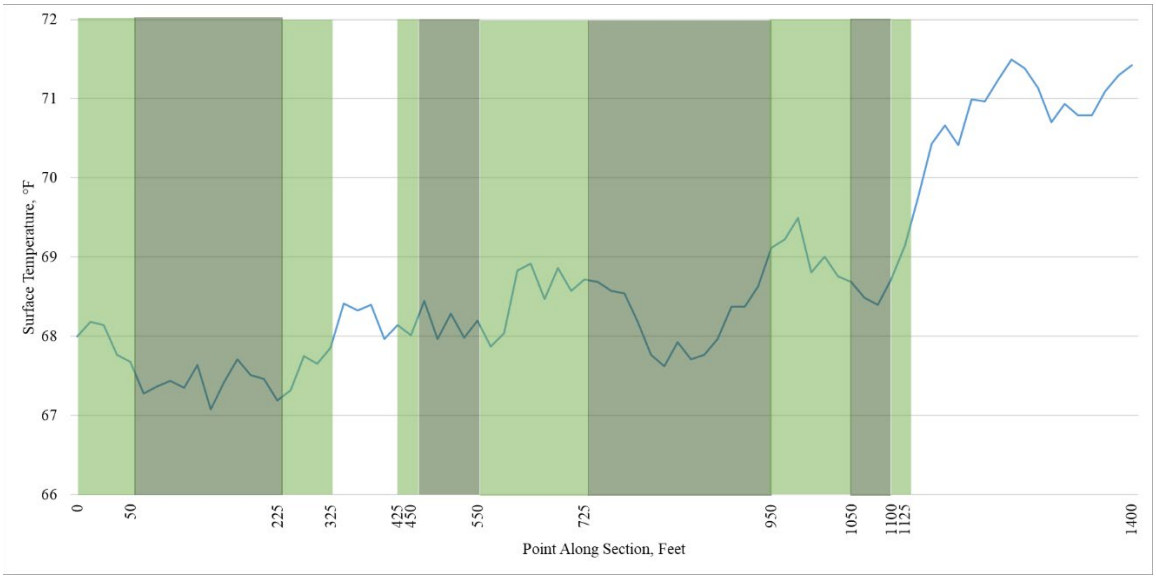

Surface temperature levels measured by MARWIS – SR 139 (EB) in Scioto County, Ohio

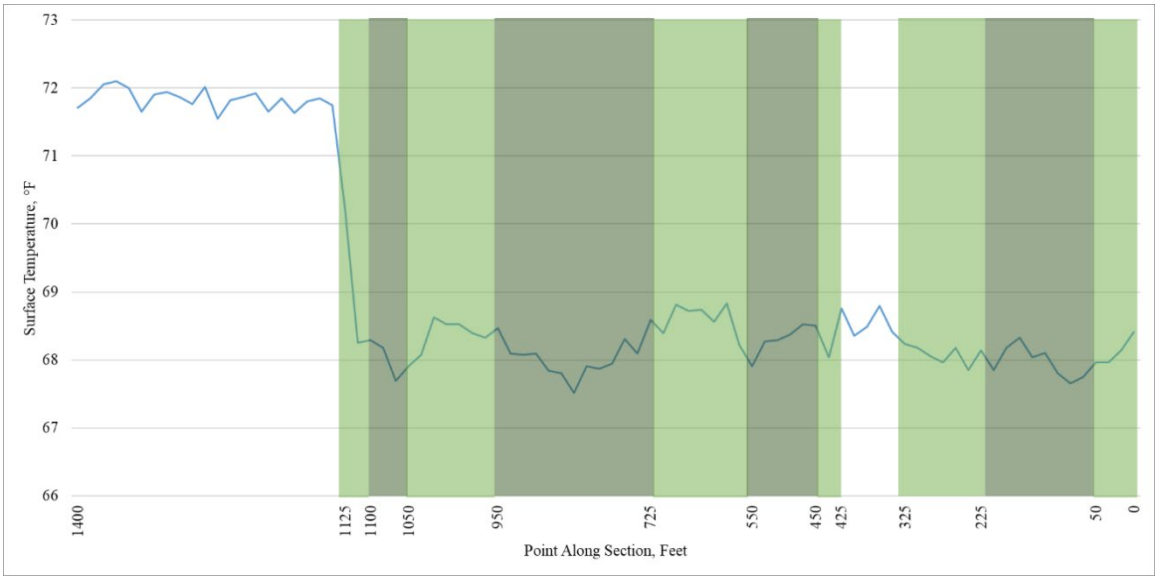

Surface temperature levels measured by MARWIS – SR 139 (WB) in Scioto County, Ohio

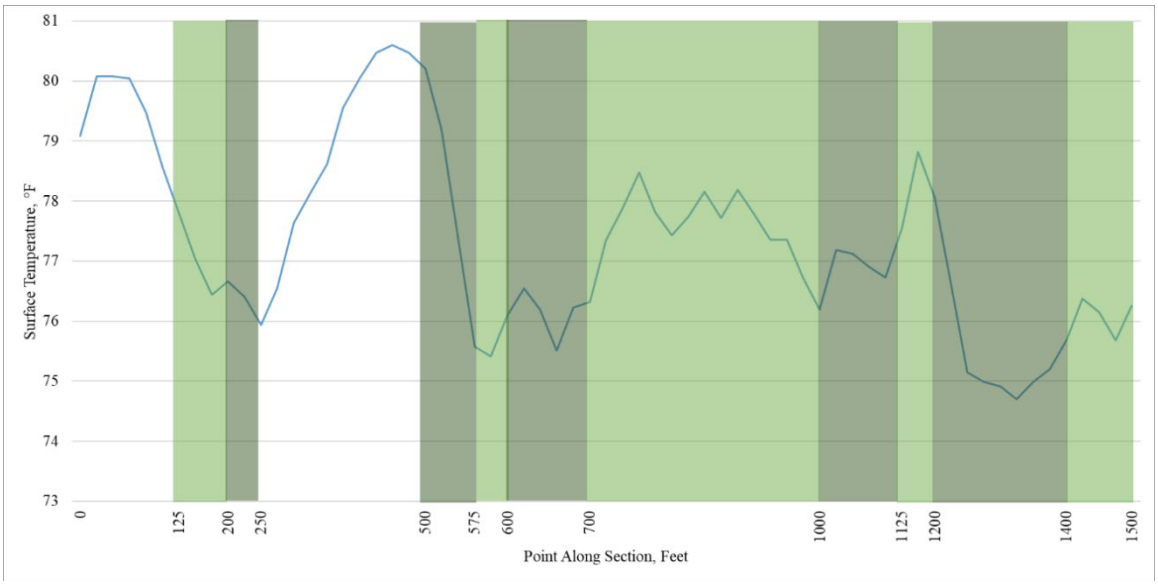


Surface temperature levels measured by MARWIS – SR 800 (1) (NB) in Tuscarawas County, Ohio


Surface temperature levels measured by MARWIS – SR 800 (1) (SB) in Tuscarawas County, Ohio

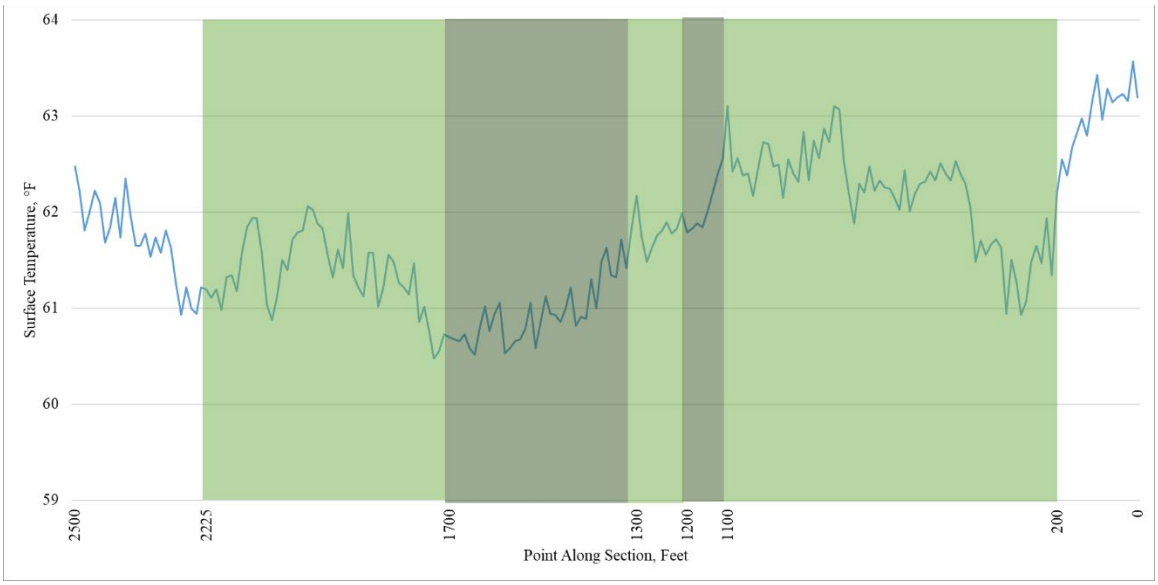

Surface temperature levels measured by MARWIS – SR 56 (EB) in Vinton County, Ohio

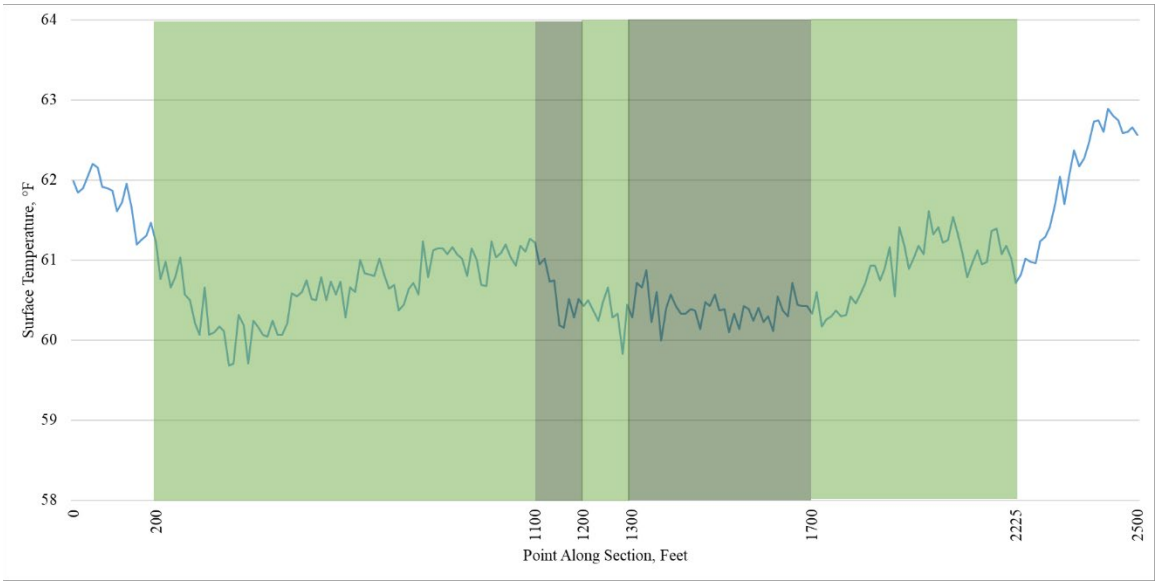

Surface temperature levels measured by MARWIS – SR 56 (WB) in Vinton County, Ohio

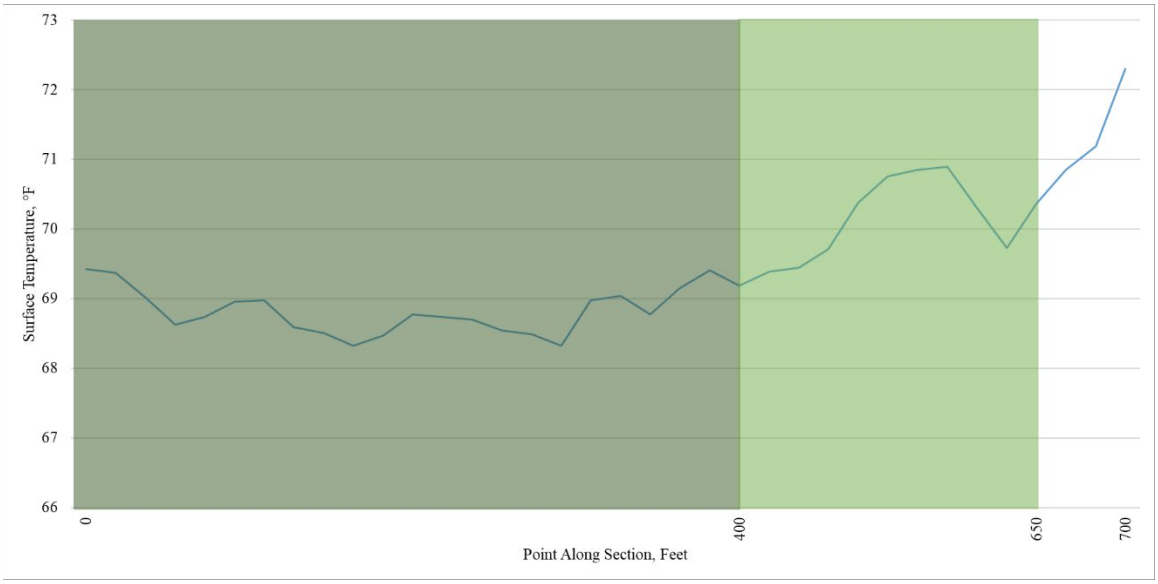

Surface temperature levels measured by MARWIS – SR 124 (EB) in Vinton County, Ohio

Surface temperature levels measured by MARWIS – SR 124 (EB) in Vinton County, Ohio

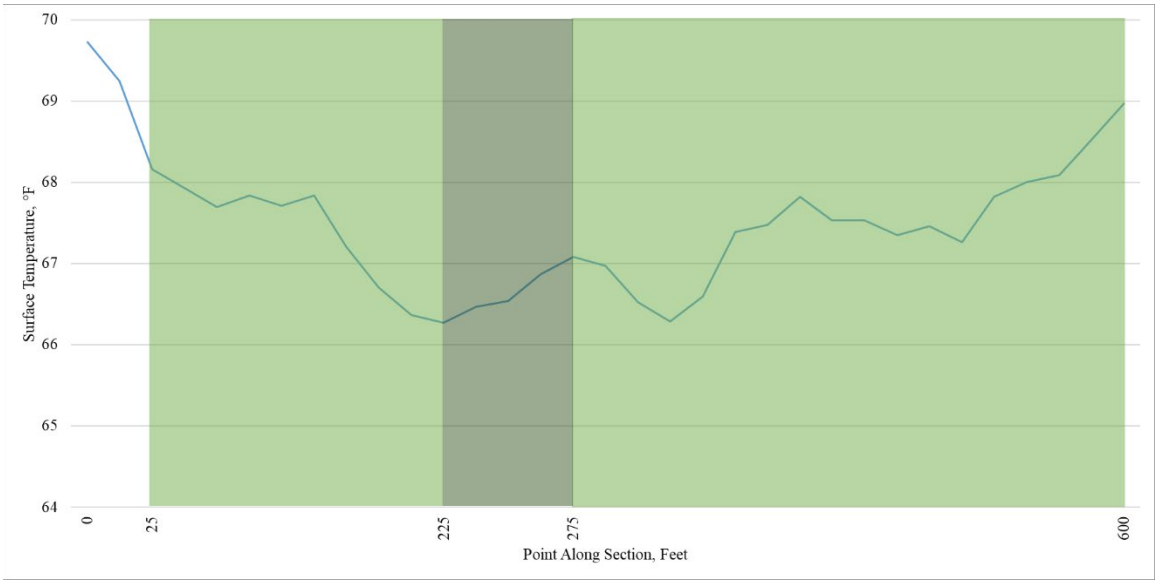

Surface temperature levels measured by MARWIS – SR 327 (1) (NB) in Vinton County, Ohio

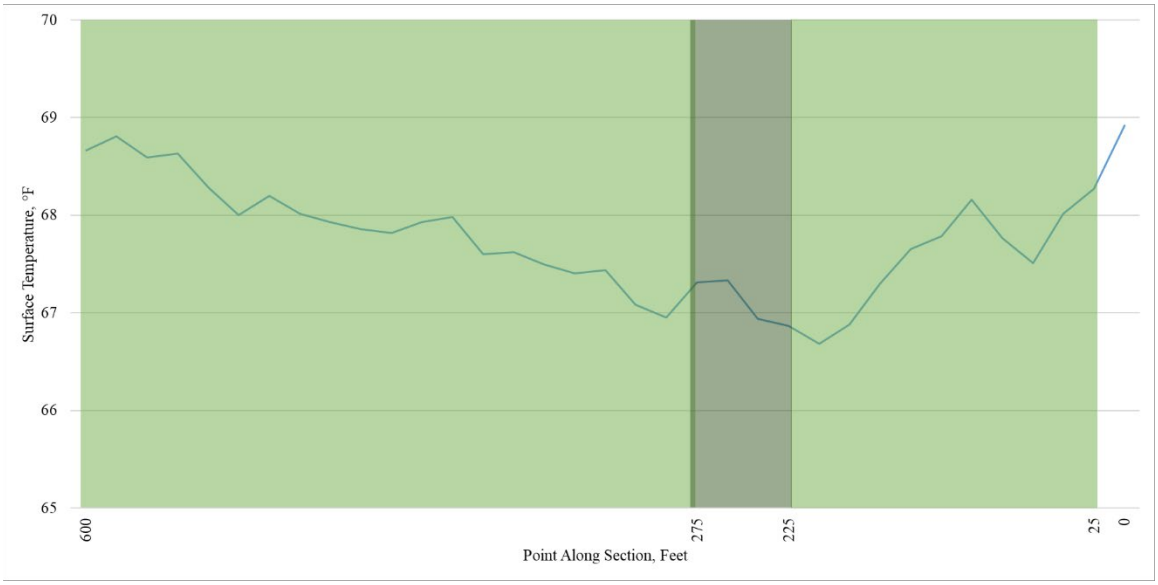

Surface temperature levels measured by MARWIS – SR 327 (1) (SB) in Vinton County, Ohio

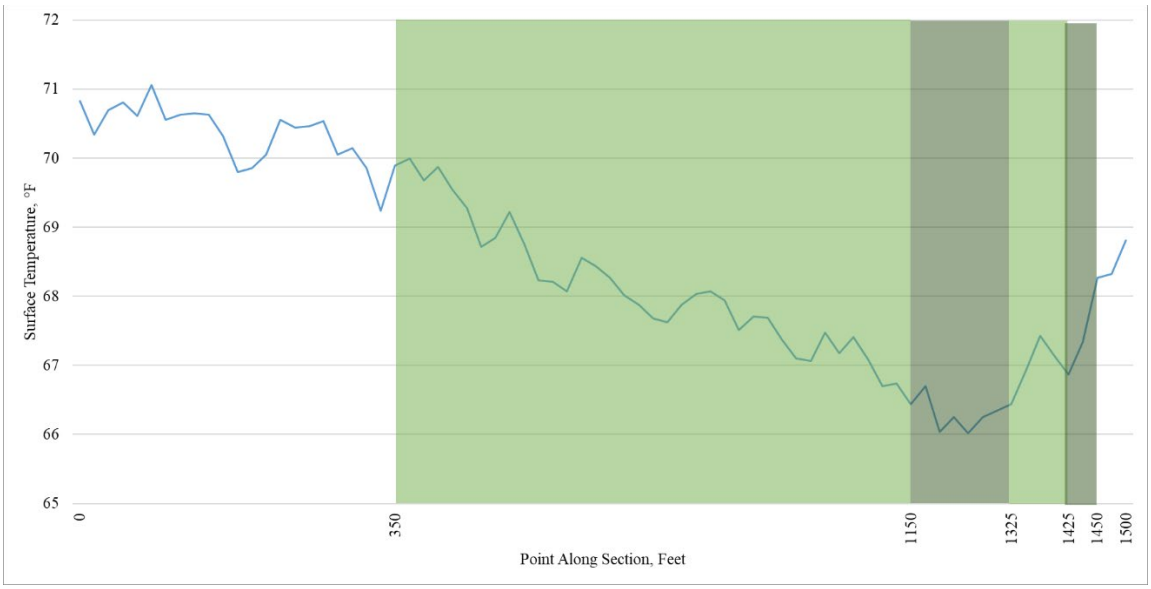

Surface temperature levels measured by MARWIS – SR 327 (2) (NB) in Vinton County, Ohio

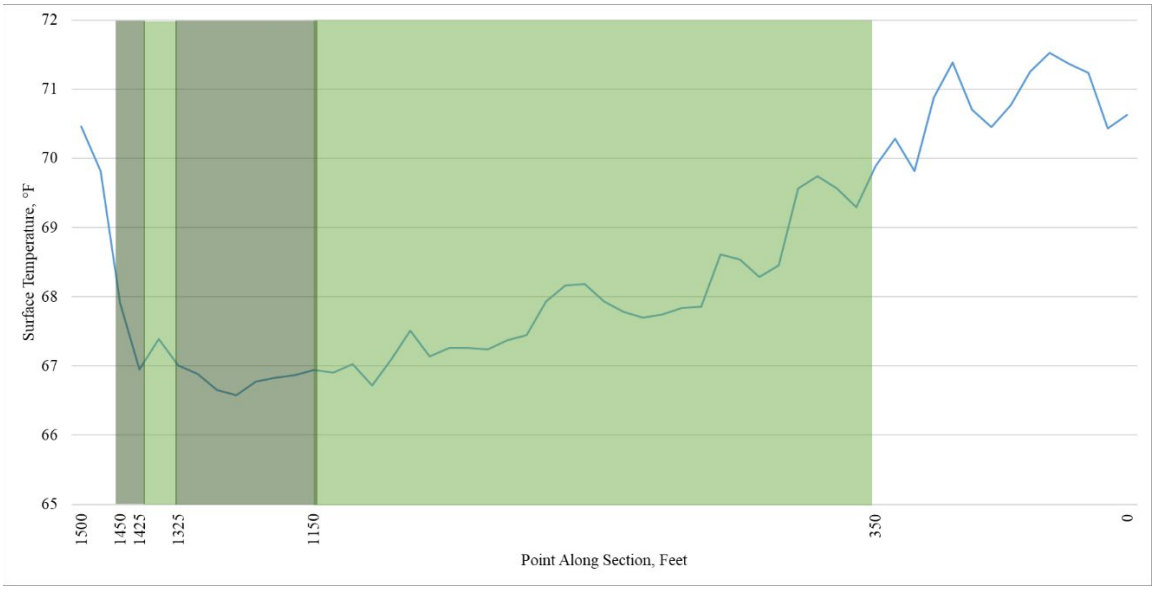

Surface temperature levels measured by MARWIS – SR 327 (2) (SB) in Vinton County, Ohio

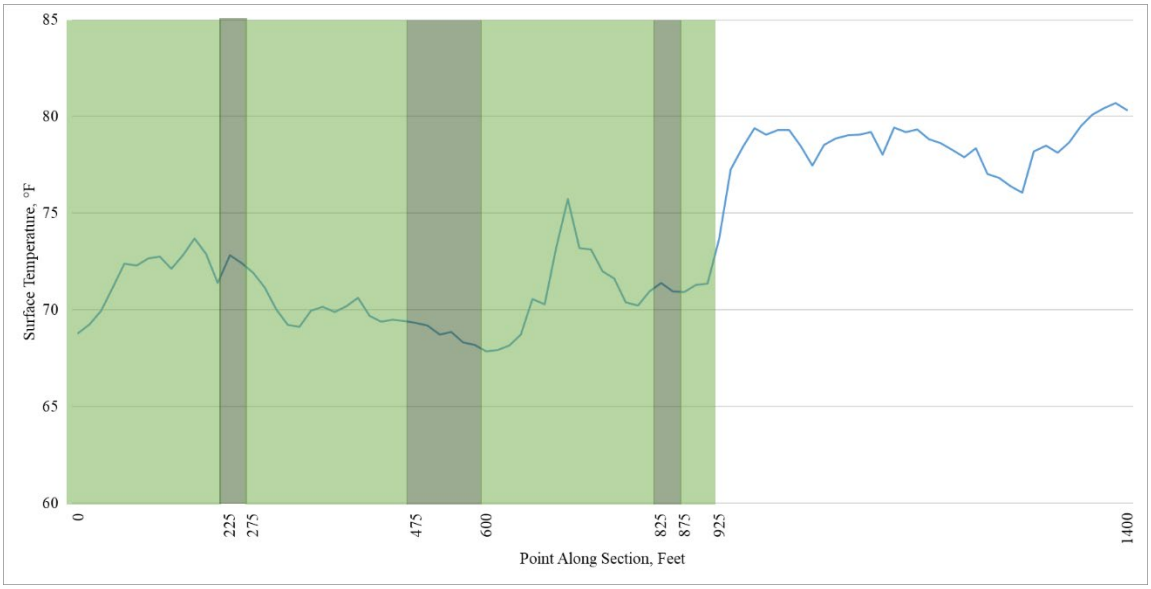

Surface temperature levels measured by MARWIS – SR 356 (NB) in Vinton County, Ohio

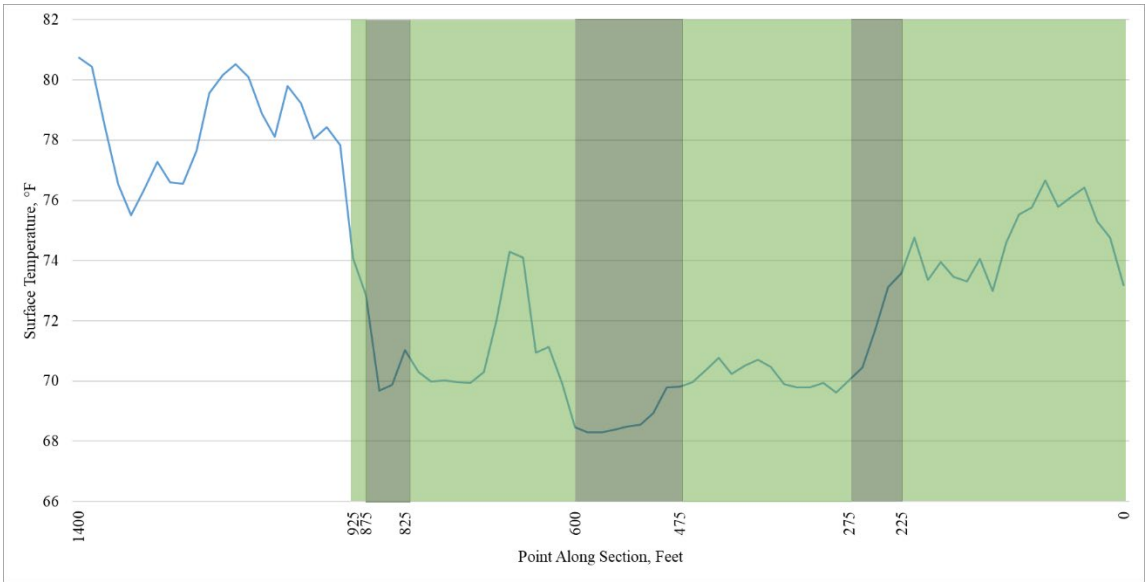

Surface temperature levels measured by MARWIS – SR 356 (SB) in Vinton County, Ohio

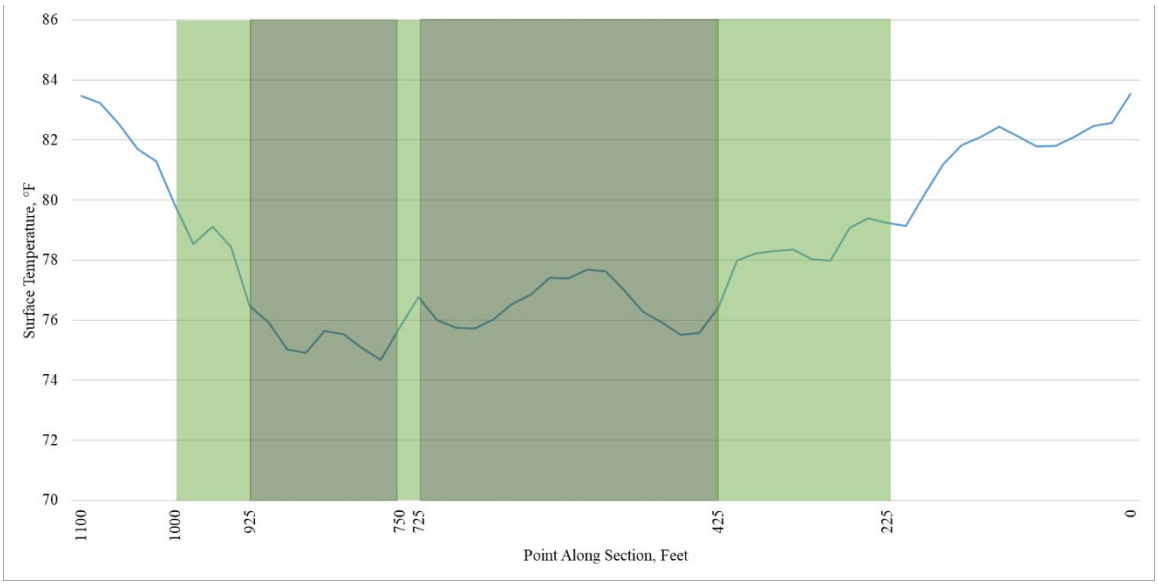

Surface temperature levels measured by MARWIS – SR 260 (NB) in Washington County, Ohio

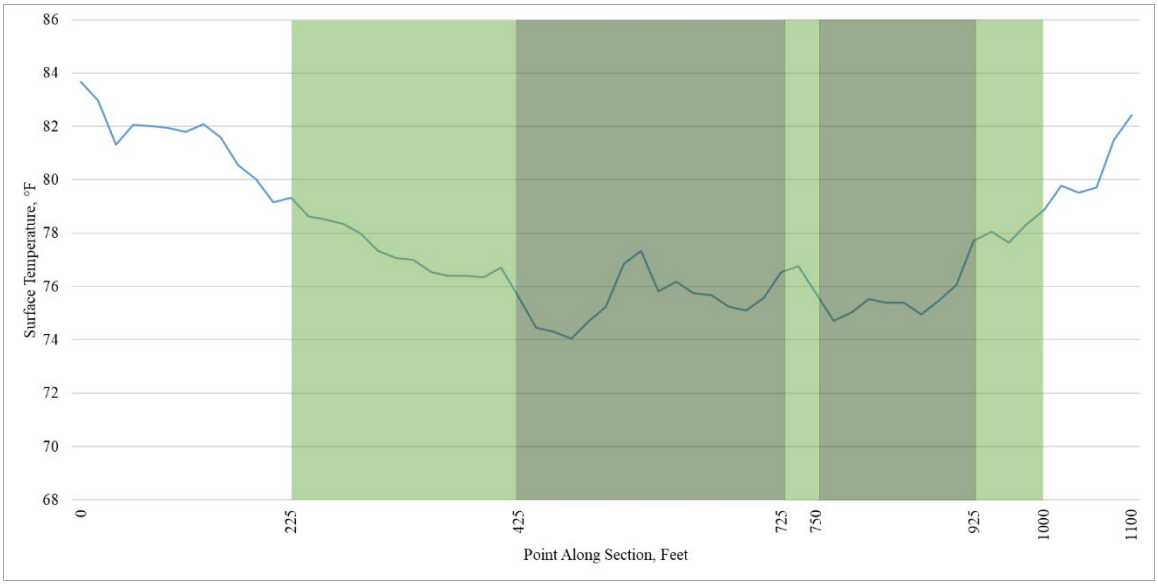

Surface temperature levels measured by MARWIS – SR 260 (SB) in Washington County, Ohio

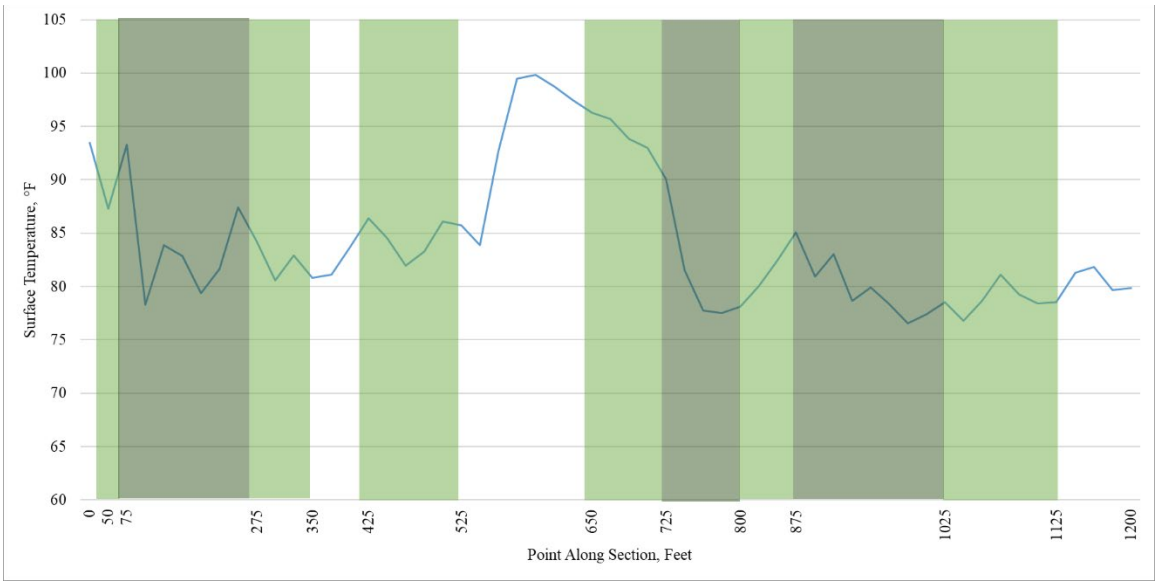


Surface temperature levels measured by MARWIS – SR 555 (NB) in Washington County, Ohio

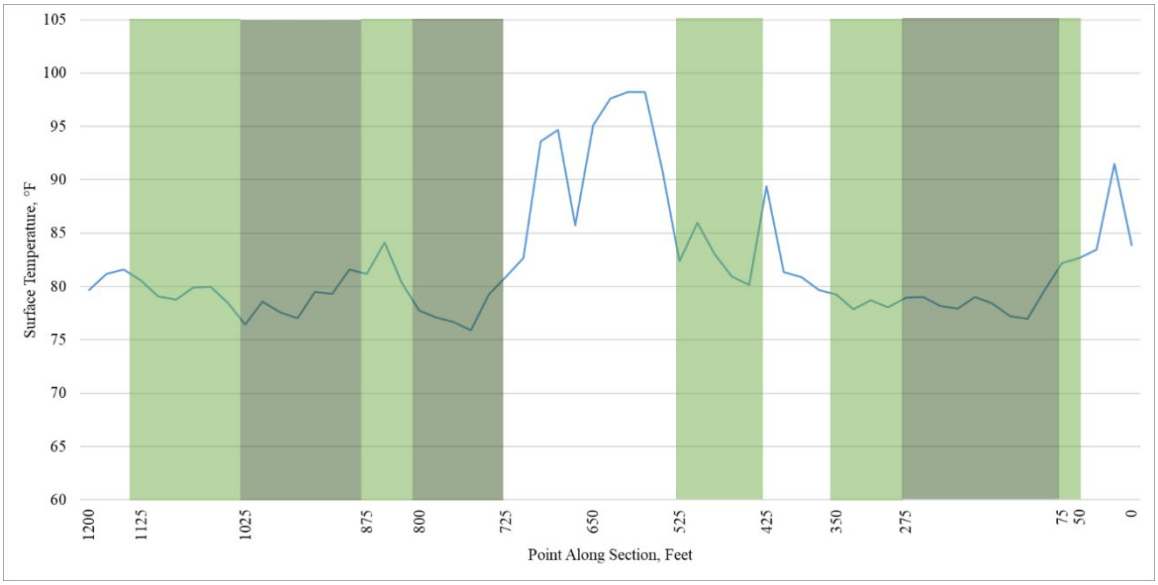


Surface temperature levels measured by MARWIS – SR 555 (SB) in Washington County, Ohio

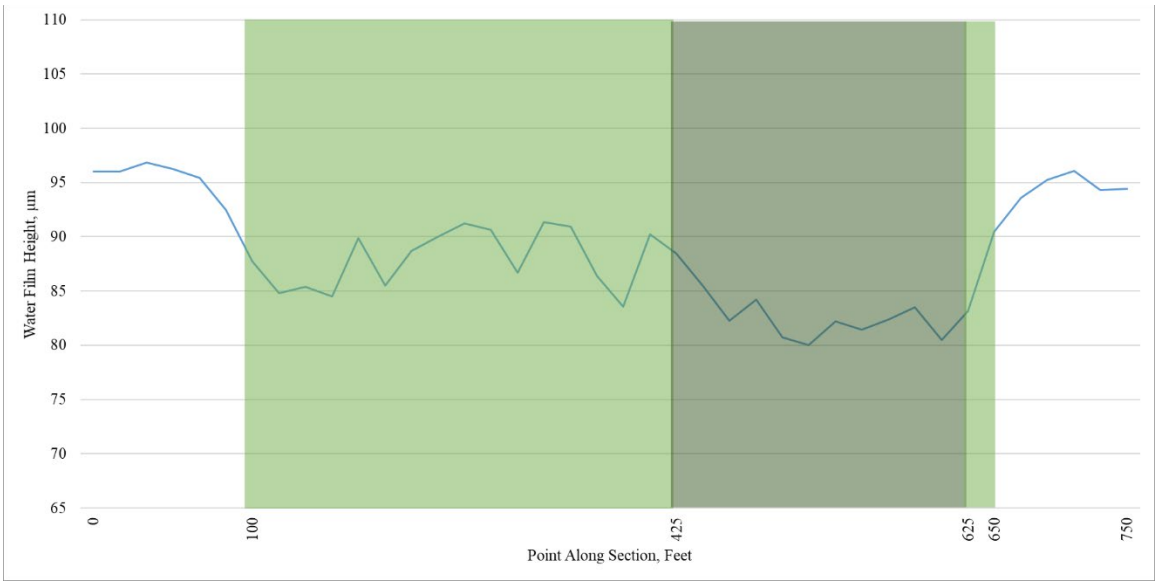

Surface temperature levels measured by MARWIS – SR 676 (1) (EB) in Washington County, Ohio

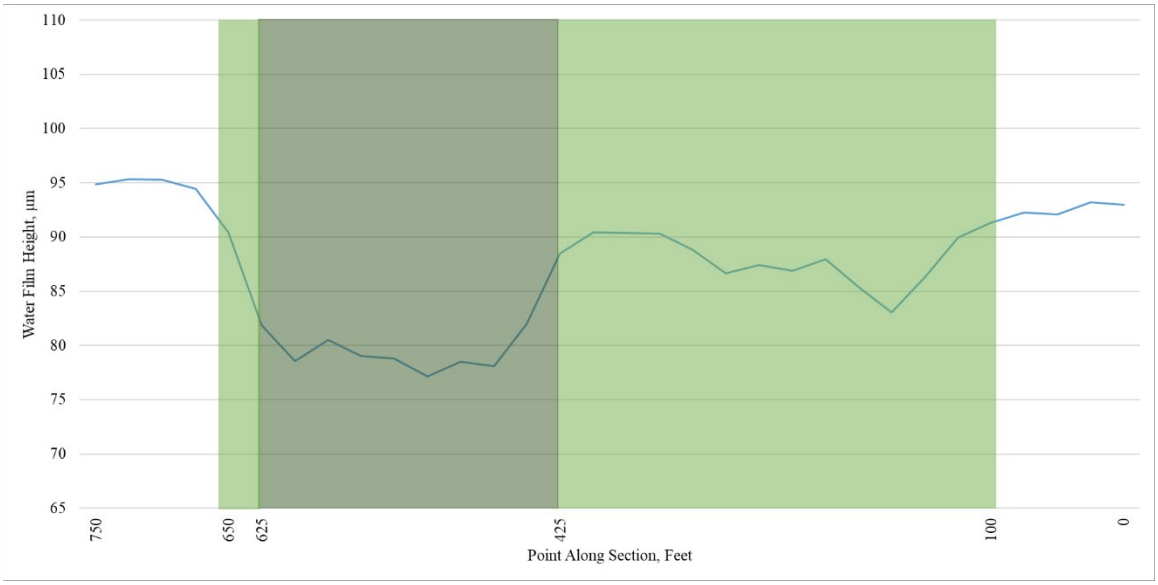

Surface temperature levels measured by MARWIS – SR 676 (1) (WB) in Washington County, Ohio

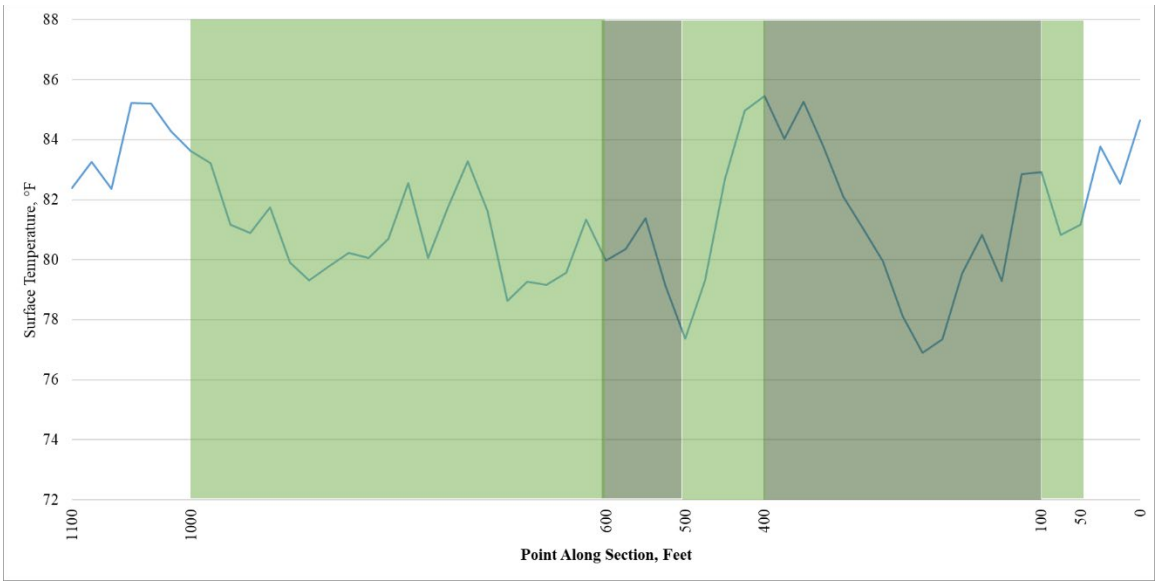


Surface temperature levels measured by MARWIS – SR 676 (2) (EB) in Washington County, Ohio

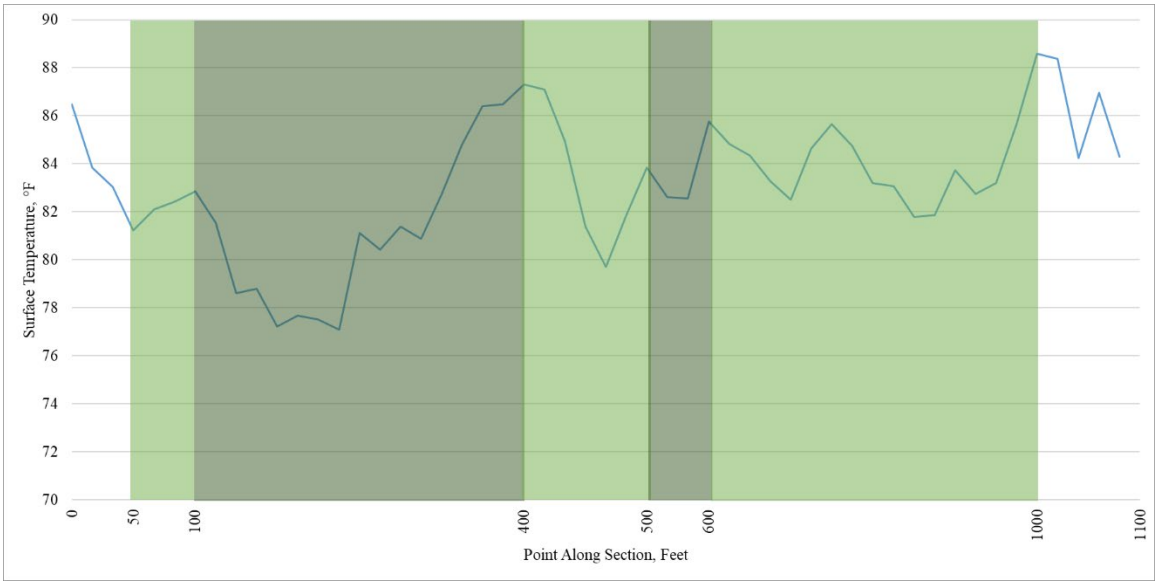


Surface temperature levels measured by MARWIS – SR 676 (2) (EB) in Washington County, Ohio

## APPENDIX J: FLIR PAVEMENT TEMPERATURE

- These graphs are listed in order by county name and state route (SR) number.
- White portions indicate densiometer measurements of tree coverage 0-25% (no canopy); light green portions indicate coverage 25-75% (partial canopy); dark green portions indicate coverage 75-100% (full canopy)
- Horizontal axis indicates distance in feet along road section (1 ft = 0.305 m)
- Vertical axis indicates surface temperature in degrees F (68°F = 20°C; 113°F = 45°C)

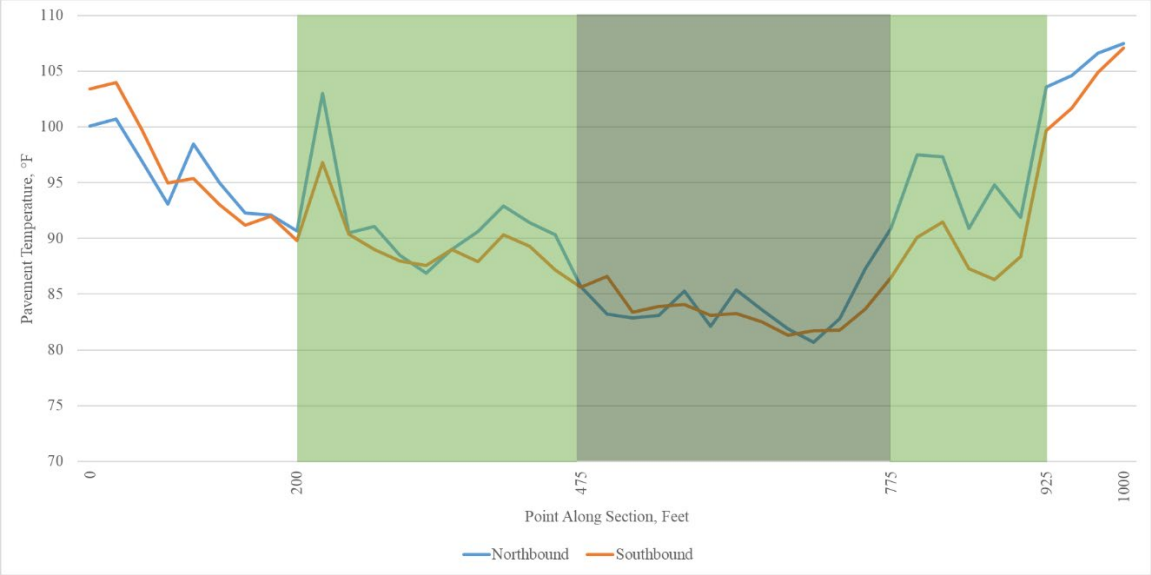


Surface temperature levels measured by FLIR – SR 13 in Athens County, Ohio

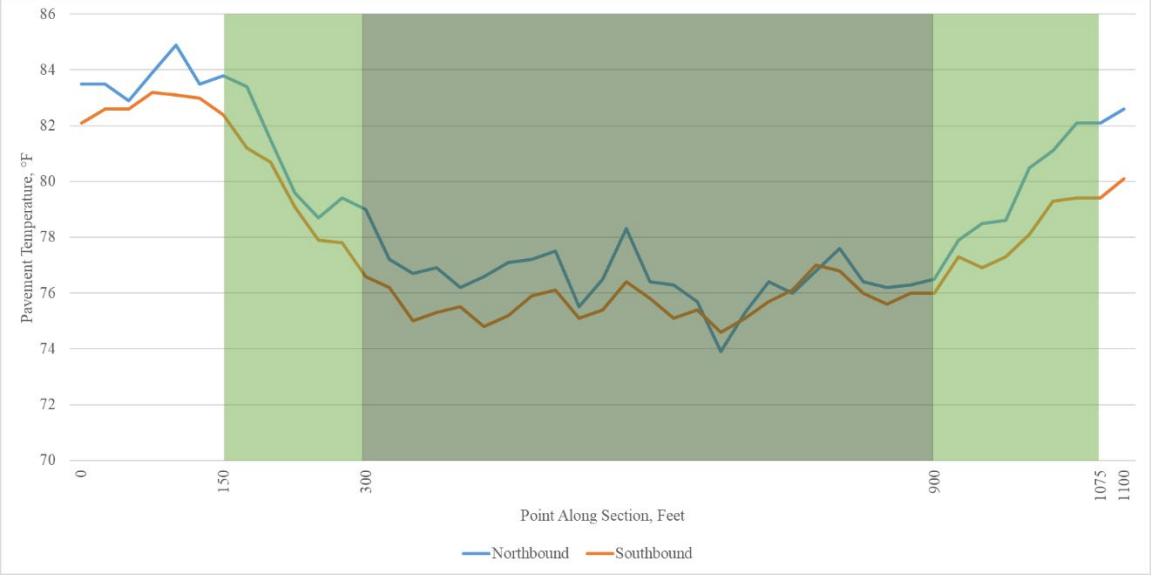


Surface temperature levels measured by FLIR – SR 258 in Harrison County, Ohio

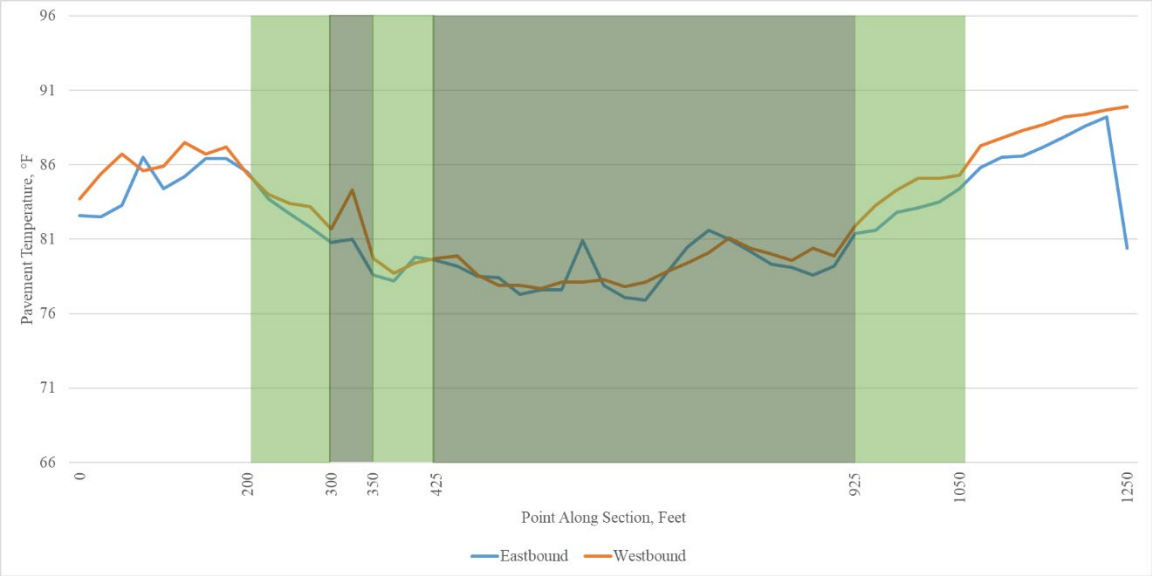

Surface temperature levels measured by FLIR – SR 56 in Hocking County, Ohio

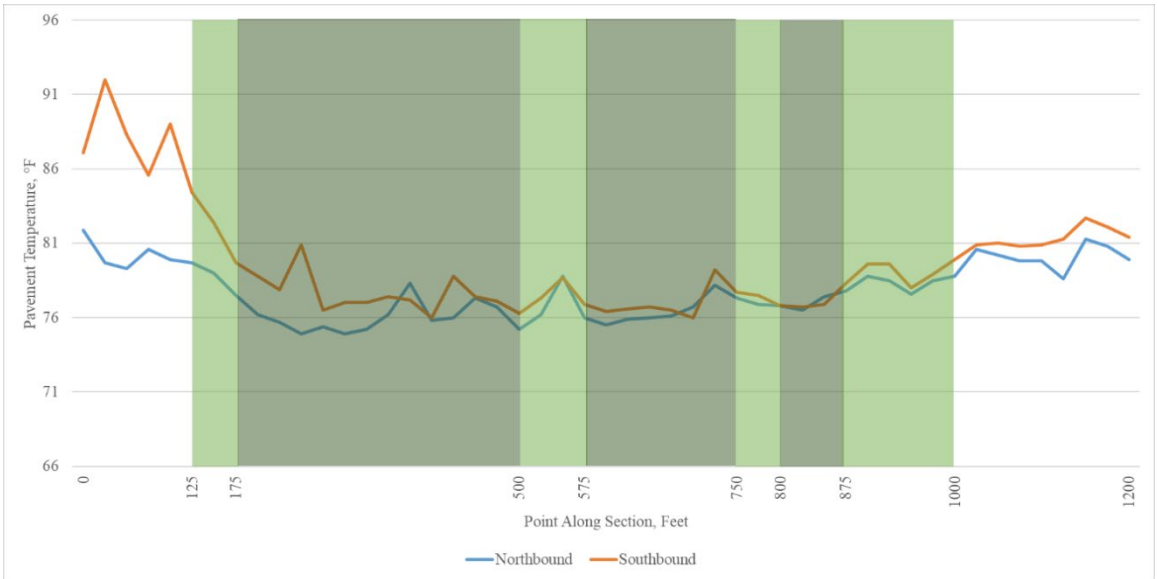

Surface temperature levels measured by FLIR – SR 374 (1) in Hocking County, Ohio

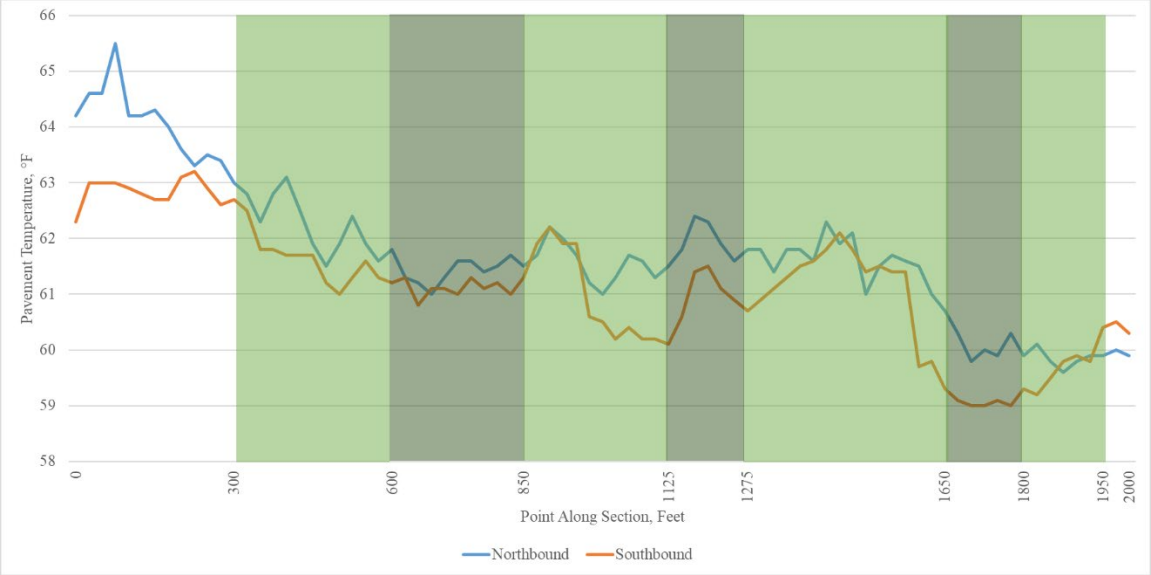

Surface temperature levels measured by FLIR – SR 374 (2) in Hocking County, Ohio

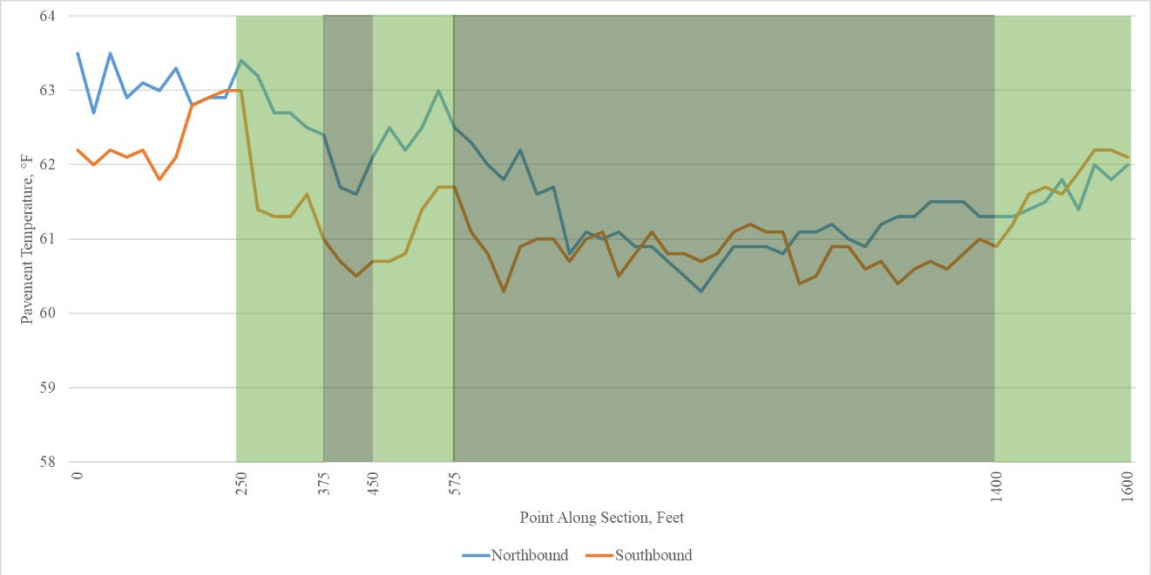

Surface temperature levels measured by FLIR – SR 374 (3) in Hocking County, Ohio

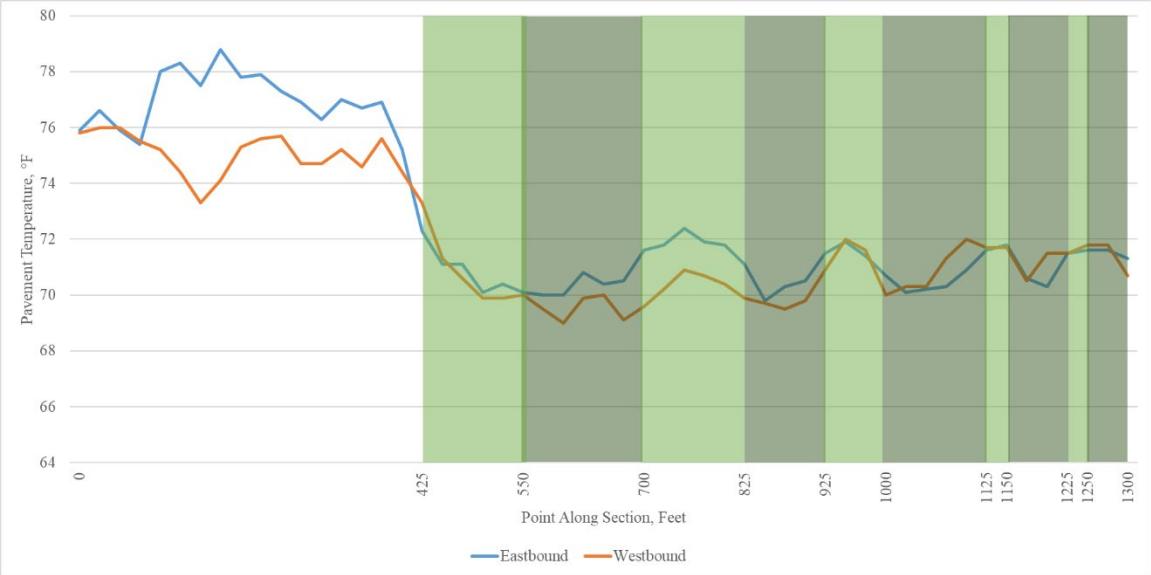

Surface temperature levels measured by FLIR – SR 124 (1) in Jackson County, Ohio

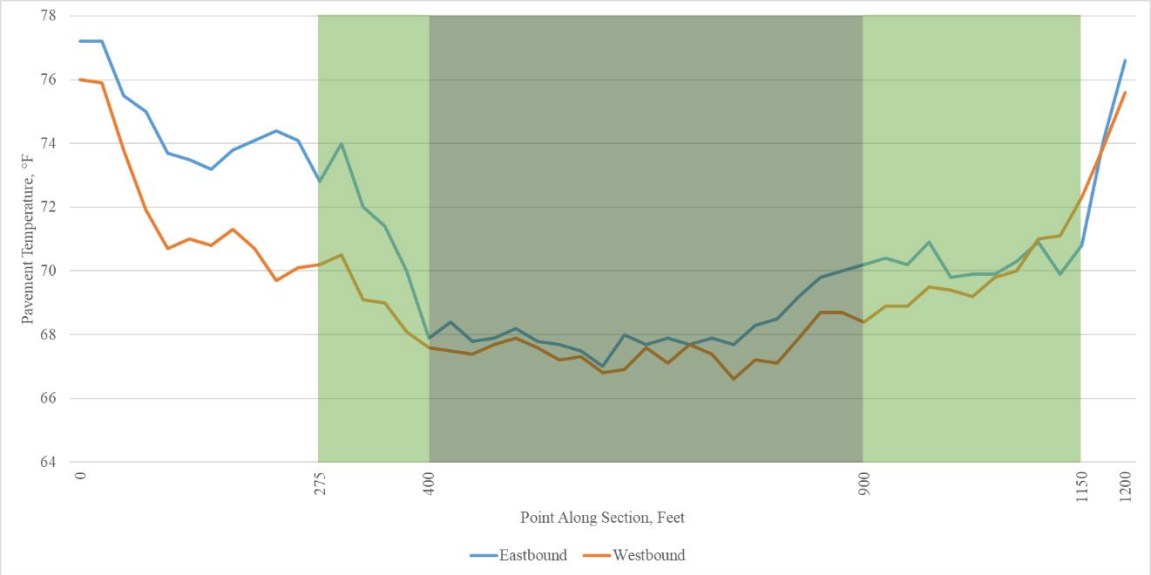

Surface temperature levels measured by FLIR – SR 124 (2) in Jackson County, Ohio

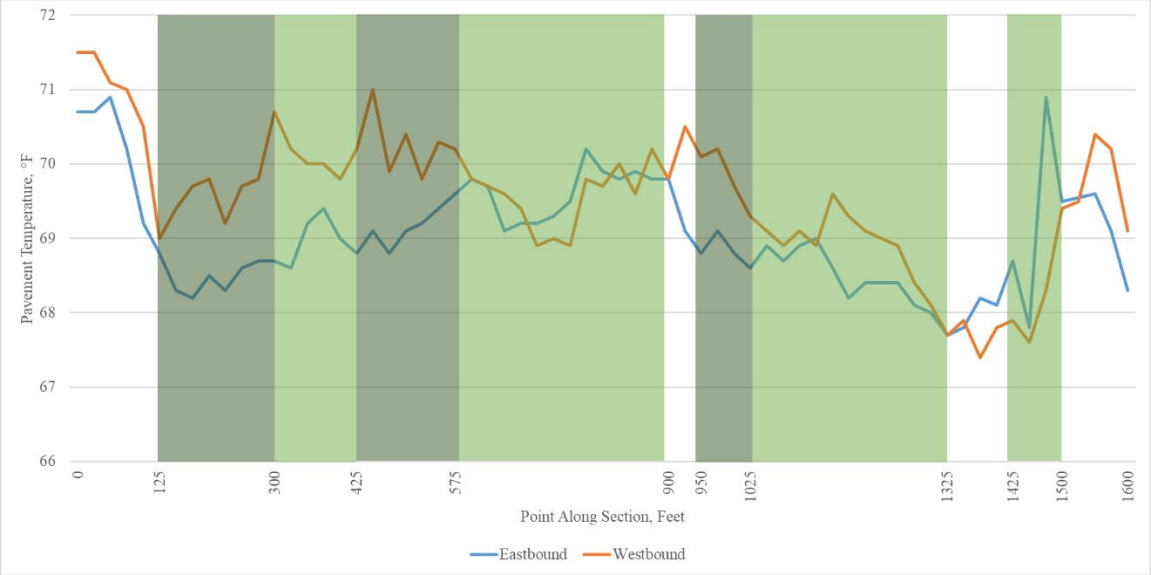

Surface temperature levels measured by FLIR – SR 335 (1) in Pike County, Ohio

Surface temperature levels measured by FLIR – SR 335 (2) in Pike County, Ohio

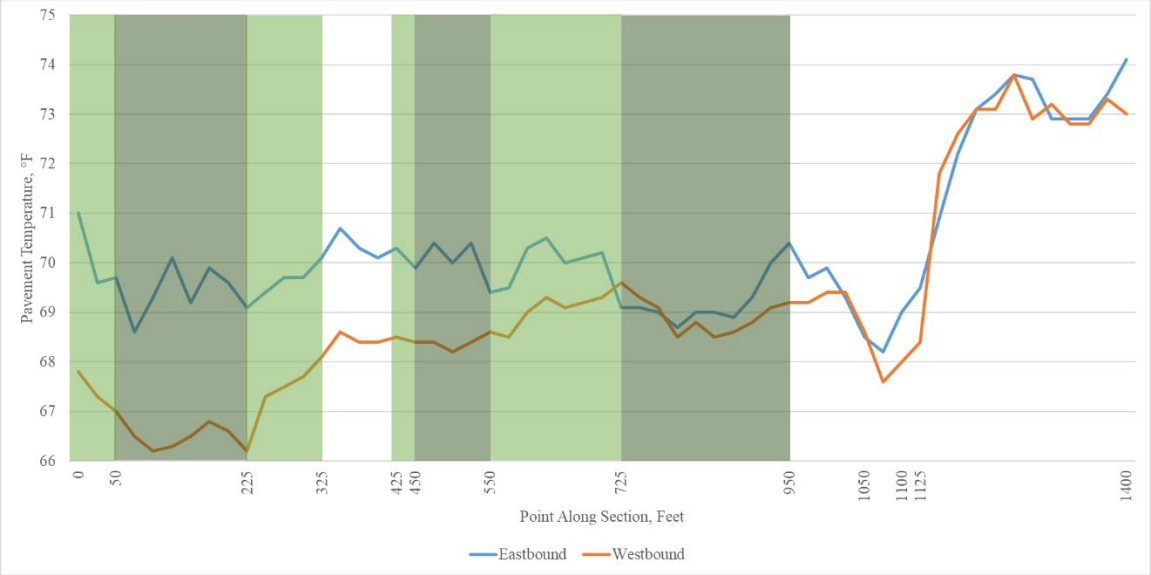

Surface temperature levels measured by FLIR – SR 139 in Scioto County, Ohio

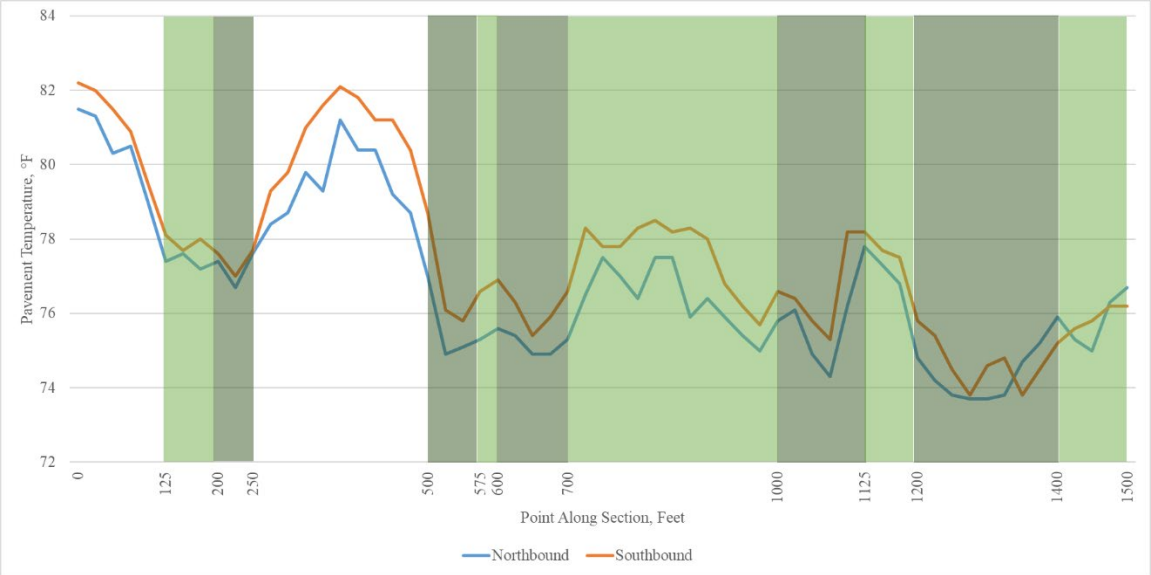

Surface temperature levels measured by FLIR – SR 800 in Tuscarawas County

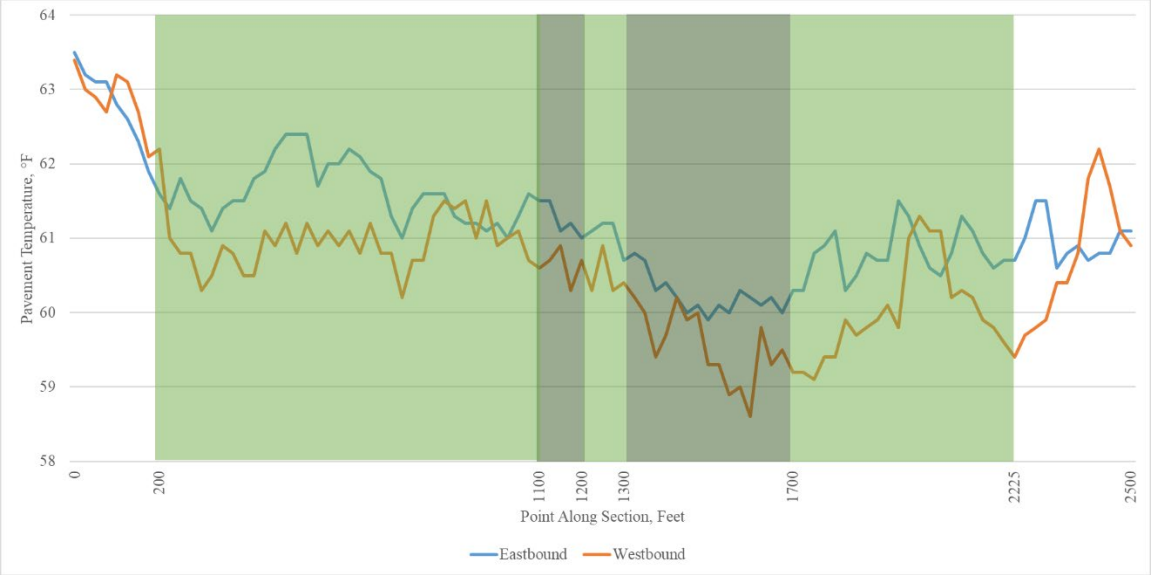

Surface temperature levels measured by FLIR – SR 56 in Vinton County

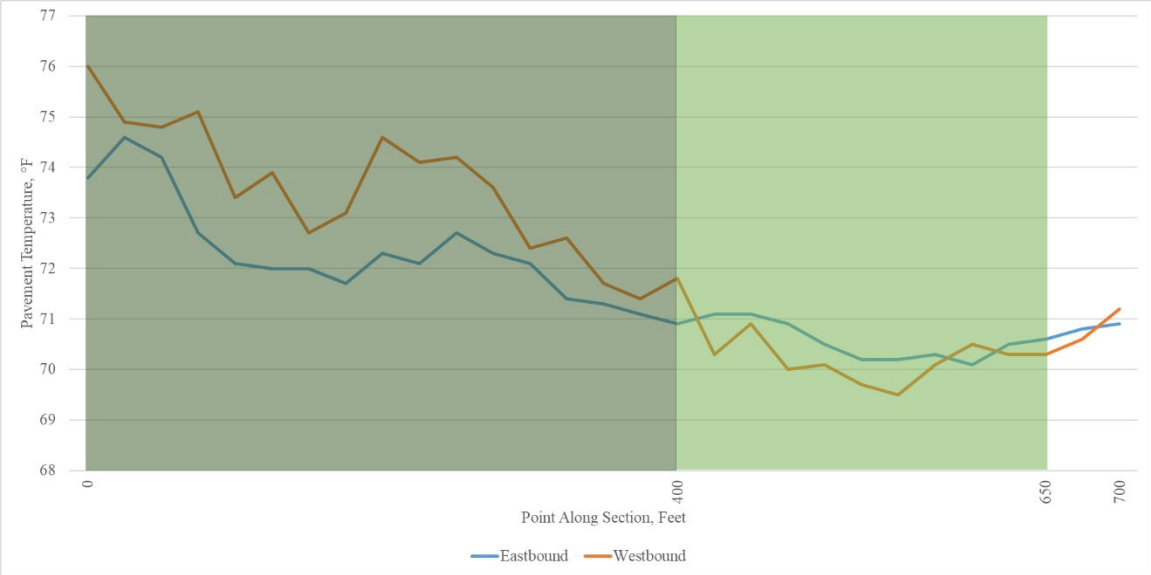

Surface temperature levels measured by FLIR – SR 124 in Vinton County, Ohio

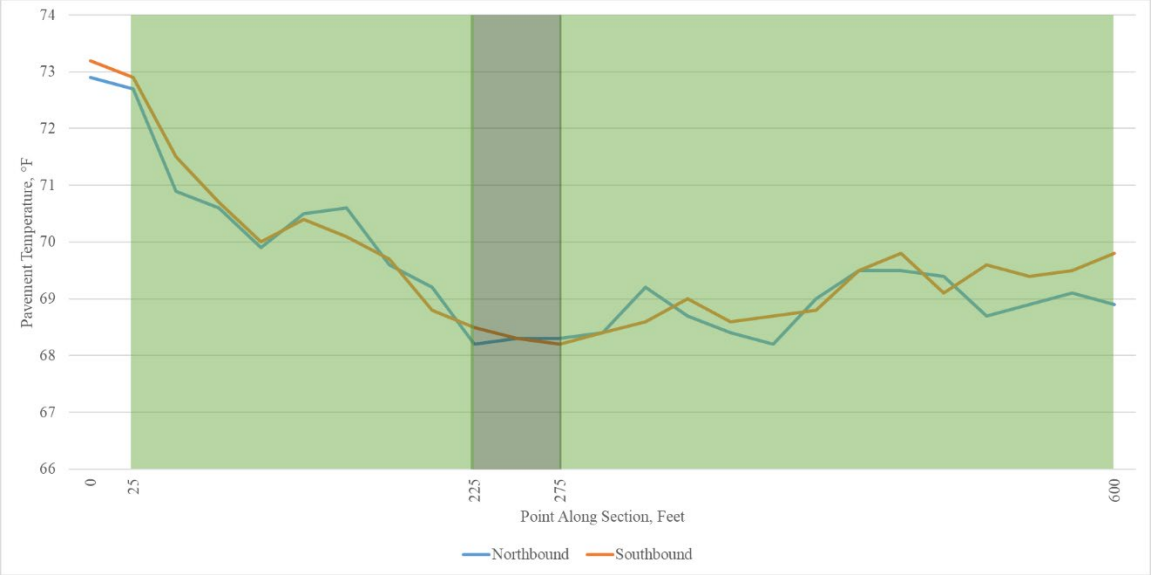

Surface temperature levels measured by FLIR – SR 327 (1) in Vinton County, Ohio

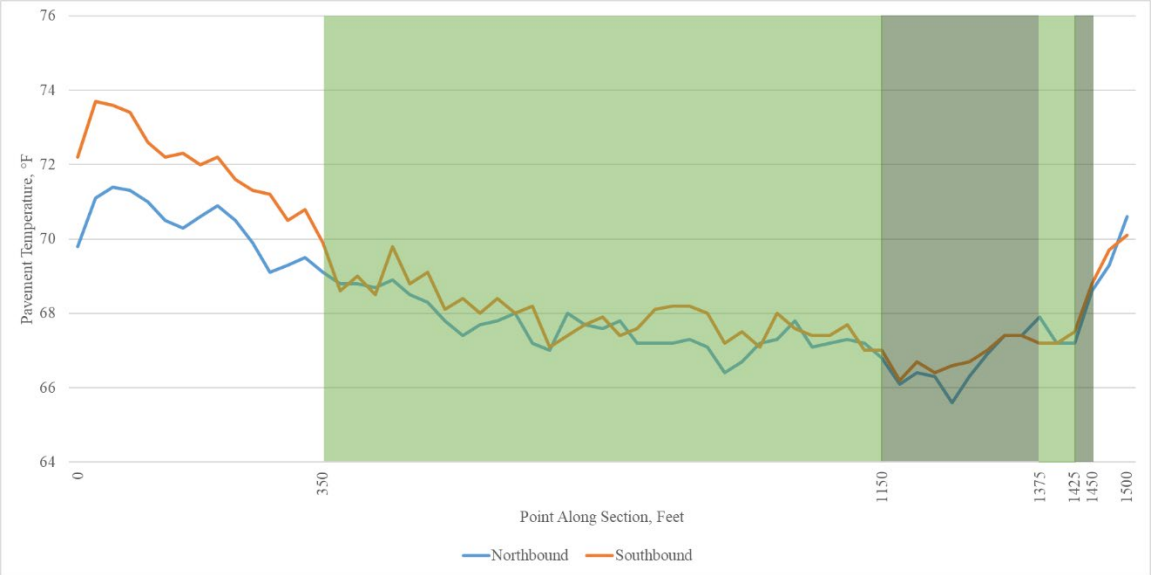

Surface temperature levels measured by FLIR – SR 327 (2) in Vinton County, Ohio

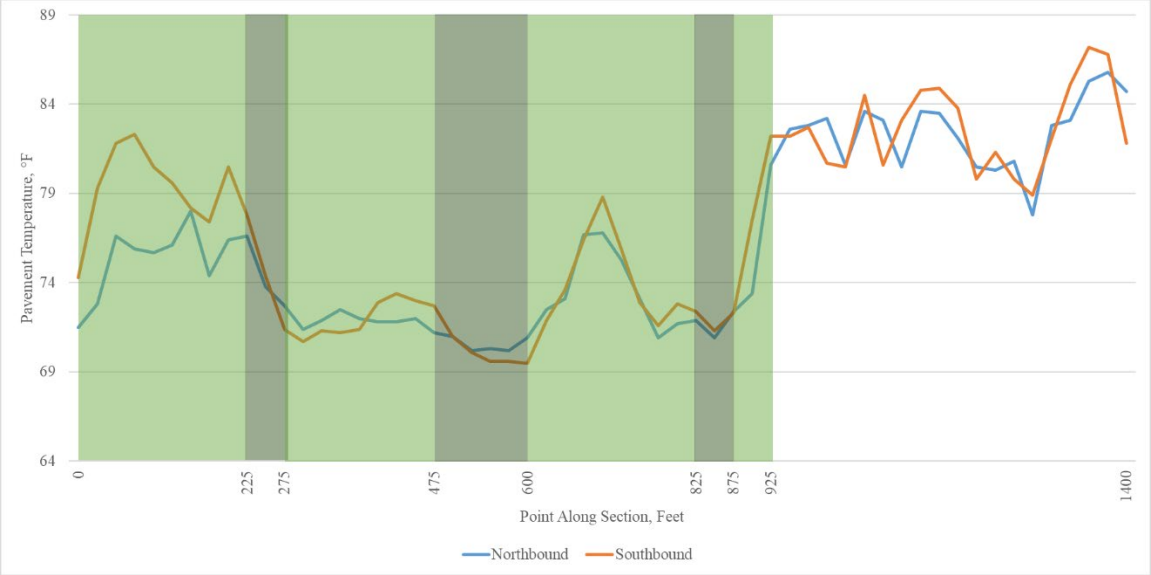

Surface temperature levels measured by FLIR – SR 356 in Vinton County, Ohio

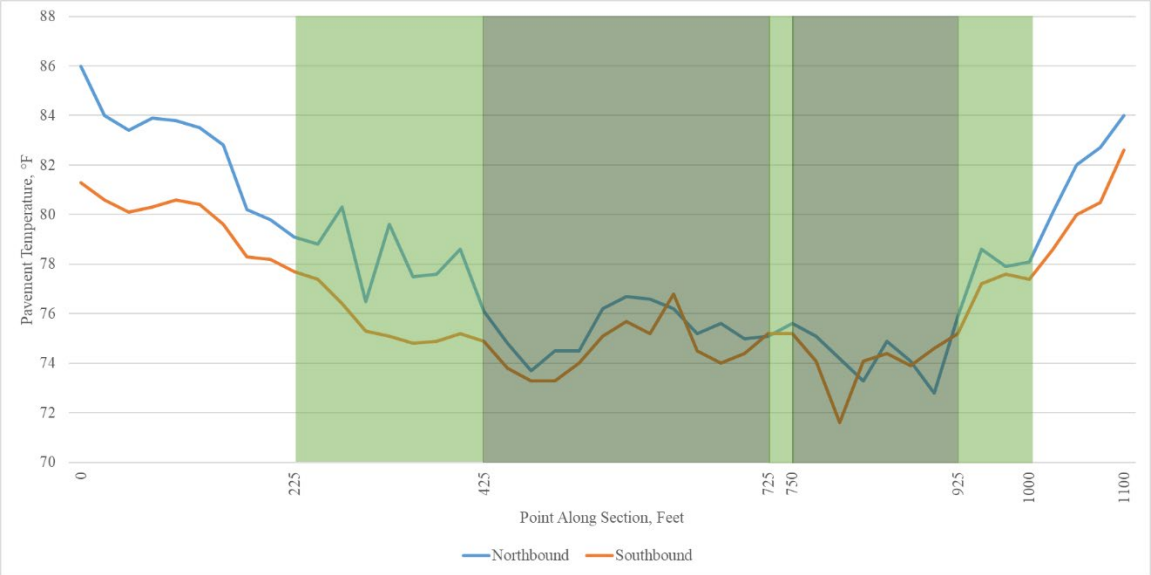

Surface temperature levels measured by FLIR – SR 260 in Washington County, Ohio

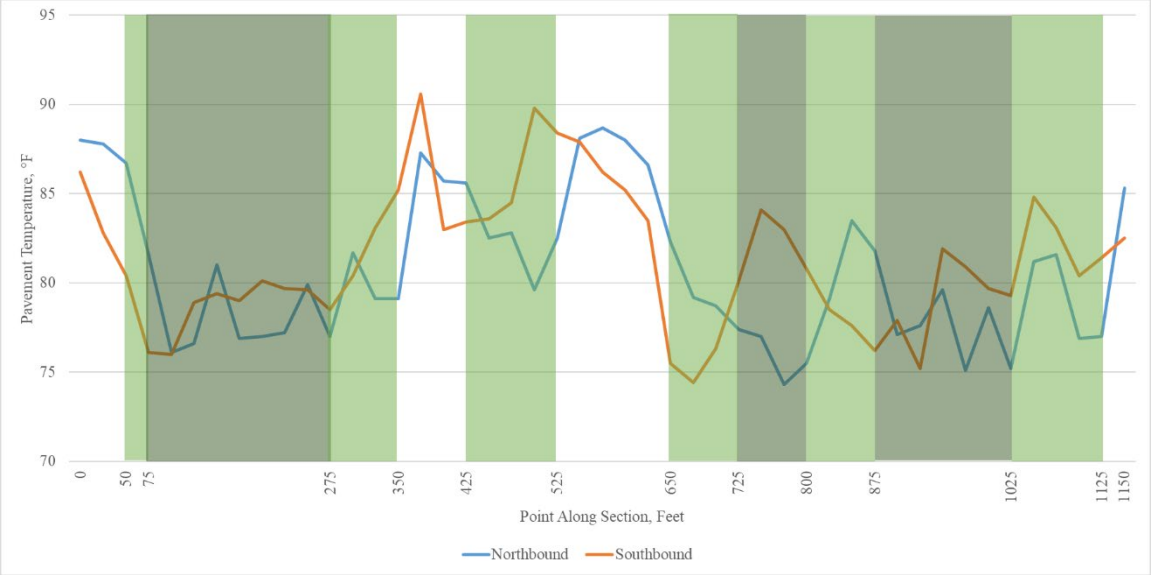

Surface temperature levels measured by FLIR – SR 55 in Washington County, Ohio

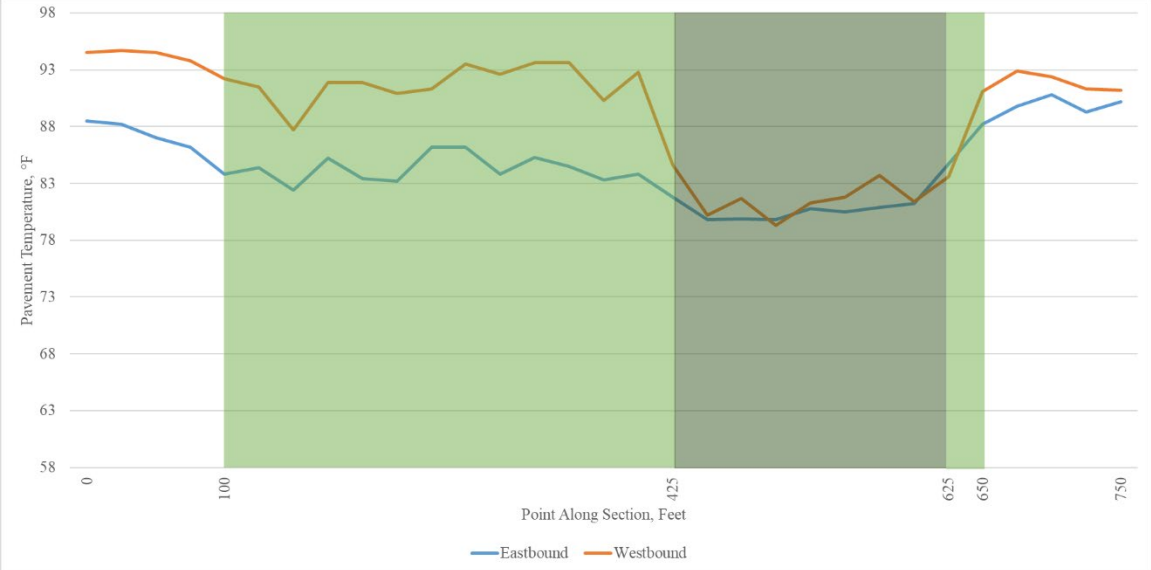

Surface temperature levels measured by FLIR – SR 676 (1) in Washington County, Ohio

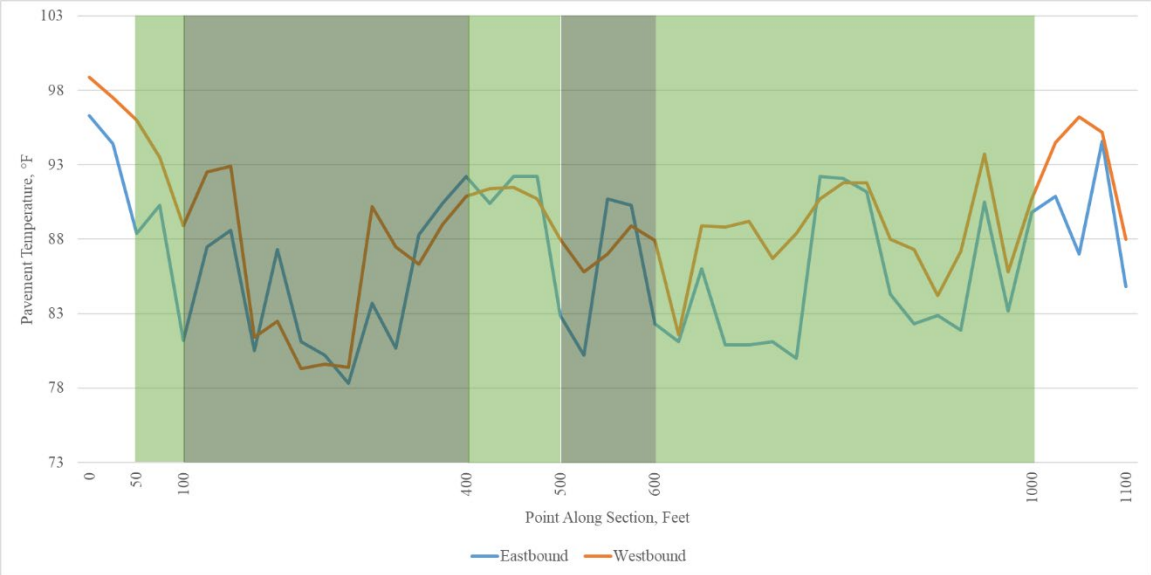

Surface temperature levels measured by FLIR – SR 676 (2) in Washington County, Ohio